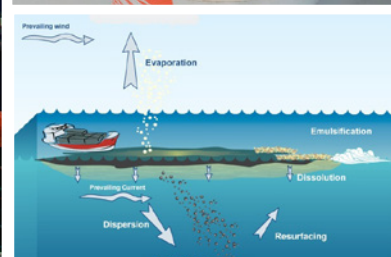
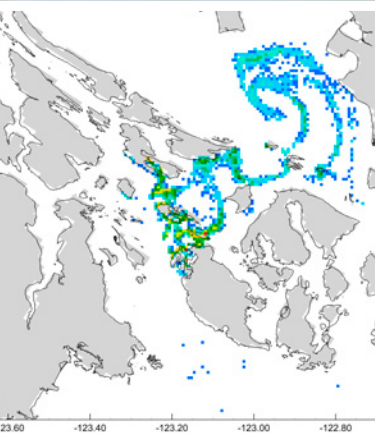


## TRANS MOUNTAIN PIPELINE ULC

# MODELLING THE FATE AND BEHAVIOUR OF MARINE OIL SPILLS FOR THE TRANS MOUNTAIN EXPANSION PROJECT



## REPORT

NOVEMBER 2013  
ISSUED FOR USE  
EBA FILE: V13203022

TRANS MOUNTAIN PIPELINES ULC

---

# MODELLING THE FATE AND BEHAVIOUR OF MARINE OIL SPILLS FOR THE TRANS MOUNTAIN EXPANSION PROJECT



## REPORT

---

NOVEMBER 2013  
ISSUED FOR USE  
EBA FILE: VI3203022

creating & delivering | BETTER SOLUTIONS

  
A TETRA TECH COMPANY



---

This page intentionally left blank.

---

## EXECUTIVE SUMMARY

Trans Mountain Pipeline ULC (Trans Mountain) proposes to increase the capacity of the Trans Mountain Pipeline system from the current 300,000 bbls/day to an estimated 890,000 bbls/day (the Project). This will result in an increased number of tankers calling at the Westridge Terminal to load crude oil cargo. As a result, Trans Mountain expects tanker traffic to the Westridge Marine Terminal to increase from about 60 vessels departing per year to 408 departing per year if the terminal and pipeline system is developed as planned.

As part of Trans Mountain's assessment of the risks of increased shipping of crude oils by tanker, including diluted bitumen oils, from their Westridge Terminal in Burnaby, several risk assessment studies have been undertaken including, but not limited to, a quantitative risk assessment (conducted by DNV, 2013), an ESA (conducted by TERA, 2013), research and tests of representative diluted bitumen crude oil to better understand the characteristics of this type of crude oil (Polaris & WCMRC, 2013) and the fate and behaviour of the oil through spill modelling by EBA, A Tetra Tech Company (EBA). This report presents the results of the spill modelling conducted by EBA.

Traditional numerical oil spill models such as OilMap and OSCAR typically use static surface currents and time-varying wind values. In the region along the shipping route, from Westridge Terminal to the open Pacific, surface currents depend on tides as well as the interaction of both wind-driven currents and tidal currents with the estuarine density stratification characterizing the region. It is crucial to obtain currents for spill simulations from an appropriate hydrodynamic numerical model which contains these processes, and which has been validated numerous times for the region of the spill. For this study, two numerical models were used: H3D, a three dimensional circulation model calibrated and validated in the area of study, to generate surface currents; and SPILLCALC, EBA's proprietary spill model, to simulate the movement and weathering of the oil slick resulting from the spill.

Modelling the fate and behaviour of the oil in the marine environment used a comprehensive approach: the release scenarios were based on a spill probability assessment conducted by Det Norske Veritas (DNV, 2013); oil trajectories, weathering and shore contact were computed by the modelling system, SPILLCALC and the models are run in both stochastic and deterministic modes. Stochastic modelling is widely used to develop an understanding of the likely behaviour of an oil slick. Deterministic modelling uses a three-dimensional model to evaluate the fate of dissolved components of the released oil, and oil-sediment interactions.

The stochastic modelling was conducted at four marine sites (Strait of Georgia, at the crossing of the route between Tsawwassen and Sidney (Location D); Haro Strait, at Arachne Reef (Location E); Juan de Fuca Strait, mid-channel off Race Rocks (Location G); and Western Entrance to the Juan de Fuca Strait, at Buoy J (Location H)); and also at the Westridge Terminal (Location A) and at Port Mann Bridge (Location FR). Further details on site selection methodology are available in the DNV report. The year was broken into four seasons: winter (January to March), spring (April to June), summer (July to September), and fall (October to December). Within each season, independent simulations starting at 6-hour intervals over the three-month period were conducted, and the resulting data summarized into various statistical products.

As part of the NEB requirements, the modelling was conducted for two spill sizes: a large or credible worst case scenario (16,500 m<sup>3</sup> for the marine site and 160 m<sup>3</sup> for the Westridge site) and a medium spill case scenario (8,250 m<sup>3</sup> for the marine site and 10 m<sup>3</sup> for the Westridge site). The Fraser site at Port Mann Bridge is different in the sense that this site corresponds to an on-land spill: one credible worst case (CWC) scenario was modelled with a spill of 1,250 m<sup>3</sup> of oil onto the Fraser River.

For the four marine locations, the duration of the oil release was 13 hours: as guided by DNV, 25% of the oil spill volume is released in the first hour, and the balance released at a uniform rate over the next 12 hours. Statistics for shoreline contact and mass balance were computed on a site and seasonal basis. Substantial differences were observed amongst the different marine sites. Spills in the inshore waters are generally larger in aerial extent than a spill at Buoy J, on the continental shelf. The extent of shoreline oiling depends on the proximity of land, and on the complexity of currents at the site: currents at the Race Rocks site and at Buoy J, in summer, are dominated by the large-scale estuarine flow in these areas, whereas in the Strait of Georgia and Haro Strait, currents tend to be more tidal. The fraction evaporated is relatively constant for all four sites. The amount remaining on the water surface is much less at the inshore sites, because of the close proximity of shorelines, which absorb the oil that comes into contact with them.

The large spill at the Westridge Terminal resulting from an incident during loading of a tanker was assessed, assuming a volume of 160 m<sup>3</sup>. At 160 m<sup>3</sup>, this spill is larger than the CWC spill resulting from a rupture of a loading arm and significantly smaller than the over 1,500 m<sup>3</sup> capacity of the precautionary boom that will be deployed around each berth while any cargo transfer activities are taking place and it is reasonable to expect that the spill would be entirely contained within the boom. In addition, observed weak currents (EBA, 2013) at the Terminal support the full containment of the oil within the pre-deployed boom. However, as a conservative approach to this scenario, it was deemed that, for oil spill modelling purposes, 20% of the oil released would escape the containment boom (i.e. 32 m<sup>3</sup>). This condition was chosen to ensure a conservative approach to spill response requirements at the site and does not reflect Trans Mountain's expectation for performance of the precautionary boom which will be in place to fully contain such a release at the terminal. For information of the reader, the CWC oil spill volume resulting from this scenario has been calculated by DNV as 103 m<sup>3</sup> and deemed as a low probability event with likelihood of occurring once every 234 years.

Statistics for shoreline contact and mass balance were computed on seasonal basis for the spill at Westridge Terminal. Results amongst the four seasons were similar: about 80% of the oil was still on water (contained in the pre-deployed boom), about 18% ended up on shore and the remaining 2% were either evaporated in the air or dissolved in the water column.

The Fraser River Site, referred as Site FR, was located downstream of the Port Mann Bridge. This location was determined to be representative of a hypothetical incident resulting from on-land pipe failure prior to crossing the Fraser River: 1,250 m<sup>3</sup> of oil was assumed to be released from the pipeline and make its way to the Fraser River. Interaction with the soils along the way to the entry point in the river was not considered in these simulations.

The length of shoreline oiled was relevant for determining potential ecological damage and for estimating shoreline clean up resources that would be required in the unlikely event of a spill. The average length of shoreline affected by the Fraser River spill ranged from a minimum of 25 km during spring to a maximum of 36 km during winter. The majority of the oil (74%) became trapped on shore. The amount of oil bound



---

up in oil-mineral aggregations was negligible, even though the potential to form OMA was greater in the Fraser River than in any other sites of study. However, the required energy level to mix the oil and form the OMA was not present in the river. The amount of submerged oil was greater than at the other sites because of the lighter surface water density in the Fraser River.

The differences observed within seasons were very interesting and reflected the strong dependence of the oil on flow conditions in the river. During the spring and summer when the freshet was at its maximum, the oil was carried out onto the Strait of Georgia and impacts were noted at shorelines along the Gulf Islands and into Boundary Bay. In fall and winter, the oil essentially remained within the river, at least for the three-day modelling period.

Specific scenarios, or deterministic simulations, were conducted using the version of SPILLCALC that is embedded in the H3D model. In order to extract a wider range of spill properties, the full 3D simulation represents an extension of the stochastic simulations: certain modules, such as dissolution, were simulated more accurately in those scenarios and the fate of pseudo-components was tracked over the entire water column. A primary purpose of these simulations was to provide information on the potential toxicity of the spill. Two deterministic simulations were conducted for this project: at the Arachne Reef site and at the Westridge Marine Terminal site.

Arachne Reef is situated on the west side of the northern end of Haro Strait. A plausible but highly unlikely event would be a powered grounding of a laden tanker on Arachne Reef. For this simulation, a total volume of 16,500 m<sup>3</sup> of oil was released over 13 hours: 25% in the first hour and the remainder released at a uniform rate over the next 12 hours.

The dissolution of all 17 pseudo-components within the water column was simulated. Since benzene has the highest solubility among the 16 other pseudo-components and is particularly toxic, this report focuses on its behaviour in the water column. The corresponding data for all the other pseudo-components was provided to TERA/Stantec for ecological impact evaluation. Stantec was part of TERA's ESA team and carried out a number of tasks in that respect and liaised closely with EBA.

After 13 hours of simulation, when the flow of oil from the tanker had just ceased, the benzene was found to extend from the release location to the northwest coast of San Juan Island, and down the eastern side of Haro Strait to its connection with the Juan de Fuca Strait. Values observed were typically about 20 times lower than the CCME threshold value for the protection of aquatic life in the marine environment, 0.11 mg/L (<http://st-ts.ccme.ca/?lang=en&factsheet=14>).

After 48 hours, the typical concentration in the surface layer is about 100 times lower than the CCME threshold value. Examination of vertical profiles indicated that the highest concentrations were at the surface.

The second deterministic simulation was the Westridge scenario, located at the Westridge Terminal in Burrard Inlet, Burnaby. A conservative value of 160 m<sup>3</sup> was retained for the spilled amount. Of the 160 m<sup>3</sup> total spill volume, about 32 m<sup>3</sup> of oil leaks through the boom and enters Burrard Inlet. The remaining 128 m<sup>3</sup> of oil is contained inside the pre-deployed boom.

The maximum concentration of benzene one hour after release is 0.06 mg/L, in the vicinity of the terminal, approximately half of the CCME threshold value.

After 12 hours the maximum concentration is still observed around the terminal with a value about three to four times lower than the CCME threshold value. The higher concentrations around the terminal are due to dissolution from the pool of oil contained inside the pre-deployed boom. It should be noted that most of the dissolved benzene has a concentration about 100 times lower than the CCME guideline.

The airborne transport of the evaporated portion of each pseudo-component was also modelled for both spills, using CALPUFF. CALPUFF is an advanced, multi-layered, multi-species, non-steady-state Gaussian puff air dispersion modeling system that can simulate the effects of time- and space-varying meteorological conditions on pollutant transport and is recommended by the B.C. Ministry of Environment for long-range transport and for short-range transport in complex, non-steady state meteorological conditions found in complex terrain and coastal situations.

Time and spatially variant evaporative flux area sources were produced at hourly intervals by SPILLCALC and written to a series of files as the emission inputs for CALPUFF. Of the 17 pseudo-components, 11 were shown to readily evaporate into the air. CALPUFF then tracked the transport of these fluxes calculating the concentration and transport time to each receptor grid point, set up at ground level over hourly intervals.

The constituent with the highest evaporative flux, benzene, is presented in this report. With the Westridge simulation, the majority of benzene is transported and dispersed to the west of the terminal, due to the predominance of easterly winds at the beginning of the spill when fluxes were highest. The highest concentrations are within two kilometres of the terminal as the majority of the flux volume (~70%) is produced from the portion of the spill that is contained behind the pre-deployed boom. The complete human health risk assessment associated with the airborne transport of the evaporated portion is described as part of the Human Health Risk Assessment Report.

## TABLE OF CONTENTS

<b>1.0 INTRODUCTION .....</b>	<b>1</b>
<b>2.0 SPILL SCENARIOS .....</b>	<b>1</b>
<b>3.0 HYDRODYNAMIC MODEL: H3D .....</b>	<b>3</b>
3.1 Description of H3D .....	3
3.1.1 Hydrodynamic Grids .....	4
3.1.1.1 Strait of Georgia 1 km Grid .....	4
3.1.1.2 Strait of Georgia 200 m Grid .....	4
3.1.1.3 Burrard Inlet 125 m Grid .....	4
3.1.1.4 Fraser River Grid .....	5
3.1.2 Tides .....	5
3.1.3 Winds .....	5
3.1.4 Meteorology .....	5
3.1.5 River Inputs .....	6
3.1.6 Vertical and Horizontal Mixing .....	6
3.1.7 Initial and Boundary Conditions .....	6
3.2 Validation of the Models .....	6
3.2.1 Tidal Validation .....	7
3.2.2 Current Meter Validation .....	8
3.2.3 The Bob Lord Drift .....	8
<b>4.0 WAVE MODEL: SWAN .....</b>	<b>10</b>
4.1 Description of SWAN .....	10
4.2 Model Configuration: Strait of Georgia 1-km Grid .....	10
4.3 Model Configuration: Strait of Georgia 200-m Grid .....	10
4.4 Model Configuration: Burrard Inlet Grid .....	10
4.5 Model Configuration: Fraser River Grid .....	11
<b>5.0 OIL SPILL MODEL: SPILLCALC .....</b>	<b>11</b>
5.1 Overview .....	11
5.2 Input and Data Forcing .....	12
5.2.1 Particle Properties .....	12
5.2.2 Transfer of Oil to the Water .....	12
5.2.3 Calculation of the Particle Velocities .....	13
5.2.4 Calculation of New Particle Positions .....	14
5.2.5 Transfer of Oil to the Shoreline .....	14
5.2.6 Properties and Weathering of Diluted Bitumen .....	15
5.2.7 Weathering Processes in SPILLCALC .....	17
5.2.7.1 Evaporation .....	17
5.2.7.2 Vertical Dispersion and Resurfacing .....	18
5.2.7.3 Oil Sinking .....	19



5.2.7.4	Contact with Beach and Intertidal Areas .....	19
5.2.7.5	Small-Scale Spreading .....	19
5.2.7.6	Oil-Sediment Interaction .....	20
5.2.7.7	Emulsification .....	20
5.2.7.8	Dissolution .....	20
5.2.7.9	Bacterial Decay .....	21
5.3	Burrard Inlet Spill Validation .....	21
<b>6.0</b>	<b>AIR DISPERSION MODEL: SPILLCALC TO CALPUFF .....</b>	<b>23</b>
6.1	Diagnostic Wind and Meteorological Modelling (CALMET) .....	23
6.1.1	Model Grids and Meteorological Data .....	23
6.1.2	CALMET Switch Settings .....	26
6.2	Air Dispersion Model (CALPUFF) .....	26
6.2.1	Evaporation Flux (Area Sources) .....	26
6.2.2	CALPUFF Switch Settings .....	27
<b>7.0</b>	<b>SIMULATION OVERVIEW .....</b>	<b>27</b>
7.1	Types of Simulations .....	27
7.1.1	Stochastic simulations .....	27
7.1.2	Specific simulations .....	27
<b>8.0</b>	<b>STOCHASTIC SIMULATIONS .....</b>	<b>27</b>
8.1	Site A: Westridge Terminal .....	28
8.1.1	Large Spill (160 m <sup>3</sup> ) .....	28
8.1.2	Small Spill (10 m <sup>3</sup> ) .....	30
8.2	Site D: Strait of Georgia .....	30
8.2.1	CWC Spill (16,500 m <sup>3</sup> ) .....	31
8.2.2	Medium Spill (8,250 m <sup>3</sup> ) .....	32
8.3	Site E: Haro Strait at Arachne Reef .....	33
8.3.1	CWC Spill (16,500 m <sup>3</sup> ) .....	33
8.3.2	Medium Spill (8,250 m <sup>3</sup> ) .....	34
8.4	Site G: Juan de Fuca Strait off Race Rocks .....	35
8.4.1	CWC Spill (16,500 m <sup>3</sup> ) .....	36
8.4.2	Medium Spill (8,250 m <sup>3</sup> ) .....	37
8.5	Site H: Buoy J .....	38
8.5.1	CWC Spill (16,500 m <sup>3</sup> ) .....	38
8.5.2	Medium Spill (8,250 m <sup>3</sup> ) .....	39
8.6	Site FR: Fraser River at Port Mann Bridge .....	40
8.7	Synthesis of Marine Spills Stochastic Results .....	41
8.7.1	CWC (16,500 m <sup>3</sup> ) .....	41
8.7.2	Medium Spill (8,250 m <sup>3</sup> ) .....	42

---

<b>9.0</b>	<b>THREE-DIMENSIONAL SPECIFIC SIMULATIONS.....</b>	<b>43</b>
9.1	Spill at Arachne Reef .....	43
9.2	Arachne Reef Simulation Results .....	44
9.3	Arachne Reef Air Dispersion .....	45
9.4	Spill at the Westridge Marine Terminal.....	45
9.5	Westridge Marine Terminal Simulation Results.....	46
9.6	Westridge Marine Terminal Air Dispersion .....	47
9.6.1	Synopsis of Burrard Inlet Winds During the Spill Simulations .....	47
9.6.2	160 m <sup>3</sup> Spill Results.....	47
<b>10.0</b>	<b>CONCLUSION .....</b>	<b>48</b>
<b>11.0</b>	<b>CLOSURE.....</b>	<b>49</b>
	<b>REFERENCES.....</b>	<b>50</b>

## TABLES

Table 2.1.1	Spill Locations
Table 3.2.1	Tidal Validation Statistics
Table 3.2.2	Summary of Bob Lord's Drift
Table 5.2.1	Pseudo-Components and Properties
Table 6.1.1	Meteorological Surface Stations, Buoys and NARR Grid Points Used in CALMET
Table 8.1.1	Statistics for Shoreline Contact for a Large Spill at Site A
Table 8.1.2	Mass Balance Summary for a Large Spill at Site A
Table 8.1.3	Mass Balance Summary for a Small Spill at Site A
Table 8.2.1	Statistics for Shoreline Contact for a Credible Worst Case Spill at Site D
Table 8.2.2	Mass Balance Summary for a Credible Worst Case Spill at Site D
Table 8.2.3	Statistics for Shoreline Contact for a Medium Case Spill at Site D
Table 8.2.4	Mass Balance Summary for a Medium Case Spill at Site D
Table 8.3.1	Statistics for Shoreline Contact for a Credible Worst Case Spill at Site E
Table 8.3.2	Mass Balance Summary for a Credible Worst Case Spill at Site E
Table 8.3.3	Statistics for Shoreline Contact for a Medium Case Spill at Site E
Table 8.3.4	Mass Balance Summary for a Medium Case Spill at Site E
Table 8.4.1	Statistics for Shoreline Contact for a Credible Worst Case Spill at Site G
Table 8.4.2	Mass Balance Summary for a Credible Worst Case Spill at Site G
Table 8.4.3	Statistics for Shoreline Contact for a Medium Case Spill at Site G
Table 8.4.4	Mass Balance Summary for a Medium Case Spill at Site G
Table 8.5.1	Statistics for Shoreline Contact for a Credible Worst Case Spill at Site H
Table 8.5.2	Mass Balance Summary for a Credible Worst Case Spill at Site H
Table 8.5.3	Statistics for Shoreline Contact for a Medium Case Spill at Site H
Table 8.5.4	Mass Balance Summary for a Medium Case Spill at Site H
Table 8.6.1	Statistics for Shoreline Contact for a Pipe Failure at Site FR
Table 8.6.2	Mass Balance Summary for a Pipe Failure at Site FR
Table 8.7.1	Summary of Stochastic Modelling Results



## FIGURES

Figure 2.1.1	Sites Location
Figure 3.1.1	Typical Grid Mesh
Figure 3.1.2	Hydrodynamic Model Grid Domains
Figure 3.2.1	Modelled and Predicted Water Levels September 2011
Figure 3.2.2	Modelled and Observed Water Levels September 2011
Figure 3.2.3	Modelled and Observed Water Levels April 2013
Figure 3.2.4	Bob Lord's Drift Path
Figure 3.2.5	Bob Lord's Drift Path Computed by CANSARP
Figure 3.2.6	Bob Lord's Drift Path Computed by SPILLCALC
Figure 5.2.1	Observed and Hind cast Density Time-Series
Figure 5.2.2	Percentage of Oil-SPM Interaction
Figure 8.1.1	Stochastic Simulation Site A (160 m <sup>3</sup> ) P <sub>50</sub> and P <sub>90</sub> after 6 Hours
Figure 8.1.2	Stochastic Simulation Site A (160 m <sup>3</sup> ) P <sub>50</sub> and P <sub>90</sub> after 12 Hours
Figure 8.2.1	Stochastic Simulation Site D (16,500 m <sup>3</sup> ) P <sub>50</sub> and P <sub>90</sub> after 24 Hours
Figure 8.2.2	Stochastic Simulation Site D (16,500 m <sup>3</sup> ) P <sub>50</sub> and P <sub>90</sub> after 48 Hours
Figure 8.2.3	Stochastic Simulation Site D (8,250 m <sup>3</sup> ) P <sub>50</sub> and P <sub>90</sub> after 24 Hours
Figure 8.2.4	Stochastic Simulation Site D (8,250 m <sup>3</sup> ) P <sub>50</sub> and P <sub>90</sub> after 48 Hours
Figure 8.3.1	Stochastic Simulation Site E (16,500 m <sup>3</sup> ) P <sub>50</sub> and P <sub>90</sub> after 24 Hours
Figure 8.3.2	Stochastic Simulation Site E (16,500 m <sup>3</sup> ) P <sub>50</sub> and P <sub>90</sub> after 48 Hours
Figure 8.3.3	Stochastic Simulation Site E (8,250 m <sup>3</sup> ) P <sub>50</sub> and P <sub>90</sub> after 24 Hours
Figure 8.3.4	Stochastic Simulation Site E (8,250 m <sup>3</sup> ) P <sub>50</sub> and P <sub>90</sub> after 48 Hours
Figure 8.4.1	Stochastic Simulation Site G (16,500 m <sup>3</sup> ) P <sub>50</sub> and P <sub>90</sub> after 24 Hours
Figure 8.4.2	Stochastic Simulation Site G (16,500 m <sup>3</sup> ) P <sub>50</sub> and P <sub>90</sub> after 48 Hours
Figure 8.4.3	Stochastic Simulation Site G (8,250 m <sup>3</sup> ) P <sub>50</sub> and P <sub>90</sub> after 24 Hours
Figure 8.4.4	Stochastic Simulation Site G (8,250 m <sup>3</sup> ) P <sub>50</sub> and P <sub>90</sub> after 48 Hours
Figure 8.5.1	Stochastic Simulation Site H (16,500 m <sup>3</sup> ) P <sub>50</sub> and P <sub>90</sub> after 24 Hours
Figure 8.5.2	Stochastic Simulation Site H (16,500 m <sup>3</sup> ) P <sub>50</sub> and P <sub>90</sub> after 48 Hours
Figure 8.5.3	Stochastic Simulation Site H (8,250 m <sup>3</sup> ) P <sub>50</sub> and P <sub>90</sub> after 24 Hours
Figure 8.5.4	Stochastic Simulation Site H (8,250 m <sup>3</sup> ) P <sub>50</sub> and P <sub>90</sub> after 48 Hours
Figure 8.6.1	Stochastic Simulation Site FR (1,250 m <sup>3</sup> ) P <sub>50</sub> and P <sub>90</sub> after 12 Hours
Figure 8.6.2	Stochastic Simulation Site FR (1,250 m <sup>3</sup> ) P <sub>50</sub> and P <sub>90</sub> after 24 Hours
Figure 9.2.1	Benzene Concentration in the Surface Layer after 13 Hours
Figure 9.2.2	Benzene Concentration in the Surface Layer after 24 Hours
Figure 9.2.3	Benzene Concentration in the Surface Layer after 48 Hours
Figure 9.2.4	Profile of Benzene Concentration
Figure 9.5.1	Benzene Concentration in the Surface Layer after 1 Hours
Figure 9.5.2	Benzene Concentration in the Surface Layer after 6 Hours
Figure 9.5.3	Benzene Concentration in the Surface Layer after 12 Hours
Figure 9.5.4	Benzene Concentration in the Surface Layer after 24 Hours
Figure 9.5.5	Benzene Concentration in the Surface Layer after 48 Hours
Figure 9.5.6	Profile of Benzene Concentration

## FIGURES

- Figure 9.6.1 Volatiles – Maximum 1-hour Average Ground Level Concentration in Air ( $\mu\text{g}/\text{m}^3$ ) - 160 m<sup>3</sup> Spill
- Figure 9.6.2 Benzene – Maximum 1-hour Average Ground Level Concentration in Air ( $\mu\text{g}/\text{m}^3$ ) - 160 m<sup>3</sup> Spill
- Figure 9.6.3 TEX – Maximum 1-hour Average Ground Level Concentration in Air ( $\mu\text{g}/\text{m}^3$ ) - 160 m<sup>3</sup> Spill
- Figure 9.6.4 Aromatics > C8-10 – Maximum 1-hour Average Ground Level Concentration in Air ( $\mu\text{g}/\text{m}^3$ ) - 160 m<sup>3</sup> Spill
- Figure 9.6.5 Aromatics > C10-12 – Maximum 1-hour Average Ground Level Concentration in Air ( $\mu\text{g}/\text{m}^3$ ) - 160 m<sup>3</sup> Spill
- Figure 9.6.6 Aromatics > C12-16 – Maximum 1-hour Average Ground Level Concentration in Air ( $\mu\text{g}/\text{m}^3$ ) - 160 m<sup>3</sup> Spill
- Figure 9.6.7 Aliphatics > C6-8 – Maximum 1-hour Average Ground Level Concentration in Air ( $\mu\text{g}/\text{m}^3$ ) - 160 m<sup>3</sup> Spill
- Figure 9.6.8 Aliphatics > C8-10 – Maximum 1-hour Average Ground Level Concentration in Air ( $\mu\text{g}/\text{m}^3$ ) - 160 m<sup>3</sup> Spill
- Figure 9.6.9 Aliphatics > C10-12 – Maximum 1-hour Average Ground Level Concentration in Air ( $\mu\text{g}/\text{m}^3$ ) - 160 m<sup>3</sup> Spill
- Figure 9.6.10 Aliphatics > C12-16 – Maximum 1-hour Average Ground Level Concentration in Air ( $\mu\text{g}/\text{m}^3$ ) - 160 m<sup>3</sup> Spill
- Figure 9.6.11 Aliphatics > C16-21 – Maximum 1-hour Average Ground Level Concentration in Air ( $\mu\text{g}/\text{m}^3$ ) - 160 m<sup>3</sup> Spill
- Figure 9.6.12 Benzene – Average Ground Level Concentration in Air ( $\mu\text{g}/\text{m}^3$ ) 0-1 Hours Following the Spill - 160 m<sup>3</sup> Spill
- Figure 9.6.13 Benzene – Average Ground Level Concentration in Air ( $\mu\text{g}/\text{m}^3$ ) 1-2 Hours Following the Spill - 160 m<sup>3</sup> Spill
- Figure 9.6.14 Benzene – Average Ground Level Concentration in Air ( $\mu\text{g}/\text{m}^3$ ) 2-3 Hours Following the Spill - 160 m<sup>3</sup> Spill
- Figure 9.6.15 Benzene – Average Ground Level Concentration in Air ( $\mu\text{g}/\text{m}^3$ ) 3-4 Hours Following the Spill - 160 m<sup>3</sup> Spill
- Figure 9.6.16 Benzene – Average Ground Level Concentration in Air ( $\mu\text{g}/\text{m}^3$ ) 4-5 Hours Following the Spill - 160 m<sup>3</sup> Spill
- Figure 9.6.17 Benzene – Average Ground Level Concentration in Air ( $\mu\text{g}/\text{m}^3$ ) 5-6 Hours Following the Spill - 160 m<sup>3</sup> Spill
- Figure 9.6.18 Benzene – Average Ground Level Concentration in Air ( $\mu\text{g}/\text{m}^3$ ) 6-7 Hours Following the Spill - 160 m<sup>3</sup> Spill
- Figure 9.6.19 Benzene – Average Ground Level Concentration in Air ( $\mu\text{g}/\text{m}^3$ ) 12-13 Hours Following the Spill - 160 m<sup>3</sup> Spill
- Figure 9.6.20 Benzene – Average Ground Level Concentration in Air ( $\mu\text{g}/\text{m}^3$ ) 24-25 Hours Following the Spill - 160 m<sup>3</sup> Spill
- Figure 9.6.21 Benzene – Average Ground Level Concentration in Air ( $\mu\text{g}/\text{m}^3$ ) 48-49 Hours Following the Spill - 160 m<sup>3</sup> Spill
- Figure 9.6.22 Volatiles – Maximum 1-hour Average Ground Level Concentration in Air ( $\mu\text{g}/\text{m}^3$ ) - 10 m<sup>3</sup> Spill
- Figure 9.6.23 Benzene – Maximum 1-hour Average Ground Level Concentration in Air ( $\mu\text{g}/\text{m}^3$ ) - 10 m<sup>3</sup> Spill

## FIGURES

- Figure 9.6.24 TEX – Maximum 1-hour Average Ground Level Concentration in Air ( $\mu\text{g}/\text{m}^3$ ) - 10 m<sup>3</sup> Spill
- Figure 9.6.25 Aromatics > C8-10 – Maximum 1-hour Average Ground Level Concentration in Air ( $\mu\text{g}/\text{m}^3$ ) - 10 m<sup>3</sup> Spill
- Figure 9.6.26 Aromatics > C10-12 – Maximum 1-hour Average Ground Level Concentration in Air ( $\mu\text{g}/\text{m}^3$ ) - 10 m<sup>3</sup> Spill
- Figure 9.6.27 Aromatics > C12-16 – Maximum 1-hour Average Ground Level Concentration in Air ( $\mu\text{g}/\text{m}^3$ ) - 10 m<sup>3</sup> Spill
- Figure 9.6.28 Aliphatics > C6-8 – Maximum 1-hour Average Ground Level Concentration in Air ( $\mu\text{g}/\text{m}^3$ ) - 10 m<sup>3</sup> Spill
- Figure 9.6.29 Aliphatics > C8-10 – Maximum 1-hour Average Ground Level Concentration in Air ( $\mu\text{g}/\text{m}^3$ ) - 10 m<sup>3</sup> Spill
- Figure 9.6.30 Aliphatics > C10-12 – Maximum 1-hour Average Ground Level Concentration in Air ( $\mu\text{g}/\text{m}^3$ ) - 10 m<sup>3</sup> Spill
- Figure 9.6.31 Aliphatics > C12-16 – Maximum 1-hour Average Ground Level Concentration in Air ( $\mu\text{g}/\text{m}^3$ ) - 10 m<sup>3</sup> Spill
- Figure 9.6.32 Aliphatics > C16-21 – Maximum 1-hour Average Ground Level Concentration in Air ( $\mu\text{g}/\text{m}^3$ ) - 10 m<sup>3</sup> Spill

## APPENDICES

- Appendix A H3D Theory
- Appendix B Diluted Bitumen Weathering Memos
- Appendix C Shoreline Retention Information
- Appendix D Burrard Inlet Spillcalc Validation
- Appendix E Stochastic Modelling Results
- Appendix F EBA's General Conditions



## **LIMITATIONS OF REPORT**

This report and its contents are intended for the sole use of Kinder Morgan Canada and their agents. EBA Engineering Consultants Ltd. does not accept any responsibility for the accuracy of any of the data, the analysis, or the recommendations contained or referenced in the report when the report is used or relied upon by any Party other than Kinder Morgan Canada, or for any Project other than the proposed development at the subject site. Any such unauthorized use of this report is at the sole risk of the user. Use of this report is subject to the terms and conditions stated in EBA's Services Agreement. EBA's General Conditions are provided in Appendix A of this report.

## 1.0 INTRODUCTION

EBA Engineering Consultants Ltd. operating as EBA, A Tetra Tech Company (EBA) was retained by Kinder Morgan Canada to conduct oil spill simulations on behalf of the Trans Mountain Expansion Project (TMEP). The TMEP involved an increase in the number of tankers calling at the Westridge Terminal to load dilute bitumen (such as Cold Lake blend, diluted with condensate). The number of vessel calls per month will increase from about 5 to 34. This report presents the results of the spill modelling investigations. The spill modelling uses a comprehensive approach: the release scenarios are based on a spill probability assessment conducted by DNV (ref); oil trajectories, weathering and shore contact are computed by the modelling system; the models are run in both stochastic and deterministic modes, and incorporate air dispersion; for selected cases, a full three-dimensional simulation is conducted, to evaluate the fate of dissolved components of the released oil, and oil-sediment interactions.

This report is organized as follows: Section 2 summarizes the spill characteristics based on the quantitative risk assessment conducted by DNV; Section 3 describes the hydrodynamic model that was used for the simulations, H3D; Section 4 describes the wave model, SWAN; Section 5 describes the spill model that was used, SPILCALC; Section 6 describe the air dispersion model CALPUFF that was used; Section 7 provides an overview of the simulations; Section 8 presents the results of the stochastic simulations; Section 9 presents the results from the deterministic modelling. Section 10 summarizes the key findings.

## 2.0 SPILL SCENARIOS

As described in Volume 8A, Section 5.2.2, the quantitative risk assessment (TERMPOL 3.15, Volume 8C) examined the risk of an accidental spill from a laden oil tanker carrying product loaded at Westridge Marine Terminal. Eight locations along the tanker transit route were selected as possible locations for a hypothetical accident involving a Project-related laden oil tanker and resulting in an oil spill. Four of the eight possible locations were selected for modelling the oil spill behaviour that is likely to be encountered in the marine environment:

1. Strait of Georgia, at the crossing of the route between Tsawwassen and Sidney (Location D);
2. Haro Strait, at Arachne Reef (Location E);
3. Juan de Fuca Strait, mid-channel off Race Rocks (Location G) and
4. Western Entrance of Juan de Fuca Strait, at Buoy J (Location H).

In addition to the marine sites, two hypothetical land-adjacent sites were selected, resulting in a spill in the surrounding waters:

1. Fraser River at Port Mann Bridge (Location FR); and
2. Westridge Terminal (Location A).

Figure 2.1.1 shows the locations of the different sites. The consequence of an oil cargo spill accident depends on the extent of the damage to the vessel's hull and the amount of oil that can spill from a ship.

The damage severity and oil outflow modelling for the marine sites shows that the 90<sup>th</sup> percentile worst case scenario is the loss of the entire contents of two cargo oil tanks to the sea, which gives an oil outflow of approximately 16,500 m<sup>3</sup> (DNV, 2013). Such an event is considered the credible worst case oil spill (CWC). The mean outflow volume (P<sub>50</sub>) is 8,250 m<sup>3</sup> for a marine spill. The large spill scenario at the Westridge Terminal was determined to be 160 m<sup>3</sup> and in the Fraser River 1,250 m<sup>3</sup>. For the Fraser River spill, a volume of 1,250 m<sup>3</sup> was considered based on pipeline failure simulations conducted by Dynamic Risk, as well as an estimated duration of the overland delivery to the river of 15 minutes. Table 2.1.1 summarizes the spill locations and volumes selected for the oil spill modelling.

**Table 2.1.1: Spill Locations**

Site	Spill location	Representative Incident	Spill Scenario	Volume Modelled
A	Westridge Terminal	Oil spill from loading operation or flow line damage.		large: 160 m <sup>3</sup> small: 10 m <sup>3</sup>
D	Main ferry route crossing	Possible collision with crossing traffic from Fraser River and ferries is a low probability event, but considered because of higher number of crossings per day.	Collision	P <sub>90</sub> : 16,500 m <sup>3</sup> P <sub>50</sub> : 8,250 m <sup>3</sup>
E	Northern Entrance to Haro Strait: Arachne Reef	Possible powered grounding is a low probability event due to pilots and tethered tug but this location is rated with greatest level of navigation complexity for the entire passage. Location also has high environmental values.	Powered Grounding	P <sub>90</sub> : 16,500 m <sup>3</sup> P <sub>50</sub> : 8,250 m <sup>3</sup>
G	Juan de Fuca Strait - South of Race Rocks	Possible collision with crossing traffic from Puget Sound and Rosario Strait or grounding at Race Rock is a low probability event, but considered because not all vessels in this location will have pilot onboard.	Collision	P <sub>90</sub> : 16,500 m <sup>3</sup> P <sub>50</sub> : 8,250 m <sup>3</sup>
H	Buoy J.	Possible collision between vessels approaching the confluence of the TSS at the entrance to Juan de Fuca Strait. It is a low probability event due to high oversight by MCTS and well established TSS.	Collision	P <sub>90</sub> : 16,500 m <sup>3</sup> P <sub>50</sub> : 8,250 m <sup>3</sup>
FR	Fraser River at Port Mann	Pipeline leak		large: 1,250 m <sup>3</sup>

For the four marine scenarios (i.e. Sites D, E, G and H), DNV estimated a spill rate of 25% of the total volume in the first hour, and the remaining 75% released at a uniform rate over the following 12 hours. For the loading scenario at the Westridge Terminal, a duration of 4 minutes was considered.

## 3.0 HYDRODYNAMIC MODEL: H3D

Surface currents for the oil spill simulations were hindcast using a proprietary three-dimensional hydrodynamic model, H3D. This model is derived from GF8 (Stronach et al. 1993) developed for Fisheries and Oceans Canada. H3D has formed the core of our consulting practice, and has been used on several extensive studies along the BC coast. An extensive application of an operational version of this model to the St. Lawrence Estuary is described in Saucier and Chassée (2000).

### 3.1 Description of H3D

H3D is a three-dimensional time stepping numerical model that computes the three components of velocity ( $u$ ,  $v$  and  $w$ ) on a regular grid in three dimensions ( $x$ ,  $y$  and  $z$ ), as well as scalar fields such as temperature, salinity and various introduced contaminants. A time stepping numerical model is one in which the period of interest (e.g., a year-long simulation of currents in the Salish Sea) is broken up into a number of small time intervals (e.g., 100 seconds each). The model then takes advantage of the fact that over a short time interval, known as a timestep, changes in currents, salinities, and other properties are small and can be computed in a rather simple fashion, suitable for coding in a numerical model. The timestep length is variable, depending on the maximum velocity present in the model at that particular timestep. During each timestep, values of velocity, temperature, and salinity are updated in each cell. Typically, for spill simulations, data are archived (i.e., saved to disk) every 15 minutes, so that a manageable amount of data was generated for subsequent spill tracking.

The spatial grid may be visualized as a number of interconnected computational cells collectively representing the water body. Figure 3.1.1 shows a schematic of a typical grid. Velocities are determined on the faces of each cell and non-vector variables, such as temperature or salinity, are situated in the centre of each cell. The selection of grid size is based on consideration of the scale of the phenomena of interest, the grid domain, and available computational resources.

In the vertical, the cells are usually configured such that they are relatively thin near the surface and increase in thickness with depth. The increased vertical resolution near the surface is needed because much of the variability (e.g., stratification, wind mixing, inputs from streams and land drainage) is concentrated near the surface.

H3D is a semi-implicit model, using the numerical scheme described in Backhaus (1983), and using a staggered Arakawa C-grid (Arakawa and Lamb 1977). It uses only two time levels, and computes internal and external modes at the same time. To allow for better simulation of features such as river plumes in conjunction with large tidal excursions, the number of layers is allowed to increase and decrease as water levels rise and fall. New layers are successively turned on as the water level rises, and are then allowed to drain as the water level falls. This feature allows river plumes that have vertical dimensions of 1 or 2 metres to be resolved in the presence of tidal ranges of 5 metres. This procedure has been shown to work well for simulations of the Fraser River as it enters the Strait of Georgia (Stronach et al., 2006).

The following sections describe further information on the inputs to and hydrodynamic characteristics of the model, as well as the model grids used for this investigation.

### **3.1.1 Hydrodynamic Grids**

The oil spill model SPILLCALC can make use of data from several hydrodynamic models simultaneously. For the stochastic simulations described in this report, four model implementations of H3D on different spatial grids were used. Figure 3.1.2 shows the domain of each model grid. Each model grid is described primarily in terms of its horizontal resolution and spatial coverage. A larger horizontal resolution allows a larger area to be covered with the same computing resources, but reduces the ability to resolve smaller-scale hydrodynamic processes. Where further hydrodynamic detail is required, additional model grids with finer horizontal resolution are nested inside the larger model, matching water level, velocity and hydrographic information at the boundaries but independently computing processes inside a smaller area, such as the Fraser River or Burrard Inlet in this case.

These models then provided current data for the spill model (SPILLCALC, see below) which tracks particles representing oil over the entire study area. For the three-dimensional deterministic simulations, only a single grid can be used, selected on the basis of spill location.

#### **3.1.1.1 Strait of Georgia 1 km Grid**

This model covers the entirety of the Strait of Georgia, Juan de Fuca Strait, Puget Sound, and a substantial part of the shelf off the entrance to Juan de Fuca Strait at a horizontal resolution of 1 km. It is driven at the boundaries by tidal and hydrographic data as discussed below. Information from this model provides boundary information for the three finer model grids. This model is validated by comparing tide heights at a number of locations, as well as by proxy in validations of the fine grids, as they could not match observations if their boundary conditions were not also correct.

The model ran from 1 January 2011 to 25 October 2012, archiving surface currents for SPILLCALC at 15 minute intervals starting in September 2011.

#### **3.1.1.2 Strait of Georgia 200 m Grid**

This model covers the Strait of Georgia between Point Grey at the north end and Point Roberts to the south. This grid provides detailed hydrodynamics on a 200 m grid in the region of the Fraser River plume and the wetting and drying of Roberts and Sturgeon Banks. This grid is validated by visually comparing performance at the boundaries with the 1 km model, and by observations of the Fraser River plume.

The model ran from September 2011 to October 2012, archiving surface currents for SPILLCALC at 15 minute intervals.

#### **3.1.1.3 Burrard Inlet 125 m Grid**

This model covers Burrard Inlet and English Bay at a resolution of 125 metres. It provides detailed hydrodynamics at First and Second Narrows as well as the region around the Westridge terminal. This model is validated by comparing modelled currents with those observed at a current meter offshore of the Westridge terminal.

The model ran from September 2011 to October 2012, archiving surface currents for SPILLCALC at 15 minute intervals.

#### **3.1.1.4 Fraser River Grid**

This model covers the Fraser River, from the Port Mann Bridge to the confluence with the Strait of Georgia. This is a curvilinear grid with grid cells that vary in size, but are nominally 50 m in the along-channel direction and 20 m in the cross-channel direction. This model has previously been validated in terms of water levels and sediment transport processes.

The model ran from September 2011 to October 2012, archiving surface currents for SPILLCALC at 15 minute intervals.

#### **3.1.2 Tides**

One of the principal driving forces is water level fluctuation, primarily tidal, derived from water level variations at the open boundaries of the model. Tidal fluctuations are computed from tidal constituents obtained from global tidal models (Schrama and Ray, 1994) and are applied to the open boundaries of the 1 km Strait of Georgia model. The other model grids obtain their tidal information from the relevant portion of the 1 km Strait of Georgia model. Tidal currents at the boundaries are generated by the model, and are the response of the basin to the fluctuating water levels on the boundaries.

#### **3.1.3 Winds**

Wind forcing causes both currents and water level differences. Consideration of wind forcing is also important because wind energy has a notable effect on vertical mixing, and therefore scalar distributions. Wind stresses acting at the water surface are derived from wind records collected from coastal Meteorological Service of Canada stations and moored buoys. Offshore winds from the North American Regional Reanalysis (NARR) were also used due to the scarcity of offshore observations. Winds from NARR matched the buoy data well, but did not accurately represent winds inland of Vancouver Island so were only used offshore. The raw or reanalysis data were processed into hourly time-series of over-water winds at the observation points, and then spatially interpolated inside H3D. For the Strait of Georgia models (1 km and 200 m), a simple inverse distance weighting scheme in H3D is used for the spatial interpolation of hourly wind data from the available locations. For Burrard Inlet, and the Fraser River, winds are first processed using CALMET and saved at a coarse grid of points, and then interpolated as required in H3D.

#### **3.1.4 Meteorology**

Besides winds, other meteorological data are also needed to compute heat flux into the waterbody and thus its temperature structure. In most applications, data are limited for calculating heat flux across the water surface. Reasonable estimates can be made from wind speed, wet bulb and dry bulb air temperatures, and cloud cover or insolation. These data are obtained from the Halibut Bank buoy, with the exception of cloud cover which was obtained from the Vancouver International Airport meteorological station. In the summer, heat input leads to increased temperature stratification. In the winter, when salinity stratification is often minimal, cooling can lead to static instabilities and overturning in the upper part of the water column. To treat winter cooling effectively, H3D includes a convective overturning mechanism, so that if, for example, the surface cell in a particular water column cools to the point that it is denser than the cell beneath it, H3D will vertically mix the water in these two cells, therefore propagating the cooling process downward. H3D's ability to simulate both summer heating and winter cooling has been rigorously verified in simulations done for freshwater lakes, where adequate temperature data is more routinely available over several years (Zaremba et al. 2005).

### **3.1.5 River Inputs**

The model incorporates inflows from 50 rivers and creeks throughout the model domain. These inflows contribute mass and momentum to the waterbody. The flow boundary condition is represented by a time-varying flow rate. Where available, all input river flows are generated from the daily hydrographs of the particular river under consideration. Where necessary, gauged rivers are supplemented with flows from nearby ungauged watersheds using basin area ratios.

### **3.1.6 Vertical and Horizontal Mixing**

Turbulence modelling is important in determining the correct distribution of velocity and scalars such as temperature and salinity. The diffusion coefficients for momentum and scalars at each computational cell depend on the level of turbulence at that point. H3D uses a shear-dependent turbulence formulation in the horizontal (Smagorinsky 1963) and a shear- and stratification-dependent formulation in the vertical for momentum, a procedure referred to as the Mellor-Yamada Level 2 scheme (Mellor and Yamada 1982), a local boundary layer simplification of the full turbulence closure model. These parameters have been shown to work well when simulating the annual cycle of salinity and temperature in the Strait of Georgia (Stronach et al. 2006) and also allowed a good calibration of the model against observed data. For scalars, such as salinity, constant horizontal eddy diffusivity is used, as well as vertical diffusivity and vertical eddy viscosity, to compute the spreading of the scalar.

### **3.1.7 Initial and Boundary Conditions**

The model is initialized with salinity and temperature fields obtained by interpolating observations archived at the Institute of Ocean Sciences. An initial condition of zero velocity is chosen, and the water level is initially set to mean sea level. The model is run in prognostic mode from this initial state, with the tide and wind being ramped up over one day. For the 1 km Strait of Georgia model, the first nine months of 2011 were used to ensure model stability and remove any start-up transients.

Oceanic boundary conditions for salinity and temperature were available via models maintained by the Alaska Ocean Observing System (AOOS). The AOOS developed and continues to maintain an implementation of the Regional Ocean Modelling System (ROMS) for the entire Gulf of Alaska. The southern boundary of this model domain is approximately 450 km south of the mouth of the Juan de Fuca Strait, and the AOOS provides and archives model predictions every 4 hours since early 2011. These data were downloaded and used to provide realistic boundary conditions to the 1 km Strait of Georgia implementation of H3D.

## **3.2 Validation of the Models**

The H3D model that forms the basis of the hydrodynamics has been extensively validated over the course of its ongoing development. Several validations relevant to the models used for oil spill simulations are described here.



### 3.2.1 Tidal Validation

The primary validation of an oceanographic model concerns the reproduction of observed tidal heights. Comparisons are made to four tide gauges at different locations in the 1 km Strait of Georgia model domain. Point Atkinson is a long-term tide gauge close to Vancouver and representing the central Strait of Georgia. Campbell River confirms that the models' northern boundary performs well. Victoria is on the other side of the Gulf Island from Point Atkinson and represents the Juan de Fuca Strait. Bamfield is on the Pacific coast of Vancouver Island and represents tides offshore. The model was compared to theoretical tide heights at all four gauges (Figure 3.2.1) and observed heights at Point Atkinson and Victoria (Figure 3.2.2). The figures show a representative month of modelled and theoretical or observed water levels. H3D reproduces the wide variety of tidal characteristics at different locations, from the mixed semidiurnal signals at Point Atkinson and Campbell River to the mainly diurnal tides at Victoria.

The statistical methods used to measure model performance are root-mean-square (RMS) error and a comprehensive 'model skill' equation (Equation 3.2.1). RMS error is presented in the same units as the original data and represents the magnitude of all errors over the entire predicted time period. Model skill, as defined by Wilmott et al. (1981), is a measure of the agreement between predicted and observed data, with a skill of 1 representing a perfect match. It differs from the statistical correlation statistic  $r$  or  $r^2$  in that a prediction that was perfect in magnitude but inverted in sign would still have a perfect  $r^2$ , whereas the skill would be negligible.

#### Equation 3.2.1 Model Skill

$$Skill = 100 \times \left( 1 - \frac{\sum |X_{Model} - X_{Data}|^2}{\sum (|X_{Model} - \bar{X}_{Data}| + |X_{Data} - \bar{X}_{Data}|)^2} \right)$$

**Table 3.2.1: Tidal Validation Statistics**

Tide Gauge	RMS Difference (m)	Model Skill
Point Atkinson	0.24	0.985
Campbell River	0.22	0.985
Victoria	0.19	0.969
Bamfield	0.10	0.995
Point Atkinson (observed)	0.23	0.986
Victoria (observed)	0.22	0.958

Modelled tide heights are generally within 0.2 m at all stations, with excellent reproduction of variations in tidal patterns throughout the modelled regions.

### 3.2.2 Current Meter Validation

Current meter data collected as part of the Westridge terminal design was used to validate the Burrard Inlet implementation of H3D, and by proxy the 1 km model which provided the boundary conditions for the finer grid. The two-month record of current meter data is described in more detail in EBA (2013a). The along-channel component of the near-surface currents was compared with currents at the same location in the 125 m Burrard Inlet model. Figure 3.2.3 shows this comparison for the month of April 2013, as well as the winds recorded at the Westridge terminal and the difference between modelled and observed currents. The phase and magnitude of the currents were well-predicted. The RMS difference in current speed was 5.8 cm/s, and the model skill was 0.947. This comparison shows that currents, an important driver of oil spill movement, were well-simulated in the region of the Westridge terminal and, by extension, elsewhere in the Burrard Inlet model. It also helps to validate the 1 km Strait of Georgia model which provided the boundary conditions for the 125 m model.

### 3.2.3 The Bob Lord Drift

Late on July 25, 1993 Bob Lord fell from a BC Ferries vessel transiting between Active Pass and Tsawwassen. He subsequently spent eight hours drifting until picked up near Orcas Island by a fishing vessel. Throughout his ordeal Mr. Lord was conscious and aware of his position in relation to Galiano Island, Mayne Island and Saturna Island. Based on his observations of the night of July 25<sup>th</sup>, Mr. Lord has recreated his likely drift path for verification of CANSARP and testing of leeway factors. [CANSARP, Canadian Search and Rescue Program, is a software product developed under Dr. Stronach's direction while he was employed by Seaconsult Marine Research Ltd. Material in this section is derived from an unpublished Seaconsult report to the Canadian Coast Guard.]

The key events noted by Bob Lord are summarized in Table 3.2.2 below. The likely drift path is plotted in Figure 3.2.4. The greatest uncertainty is associated with the initial location. The time that Mr. Lord fell from the ferry is quite accurate; however, the ferry's actual position at that time has not been confirmed. Notable features of the drift include the initial sweep toward Active Pass on the falling tide, followed by the steady southward drift for about six hours, the patches of warm and cold water in Boundary Pass, indicating strong vertical mixing, and the final period of meandering motion near Sucia Islands in US waters just before he was picked up.

**Table 3.2.2: Summary of Bob Lord's Drift**

Time (PDT)	Event
93/07/25 11:15	Fell from BC Ferry about 5-6 km east of Active Pass
93/07/26 00:30 – 01:30	Observed 2 shore lights & flashing white light, also a tower with 3 red lights. Suspect position within 0.5 km of Gossip Island
93/07/26 02:30 - 03:00	Sighted two empty freighters moving south, second freight passed within 1 km
93/07/26 Shortly before first light	12" to 18" waves in area of tide rips about 4-5 km NE of East Point

**Table 3.2.2: Summary of Bob Lord's Drift**

Time (PDT)	Event
93/07/26 First light	Felt cold and warm patches of water, changing rapidly about 2 km E of flashing green light on a line with Alden Pt., Patos I.
93/07/26 Sunrise	8" to 12" waves in tide rips about 1.5 km W of Alden Pt.
93/07/26 06:00 – 07:15	Drifting slowly about 2-3 km SSW of Sucia Is.
93/07/26 07:15	Picked up by a fish boat about 2 km SSW of Sucia Is.

Two different approaches were used to compute Mr. Lord's drift. First, a traditional method, relying on currents from harmonic constants plus wind leeway plus an estimate of wind-driven currents was used. The specific software package was CANSARP, a Search and Rescue system developed by Seaconsult Marine Research Ltd. with funding by the Canadian Coast Guard. The simulation process in CANSARP is similar to procedures used in SPILLCALC. The second method used a full three-dimensional model to compute currents. The specific program was GF9, a pre-cursor to H3D, the model used for the Trans Mountain simulations. Mr. Lord's drift was then computed using SPILLSIM, which had a similar Monte Carlo particle tracking algorithm to SPILLCALC. All models were run using the standard data inputs available to them, and without any specific tuning to improve their simulation of Mr. Lord's drift.

### CANSARP Results

The drift path computed by CANSARP is shown in Figure 3.2.5. Because CANSARP is a Search and Rescue program, the results are expressed in a circular computed search area, the envelope of several smaller search areas, each of which represents the drift under a range of wind leeway and direction offsets. It can be seen that the computed drift is about half as long as the actual drift.

### SPILLSIM Results

The drift path computed by SPILLSIM is shown in Figure 3.2.6. Because SPILLSIM is an oil simulation model, the results are presented in terms of a surface slick, which maps out the highest probability area for finding the drifting object, in this case Mr. Lord. The recovery point is almost exactly in the middle of the computed drift pattern.

### Summary

It is clear from these results that the calculations with the full three-dimensional model were able to reliably hindcast Mr. Lord's drift, but methods relying on stored harmonic constants plus winds, for instance, estimated a drift track that was only half of what actually occurred. The reason is that the full hydrodynamic model included all processes, and that the relaxation currents following the strong southerly winds on the day preceding Mr. Lord's drift were a major factor in determining currents over the course of his drift.

## **4.0 WAVE MODEL: SWAN**

The oil spill model, SPILLCALC, requires wave conditions as an input to its weathering processes. Wave conditions for the simulation period were hindcast using SWAN version 40.72 (Simulating Waves Nearshore; Booij, 2006). For consistency with the hydrodynamic inputs, wave conditions were simulated on the same set of computational grids. Further details are provided below.

### **4.1 Description of SWAN**

SWAN is a third-generation wave model for obtaining realistic estimates of wave parameters in coastal areas, lakes, reservoirs and estuaries from given wind and bottom conditions. SWAN utilizes a finite difference scheme to compute random, short-crested wind generated waves. SWAN incorporates physical processes such as wave propagation, wave generation by wind, whitecapping, shoaling, wave breaking, bottom friction, sub-sea obstacles, wave setup and wave-wave interactions in its computations. It is thus well-suited to computing a wave field as it propagates from the Pacific into the Strait of Georgia, Burrard Inlet and the Fraser estuaries.

### **4.2 Model Configuration: Strait of Georgia 1-km Grid**

This implementation of SWAN used the same computational domain and bathymetry as the corresponding hydrodynamic model. The wind inputs were also the same as those used in H3D. Wave boundary conditions along the southwest and northwest edges of the domain were taken from the La Perouse Bank and South Brooks wave buoys. These buoys do not record wave direction. Therefore, to best agree with the wave directions observed at Neah Bay, boundary waves were assumed always to come from the west.

The model ran from September 30, 2011 to October 25, 2012, archiving significant wave height and peak period in each model cell on an hourly time step.

### **4.3 Model Configuration: Strait of Georgia 200-m Grid**

This implementation of SWAN used the same computational domain and bathymetry as the corresponding hydrodynamic model. The wind inputs were the same as those used for the 1-km SWAN model. Wave boundary conditions along the north and south edges of the domain were taken from the 1-km SWAN model.

The model ran from September 30, 2011 to October 25, 2012, archiving significant wave height and peak period in each model cell on an hourly time step.

### **4.4 Model Configuration: Burrard Inlet Grid**

This implementation of SWAN used the same computational domain and bathymetry as the corresponding hydrodynamic model. The wind inputs were also the same as those used in H3D. Wave boundary conditions along the west edge of the domain were taken from the Halibut Bank wave buoy.

The model ran from September 30, 2011 to October 18, 2012, archiving significant wave height and peak period in each model cell on an hourly time step. Additionally, for the SPILLCALC validation in July 2007 the model ran from July 20 to August 4, 2007.

## 4.5 Model Configuration: Fraser River Grid

This implementation of SWAN used the same computational domain and bathymetry as the corresponding hydrodynamic model. The wind inputs were also the same as those used in H3D. Wave boundary conditions along the west edge of the domain were taken from the Halibut Bank wave buoy.

The model ran from September 30, 2011 to October 18, 2012, archiving significant wave height and peak period in each model cell on an hourly time step.

## 5.0 OIL SPILL MODEL: SPILLCALC

### 5.1 Overview

SPILLCALC is a timestepping model that computes the motion and weathering of liquid hydrocarbon spills. It can be implemented in one of two different versions: a stand-alone version and a version embedded within the hydrodynamic model H3D. The stand-alone version contains interfaces to the output from one or more H3D circulation models, and can access data from these grids simultaneously, depending on spill location. For the simulations reported herein, data from four hydrodynamic models were used: the 1 km resolution Regional Model of the Strait of Georgia-Juan de Fuca – Puget Sound system, extending out onto the shelf at the western end of Juan de Fuca; a 125 m resolution model of Burrard Inlet and English Bay; a 200 m resolution model of the south-central Strait of Georgia, roughly from Tsawassen to Point Grey and including Roberts and Sturgeon Banks, and a 50 m x 20 m resolution model of the Fraser River. The Fraser River grid is curvilinear, to better follow the configuration of the river. For the three-dimensional deterministic simulations, only a single grid can be used, selected on the basis of spill location.

SPILLCALC uses currents from these models to move the spill. Oil released on the water surface is represented as a large number of independent floating particles, referred to as “slicklets” in this report. Individual slicklets are not intended to be physically meaningful, but they do carry significant information regarding their aliquot of the total spill, such as age, density, and fractions lost to evaporation, dissolution and shore contact. The cloud of particles as a whole represents the area covered by the spill, and its progress is the spill’s dispersion and trajectory. SPILLCALC uses a timestep appropriate to the grid size and drift velocities. To adequately resolve the slick movement and shore contact a 500 m resolution grid was used for spills in the marine waters, while a 125 m grid was used for spills in Burrard Inlet, and a 100 m grid was used for spills in the Fraser River.

The key processes determining the fate of slicklets are:

- Advection, based on surface currents obtained from H3D;
- Wind stress, using winds interpolated from several stations over the Strait of Georgia and Juan de Fuca Strait;
- Eddy diffusion by oceanic turbulence, simulated through the Monte Carlo method as a random velocity component;
- Shoreline retention; and
- Weathering.

These components are described in detail in Section 5.2. A validation of SPILLCALC against observations of the 2007 accidental hydrocarbon release at Westridge Terminal is presented in Section 5.3.

## 5.2 Input and Data Forcing

### 5.2.1 Particle Properties

The following attributes are associated with each particle:

- Location (latitude, longitude);
- Status: “unreleased”, “on water” or “on land”;
- Volume: quantity released as represented by the particle;
- Age: time since release;
- Tar ball: formed or not;
- Density;
- Depth;
- Amount evaporated;
- Volume dispersed; and
- Pseudo-component fractions.

For each timestep, the particles are moved according to the algorithms outlined below. All the particles begin the simulation at the release location with a status of “unreleased” and an initial volume of “V/N”, where “V” is the total volume of oil to be released and “N” is the number of particles.

### 5.2.2 Transfer of Oil to the Water

Between the start and end times of the release, particles are continuously introduced at the release location. The number of particles released at each timestep is calculated from the particles’ volumes and the release rate. As each particle is released, its status is switched from “unreleased” to “on water”. Particles begin to move with the timestep immediately following their release.

When oil is released in a large quantity over a short time, it spreads rapidly under the influence of gravity. It is assumed that the oil released over one timestep spreads instantaneously to a thickness of 2 centimetres. To represent this spreading, the particles are initialized with positions randomly assigned in a circular zone centered at the release location.

If the current speed is insignificant, the initial diameter of the spill can be computed based on the spill volume and thickness as follows:

$$D = \sqrt{\frac{4V}{\pi t}}$$

Where: “D” is the diameter

“V” is the volume of released oil

“t” is the initial thickness of the slick (2 centimetres).

If the current is significant, the spill is dragged to a longer, narrower streak, with a width given by:

$$D = \frac{Q}{U_t}$$

Where: “Q” is the oil flow rate

“U” is the local surface current speed.

The diameter (“D”) is taken as the lower value of that determined by the two methods. Particles are initialized at random positions within a radius of “D/2” from the release site.

Due to this spreading, which involves an initial displacement from the release site, some particles may contact land immediately, depending on their release site. As the particles are initialized, those that would contact land are stopped at the shore and deactivated, following the process described below.

### 5.2.3 Calculation of the Particle Velocities

In the stochastic modelling, the spill trajectory is updated every timestep, with timesteps ranging from 30 seconds to 300 seconds, depending on the grid size and water currents. At each timestep, particle positions are updated as follows. Each particle “on water” is assigned a velocity, the sum of three components. The first component of a particle’s velocity is a result of currents at the water surface. In the absence of wind and diffusion, a particle’s velocity exactly matches the current; that is:

$$\vec{V}_{Oil, advection} = \vec{V}_{current}$$

No provision is made for internal forces in the spill, such as the initial gravity-dominated spreading, since the spatial zone in which internal forces would be significant is quite small compared to the area reached by the spill as it evolves.

The second component is a result of the wind force against the oil surface, often referred to as the “leeway”. This component is expressed as a fraction of the wind speed, taken to be 1% for this study, as follows:

$$\vec{V}_{Oil, wind\ shear} = 0.01 \vec{V}_{wind}$$

The final component is a random velocity, representing diffusion, as follows:

$$\vec{V}_{Oil, diffusion}$$

It is uniformly distributed and each of the “U” and “V” components has a value of:

$$RAND \times \sqrt{6D/dt}$$

where “D” is the eddy diffusion coefficient specified in the model input, “dt” is the model timestep and “RAND” is a random number between –1 and 1. This component has the effect of increasing the spill’s area. By random diffusion alone, the release’s statistical radius increases as the square root of time, as follows:



$$\sqrt{\frac{1}{N} \sum_N (x - \bar{x})^2 + (y - \bar{y})^2} \cong \sqrt{2Dt}$$

In practice, shear in the horizontal velocity field, especially in the Fraser River plume and regions in the Gulf and San Juan Islands, is responsible for even greater spreading than that arising from eddy diffusion alone.

Each particle's velocity is computed as the vector sum of its three components, as follows:

$$\vec{V}_{Oil} = \vec{V}_{Oil: advection} + \vec{V}_{Oil: wind} + \vec{V}_{Oil: diffusion}$$

The correct operation of the above three terms was checked for simple cases, where the outcome could be predicted analytically: steady currents, steady wind, and comparisons with the analytical solution of the diffusion equation for an instantaneous release. The methods described above are standard and, for instance, are used in commercial models such as OilMAP™ (developed by Applied Science Associates, Inc.). A similar procedure, excluding the wind "leeway" but adding a sinking velocity, was also used in a sediment transport simulation of Howe Sound (Stronach et al., 1993b).

#### 5.2.4 Calculation of New Particle Positions

A potential new position is calculated for each particle on water, as follows:

$$\vec{X}_{new} = \vec{X}_{old} + \vec{V}_{Oil} dt$$

The model then checks whether the oil particle would have to cross any shoreline segment to reach its new position. If it would, the particle is left in its previous position and some or all of its volume may be transferred to the shore, according to that shore's oil retention capacity. If it would not reach or cross the shoreline, the particle is moved to the new position.

#### 5.2.5 Transfer of Oil to the Shoreline

Each segment of shoreline can retain a certain maximum volume of oil. Whenever a particle's new position would bring it in contact with the shore, the shoreline is checked to determine if it has reached its full retention capacity. If it has, the status and volume of the particle remain unchanged. If the shoreline is below capacity, some volume of oil is transferred from the particle to the shore.

If the remaining capacity of the shoreline segment is greater than the particle's volume, the entire volume is transferred to the shore and the particle's status is switched to "on land". Otherwise, the remaining capacity of the shoreline segment is filled, the particle's volume is reduced correspondingly, and its status remains "on water". Once oil is "on land", it is held there for the remainder of the simulation, because the spill model does not allow the tide or waves to move it back onto the water. Furthermore, the model does not compute the evaporation of oil once it has contacted land, either through shore retention or stranding in intertidal areas during a falling tide.

SPILLCALC uses a shoreline provided by Coastal and Ocean Sciences (Methods for Estimating Shoreline Oil Retention, in Volume 8B). The shoreline is based on British Columbia and Washington State databases, and includes not only shore location, but also coastline type, and a value for oil retention. Oil retention was calculated based on shore types and the known properties of diluted bitumen – especially its relatively high viscosity.

### 5.2.6 Properties and Weathering of Diluted Bitumen

The main difference between oil sands deposits and those from the rest of the western Canadian sedimentary basin is that oil sands hydrocarbons formed nearer to the surface. In doing so they were subject to more microbial activity - most of the lighter fractions in these deposits, characterized by fewer carbon atoms in their molecules, lower densities and higher vapour pressures have been digested by microbes. What remains are the heavier fractions that result in the denser more viscous crude oil known as bitumen.

Once sand and water have been removed from extracted oil sands deposits, the remaining bitumen is too dense and viscous to meet pipeline specifications, so it is mixed with diluent. Typical diluents are natural gas condensate (light oil recovered from natural gas production) and synthetic crude oil (partially refined bitumen). In effect the diluent is added to replace the light hydrocarbons lost from microbial degradation of the oil sands. Adding diluent creates a stable homogeneous mixture that behaves in a similar manner to other natural crude oils.

Bitumen that has not been diluted is denser than water, while diluent is lighter than water. When the diluent is blended with the bitumen, resulting in a product known as diluted bitumen or “dilbit”, its relative density is 0.94. Properties of both the undiluted bitumen and the dilbit are regularly reported on [www.crudemonitor.ca](http://www.crudemonitor.ca). Dilbit is expected to form a large proportion of the crude oil shipped from the Westridge Marine Terminal once the Project is in operation.

In May 2013, Trans Mountain conducted applied research (Gainford study, Polaris and WCMRC, 2013) on the fate and behaviour of dilbit in a marine environment. The Gainford study included a weathering test of dilbit spilled in a marine environment over a 10-day period. That study and other tests have shown that, like other crude oils, while the density increases as the lighter components evaporate, the rate at which this occurs diminishes as the density and viscosity of the oil increases. Although the relative density of the dilbit observed in the Gainford study reached that of fresh water, it took 8-10 days for this to happen. No evidence of sunken or submerged dilbit in the marine environment simulated for the tests was observed during the Gainford study.

Typically, once released into the marine environment all hydrocarbons begin to “weather” and after a period of time can submerge or begin to sink. When released into water lighter components of hydrocarbons will begin to evaporate, some will dissolve into the water column, and the remainder will float as long as the density of the remaining oil is less than the density of the water into which it was released. Wave action can cause water-in-oil emulsions which will drive the mixture towards neutral buoyancy. Adhesion to bottom sediment (e.g., beaches, riverbeds) or other sinking material can cause the oil to be submerged. These are the mechanisms that caused some of the oil released in the Enbridge Kalamazoo spill to submerge in the river. The question then, especially for heavier oils like dilbit, is about the weathering process and the mechanisms which can cause it to submerge or sink.

To support the discussion of dilbit properties and behaviour in the marine environment, it is worth describing briefly the chemical composition of the dilbit that will be shipped. Like other crude oils, dilbit is a mixture of many hydrocarbon species. Characterizing the oil by its pseudo-component composition facilitates the calculation of the effects of weathering on dilbit in the marine environment, and the analysis of toxicity of the various fractions that enter the receiving environment once the oil is spilled. Whereas a product such as crude oil contains many chemical species (e.g., benzene, heptane, octane, etc.), a pseudo-component is a group of these chemical species with relatively similar properties (e.g. aromatics with carbon numbers 6 to 10). The Canada Wide Standard for Petroleum Hydrocarbons (CCME 2008) describes a method for characterizing hydrocarbons from a toxicity point of view using four fractions: F1 to F4. Each fraction (or pseudo-component) represents a range of carbon atoms in the molecule. For example, F1 represents the C6 to C10 band. Sub-categories of aromatics and aliphatics are also recognized in the Canada Wide Standard (CWS).

Based on these considerations, the Project environmental assessment team developed a pseudo-component description with greater resolution (smaller ranges of carbon numbers in each fraction). Three additional components were added to this list of 14 pseudo-components: C34 and greater, resins and asphaltenes. These two additional pseudo-components account for about 28% of the oil mass, but have limited solubility, very high boiling points, and hence limited evaporability, and are generally not significant toxicologically. However, they represent a significant part of the molar composition of the oil, which influences the evaporation and dissolution rates of the lighter fractions through Raoult's Law. These two heavier fractions also figure prominently in the formation of tar balls, making them important for the overall simulations.

Table 5.1 is the pseudo-component description of a Cold Lake Winter Blend bitumen sample, using the pseudo-component categories adopted for this project (Sample BG5490, collected February 19, 2013 at the Westridge Terminal). This composition was used for the modelling simulations described later in this report. The selection of this particular dilbit as a suitable representative product is discussed in Volume 8 of the Application.

**Table 5.2.1: Pseudo-Components and Properties**

Pseudo-Component	Description	Concentration (mg/kg)	Molar Fraction	Molar Weight (g/mol)	Vapour Pressure (Pa)	Water Solubility (mol/m <sup>3</sup> )	Effective Density @ 25°C (kg/m <sup>3</sup> )
VOL	Volatiles	72,310	2.55E-01	70.8	9.98E+04	2.28E+00	612
AR1	Benzene	1,800	5.76E-03	78.1	1.27E+04	2.28E+01	867
AR2	TEX	7,870	1.98E-02	99	2.47E+03	2.05E+00	860
AR3	Aromatics >C8-C10	3,000	6.25E-03	120	1.27E+03	3.90E-01	866
AR4	Aromatics >C10-C12	4,100	7.88E-03	130	4.14E+00	2.35E-01	888
AR5	Aromatics >C12-C16	22,000	3.66E-02	150	8.72E-03	1.10E-01	1,156
AR6	Aromatics >C16-C21	47,000	6.18E-02	190	2.13E-05	3.10E-02	1,235

**Table 5.2.1: Pseudo-Components and Properties**

Pseudo-Component	Description	Concentration (mg/kg)	Molar Fraction	Molar Weight (g/mol)	Vapour Pressure (Pa)	Water Solubility (mol/m <sup>3</sup> )	Effective Density @ 25°C (kg/m <sup>3</sup> )
AR7	Aromatics >C21-C32	120,000	1.25E-01	240	9.16E-08	3.17E-03	1,216
AL1	Aliphatics >C6-C8	55,000	1.37E-01	100	6.38E+03	1.42E-01	695
AL2	Aliphatics >C8-C10	20,000	3.84E-02	130	6.38E+02	1.45E-02	721
AL3	Aliphatics >C10-C12	16,000	2.50E-02	160	6.38E+01	1.48E-03	740
AL4	Aliphatics >C12-C16	40,000	5.00E-02	200	4.86E+00	5.51E-05	765
AL5	Aliphatics >C16-C21	46,000	4.26E-02	270	1.11E-01	2.70E-07	781
AL6	Aliphatics >C21-C32	60,000	3.84E-02	390	2.59E-06	6.31E-12	8000
RES	F4 >C34-C50+	110,000	4.82E-02	570	1.00E-10	5.25E-15	998
RES2	Resins	294,920	8.93E-02	825	1.00E-10	9.55E-08	1008
RES3	Asphaltenes	80,000	1.25E-02	1599	1.00E-10	3.24E-16	1166

## 5.2.7 Weathering Processes in SPILLCALC

The following sections provide details on the weathering processes included in SPILLCALC.

### 5.2.7.1 Evaporation

In SPILLCALC, there are two mechanisms to specify the evaporation process. First, there is the fairly standard mass transfer approach of calculating the mass flux based on wind speed, equilibrium pressure for the constituent and molar concentration of the constituent in the total product. This method is used in ADIOS2. However, SPILLCALC includes an additional mechanism, the effect of the slow rate of molecular diffusion within diluted bitumen. Molecular diffusion is responsible for bringing the lighter fractions from within the dilbit layer to the evaporating surface to replace the losses due to evaporation. In general the rate of molecular diffusion through the vertical extent of the slick is slower than the rate of evaporation from the surface, so the controlling mechanism is the internal diffusion process.

The two processes interact in SPILLCALC. Surface evaporation proceeds using the standard formulas; however the concentration of the evaporating constituent is limited by the concentration that the diffusion process delivers at the surface of the slick. The slower of these two rates determines the rate of evaporation. The diffusion coefficient used was similar to those reported by Afsahi and Kantzas (2006) for pentane diffusion in Cold Lake bitumen, but was adjusted slightly to values that would reproduce the Gainford results, as described in a Technical Memo provided in Appendix B. Figure 5.2.1 shows the

simulation of the observed density in the Gainford static Cold Lake Winter Blend Bitumen test. The density of the oil is a relatively sensitive indicator of the amount of evaporation; the faster evaporation occurs, the faster the density will increase. The near-exact reproduction of the rate of change of density in Figure 5.2.1 is a strong indicator that the dilbit's reluctance to sink in brackish waters is supported by a reasonable theoretical explanation.

#### **5.2.7.2 Vertical Dispersion and Resurfacing**

Breaking waves drive small droplets of the oil into the water column. Depending on the natural turbulence in the water and the size and density of the droplets, the dispersed oil will generally stay suspended in the water column and will be prevented from resurfacing as long as the dispersing mechanism, breaking surface waves, remains active. When wind and waves die down, the dispersed oil will generally rise to the surface. The process of vertical dispersion has been implemented in SPILLCALC using equations developed by Delvigne and Sweeney (1988), which are also used to compute dispersion in the NOAA ADIOS2 model. The process of resurfacing was implemented in SPILLCALC using the equations developed by Tkalic and Chan (2002). A unique feature of SPILLCALC is that the wave field was generated by a reliable and widely used wave model SWAN, whereas most spill models estimate waves from wind speed and fetch. The use of SWAN provides much more realistic wave energy for computing vertical dispersion.

The dispersion process is a function of wind speed, wave height, the fraction of waves that are breaking, and the size of the droplets.

As suggested in ADIOS2, the size of the droplets has been set to 70 microns, which is the criterion for a droplet to stay inside the water column because of natural turbulence. Droplets larger than 70 microns will resurface in less time than it takes for the surface spill to move.

In the ADIOS2 formulation, dispersion is set to zero for wind speeds less than 5 metres per second, reflecting the absence of breaking waves at low wind speeds. A similar procedure is used in SPILLCALC for the dispersal of oil into the water column. However, unlike ADIOS2, and to provide a more realistic simulation, a continuous process of bubble rise is included in SPILLCALC. Under strong wind and wave conditions, the sinking mechanism dominates, and under weak wind and wave conditions, the bubble rise mechanism dominates (Tkalic and Chan, 2002).

In SPILLCALC, the horizontal and vertical position of each dispersed oil particle is updated at each timestep. Two modes of implementation are operative. In the stand-alone version of SPILLCALC, it is assumed that the oil is uniformly dispersed in a 2 metre thick layer of water, and moves according to the surface currents provided by H3D. Since the surface slick moves according to surface currents, diffusion and a wind leeway, the two oil compartments (i.e., on the surface and dispersed) do not travel together, becoming spatially separated, especially during periods of strong winds. Oil that was dispersed and then rises can undergo evaporation as soon as it reaches the surface. Because strong winds do not occur continuously in both Straits, it was found that oil which was dispersed into the water column generally started to rise shortly after the wind event died down, and that the rate of evaporation generally kept up with the rate of rise; oil that was dispersed into the water column was only passing through a transient state on its way to its ultimate fate, evaporation.

For the version of SPILLCALC that is embedded in H3D, the slicklets representing the dispersed oil are assumed to be driven to the dispersal depth by breaking wave action, and then travel with the currents at that depth. The assumption of a 2 m thick layer into which the oil droplets can disperse is thereby relaxed, although, there appeared to be no occasions in which the depth of dispersal was greater than 2 m.

#### **5.2.7.3 Oil Sinking**

The density of each particle is updated on a timestep basis, using the concentration and density of each pseudo-component. When the density of one oil particle becomes greater than the ambient water density, the particle sinks until it reaches an equilibrium depth. The deterministic simulation, with SPILLCALC embedded into the circulation model H3D, computes the horizontal and vertical advection of the sunken oil particle. The sunken particle will move based on currents, turbulence and density of the surrounding waters.

#### **5.2.7.4 Contact with Beach and Intertidal Areas**

A potential issue of concern is the extent to which oil would come into contact with intertidal sand and mud flats and adversely affects benthic invertebrates and bio-films. In addition to entering beach and mud flat sediment via the shore contact process, SPILLCALC contains an algorithm to simulate stranding of oil as water levels fall below the level of the beach or sand flat in a model cell. The algorithm used assumed that all the oil on the water surface in a particular cell would be transferred to the sediment on a falling tide, once the water depth dropped below 2 centimetres. No provision was made to re-float the trapped oil on a rising tide. This procedure is likely to overestimate the amount of oil that is stranded, and hence overestimates the amount of oil trapped in the intertidal zone. Despite that shortcoming, it was found during preliminary testing that virtually no oil was deposited on Roberts or Sturgeon Banks during a typical scenario: oil entered the banks on a rising tide, and left on a falling tide, but in such a way that there was always more than 2 cms depth of water between the oil and the intertidal flats. As a test, a simulation was done whereby oil was released continuously over the month of March 2002 at Sand Heads. Virtually no oil was found to be trapped on either Roberts or Sturgeon Bank.

#### **5.2.7.5 Small-Scale Spreading**

In addition to the vertical diffusion within the slick, the area covered by the slick plays a major role in the evaporation subroutine. A spreading experiment which was conducted at the WCMRC facility showed that the lateral spreading of the oil is limited and that a minimum thickness is observed. This minimum thickness is 0.4 mm, as described in the Spreading Observation Memo, Appendix B of the Technical Report. As a result, a reduced “effective” area was used in the evaporation process, based on the volume of oil in one cell and the minimum thickness it can reach. The ratio of the effective area to the total cell area ranges from 0 to 1. At the beginning of the simulation, the effective area is very close to the cell area, since the oil slick generally thicker. As time goes by, the effective area becomes smaller, representing the patchiness developing in the slick, and thereby reducing the rate of evaporation.



#### 5.2.7.6 Oil-Sediment Interaction

The formation of oil-mineral aggregate is another process that can affect the behavior of an oil slick. In river and estuary areas, where the fine sediment load is usually higher than the one in the ocean, the interaction between oil and fine sediment is crucial in assessing the impact of a spill on the environment.

The method used in the SPILLCALC model follows the same approach as in the NOAA ADIOS2 model. The approach was proposed by J.R. Payne in 1987 (Integration of Suspended Particulate Matter and Oil Transportation Study) and incorporates the effect of water turbulence.

The oil spill model, SPILLCALC, uses time-varying wave data computed by SWAN and time-varying sediment concentration computed by H3D to calculate the interaction of oil with sediments, making it difficult to reproduce laboratory conditions.

The calibration and the validation of the SPILLCALC oil-sediment interaction module was conducted using data reported by Khelifa, Fingas and Brown (2008). The rate of energy dissipation in the breaking wave field was used in place of the mechanical agitation energy in the reported experiments. Good agreement was obtained using the SPILLCALC formulation in a hindcast of these experiments, as shown in Figure 5.2.2. The technical memo describing the calibration and the validation is located in Appendix B.

#### 5.2.7.7 Emulsification

Emulsification is a process whereby oil and water co-mingle and form an emulsion, usually requiring wave energy to mix the two liquids. The emulsification process can be qualitatively seen as the opposite of the vertical dispersion process; during oil emulsification, oil takes up water to form the emulsion, whereas during vertical dispersion, the oil droplets are driven down and mixed in the water column.

The formation of emulsions can change the properties and characteristics of the oil drastically. Depending on the state of the emulsion (stable, meso-stable or unstable), the volume of the slick may be up to 80% water, thus expanding the volume of the slick by several times (Xie et al., 2007)

The formulas used by SPILLCALC for the water uptake and the emulsion stability were proposed by Mackay et al. (1980) and Mackay and Zagorsky (1982) respectively. Amongst others, the emulsification has a strong impact on the evaporation process. The inhibition of evaporation rises with increasing water content and slick thickness. SPILLCALC follows the method developed by Ross and Buist (1995); evaporation is assumed to have a linear relationship with the water content.

#### 5.2.7.8 Dissolution

Some of the lighter hydrocarbon fractions are soluble in water; they will dissolve in the underlying water column. The solubility of the pseudo-components are given in Table 5.3.6. The potential for dissolution is a function of the pure component solubility, the mole fraction of the hydrocarbon and the mass transfer coefficient. The rate of dissolution is computed according to the equation published by MacKay and Leinonen (1977) and uses their value for a mass transfer coefficient:  $2.36 \times 10^{-6}$  m/s.

This flux is applied as a loss to the oil slick, in a similar manner to the evaporation process. In order to compute concentrations in the water column of these lighter fractions, some of which are quite toxic, SPILLCALC is operated within the hydrodynamic model H3D. The flux from the oil slick enters the top layer



of H3D, and is then acted on by the same processes of advection and diffusion that apply to all the other scalars, such as temperature and salinity. This method is applicable to a three dimensional simulation of the dissolved oil in the water column.

In the two-dimensional SPILLCALC implementation, the same mass transfer equation is used, but since the two-dimensional model does not keep track of concentration in the water column, SPILLCALC assumes that concentration to be zero, which leads to a somewhat higher mass transfer rate.

#### 5.2.7.9 Bacterial Decay

Despite its toxicity, a considerable fraction of petroleum oil entering marine systems is eliminated by the hydrocarbon-degrading activities of microbial communities, in particular the so-called hydrocarbonoclastic bacteria (HCB). *Alcanivorax borkumensis* is one of the HCB family and is an alkane-degrading marine bacterium which naturally propagates and becomes predominant in crude-oil-containing seawater when nitrogen and phosphorus nutrients are supplemented. They are currently thought to be the world's most important oil-degrading organisms.

The biodegradability of the oil components generally decreases in the following order: n-alkanes, branched-chain alkanes, branched alkenes, low molecular-weight n-alkyl aromatics, mono-aromatics, cyclic alkanes, polycyclic aromatic hydrocarbons (PAHs) and asphaltenes.

Uncertainty is present regarding the population size of such bacteria along the tanker route. Since the initial bacteria population is rarely well known, most models having a biodegradation module use a first order bacterial decay process in which the rate of oil biodegraded is proportional to the initial mass and an empirical decay coefficient, i.e.  $m = m_0 \cdot e^{-kt}$ . The empirical decay coefficient was selected as being in the same order of magnitude than the first order biodegradation rate constants from field studies (Niu et al., 2011 and Zhu et al., 2004).

### 5.3 Burrard Inlet Spill Validation

At 12:32 p.m. on 24 July 2007, a backhoe accidentally ruptured a pipeline carrying crude oil in Burnaby, BC. Approximately 224 m<sup>3</sup> of oil escaped the pipeline, some of which entered city storm sewers and was released into Burrard Inlet near Kinder Morgan's Westridge Terminal. Emergency responders contained and ultimately recovered most of the oil that entered the sewers, using booms, vacuum trucks and skimmers. According to the Environmental Impact Statement (EIS; TERA/Stantec, 2010), 5.636 m<sup>3</sup> of oil was estimated to have been released to Burrard Inlet, excluding recovered oil and volatilization.

EBA used H3D/SPILLCALC to hindcast the trajectory of the released oil as a validation of the model. Model inputs are described in Appendix C. Predictions made by SPILLCALC were compared against observations reported in the EIS as well as archived news articles available online.

According to Table 2.1.1 of the EIS, the first report of oil coming out of the sewer was at 1:35 p.m. on July 24, (one hour after the rupture), and the first booms were deployed at 2:15 p.m. By 4:40 p.m. on July 26, most of the oil was removed from inside the boomed area. In the intervening time, small amounts of oil escaped from the boomed area as a result of wave action. Therefore, the oil release in SPILLCALC was assumed to occur at a steady rate over a period of 51 hours, from 1:35 p.m. on July 24 to 16:35 p.m. on July 26.

The SPILLCALC predictions were validated against observations in the EIS and new reports, as detailed in Appendix C and summarized below.

### **Shore Impacts**

The SPILLCALC predictions showed good general agreement with the extent and degree of shoreline oiling reported in the EIS. The heaviest observed shore oiling was adjacent to the spill site, from the Chevron refinery to Barnet Marine Park. The heaviest predicted shore oiling was in the same area. In agreement with the EIS observations, SPILLCALC predicted oiling on shore near the Dollarton Highway, along the south shore at the Second Narrows, and in Belcarra Bay. No oil was observed in Port Moody; neither did SPILLCALC predict any oil impact there.

SPILLCALC predicted shore oiling south of Belcarra Bay, north of Cates Park and around Deep Cove; however, no shore oiling was observed in those locations. The most likely reason for this disagreement is the uncertainty in the timing of the oil release: oil probably escaped from the containment booms in intermittent bursts, rather than the steady flow assumed in SPILLCALC. Additionally, it is possible that the predicted slight degree of oiling actually occurred and escaped detection.

### **Duration of Oil on Water**

The SPILLCALC model ran for about 85 hours, terminating at 3:00 a.m. on Saturday July 28, 2007, at which time there was no oil remaining on the water surface. About three quarters of the oil reached shore, while most of the remainder had evaporated. According to the EIS, oil persisted longer on the water, until “by August 2 only a few patches of sheen and mousse remained outside of the spill site”. The predicted lifespan of oil on water is underestimated by the model due to complete and permanent stranding of the oil on shore. In reality, oil on shore can be re-suspended and continue to move, but this mechanism is not supported in the model.

### **Slick Motion**

The SPILLCALC predictions showed good general agreement with the observations recorded in the EIS. According to the EIS, “the greatest concentration of oil was reported east of Second Narrows and west of Port Moody;” SPILLCALC predicted the same. A small amount of oil was observed west of the Second Narrows Bridge; again, this was correctly predicted by SPILLCALC. Oil was not observed going toward Port Moody until 29 July; SPILLCALC agreed, predicting no oil entering Port Moody, although the simulation ended on 28 July. SPILLCALC predicted oil entering Belcarra Bay and Deep Cove in agreement with observations, but approximately 6-12 hours early. This difference in timing can be attributed to the uncertainty in the oil release timing.

### **Summary**

The predictions made by SPILLCALC of oil motion and shore impacts during the 2007 spill in Burrard Inlet were compared with recorded observations. The general movement of the oil, the locations of heavily affected shorelines and the extent of the affected area are in agreement. Some differences appear in the timing of the oil motion and the duration of oil on water. These differences are mainly attributed to uncertainty in the timing of the release and to the permanence of oil on shore in SPILLCALC.

## 6.0 AIR DISPERSION MODEL: SPILLCALC TO CALPUFF

Evaporation accounts for up to 25% of the fate of spilled diluted bitumen, and the bulk of the evaporation occurs within the first two days. Thus, in a major release, as much as 4,000 m<sup>3</sup> of volatile hydrocarbons will be released to the atmosphere. These volatiles contain significant toxic components, so their distribution in space and time is significant for both human and ecological health. Human health concerns arise for both the transport ship's crew and for first responders, as well as people living or working near the shore in adjacent areas. Because the source covers a wide area and is moving, the behaviour of the evaporated hydrocarbons is relatively complex, and will be treated using a numerical air dispersion model.

CALPUFF is an advanced, multi-layered, multi-species, non-steady-state Gaussian puff air dispersion modeling system which can simulate the effects of time- and space-varying meteorological conditions on pollutant transport. The model is recommended by the B.C. Ministry of Environment for long-range transport and for short-range transport in complex, non-steady state meteorological conditions found in complex terrain and coastal situations. CALPUFF differs from most other air dispersion models in that it has the ability to model several time- and spatially-variant area sources.

The main components of the modeling system are CALMET (a diagnostic three-dimensional meteorological model), CALPUFF (an air quality dispersion model), and a post-processing package. In addition to these components, there are numerous other processors that are used to prepare geophysical (land use and terrain) and meteorological data (surface, upper air, precipitation, and buoy data).

### 6.1 Diagnostic Wind and Meteorological Modelling (CALMET)

CALMET's wind module contains algorithms for calculating kinematic effects of terrain, slope flows and terrain blocking which alter domain-scale winds at the resolution of the meteorological grid size. Surface winds for the three spill scenarios (Arachne Reef, Westridge Terminal and Fraser River) were modelled using meteorological grids of varying spatial extent and resolution based on the size of the domain, the complexity of the terrain and the availability of surface meteorological data. In addition to transport modelling of the evaporated fraction of hydrocarbons in air, the wind field created by CALMET was used for the SWAN and SPILLCALC models for Burrard Inlet and the Fraser River, as CALMET provided a higher-resolution wind field than could be produced using simple interpolation schemes.

#### 6.1.1 Model Grids and Meteorological Data

##### Surface Data

Hourly data was acquired from several meteorological stations located in close proximity to the water operated by various organizations and ocean buoys. Only stations and buoys which report QA/QC'd data were used (Environment Canada, NOAA, B.C. Ministry, Metro Vancouver). All surface data was reviewed for representativeness and subjected to QA/QC and substitution methods described in 'Guidelines for Air Dispersion Modelling in British Columbia' (MoE 2008). In addition, three North American Regional Reanalysis (NARR) grid points were added west of the entrance to Juan de Fuca Strait, south of Vancouver Island, to provide wind conditions near the domain boundaries where station observations were absent. The stations are listed in Table 5.1 along with the model grid in which they were included.

**Table 6.1.1: Meteorological Surface Stations, Buoys and NARR Grid Points Used in CALMET**

Meteorological Station/Buoy	Location	Body	Latitude	Longitude	Grid		
					Arachne Reef	Westridge Terminal	Fraser River
Howe Sound – Pam Rocks	Howe Sound	EC	49.488 N	123.299 W	*	*	
Kensington Park	Burnaby	MV	49.279 N	123.971 W		*	
Second Narrows	North Vancouver	MV	49.302 N	123.020 W		*	
Mahon Park	West Vancouver	MV	49.324 N	123.084 W		*	
Rocky Pt. Park	Port Moody	MV	49.281 N	122.849 W		*	
Point Atkinson	West Vancouver	EC	49.330 N	123.265 W	*	*	
Burnaby North	Burnaby	MV	49.288 N	123.008 W		*	
Vancouver Int'l Airport	Richmond	EC	49.195 N	123.182 W	*	*	*
Burns Bog	Richmond	EC	49.126 N	123.002 W			*
Seymour	North Vancouver	MoF	49.483 N	122.950 W		*	
North Delta	Delta	MV	49.158 N	122.902 W			*
Annacis Island	Richmond	MV	49.166 N	122.961 W			*
Richmond South	Richmond	MV	49.141 N	123.108 W			*
Burnaby South	Burnaby	MV	49.215 N	122.986 W			*
Pitt Meadows A	Pitt Meadows	EC	49.216 N	122.683 W	*	*	*
Halibut Bank Buoy	Strait of Georgia	EC	49.340 N	123.727 W	*	*	
New Dungeness Buoy	Juan de Fuca Strait	NDBC	48.336 N	123.159 W	*		
Neah Bay Buoy	Juan de Fuca Strait	NDBC	48.494 N	124.728 W	*		
Sentry Shoal Buoy	Strait of Georgia	EC	49.92 N	125.0 W	*		
Kelp Reefs	Haro Strait	EC	48.548 N	123.236 W	*		
Campbell River	N Vancouver Is.	EC	49.952 N	125.467 W	*		
Grief Point	Sunshine Coast	EC	49.805 N	124.525 W	*		
Discovery Island	Haro/Juan de Fuca Strait	EC	48.424 N	123.225 W	*		
Sand Heads	Strait of Georgia	EC	49.106 N	123.303 W	*		*
Saturna Island	Boundary Pass	EC	48.783 N	123.045 W	*		
Ballenas Island	Strait of Georgia	EC	49.350 N	124.158 W	*		
Entrance Island	Strait of Georgia	EC	49.217 N	123.800 W	*		
Race Rocks	S Vancouver Is.	EC	48.299 N	123.531 W	*		
Sheringham Point	SW Vancouver Is.	EC	48.377 N	123.921 W	*		
Sisters Island	Strait of Georgia	EC	49.487 N	124.435 W	*		
Comox A	N Vancouver Is.	EC	49.717 N	124.900 W	*		
North Cowichan	Vancouver Island	EC	48.817 N	123.717 W	*		
Cherry Point	Washington State	NOAA	48.863 N	122.758 W	*		
Bellingham Airport	Washington State	NOAA	48.794 N	122.537 W	*		
Port Angeles	N Olympic Peninsula	NOAA	48.117 N	123.417 W	*		

**Table 6.1.1: Meteorological Surface Stations, Buoys and NARR Grid Points Used in CALMET**

Meteorological Station/Buoy	Location	Body	Latitude	Longitude	Grid		
					Arachne Reef	Westridge Terminal	Fraser River
Port Townsend	NE Olympic Peninsula	NOAA	48.112 N	122.758 W	*		
Smith Island	E. Juan de Fuca Strait	NOAA	48.317 N	122.843 W	*		
Skagit Regional Airport	Washington State	NOAA	48.317 N	122.843 W	*		
Orcas Island Airport	San Juan Islands	NOAA	48.466 N	122.416 W	*		
Friday Harbor	San Juan Islands	NOAA	48.522 N	123.023 W	*		
Whidbey Island	Washington State	NOAA	48.350 N	122.666 W	*		
Everett/Paine Field	Washington State	NOAA	47.907 N	122.280 W	*		
Arlington Municipal Airport	Washington State	NOAA	48.160 N	122.158 W	*		
Tatoosh Island	NW Olympic Peninsula	NOAA	48.383 N	124.733 W	*		
NARR Pt205_60	Mouth of Juan de Fuca	NARR	48.567 N	125.383 W	*		
NARR Pt230_60	Mouth of Juan de Fuca	NARR	48.433 N	125.010 W	*		
NARR Pt230_10	Offshore O. Peninsula	NARR	48.067 N	125.466 W	*		

EC: Environment Canada; MV: Metro Vancouver; MoF: BC Ministry of Forests; NDBC: National Data Buoy Center (USA); NOAA – National Oceanic and Atmospheric Administration (USA); NARR: North American Regional Reanalysis.

### **Arachne Reef (Strait of Georgia/ Juan de Fuca) Grid**

The Strait of Georgia/ Juan de Fuca grid was used to provide wind inputs for SWAN and SPILLCALC and to model the transport of evaporated hydrocarbons for spill scenarios at Arachne Reef. The meteorological grid uses a 1 km resolution over a domain of 210 km by 210 km, centered over 460 km east, 5380 km north, Zone 10 (UTM). The domain covers the expanse of oil migration, spanning approximately 20 km past the entrance to Juan de Fuca Strait to the west, the southern portion of Texada Island to the north and the northern passages of Puget Sound to the south. In addition to the representative coastal EC and NOAA meteorological stations and DFO and NDBC buoys identified in the MetOcean report prepared by EBA (EBA 2012), additional NOAA stations were added which provided meteorology over the southeast portion of the grid into Washington State and NARR grid points which provided winds over the Pacific Ocean west of the Juan de Fuca.

### **Westridge Terminal (Burrard Inlet) Grid**

The Burrard Inlet grid was used to provide wind inputs for SWAN and SPILLCALC and to model the transport of evaporated hydrocarbons for spill scenarios at the Westridge Terminal. The meteorological grid uses a 300 m resolution over a model domain of 63 km in the east-west by 45 km in the north-south, centered at 496.369 km east, 5467.478 km north, zone 10 (UTM). In addition to stations identified in the MetOcean report, Metro Vancouver meteorological stations located near the shore of Burrard Inlet were included in the meteorological station network to increase wind resolution. For the purpose of retaining recorded over-water winds along the western domain boundary, the Halibut Bank buoy data was replicated 17 kilometres east (49.34° N, 123.48° W) of its actual position to include it within the domain boundaries.

## Fraser River Grid

The Fraser River grid provided wind inputs for SWAN and SPILLCALC. The grid uses a 200 m resolution and is 40 km in the east-west by 22 km in the north-south, centered over the Fraser River near Tilbury (497.044 km east, 5442.928 north, Zone 10, UTM). The grid is aligned with the SPILLCALC grid. Pitt Meadows station was replicated at a location on Douglas Island (523.093 km east, 5449.737 km north) to provide boundary conditions at the easternmost edge of the domain.

Upper air soundings, recorded at the NOAA upper air station located at Quillayute, Washington were used in CALMET to provide the first-guess wind field. Where a sounding or sequential soundings were missing, temporal or spatial substitution methods were used. Spatial substitution from the nearest representative station (Port Hardy) was the preferred method. Because the network of surface stations provided very good coverage, using the single station as the initial guess was adequate and prognostic meteorological data was not necessary. Furthermore since the pseudo-components being modelled were dense relative to air, winds in the surface layer were much more crucial to predict transport than three-dimensional stability aloft.

For the Arachne Reef grid, SRTM1 (USA) and 1:50,000 Canadian Digital Elevation Data (Canada) at ~30 m resolution were downloaded and used in CALMET's geophysical processor along with a USGS Global Land Cover Characterization (GLCC) data set (resolution ~1 km). For the Westridge Terminal and Fraser River grids, 1:50,000 Canadian Digital Elevation Data and a 1:250,000 Land Cover data set from GeoBase (LCC2000) were used.

### 6.1.2 CALMET Switch Settings

The model settings for CALMET were defined in compliance with Table 9.6 in 'Guidelines for Air Dispersion Modelling in British Columbia' (MoE 2008). Default settings were used where required or recommended. Where expert judgement was required, choices were evaluated on the best surface layer wind field. These switch settings included radius of influence of terrain and radius of influence of observed meteorological data.

## 6.2 Air Dispersion Model (CALPUFF)

### 6.2.1 Evaporation Flux (Area Sources)

CALPUFF has the ability to model time- and spatially-varying area sources through an external buoyant area source file. The external file is designed for tracking the effects from buoyant area sources such as forest fires, but contains changeable parameters to more closely simulate a non-buoyant source such as an evaporating hydrocarbon pool (Table 6.2.1). The file allows for up to 200 area sources with an emission rate defined for each species (pseudo-component) (in g/s) over each timestep (one hour).

The average evaporation flux (emission rate) for each of the 17 pseudo-components was determined by SPILLCALC in hourly intervals and written to an output file. The total source area (oil on the surface of the water) was then divided into smaller area sources (500 m<sup>2</sup> for Arachne Reef, 62.5 m<sup>2</sup> for Westridge) for each hour. The flux rate for each smaller source polygon is assumed to occur homogeneously over the entire surface area.



## 6.2.2 CALPUFF Switch Settings

The model settings for CALPUFF were defined in compliance with Table 9.7 in 'Guidelines for Air Dispersion Modelling in British Columbia' (MoE 2008). Default settings were used where required or recommended.

## 7.0 SIMULATION OVERVIEW

### 7.1 Types of Simulations

#### 7.1.1 Stochastic simulations

A stochastic simulation is essentially a collection of separate spill simulations, holding most aspects of the spill, such as location and volume, constant, but varying the start time and date of the spill. The resulting set of spills can be analyzed to obtain statistical information on the extent of the spill, the probability to reach a certain area, and the amount of shoreline (minimum, average, median, maximum length) that can be potentially contacted. The intent of a stochastic simulation is to simulate a wide range of environmental conditions without bias to any particular set of conditions.

#### 7.1.2 Specific simulations

Specific scenarios, also called deterministic scenarios, were chosen based on results from the stochastic simulations or according to other criteria. Typically, the stochastic simulations represent the envelope of a large number of independent spills that could occur in a given time frame. The worst scenario, i.e. largest spill extent and highest amount of shoreline contacted, can be extracted to gain an understanding of how bad a spill could be. In general, they are done using the version of SPILLCALC that is embedded in the H3D model. The full 3D simulation represents an extension of the specific simulations: different modules, such as the dissolution, are simulated in those scenarios and the fate of pseudo-components is tracked over the entire water column and model domain. The primary purpose of these simulations is to provide information on the potential toxicity of the spill.

## 8.0 STOCHASTIC SIMULATIONS

The figures corresponding to the stochastic modelling are located in Appendix D. The numbering system is the following: Figure A.m-n with "A" referencing to the site letter (i.e. Strait of Georgia is site D – Table 2.1.1), "m" being the season (1 for winter, 2 for spring, 3 for summer, 4 for fall) and "n" being the sequential numbering for this particular site and season. For example, Figure D.3-3 would refer to Figure 3 of Site D, Strait of Georgia, Summer season.

For each season, the following stochastic package was produced:

- Environmental conditions, wind conditions and Fraser flow (Figure 1);
- Maps showing the probability of oil presence, shoreline oiled probability and first contact (Figures 2 to 4);



- Time series of length of shoreline contacted (total and per coastal class) and amount dissolved (Figures 5 to 7);
- Time series of mass balance (Figures 8 to 9);
- Statistics on area and thickness (Figure 10); and
- $P_{50}$  and  $P_{90}$  after 6/12/24/48 hours (Figures 11 to 14).

## 8.1 Site A: Westridge Terminal

### 8.1.1 Large Spill (160 m<sup>3</sup>)

The large spill at the Westridge Terminal resulting from an incident during loading of a tanker was assessed under conservative conditions, assuming a volume of 160 m<sup>3</sup>. The simulated incident occurs during a tanker loading activity: the transfer rate is about 1,545 m<sup>3</sup>/hr per loading arm and it is calculated that a 160 m<sup>3</sup> oil spill could have resulted from a complete rupture of one loading arm based upon an earlier design of the dock complex. Although optimisation of the dock design resulted in a significant reduction of such an oil spill quantity to 103 m<sup>3</sup>, the simulation, which had been planned prior to such optimisation having taken place, was kept to the higher release volume and is therefore a more conservative assumption (i.e. 160 m<sup>3</sup> spill).

At 160 m<sup>3</sup>, this spill is larger than the CWC spill resulting from a rupture of a loading arm but significantly smaller than the over 1,500 m<sup>3</sup> capacity of the precautionary boom that will be deployed around each berth while any cargo transfer activities are taking place. It is reasonable to expect that the spill would be entirely contained within the boom. In addition, observed weak currents (EBA, 2013) at the Terminal support the full containment of the oil within the pre-deployed boom.

However, as a conservative approach to this scenario, it was deemed that, for oil spill modeling purposes, 20% of the oil released would escape the containment boom (i.e. 32 m<sup>3</sup>). This condition was chosen to ensure a conservative approach to spill response requirements at the site and does not reflect Trans Mountain's expectation for performance of the precautionary boom which will be in place to fully contain such a release at the terminal. For information of the reader, the CWC oil spill volume resulting from this scenario has been calculated by DNV as 103 m<sup>3</sup> and was deemed as a low probability event with an estimated likelihood of occurring once every 234 years.

The general wind pattern at Site A is mainly north-west winds which rarely exceed 10 m/s.

Figures 8.1.1 and 8.1.2 show the 50% ( $P_{50}$ ) and 90% ( $P_{90}$ ) probability maps at Hour 6 (i.e., 6 hours after the start of the incident) and Hour 12. Individual figures after 6, 12 and 24 hours for each season are available in Appendix D.

The length of shoreline oiled is relevant for determining potential ecological damage, and for estimating shoreline clean up resources that would be required in the unlikely event of a spill. Figure A.3-5 illustrates the length of shoreline contacted by oil for the summer simulations. Basic statistics on shoreline oiling for all seasons are presented in Table 8.1.1.

**Table 8.1.1: Statistics for Shoreline Contact for a Large Spill at Site A**

	Median (km)	Average (km)	Maximum (km)	Minimum (km)
Winter	13	15	44	2
Spring	16	17	43	2
Summer	20	19	37	2
Fall	14	15	38	2

The mass balance of the spilled oil provides a good summary of a particular spill, or, when averaged across all spills, a good understanding of spill behaviour for a spill that would occur in a particular season. Figures A.3-8 and A.3-9 show the mass balance for the summer spill scenario. Figure A.3-8 shows the major components: on water, on shore and evaporated. Figure A.3-9 shows the minor components: dispersed, biodegraded, on banks and dissolved. Table 8.1.2 summarizes the mass balance for all four seasons at the end of the tracking period. It should be noted that, due to the small amount released onto Burrard Inlet, most of the oil, which escaped the pre-deployed boom, disappears from the water surface after a short number of days. The amount of oil bound up in oil-mineral aggregations was negligible. The evaporation process is limited for the oil that escaped the pre-deployed boom, since the oil is very thin and spread over a somewhat large area; on the other hand, the slick contained inside the pre-deployed boom is diffusion-limited.

**Table 8.1.2: Mass Balance Summary for a Large Spill at Site A**

Component	Winter	Spring	Summer	Fall	Yearly Average
Fraction on shore (%)	18.0	18.0	17.9	18.0	18.0
Fraction evaporated (%)	19.4	19.1	19.6	19.5	19.4
Fraction on water (%)	54.2	55.0	54.0	54.1	54.3
Fraction dissolved (%)	1.2	1.3	1.3	1.2	1.3
Fraction biodegraded (%)	7.2	6.6	7.2	7.2	7.0
Fraction on banks (%)	0	0	0	0	0
Fraction OMA (%)	0	0	0	0	0
Fraction dispersed (%)	0	0	0	0	0

Results amongst the four seasons are similar; about 55 % of the oil was still on water (mainly contained in the pre-deployed boom), about 18% ends up on shore, about 19% evaporated and the remaining 8% is either biodegraded or dissolved in the water column. The maximum extent of the spill (1% probability line) is observed between Lion's Gate Bridge, Port Moody and Indian Arm. A single spill would not cover this entire area, but could reach part of an area bounded by Lion's Gate Bridge to the west with Port Moody to the east and Indian Arm to the north, depending on specific environmental conditions.

### 8.1.2 Small Spill (10 m<sup>3</sup>)

The small spill at the Westridge Terminal resulting from an incident during loading of a tanker was estimated to be 10 m<sup>3</sup> (Termopol 3.15). At 10 m<sup>3</sup>, this spill is significantly smaller than the over 1,500 m<sup>3</sup> capacity of the precautionary boom that will be deployed around each berth and it is reasonable to expect that the spill would be entirely contained within the boom. In addition, observed weak currents (EBA, 2013) at the Terminal support the full containment of the oil within the pre-deployed boom. As a result, since the spill is fully contained, there is no spreading or advection onto Burrard Inlet. The only weathering occurring are the evaporation, dissolution and biodegradation.

The general wind pattern at Site A is mainly north-west winds which rarely exceed 10 m/s.

Table 8.1.3 summarizes the mass balance for all four seasons at the end of the tracking period.

**Table 8.1.3: Mass Balance Summary for a Small Spill at Site A**

Component	Winter	Spring	Summer	Fall	Yearly Average
Fraction on shore (%)	0	0	0	0	0
Fraction evaporated (%)	22.7	22.4	21.7	22.9	22.4
Fraction on water (%)	72.3	72.6	73.1	72.1	72.5
Fraction dissolved (%)	1.8	1.8	1.9	1.8	1.8
Fraction biodegraded (%)	3.2	3.2	3.3	3.2	3.2
Fraction on banks (%)	0	0	0	0	0
Fraction OMA (%)	0	0	0	0	0
Fraction dispersed (%)	0	0	0	0	0

Results amongst the four seasons are similar: about 73% of the oil is still on water after 5 days, about 22% evaporates and the remaining 5% are either dissolved or biodegraded.

## 8.2 Site D: Strait of Georgia

Site D is located in the Strait of Georgia between the Tsawwassen Ferry Terminal and the southern Gulf Islands, as shown in Figure 2.1.1. This location has been determined to be representative of a collision with crossing traffic from the Fraser River and ferries. The potential volume of oil spilled was determined by DNV (Volume 8A). The credible worst case spill (CWC) resulting from side damage or collision would release 16,500 m<sup>3</sup>; the medium size spill resulting from side damage or collision, P<sub>50</sub> probability, would result in 8,250 m<sup>3</sup> spilled. The duration of the spill in both cases is 13 hours with 25% released during the first hour and the balance released at a uniform rate over the next 12 hours.

To capture the seasonal variation observed in wind and currents in the Strait of Georgia, a full year of stochastic simulation was conducted. This site is especially sensitive to the seasonal pattern of the currents in this part of the Strait of Georgia due to its close proximity to the Fraser River. The results are presented per season: January-February-March for winter, April-May-June for spring, July-August-September for summer and October-November-December for fall.

The general wind pattern at Site D is mainly south-west and north-west winds which rarely exceed 20 m/s.

## 8.2.1 CWC Spill (16,500 m<sup>3</sup>)

Figures 8.2.1 and 8.2.2 show the 50% (P<sub>50</sub>) and 90% (P<sub>90</sub>) probability maps at Hour 24 (i.e., 24 hours after the start of the incident) and Hour 48. Individual figures for 6 hours, 12 hours, 24 hours, 48 hours and 15 days after the incident for each season are located in Appendix D.

Figure 8.2.1, 24 hours after the incident, illustrates the importance of using an adequate hydrodynamic model. The combination of prevailing northwest winds and the influence of the Fraser River are key factors in determining the seasonal variability, which causes the summer P<sub>50</sub> contours to extend over an area about 50% larger than the winter P<sub>50</sub> region. As well, northwest winds and the estuarine flow, causing surface water to leave the Strait and flow toward the open Pacific, lead to an elongation of the spill to the southwest in the summer and fall. After 48 hours, the P<sub>50</sub> contour has moved into Boundary Pass and almost to the top end of Haro Strait. The most striking difference between the situation at 25 hours and at 48 hours, regardless of season, is a two- to three-fold increase in the area within a particular probability contour. This comparison profoundly illustrates the benefit to be gained by developing mitigation strategies that are in the field and operational within a very few hours of the start of the incident. Although not shown here, the minimum time to reach a particular location or shoreline is also helpful in developing mitigation strategies.

The length of shoreline oiled is relevant for determining potential ecological damage, and for estimating shoreline clean up resources that would be required in the unlikely event of a spill. Figure D.3-5 illustrates the length of shoreline contacted by oil for each member of the summer simulations. The variability across all the spills within one season is quite remarkable, and illustrates the significant day to day changes in winds and currents that can occur in the study area. Basic statistics on shoreline oiling for all seasons are presented in Table 8.2.1.

**Table 8.2.1: Statistics for Shoreline Contact for a Credible Worst Case Spill at Site D**

	Median (km)	Average (km)	Maximum (km)	Minimum (km)
Winter	271	263	388	105
Spring	296	291	436	97
Summer	284	279	414	71
Fall	296	293	425	106

The mass balance of the spilled oil provides a good summary of a particular spill, or, when averaged across all spills, a good understanding of spill behaviour for a spill that would occur in a particular season. Figures D.3-8 and D.3-9 show the mass balance for the summer spill scenario. Figure D.3-8 shows the major components: on water, on shore and evaporated. Figure D.3-9 shows the minor components: dispersed, bio-degraded, on banks and dissolved. Table 8.2.2 summarizes the mass balance for all four seasons at the end of the 15-day stochastic simulation period. The amount of oil bound up in oil-mineral aggregations was negligible, even for this site which would be influenced by the Fraser River Plume.

**Table 8.2.2: Mass Balance Summary for a Credible Worst Case Spill at Site D**

Component	Winter	Spring	Summer	Fall	Yearly Average
On Shore	63.8	67.4	66.4	66.8	66.1
Evaporated	21.7	19.8	19.3	20.7	20.4
Left on Water	2.6	1.7	2.4	1.4	2.0
Dissolved	6.7	6.8	6.7	6.9	6.8
Biodegraded	3.2	2.8	2.7	2.8	2.9
OMA	0.06	< 0.01	< 0.01	0.08	0.04
On Banks	1.9	0.7	2.4	1.4	1.6
Dispersed	0.1	0	0	0.1	0.1

## 8.2.2 Medium Spill (8,250 m<sup>3</sup>)

Similarly to the CWC spill scenario, figures for the medium spill scenario are located in the Appendix D. To avoid redundancy, only the summary tables are presented in this section.

Figures 8.2.3 and 8.2.4 show the 50% (P<sub>50</sub>) and 90% (P<sub>90</sub>) probability maps at Hour 24, i.e., 24 hours after the start of the incident, and Hour 48.

The length of shoreline oiled is relevant for determining potential ecological damage, and for estimating shoreline clean up resources that would be required in the unlikely event of a spill. Basic statistics on shoreline oiling for all seasons are presented in Table 8.2.3.

**Table 8.2.3: Statistics for Shoreline Contact for a Medium Case Spill at Site D**

	Median (km)	Average (km)	Maximum (km)	Minimum (km)
Winter	189	185	307	57
Spring	218	217	344	58
Summer	208	205	316	59
Fall	213	211	314	74

The mass balance of the spilled oil provides a good summary of a particular spill, or, when averaged across all spills, a good understanding of spill behaviour for a spill that would occur in a particular season. Table 8.2.4 summarizes the mass balance for all four seasons at the end of the 10-day stochastic simulation period. The amount of oil bound up in oil-mineral aggregations was negligible, even for this site which would be somewhat influenced by the Fraser River Plume.

**Table 8.2.4: Mass Balance Summary for a Medium Case Spill at Site D**

Component	Winter	Spring	Summer	Fall	Yearly Average
On Shore	62.1	66.3	66.1	66.0	65.1
Evaporated	19.4	17.8	17.2	18.2	18.2
Left On Water	6.0	4.2	4.1	3.7	4.5
Dissolved	8.7	8.9	8.8	9.1	8.8
Biodegraded	2.5	2.2	2.1	2.3	2.3
OMA	0.07	< 0.01	< 0.01	0.04	0.03
On Banks	1.2	0.6	1.7	0.7	1.1
Dispersed	0.3	< 0.01	< 0.01	0.4	0.18

### 8.3 Site E: Haro Strait at Arachne Reef

Site E is located at Arachne Reef, at the northern end of Haro Strait. This location has been determined to be representative of an incident resulting from powered grounding and/or a collision. The potential volume of oil spilled was determined by DNV for the CWC and P<sub>50</sub> scenario. A CWC side damage incident would result in 16,500 m<sup>3</sup> spilled; the corresponding P<sub>50</sub> probability, would result in 8,250 m<sup>3</sup> spilled. The simulated duration of the release in both incidents is 13 hours with 25% of the oil released in the first hour, and a constant hourly spill rate for the next 12 hours.

Winds at Site E (as recorded at Kelp Reef) are mainly oriented north-south with strong storms occurring in the fall-winter periods with winds reaching 20 m/s. The spring-summer period is characterized by weaker winds, rarely exceeding 10 m/s.

A full year of stochastic simulation was conducted. The results are presented per season: January-February-March for winter, April-May-June for spring, July-August-September for summer and October-November-December for fall.

#### 8.3.1 CWC Spill (16,500 m<sup>3</sup>)

Figures 8.3.1 and 8.3.2 show the 50% (P<sub>50</sub>) and 90% (P<sub>90</sub>) probability maps at Hour 24, i.e., 24 hours after the start of the incident, and Hour 48. Individual figures after 6/12/24/48 hours and after 15 days are located for each season in the Appendix D.

The length of shoreline oiled is relevant for determining potential ecological damage, and for estimating shoreline clean up resources that would be required in the unlikely event of a spill. Figure E.3-5 illustrates as an example the length of shoreline contacted by oil for the summer simulation. Basic statistics on shoreline oiling for all seasons are presented in Table 8.3.1.

**Table 8.3.1: Statistics for Shoreline Contact for a Credible Worst Case Spill at Site E**

	Median (km)	Average (km)	Maximum (km)	Minimum (km)
Winter	290	292	387	162
Spring	304	306	427	206
Summer	312	309	407	174
Fall	301	301	391	169

The mass balance of the spilled oil provides a good summary of a particular spill, or, when averaged across all spills, a good understanding of spill behaviour for a spill that would occur in a particular season. Figures E.3-8 and E.3-9 show the mass balance for the summer spill scenario. Figure E.3-8 shows the major components: on-water, on-shore and evaporated, and Figure E.3-9 shows the minor components: dispersed, biodegraded, on banks and dissolved. Table 8.3.2 summarizes the mass balance for all four seasons at the end of the 15-day stochastic simulation period.

**Table 8.3.2: Mass Balance Summary for a Credible Worst Case Spill at Site E**

Component	Winter	Spring	Summer	Fall	Yearly Average
On-Shore	68.9	69.5	69.8	71.1	69.8
Evaporated	21.5	19.7	18.8	19.1	19.8
Left On-Water	1.6	2.3	2.9	1.9	2.2
Dissolved	5.2	5.8	5.7	5.3	5.5
Biodegraded	2.8	2.7	2.8	2.6	2.7
OMA	< 0.01	< 0.01	< 0.01	< 0.01	< 0.01
On-Banks	0	0	0	0	0.0
Dispersed	0	0	0	0	0.0

### 8.3.2 Medium Spill (8,250 m<sup>3</sup>)

Similarly to the CWC spill scenario, figures for the medium spill scenario are located in the Appendix D. To avoid redundancy, only the summary tables are presented in this section.

Figures 8.3.3 and 8.3.4 show the 50% (P<sub>50</sub>) and 90% (P<sub>90</sub>) probability maps at Hour 24, i.e., 24 hours after the start of the incident, and Hour 48.

The length of shoreline oiled is relevant for determining potential ecological damage, and for estimating shoreline clean up resources that would be required in the unlikely event of a spill. Basic statistics on shoreline oiling for all seasons are presented in Table 8.3.3.



**Table 8.3.3: Statistics for Shoreline Contact for a Medium Case Spill at Site E**

	Median (km)	Average (km)	Maximum (km)	Minimum (km)
Winter	211	207	284	103
Spring	223	223	326	139
Summer	222	224	317	128
Fall	215	211	305	97

The mass balance of the spilled oil provides a good summary of a particular spill, or, when averaged across all spills, a good understanding of spill behaviour for a spill that would occur in a particular season. Table 8.3.4 summarizes the mass balance for all four seasons at the end of the 10-day stochastic simulation period. The amount of oil bound up in oil-mineral aggregations was negligible.

**Table 8.3.4: Mass Balance Summary for a Medium Case Spill at Site E**

Component	Winter	Spring	Summer	Fall	Yearly Average
On Shore	70.1	71.5	71.7	72.4	71.4
Evaporated	19.1	17.2	16.8	17.1	17.5
Left On Water	2.5	2.6	2.8	2.6	2.6
Dissolved	6.2	6.8	6.7	6.1	6.5
Biodegraded	2.1	1.9	2.0	1.9	2.0
OMA	< 0.01	< 0.01	< 0.01	< 0.01	< 0.01
On Banks	< 0.01	0	< 0.01	< 0.01	< 0.01
Dispersed	0.1	0.05	0.01	0.06	0.06

## 8.4 Site G: Juan de Fuca Strait off Race Rocks

Site G is located in Juan de Fuca Strait between Race Rocks and Port Angeles, as shown in Figure 2.1.1. This location has been determined to be representative of a hypothetical collision with crossing traffic from Puget Sound and Rosario Strait. The potential volume of oil spilled was determined by DNV to be 16,500 for the Credible Worst Case; the medium size spill resulting from side damage or collision, with P<sub>50</sub> probability, would result in 8,250 m<sup>3</sup> spilled. Twenty-five percent of the oil would be released in the first hour, and the balance over the succeeding 12 hours.

The winds at Site G (as recorded at Port Angeles) blow either along the Strait from the northwest or off the land from the south-southwest. The winds blowing along the Strait are frequently up to 10 m/s and occur almost continuously in spring and summer but only intermittently in fall and winter. The winds coming off the land, however, are typically less than 5 m/s and dominate the fall and winter periods.

A full year of stochastic simulation was conducted. The results are presented per season: January-February-March for winter, April-May-June for spring, July-August-September for summer and October-November-December for fall.

#### 8.4.1 CWC Spill (16,500 m<sup>3</sup>)

Figures 8.4.1 and 8.4.2 show the 50% (P<sub>50</sub>) and 90% (P<sub>90</sub>) probability maps at Hour 24, i.e., 24 hours after the start of the incident, and Hour 48. Individual figures after 6/12/24/48 hours and after 15 days are located for each season in the Appendix D.

The length of shoreline oiled is relevant for determining potential ecological damage, and for estimating shoreline clean up resources that would be required in the unlikely event of a spill. Figure G.3-5 illustrates the length of shoreline contacted by oil for the summer simulation. Basic statistics on shoreline oiling for all seasons are presented in Table 8.4.1.

**Table 8.4.1: Statistics for Shoreline Contact for a Credible Worst Case Spill at Site G**

	Median (km)	Average (km)	Maximum (km)	Minimum (km)
Winter	183	175	316	33
Spring	129	136	259	44
Summer	110	114	196	44
Fall	140	141	296	42

The mass balance of the spilled oil provides a good summary of a particular spill, or, when averaged across all spills, a good understanding of spill behaviour for a spill that would occur in a particular season. Figures G.3-8 and G.3-9 show the mass balance for the summer spill scenario. Figure G.3-8 shows the major components: on water, on shore and evaporated, and Figure G.3-9 shows the minor components: dispersed, bio-degraded, on banks and dissolved. Table 8.4.2 summarizes the mass balance for all four seasons at the end of the 15-day stochastic simulation period.

**Table 8.4.2: Mass Balance Summary for a Credible Worst Case Spill at Site G**

Component	Winter	Spring	Summer	Fall	Yearly Average
On Shore	66.5	65.7	67.1	66.1	66.4
Evaporated	20.9	20.3	19.7	20.1	20.3
Left On Water	2.9	4.5	4.3	4.2	4.0
Dissolved	6.6	6.4	6.1	6.6	6.4
Biodegraded	3.1	3.1	2.7	2.9	3.0
OMA	< 0.01	0.01	0.02	0.01	0.01
On Banks	0	0	0	0	0.0
Dispersed	0	0	0	0	0.0

## 8.4.2 Medium Spill (8,250 m<sup>3</sup>)

Similarly to the CWC spill scenario, figures for the medium spill scenario are located in the Appendix D. To avoid redundancy, only the summary tables are presented in this section.

Figures 8.4.3 and 8.4.4 show the 50% (P<sub>50</sub>) and 90% (P<sub>90</sub>) probability maps at Hour 24, i.e., 24 hours after the start of the incident, and Hour 48.

The length of shoreline oiled is relevant for determining potential ecological damage, and for estimating shoreline clean up resources that would be required in the unlikely event of a spill. Basic statistics on shoreline oiling for all seasons are presented in Table 8.4.3.

**Table 8.4.3: Statistics for Shoreline Contact for a Medium Case Spill at Site G**

	Median (km)	Average (km)	Maximum (km)	Minimum (km)
Winter	123	124	224	26
Spring	92	99	202	40
Summer	87	88	177	37
Fall	111	112	233	29

The mass balance of the spilled oil provides a good summary of a particular spill, or, when averaged across all spills, a good understanding of spill behaviour for a spill that would occur in a particular season. Table 8.4.4 summarizes the mass balance for all four seasons at the end of the 10-day stochastic simulation period. The amount of oil bound up in oil-mineral aggregations was negligible.

**Table 8.4.4: Mass Balance Summary for a Medium Case Spill at Site G**

Component	Winter	Spring	Summer	Fall	Yearly Average
On Shore	64.8	65.7	67.6	64.3	65.6
Evaporated	18.9	18.3	17.7	18.3	18.3
Left On Water	5.0	5.1	4.4	6.1	5.1
Dissolved	8.8	8.6	8.3	8.9	8.6
Biodegraded	2.5	2.3	2.0	2.4	2.3
OMA	< 0.01	0.02	0.03	0.01	0.02
On Banks	0	0	0	0	0
Dispersed	0.4	0.03	< 0.01	0.2	0.2

## 8.5 Site H: Buoy J

Site H is located at the entrance to Juan de Fuca Strait at Buoy J, as shown in Figure 2.1.1. This location has been determined to be representative of a hypothetical incident resulting from a collision. The potential volume of oil spilled was determined by DNV as 16,500 m<sup>3</sup> for a credible worst case; the medium size spill, with P<sub>50</sub> probability, would result in 8,250 m<sup>3</sup> spilled. Twenty-five percent of the spill would be released in the first hour, and the balance at a uniform rate over the succeeding 12 hours. This location has very low probability for an oil spill from a laden tanker. However, this location represents the outer part of the assessment area, hence should be considered.

Winds at Site H are primary from the south. Strong storms are observed in the fall-winter periods with winds reaching 20 m/s. The spring-summer period is characterized by weaker winds, about 10 m/s.

A full year of stochastic simulation was conducted. The results are presented per season: January-February-March for winter, April-May-June for spring, July-August-September for summer and October-November-December for fall.

### 8.5.1 CWC Spill (16,500 m<sup>3</sup>)

Figures 8.5.1 and 8.5.2 show the 50% (P<sub>50</sub>) and 90% (P<sub>90</sub>) probability maps at Hour 24, i.e., 24 hours after the start of the incident, and Hour 48. Individual figures after 6/12/24/48 hours and after 15 days are located for each season in the Appendix D.

The length of shoreline oiled is relevant for determining potential ecological damage, and for estimating shoreline clean up resources that would be required in the unlikely event of a spill. Figure H.3-5 illustrates the length of shoreline contacted by oil for the summer simulation. Basic statistics on shoreline oiling for all seasons are presented in Table 8.5.1.

**Table 8.5.1: Statistics for Shoreline Contact for a Credible Worst Case Spill at Site H**

	Median (km)	Average (km)	Maximum (km)	Minimum (km)
Winter	145	143	271	23
Spring	103	101	208	0
Summer	88	81	143	0
Fall	107	114	314	0

The mass balance of the spilled oil provides a good summary of a particular spill, or, when averaged across all spills, a good understanding of spill behaviour for a spill that would occur in a particular season. Figures H.3-8 and H.3-9 show the mass balance for the summer spill scenario. Figure H.3-8 shows the major components: on water, on shore and evaporated, and Figure H.3-9 shows the minor components: dispersed, bio-degraded, on banks and dissolved. Table 8.5.2 summarizes the mass balance for all four seasons at the end of the 15-day stochastic simulation period.

**Table 8.5.2: Mass Balance Summary for the 16,500 m<sup>3</sup> Spill at Site H**

Component	Winter	Spring	Summer	Fall	Yearly Average
On Shore	59.6	34.3	28.2	41.5	40.9
Evaporated	22.7	23.6	24.2	23	23.4
Left On Water	6.9	26.4	31	21.5	21.5
Dissolved	6.9	9.5	10	8.8	8.8
Biodegraded	3.9	6.1	6.6	5.3	5.5
OMA	< 0.01	< 0.01	< 0.01	< 0.01	< 0.01
On Banks	0	0	0	0	0.0
Dispersed	1	2.2	8.7	1	3.2

### 8.5.2 Medium Spill (8,250 m<sup>3</sup>)

Similarly to the CWC spill scenario, figures for the medium spill scenario are located in the Appendix D. To avoid redundancy, only the summary tables are presented in this section.

Figures 8.5.3 and 8.5.4 show the 50% (P<sub>50</sub>) and 90% (P<sub>90</sub>) probability maps at Hour 24, i.e., 24 hours after the start of the incident, and Hour 48.

The length of shoreline oiled is relevant for determining potential ecological damage, and for estimating shoreline clean up resources that would be required in the unlikely event of a spill. Basic statistics on shoreline oiling for all seasons are presented in Table 8.5.3.

**Table 8.5.3: Statistics for Shoreline Contact for a Medium Case Spill at Site H**

	Median (km)	Average (km)	Maximum (km)	Minimum (km)
Winter	98	102	220	3
Spring	59	58	137	0
Summer	49	48	134	0
Fall	61	69	195	0

The mass balance of the spilled oil provides a good summary of a particular spill, or, when averaged across all spills, a good understanding of spill behaviour for a spill that would occur in a particular season. Table 8.5.4 summarizes the mass balance for all four seasons at the end of the 10-day stochastic simulation period. The amount of oil bound up in oil-mineral aggregations was negligible.

**Table 8.5.4: Mass Balance Summary for a Medium Case Spill at Site H**

Component	Winter	Spring	Summer	Fall	Yearly Average
On Shore	55.1	25.8	20.5	35.0	34.1
Evaporated	20.3	21.3	21.3	20.5	20.9
Left On Water	12.2	36.9	41.0	29.3	29.8
Dissolved	9.2	11.4	12.1	11.0	10.9
Biodegraded	3.2	4.7	5.1	4.1	4.3
OMA	< 0.01	< 0.01	< 0.01	< 0.01	< 0.01
On Banks	0	0	0	0	0
Dispersed	1.2	1.8	4.5	0.9	2.1

## 8.6 Site FR: Fraser River at Port Mann Bridge

The Fraser River Site, referred as Site FR, is located downstream of the Port Mann Bridge. This location has been determined to be representative of a hypothetical incident resulting from on-land pipe failure prior to crossing the Fraser River. About 1,250 m<sup>3</sup> of oil are spilled and enter the Fraser River.

Figures 8.6.1 and 8.6.2 show the 50% (P<sub>50</sub>) and 90% (P<sub>90</sub>) probability maps at Hour 12 i.e., 12 hours after the start of the incident, and Hour 24.

The length of shoreline oiled is relevant for determining potential ecological damage, and for estimating shoreline clean up resources that would be required in the unlikely event of a spill. Figure FR.3-5 illustrates the length of shoreline contacted by oil for the summer simulations. Basic statistics on shoreline oiling for all seasons are presented in Table 8.6.1.

**Table 8.6.1: Statistics for Shoreline Contact for a Pipe Failure at Site FR**

	Median (km)	Average (km)	Maximum (km)	Minimum (km)
Winter	35	34	53	13
Spring	23	25	63	5
Summer	31	33	65	8
Fall	35	36	63	8

The mass balance of the spilled oil provides a good summary of a particular spill, or, when averaged across all spills, a good understanding of spill behaviour for a spill that would occur in a particular season. Figures FR.3-8 and FR.3-9 show the mass balance for the summer spill scenario. Figure FR.3-8 shows the major components: on water, on shore and evaporated, and Figure FR.3-9 shows the minor components: dispersed, bio-degraded, on banks and dissolved.

Table 8.6.2 summarizes the mass balance for all four seasons at the end of the tracking period. The amount of oil bound up in oil-mineral aggregations was negligible: the potential to form OMA was greater in the Fraser River than in any other sites of study. However, the required energy level to mix the oil and form the

OMA wasn't present in the river. The amount of sunken oil was greater than at the other sites because of the lighter surface water density in the Fraser River.

**Table 8.6.2: Mass Balance Summary for a Pipe Failure at Site FR**

Component	Winter	Spring	Summer	Fall	Yearly Average
Fraction on shore (%)	84.2	58.7	69.1	83.1	73.8
Fraction evaporated (%)	11.0	8.8	9.8	10.5	10.0
Fraction on water (%)	2.9	30.7	19.3	4.7	14.4
Fraction dissolved (%)	0.5	0.5	0.6	0.7	0.6
Fraction biodegraded (%)	0.5	1.0	0.8	0.6	0.7
Fraction on banks (%)	0	0	0	0	0
Fraction OMA (%)	0	0	0	0	0
Fraction Sunk (%)	0.9	0.3	0.4	0.4	0.5
Fraction dispersed (%)	0	0	0	0	0

The differences observed within seasons are very interesting and reflect the strong dependence of the oil on the state of currents. During the spring season, when the freshet is at its maximum, the oil is carried out onto the Strait of Georgia, whereas other seasons show the oil going upstream and downstream the river, depending on tide conditions, and becoming mainly retained by the shores of the river.

## 8.7 Synthesis of Marine Spills Stochastic Results

### 8.7.1 CWC (16,500 m<sup>3</sup>)

In order to obtain a general understanding of spill behaviour in the CWC scenario in the marine environment (Sites D, E, G and H), the stochastic results corresponding to the summer season are summarized into the following Table 8.7.1.

**Table 8.7.1: Summary of Stochastic Modelling Results**

Property	Strait of Georgia	Arachne Reef	Race Rocks	Buoy J	Group Average
P <sub>50</sub> area at 24 hours (km <sup>2</sup> )	364	196	372	261	298
P <sub>50</sub> area at 48 hours (km <sup>2</sup> )	1,033	646	674	592	736
Shore oiled at 24 hours (km)	15	36	7	0	15
Shore oiled at 48 hours (km)	78	85	29	< 1	64
Shore oiled at 15 days (km)	279	309	114	81	196
Fraction on shore at 15 days (%)	66.4	69.8	67.1	28.2	57.8
Fraction evaporated 15 days (%)	19.3	18.8	19.7	24.2	20.4



**Table 8.7.1: Summary of Stochastic Modelling Results**

Property	Strait of Georgia	Arachne Reef	Race Rocks	Buoy J	Group Average
Fraction on water at 15 days (%)	2.4	2.9	4.3	31	10.1
Fraction dissolved at 15 days (%)	6.7	5.7	6.1	10	7.2
Fraction biodegraded at 15 days (%)	2.7	2.8	2.7	6.6	3.7
Fraction on banks at 15 days (%)	2.5	< 0.01	0	0	0.8
Fraction OMA at 15 days (%)	< 0.01	< 0.01	0.02	< 0.01	< 0.01
Fraction dispersed at 15 days (%)	0	< 0.01	0.1	8.7	2.9

It is clear that there are substantial differences. Spills in the inshore waters are generally larger in aerial extent than a spill at Buoy J, on the continental shelf. The extent of shoreline oiling depends on the proximity of land, and on the complexity of currents at the site: currents at the Race Rocks site and at Buoy J, in summer, are dominated by the large-scale estuarine flow in these areas, whereas in the Strait of Georgia and Haro Strait, currents tend to be more tidal. The fraction evaporated is relatively constant for all four sites. The amount remaining on the water surface is much less at the inshore sites, because of the close proximity of shorelines. Biodegraded fractions are generally small, and it is not clear why the greatest biodegradation occurs at Buoy J. The fraction on banks is highest at the Strait of Georgia site, because of the proximity of Roberts and Sturgeon Banks, and the fraction dispersed is highest at Buoy J, because of the greater wave action in the open waters.

## 8.7.2 Medium Spill (8,250 m<sup>3</sup>)

In order to obtain a general understanding of spill behaviour corresponding to a medium size spill in the marine environment (Sites D, E, G and H), the stochastic results corresponding to the summer season are summarized into the following Table 8.7.2.

**Table 8.7.2: Summary of Stochastic Modelling Results**

Property	Strait of Georgia	Arachne Reef	Race Rocks	Buoy J	Group Average
P <sub>50</sub> area at 24 hours (km <sup>2</sup> )	365	195	373	260	298
P <sub>50</sub> area at 48 hours (km <sup>2</sup> )	1,023	628	670	590	728
Shore oiled at 24 hours (km)	14	32	7	0	13
Shore oiled at 48 hours (km)	72	75	29	0.1	44
Shore oiled at 10 days (km)	205	224	88	48	141
Fraction on shore at 10 days (%)	66.1	71.7	67.6	20.5	56.4
Fraction evaporated 10 days (%)	17.2	16.8	17.7	21.3	18.2
Fraction on water at 10 days (%)	4.1	2.8	4.4	41.0	13.1
Fraction dissolved at 10 days (%)	8.8	6.7	8.3	12.1	8.9

**Table 8.7.2: Summary of Stochastic Modelling Results**

Property	Strait of Georgia	Arachne Reef	Race Rocks	Buoy J	Group Average
Fraction biodegraded at 10 days (%)	2.1	2.0	2.0	5.1	2.8
Fraction OMA at 10 days (%)	< 0.01	< 0.01	0.03	< 0.01	< 0.01
Fraction on banks at 10 days (%)	1.7	< 0.01	0	0	0.6
Fraction dispersed at 10 days (%)	< 0.01	0.01	< 0.01	4.5	1.1

The results for the medium size spill are very similar to the CWC scenarios: spills in the inshore waters, such as Site D and Site E, contact a larger length of shoreline than spills closer to the continental shelf, such as Site G and Site H. Patterns regarding the oil weathering is also very similar to the CWC scenario.

The stochastic simulations are invaluable because of their ability to show the consequences of the oceanographic and meteorological forcings in the area, as well as the consequences of the particular characteristics of the transported product, dilbit. However, they achieve greater relevance when these are used as part of the mitigation planning, and as part of the environmental risk assessment, to be discussed in subsequent sections of this document.

## 9.0 THREE-DIMENSIONAL SPECIFIC SIMULATIONS

Specific scenarios, or deterministic simulations, are conducted using the version of SPILLCALC that is embedded in the H3D model. In order to extract a wider range of spill properties, the full 3D simulation represents an extension of the stochastic simulations: certain modules, such as dissolution, are simulated more accurately in those scenarios and the fate of pseudo-components is tracked over the entire water column and model domain. A primary purpose of these simulations is to provide information on the potential toxicity of the spill. A specific scenario can be chosen based on results from the stochastic simulations or according to other criteria. Two deterministic simulations were conducted at Arachne Reef and Westridge Marine Terminal.

### 9.1 Spill at Arachne Reef

The waters between Moresby Island and Stuart Island mark the northern entrance to Haro Strait, which runs south-southeasterly between the Gulf Islands on the Canadian side and the San Juan Islands on the US side. Arachne Reef is situated at the northern end of Haro Strait, off to the west side of the Strait. It consists of three drying heads (Sailing Directions, 1979), and has a navigation aid in the form of a light beacon. A plausible but highly unlikely event would be a powered grounding of a laden tanker on Arachne Reef. The northern entrance to Haro Strait has the greatest level of navigation complexity for the entire passage of a Project-related tanker, as well as significant numbers of vessels transiting the Strait. The location also has a very high environmental value for the route with the potential to affect several distinct areas and habitats, including but not limited to Boundary / Semiahmoo Bay, the Gulf / San Juan Islands, the Salish Sea, and Juan de Fuca Strait. The event of a powered grounding of a laden Project-related tanker has low probability due to the proposed use of a tethered tug through this part of the route.

The hypothetical incident is assumed to have occurred at 07:00 on August 23, 2013 and was selected from the 368 independent simulations of the stochastic modelling for a summer spill event. The selection was based on the representativeness of the resulting spill in terms of environmental and human damages: the summer season was selected for the deterministic modelling, as warmer water and air temperatures would facilitate more rapid dissolution and/or volatilization of lighter pseudo-components into water or air, respectively. This is conservative, as the concentration in water or air would be increased by rapid dissolution and/or volatilization. At the same time, generally lower wind speeds during the summer would result in less wave action (hence, less vertical mixing of the water column, and higher concentrations of dissolved hydrocarbons in the surface water layer), as well as less dispersion of evaporated vapours in air. The use of the CLWB product under summer oil spill conditions complements these conservative assumptions, due to the higher concentrations of volatile hydrocarbons in CLWB than in other products with either less condensate, or an alternative diluent such as synthetic oil.

Resulting from the incident, 25% of the impacted tank volume is lost in the first hour and 1,000 m<sup>3</sup> of cargo will flow out of the vessel every hour thereafter until the total spilled volume is reached. A total volume of 16,500 m<sup>3</sup> of oil is released over 13 hours, which is the amount DNV calculated as credible worst case oil spill for a partly loaded Aframax tanker.

## 9.2 Arachne Reef Simulation Results

As described in Section 5.3, the oil spill tracking model SPILLCALC is coupled and runs with the three dimensional hydrodynamic model H3D. When dissolution occurs in SPILLCALC, H3D uses it as an input and tracks the dissolved hydrocarbon being advected horizontally and vertically in the water column.

Since benzene has the highest solubility amongst the 16 other pseudo-components and is particularly toxic, for purposes of describing model outputs, a focus was put on its behaviour in the water column. Figures 9.2.1 to 9.2.3 show the surface dissolved benzene concentration after 13 hours, 24 hours and 48 hours respectively.

Figure 9.2.1 shows the benzene concentration in the surface layer after 13 hours. The maximum concentration area is located in the northern part of Haro Strait, around the release location down to the northwest coast of San Juan Island. A plume of dissolved benzene can be observed (greenish colours) covering the eastern side of Haro Strait down to its connection with the Juan de Fuca Strait. Values observed are typically about 20 times lower than the CCME threshold value.

Figure 9.2.2 shows the benzene concentration in the surface layer after 24 hours. Contrary to Figure 9.2.1, the areas of high concentrations after 24 hours are much less spread out than after 13 hours and occur maximum concentrations between the release site and San Juan Island.

Figure 9.2.3 shows the benzene concentration in the surface layer after 48 hours. The typical concentration at this time in the surface layer is about 100 times lower than the CCME threshold value.

Figure 9.2.4 shows the benzene concentration profile after 13 hours, 24 hours and 48 hours. For each specific time, the profile was plotted at the location presenting the maximum benzene concentration over the entire water column over the entire domain. One can notice that the region of maximum benzene concentration moves southward, following the general current pattern at this time of the year: an outflow from Haro Strait towards the Juan de Fuca Strait and then the Pacific Ocean. This result is an agreement with the stochastic probability map presenting in Section 8. After 13 hours, at the end of the release, a maximum concentration of approximately 0.06 mg/L is observed near the surface. For comparison purpose, the CCME guideline indicates that the threshold for the protection of aquatic life in the marine environment is 0.11 mg/L (<http://st-ts.ccme.ca/?lang=en&factsheet=14>). As time goes on, the maximum benzene concentration, still observed near the surface, decreases to show a maximum value of about 0.01 mg/L after 48 hours. Examination of concentration maps at depths below the surface confirmed that the highest concentrations were found at the surface, and generally immediately under the slick.

Overall, the modelling shows that the dissolved benzene concentration rapidly dilutes with seawater and also diffuses as it enters the water column.

### 9.3 Arachne Reef Air Dispersion

(To be completed in early 2014.)

### 9.4 Spill at the Westridge Marine Terminal

The Westridge scenario is located at the Westridge Terminal in Burrard Inlet, Burnaby. Currents in this area of the inlet are weak: the 95th percentile of ADCP data (Summer Period) installed at the terminal indicates currents under 0.5 m/s (EBA Oceanographic ADCP Report, 2013).

The large spill scenario at the Westridge Terminal occurs during a tanker loading activity: the transfer rate is about 1,545 m<sup>3</sup>/hr per loading arm and it is calculated that a 160 m<sup>3</sup> oil spill could have resulted from a complete rupture to one loading arm based upon an earlier design of the dock complex. Although optimisation of the dock design resulted in a significant reduction of such an oil spill quantity to 103 m<sup>3</sup>, the simulation, which had been planned prior to such optimisation having taken place, was kept to the higher release volume and is therefore a more conservative assumption, i.e. 160 m<sup>3</sup> spill.

It is standard procedure that the receiving tanker be pre-boomed prior to commencement of loading. Since most of the currents are under 0.5 m/s, the threshold for entrainment (i.e. oil leaking through the boom as a result of a swift current) is not reached. To be conservative, a leakage amount of 20% was assumed to have occurred for spill modeling purpose only. Under such an assumption, of the 160 m<sup>3</sup> total spill volume, about 32 m<sup>3</sup> of oil leaks through the boom and enters Burrard Inlet. The remaining 128 m<sup>3</sup> of oil remains contained inside the pre-deployed boom.

The hypothetical incident is assumed to occur at 22:00 on August 21, 2012. Similar to the selection of the Arachne Reef mitigation scenario, the Westridge scenario was selected based on the environmental conditions from the 368 stochastic simulations of the stochastic modelling for a summer spill event. The selection was based on the representativeness of the resulting spill in terms of environmental and human risks: the summer season was selected for the deterministic modeling, as warmer water and air temperatures would facilitate more rapid dissolution and/or volatilization of lighter pseudo-components

into water or air, respectively. This is conservative, as the concentration in water or air would be increased by rapid dissolution and/or volatilization. At the same time, generally lower wind speeds during the summer would result in less wave action (hence, less vertical mixing of the water column, and higher concentrations of dissolved hydrocarbons in the surface water layer), as well as less dilution of vapours in air. The use of the CLWB product under summer oil spill conditions complements these conservative assumptions, due to the higher concentrations of volatile hydrocarbons in CLWB than in other products with either less condensate, or an alternative diluent such as synthetic oil.

## 9.5 Westridge Marine Terminal Simulation Results

As described in Section 5, the oil spill tracking model SPILLCALC is coupled and runs with the three dimensional hydrodynamic model H3D for the deterministic simulations. When dissolution occurs in SPILLCALC, H3D uses it as an input and tracks the dissolved hydrocarbon being advected horizontally and vertically in the water column.

Since benzene has the highest solubility amongst the 16 other pseudo-components and is particularly toxic, a focus was put on its behaviour in the water column. Figures 9.5.1 to 9.5.5 show the surface dissolved benzene concentration after 1 hour, 6 hours, 12 hours, 24 hours and 48 hours respectively.

Figure 9.5.1 shows the benzene concentration in the surface layer after 1 hour. The maximum concentration area is located in the vicinity of the terminal. The maximum concentration modelled after 1 hour is 0.06 mg/L, hence lower than the CCME threshold value.

Figures 9.5.2 and 9.5.3 show the dissolved benzene concentration in the surface layer after 6 hours and 12 hours respectively. One can see the plume of dissolved benzene travelling with the currents: going towards the west during the first six hours and backing up towards the terminal and Indian Arm when the tide reversed. The maximum concentration is still observed around the terminal with a value about three to four times lower than the CCME threshold value. These high concentrations around the terminal are due to dissolution from the pool of oil contained inside the pre-deployed boom keeping dissolving. It should be noted that most of the dissolved benzene has a concentration about 100 times lower than the CCME guideline.

Finally, Figures 9.5.4 and 9.5.5 show the dissolved benzene concentration in the surface layer after 24 hours and 48 hours. The dissolved benzene spreads over a larger area during this time and shows concentrations becoming much lower. Again, due to the oil contained in the pre-deployed boom and considered to be un-mitigated, the maximum concentration is found in the vicinity of the terminal: about 0.01 mg/L. The typical concentration at this time in the surface layer is about 100 times lower than the CCME threshold value.

Figure 9.5.6 shows vertical profiles of dissolved benzene concentration after 1 hour, 6 hours, 24 hours and 48 hours. The location of the profile is in the close vicinity of the terminal, which is where the maximum concentration is found at all times. The concentration at the surface indicates the on-going dissolution process from the slick inside the pre-deployed boom. In fact, when one considers mitigation, the slick will be pumped out of the pre-deployed boom, resulting in less dissolution.

Overall, the modelling shows that the dissolved benzene concentration rapidly dilutes with seawater and also diffuses as it enters the water column.

## 9.6 Westridge Marine Terminal Air Dispersion

### 9.6.1 Synopsis of Burrard Inlet Winds During the Spill Simulations

Winds through Burrard Inlet at the beginning of the simulation were relatively strong and from the east, with some terrain-influenced southeast winds around the terminal. This pattern begins to shift to southerlies approximately 12 hours following the spill, influenced at the western portion of the inlet by onshore flow which begins to intensify in the afternoon (+15 hrs). Towards late afternoon (+18 hrs), the westerly onshore winds begin to push into the inner portion of Burrard Inlet, funneling into Indian Arm, resulting in a southwesterly pattern around the terminal. Twenty-four hours following the spill, the easterly offshore pattern begins to re-establish, however winds are calmer than the previous day so northeasterly slope flows are also observed. Stronger easterlies begin to develop and persist overnight (+27 hrs). Thirty-six hours following the spill, strong westerlies from Georgia Strait push through the Inlet, persisting until +48 hours when light north-easterly flows are observed once again.

### 9.6.2 160 m<sup>3</sup> Spill Results

Figures 9.6.1 through 9.6.11 show the spatial extent of maximum 1-hour averaged concentrations at ground level over the duration of the simulation for each pseudo-component. The spatial variation in the observed patterns are a function of the relative time variance in the evaporation flux of each pseudo-component from the oil's surface, the migration of the oil escaping the boom and the predominant wind pattern. The evaporated portion of the pseudo-components exhibit a similar transport pattern (fractions that evaporate readily first generally transport to the west; fluxes occurring after 12 hours transport a shorter distance from the terminal in the direction of the wind at the time), however because benzene is most sensitive with respect to human health risk assessment, Figure 9.6.2 (benzene) is described in more detail.

The highest levels (>200 µg/m<sup>3</sup>) were predicted immediately west of the terminal. This is expected because the majority of the spill volume is contained within the berm, the highest evaporation of benzene occurs at the beginning of the simulation and the winds are blowing from the east over this period. The highest amount of benzene which evaporates in the first few hours is transported west down Burrard Inlet with the easterly winds, however these levels are well below 100 µg/m<sup>3</sup>. The shift in the winds described in Section 9.6.1 results in the overall patterns observed in the figure, described in more detail, below.

#### Time Series

Figures 9.6.12 through 9.6.21 show hourly snapshots of the ground level concentration of the evaporated benzene. During the first three hours, a significant amount of benzene evaporates from the oil surface which is either contained within the boom or remains in the water near the terminal. It appears that this benzene transports westward and disperses both laterally and vertically over the first three hours. At +4 hrs, the initial benzene has dispersed below background concentrations west of Burrard Inlet and the pattern predicted by CALPUFF in each individual hour is a result of the prevailing wind direction during that hour. The evaporation flux of benzene has dropped to levels where lateral and vertical dispersion of the initial release lowers the ground level concentration below background in the subsequent hour and the pattern observed is due to the flux occurring only in the current hour.

At +4 hrs, northeasterly winds push the benzene along the southern shore of Burrard Inlet west of the terminal. CALPUFF predicts that low levels of benzene may be observed upslope of Burrard Inlet at Capitol Hill and Burnaby Heights. Since benzene density is three times the density of air, the effects of wind forcing and vertical mixing may account for this.



## 10.0 CONCLUSION

This report documents an investigation into the consequences of a spill of diluted bitumen at a number of candidate locations in the Salish Sea and one location in the Fraser River. This investigation was done on behalf of Trans Mountain Pipelines ULC, as part of their risk assessment for a proposed pipeline expansion and associated increase in marine shipping traffic.

The probability of a spill at several locations was evaluated by DNV. EBA, as described in this report, then conducted spill simulations at selected release points, using the combination of a three-dimensional hydrodynamic circulation model and a coupled oil spill model. Both models are leading-edge investigation tools: the circulation model, H3D, has been widely used in coastal areas, and extensively validated. The oil spill model SPILLCALC incorporates all of the significant processes affecting the behaviour and fate of an oil spill, and includes some new quantitative information on weathering specific to diluted bitumen.

Two types of modelling were conducted: stochastic and deterministic. In stochastic modelling, a primary goal is to generate a probability map for oil exposure for the study area, in this case the Salish Sea and the adjacent waters on the continental shelf off the mouth of Juan de Fuca Strait. A different map is generated for each different spill location, and the maps have been segregated, for this report, into seasonal maps. The stochastic modelling was implemented by executing the spill model, for the specific release, every six hours over a full calendar year, to capture the effects of tides, winds, estuarine flow and forcing from the open Pacific. The resulting probability maps do not provide information on a specific spill, but indicate the area that is at risk. An actual spill would only affect a small part of this area, but all parts are at risk.

Next, specific dates and times were selected from the stochastic spills and the simulation repeated, using a full three-dimensional modelling approach. Such deterministic simulations provide an indication of the amount of exposure that would happen as a result of a specific spill.

The results of the modelling have been passed on to TERA/Stantec for ecological assessment. They have also been used by EBA and WCMRC in a companion report, “Trans Mountain Expansion Project Oil Spill Response Simulation Study, Arachne Reef & Westridge Marine Terminal”, to evaluate and potentially optimize spill mitigation practices.



## 11.0 CLOSURE

We trust this report meets your present requirements. If you have any questions or comments, please contact the undersigned.

Sincerely,  
EBA Engineering Consultants Ltd.

Prepared by:



Aurelien Hospital, M.Eng., M.Sc.  
Marine Scientist  
Direct Line: 604. 875.0275 x330  
ahospital@eba.ca

Prepared by:



Travis Miguez, B.Sc.  
Project Scientist – Air Dispersion Meteorology  
Direct Line: 604. 875.0275 x294  
jstronach@eba.ca

Reviewed by:



Jim Stronach, Ph.D. P.Eng.  
Principal Specialist  
Direct Line: 604. 875.0275 x251  
jstronach@eba.ca

AH/JAS/rbt

## REFERENCES

- Arakawa, A. and V.R. Lamb, 1977: Computational design of the basic dynamic processes of the UCLA general circulation model. *Methods of Computational Physics*, 16, 173-263.
- Backhaus, J.O., 1983: A semi-implicit scheme for the shallow water equations for application to shelf sea modelling. *Continental Shelf Research*. 2, 243-254.
- Belore, R. 2010a. Properties and fate of hydrocarbons associated with hypothetical spills in the at the Marine Terminal and in the confined channel assessment area. Contract Report by SL Ross Environmental Research Limited, Ottawa, ON, for the Enbridge Northern Gateway Project, 132 p.
- Belore, R. 2010b. Properties and Fate of Hydrocarbons Associated with Hypothetical Spills in the Open Water Area. Contract Report by SL Ross Environmental Research Limited, Ottawa, ON, for the Enbridge Northern Gateway Project, 44 p.
- Booij, N., IJ. Haagsma, Holthuijsen, L., A. Kieftenburg, R. Ris, A. van der Westhuysen and M. Zijlema, 2006. SWAN User Manual, Cycle III Version 40.51. Delft University of Technology, Netherlands, 111 pp.
- Canadian Council of Ministers of the Environment (CCME) 2008. Canada-Wide Standard for Petroleum Hydrocarbons (PHC) in Soil: Scientific Rationale. Supporting Technical Document.
- Delvigne, G.A.L. and C.E. Sweeney, 1988. Natural Dispersion of Oil. *Oil & Chemical Pollution*, 4, pp. 281-310.
- Det Norske Veritas 2013. General Risk Analysis and Intended Methods of Reducing Risks.
- Det Norske Veritas 2013. Trans Mountain Pipeline Expansion Project – Marine Risk Assessment. Report prepared for Trans Mountain Expansion Project.
- EBA, 2013. Meteorological and Oceanographic Data Relevant to the Proposed Westridge Terminal Shipping Expansion. Report prepared for Trans Mountain Pipeline LP by EBA Engineering Consultants Ltd. 43 pp + figures.
- Environment Canada (EC). 1999. Marine Weather Hazards along the British Columbia Coast.
- Harper, J.R. and M. Kory. 1995. Stranded oil in coarse sediment experiments. Contract Report by Coastal & Ocean Resources Inc., Sidney, BC for Environment Canada, Edmonton, AB, 60 p.
- Khelifa, A., M. Fingas and C. Brown, 2008. "Effects of Dispersants on Oil-SPM Aggregation and Fate in US Coastal Waters". Final Report to the Coastal Research Response Center, University of New Hampshire, July 2008, 38 pp.
- Labrecque, A.J.M., Thomson, R.E., Stacey, M.W. 1994. Residual Currents in Juan de Fuca Strait. *Atmospheric Ocean*. 32(2): 375-394.
- Lange, O.S., 1998. The Wind Came All Ways. Environment Canada, Atmospheric Environment Service.
- Lange, O.S., 2003. Living with Weather along the British Columbia Coast. Environment Canada.

- MacKay, D. and P.J. Leinonen. 1977. Mathematical Model of the Behaviour of Oil Spills on Water with Natural and Chemical Dispersion, Report Submitted to Environmental Protein Service, Department of Fisheries and the Environment. EPS-3-EC-77-19.
- Mackay, D. and W. Zagorsky, 1982. Water-in-oil emulsions: a stability hypothesis. Proceedings, 5<sup>th</sup> Arctic Marine Oilspill Program, Technical Seminar, Environment Canada, pp 61-74.
- Mackay, D.I., I.A. Buist, R. Mascarenhas, and S. Paterson. 1980. Oil spill processes and models. Manuscript Report, Vol. EE-8, Environment Canada, Ottawa.
- Masson, D., 2006. Seasonal Water Mass Analysis for the Strait of Juan de Fuca and Georgia. Atmospheric Ocean. 44(1): 1-15.
- Ministry of Environment (MoE) 2008. Guidelines for Air Dispersion Modelling in British Columbia.
- Murty, T.S., G.A. McBean and B. McKee. 1983. Explosive Cyclogenesis over the Northeast Pacific Ocean. Monthly Weather Review. Vol. 111, 1131-1135.
- Niu, H., L. Zhengkai, K. Lee, P. Kepkay. and J. Mullin. 2011. et al., 2011. Modeling the Long Term Fate of Oil-Mineral-Aggregates (OMAs) in the Marine Environment and Assessment of their Potential Risks. 2011 International Oil Spill Conference. 13 pp.
- Payne, J.R., B.E. Kirstein, J.R. Clayton, C. Clary, R. Redding, D. McNabb and G. Farmer. 1987. Integration of Suspended Particulate Matter and Oil Transportation Study. Report Submitted to Minerals Management Service by Science Application International Corporation. 215 pp.
- Ross, R and I. Buist. 1995. Preliminary laboratory study to determine the effect of emulsification on oilspill evaporation. Proceeding, 18<sup>th</sup> Arctic Marine Oilspill Program, Technical Seminar. Environment Canada, Edmonton, Alberta. pp 61-74.
- Saucier, F.J. and J. Chasseé. 2000: Tidal Circulation and Buoyancy Effects in the St. Lawrence Estuary. Atmosphere-Ocean, 38, 505-556.
- Schrama, E.J. O., and R Ray. 1994. A Preliminary Tidal Analysis of Topex/Poseidon Altimetry. Journal of Geophysical Research, v.99, p 24799.
- Ross, S.L. 2012. Meso-scale weathering of Cold Lake Bitumen/Condensate Blend. Contract Report by SL Ross Environmental Research Limited, Ottawa, ON, 27 p.
- Smagorinsky, J., 1963: General circulation experiments with the primitive equations, I. The basic experiment. Mon. Wea. Rev., 91, 99-164.
- Stronach, J., L. Zaremba, L. Neil, M. Wong, N. McLennan. 2006. Wave and Current Forecast System for the Mouth of the Fraser River. In 9<sup>th</sup> International Workshop on Wave Hindcasting and Forecasting, Victoria, British Columbia, September 24-29, 2006.
- Stronach, J.A., J.O. Backhaus, and T.S. Murty. 1993. An update on the numerical simulation of oceanographic processes in the waters between Vancouver Island and the mainland: the GF8 model, Oceanography and Marine Biology Annual Review, 31:1-86.
- Thompson, R.E., 1981: Oceanography of the British Columbia Coast, Can. Spec. Publ. Fish. Aquat. Sci. 56, 291 pp.

- Tkalich, P. and E.S. Chan, 2002. Vertical mixing of oil droplets by breaking waves, *Marine Pollution Bulletin*, 44, pp 1219-1229.
- Waldichuk M. 1957. Physical Oceanography of the Strait of Georgia, British Columbia. *J. Fish. Res. Board Can.* 14(3): 321-486.
- Witt O'Brien's Polaris Sciences and WCMRC. 2013. A Study of Fate and Behaviour of Diluted Bitumen Oils on Marine Water Dilbit experiments, Gainford, Alberta, Polaris Applied Sciences, Western Canada Marine Response Corporation. Attached to 3.1.
- Xie, H., P.D.Yapa and K. Nakata. 2007. Modelling emulsification after an oil spill in the sea. *Journal of Marine Systems*, 68, pp 489-506.
- Zaremba, L., E. Wang, and J. Stronach, 2005. The physical limnology of Okanagan Lake. In "Water – Our Limiting Resource": Towards Sustainable Water Management in the Okanagan, Proceedings of Canadian Water Resources Association B.C. Branch Conference, Feb. 23-25, 2005, Kelowna, BC. ISBN 1-896513-28-X.
- Zhu, X., A.D. Venosa, M.T, Suidan and K. Lee. 2004. Guideline for the bioremediation of oil-contaminated salt marshes. U.S. EPA Report: EPA/600/R-04/074. et al., 2004).

# FIGURES

---

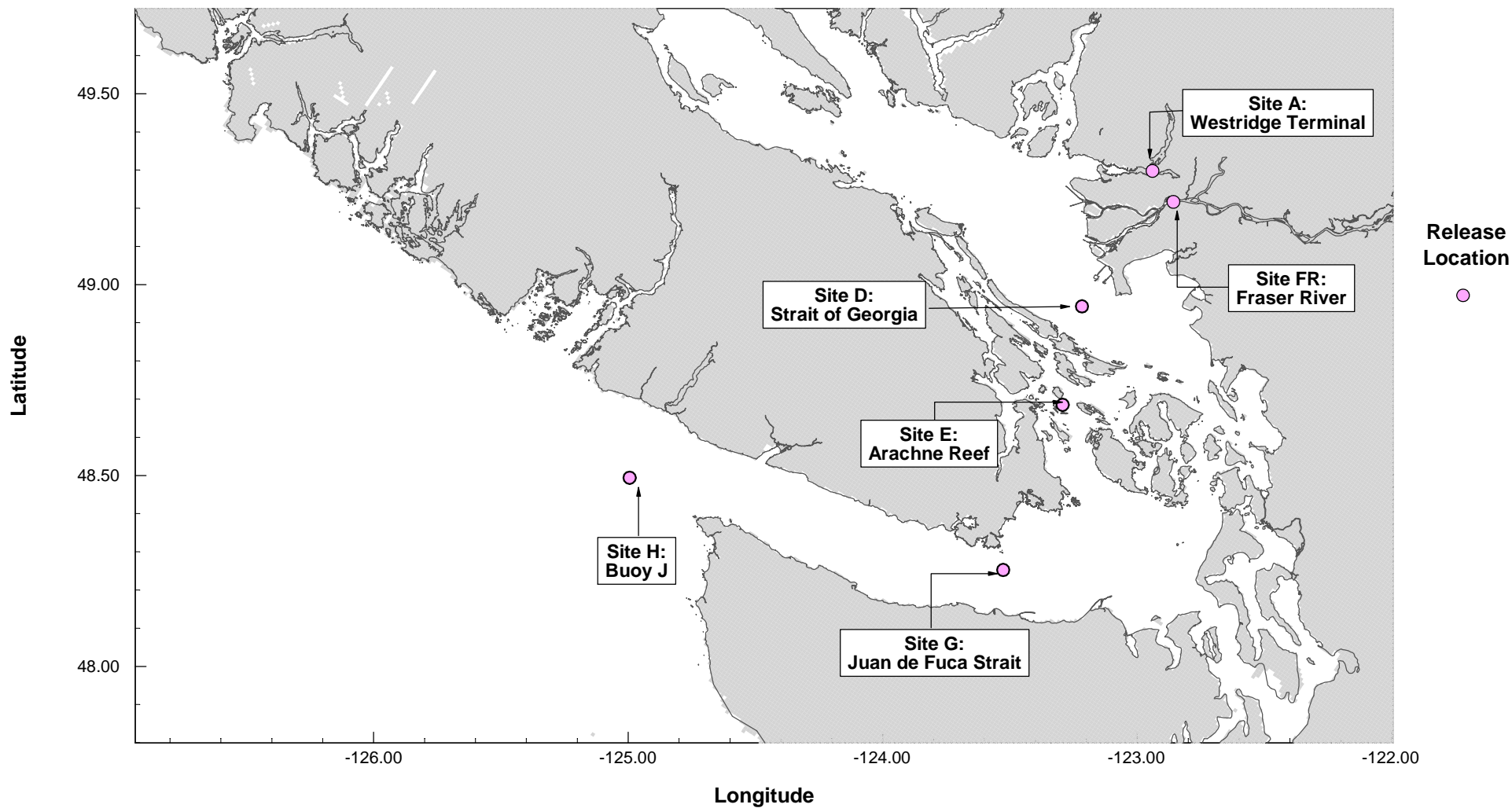
Figure 2.1.1	Sites Location
Figure 3.1.1	Typical Grid Mesh
Figure 3.1.2	Hydrodynamic Model Grid Domains
Figure 3.2.1	Modelled and Predicted Water Levels September 2011
Figure 3.2.2	Modelled and Observed Water Levels September 2011
Figure 3.2.3	Modelled and Observed Water Levels April 2013
Figure 3.2.4	Bob Lord's Drift Path
Figure 3.2.5	Bob Lord's Drift Path Computed by CANSARP
Figure 3.2.6	Bob Lord's Drift Path Computed by SPILLCALC
Figure 5.2.1	Observed and Hind cast Density Time-Series
Figure 5.2.2	Percentage of Oil-SPM Interaction
Figure 8.1.1	Stochastic Simulation Site A (160 m <sup>3</sup> ) P <sub>50</sub> and P <sub>90</sub> after 6 Hours
Figure 8.1.2	Stochastic Simulation Site A (160 m <sup>3</sup> ) P <sub>50</sub> and P <sub>90</sub> after 12 Hours
Figure 8.2.1	Stochastic Simulation Site D (16,500 m <sup>3</sup> ) P <sub>50</sub> and P <sub>90</sub> after 24 Hours
Figure 8.2.2	Stochastic Simulation Site D (16,500 m <sup>3</sup> ) P <sub>50</sub> and P <sub>90</sub> after 48 Hours
Figure 8.2.3	Stochastic Simulation Site D (8,250 m <sup>3</sup> ) P <sub>50</sub> and P <sub>90</sub> after 24 Hours
Figure 8.2.4	Stochastic Simulation Site D (8,250 m <sup>3</sup> ) P <sub>50</sub> and P <sub>90</sub> after 48 Hours
Figure 8.3.1	Stochastic Simulation Site E (16,500 m <sup>3</sup> ) P <sub>50</sub> and P <sub>90</sub> after 24 Hours
Figure 8.3.2	Stochastic Simulation Site E (16,500 m <sup>3</sup> ) P <sub>50</sub> and P <sub>90</sub> after 48 Hours
Figure 8.3.3	Stochastic Simulation Site E (8,250 m <sup>3</sup> ) P <sub>50</sub> and P <sub>90</sub> after 24 Hours
Figure 8.3.4	Stochastic Simulation Site E (8,250 m <sup>3</sup> ) P <sub>50</sub> and P <sub>90</sub> after 48 Hours
Figure 8.4.1	Stochastic Simulation Site G (16,500 m <sup>3</sup> ) P <sub>50</sub> and P <sub>90</sub> after 24 Hours

Figure 8.4.2	Stochastic Simulation Site G (16,500 m <sup>3</sup> ) P <sub>50</sub> and P <sub>90</sub> after 48 Hours
Figure 8.4.3	Stochastic Simulation Site G (8,250 m <sup>3</sup> ) P <sub>50</sub> and P <sub>90</sub> after 24 Hours
Figure 8.4.4	Stochastic Simulation Site G (8,250 m <sup>3</sup> ) P <sub>50</sub> and P <sub>90</sub> after 48 Hours
Figure 8.5.1	Stochastic Simulation Site H (16,500 m <sup>3</sup> ) P <sub>50</sub> and P <sub>90</sub> after 24 Hours
Figure 8.5.2	Stochastic Simulation Site H (16,500 m <sup>3</sup> ) P <sub>50</sub> and P <sub>90</sub> after 48 Hours
Figure 8.5.3	Stochastic Simulation Site H (8,250 m <sup>3</sup> ) P <sub>50</sub> and P <sub>90</sub> after 24 Hours
Figure 8.5.4	Stochastic Simulation Site H (8,250 m <sup>3</sup> ) P <sub>50</sub> and P <sub>90</sub> after 48 Hours
Figure 8.6.1	Stochastic Simulation Site FR (1,250 m <sup>3</sup> ) P <sub>50</sub> and P <sub>90</sub> after 12 Hours
Figure 8.6.2	Stochastic Simulation Site FR (1,250 m <sup>3</sup> ) P <sub>50</sub> and P <sub>90</sub> after 24 Hours
Figure 9.2.1	Benzene Concentration in the Surface Layer after 13 Hours
Figure 9.2.2	Benzene Concentration in the Surface Layer after 24 Hours
Figure 9.2.3	Benzene Concentration in the Surface Layer after 48 Hours
Figure 9.2.4	Profile of Benzene Concentration
Figure 9.5.1	Benzene Concentration in the Surface Layer after 1 Hours
Figure 9.5.2	Benzene Concentration in the Surface Layer after 6 Hours
Figure 9.5.3	Benzene Concentration in the Surface Layer after 12 Hours
Figure 9.5.4	Benzene Concentration in the Surface Layer after 24 Hours
Figure 9.5.5	Benzene Concentration in the Surface Layer after 48 Hours
Figure 9.5.6	Profile of Benzene Concentration
Figure 9.6.1	Volatiles – Maximum 1-hour Average Ground Level Concentration in Air (µg/m <sup>3</sup> ) - 160 m <sup>3</sup> Spill
Figure 9.6.2	Benzene – Maximum 1-hour Average Ground Level Concentration in Air (µg/m <sup>3</sup> ) - 160 m <sup>3</sup> Spill
Figure 9.6.3	TEX – Maximum 1-hour Average Ground Level Concentration in Air (µg/m <sup>3</sup> ) - 160 m <sup>3</sup> Spill
Figure 9.6.4	Aromatics > C8-10 – Maximum 1-hour Average Ground Level Concentration in Air (µg/m <sup>3</sup> ) - 160 m <sup>3</sup> Spill
Figure 9.6.5	Aromatics > C10-12 – Maximum 1-hour Average Ground Level Concentration in Air (µg/m <sup>3</sup> ) - 160 m <sup>3</sup> Spill
Figure 9.6.6	Aromatics > C12-16 – Maximum 1-hour Average Ground Level Concentration in Air (µg/m <sup>3</sup> ) - 160 m <sup>3</sup> Spill
Figure 9.6.7	Aliphatics > C6-8 – Maximum 1-hour Average Ground Level Concentration in Air (µg/m <sup>3</sup> ) - 160 m <sup>3</sup> Spill
Figure 9.6.8	Aliphatics > C8-10 – Maximum 1-hour Average Ground Level Concentration in Air (µg/m <sup>3</sup> ) - 160 m <sup>3</sup> Spill
Figure 9.6.9	Aliphatics > C10-12 – Maximum 1-hour Average Ground Level Concentration in Air (µg/m <sup>3</sup> ) - 160 m <sup>3</sup> Spill
Figure 9.6.10	Aliphatics > C12-16 – Maximum 1-hour Average Ground Level Concentration in Air (µg/m <sup>3</sup> ) - 160 m <sup>3</sup> Spill
Figure 9.6.11	Aliphatics > C16-21 – Maximum 1-hour Average Ground Level Concentration in Air (µg/m <sup>3</sup> ) - 160 m <sup>3</sup> Spill
Figure 9.6.12	Benzene – Average Ground Level Concentration in Air (µg/m <sup>3</sup> ) 0-1 Hours Following the Spill - 160 m <sup>3</sup> Spill

---

Figure 9.6.13	Benzene – Average Ground Level Concentration in Air ( $\mu\text{g}/\text{m}^3$ ) 1-2 Hours Following the Spill - 160 $\text{m}^3$ Spill
Figure 9.6.14	Benzene – Average Ground Level Concentration in Air ( $\mu\text{g}/\text{m}^3$ ) 2-3 Hours Following the Spill - 160 $\text{m}^3$ Spill
Figure 9.6.15	Benzene – Average Ground Level Concentration in Air ( $\mu\text{g}/\text{m}^3$ ) 3-4 Hours Following the Spill - 160 $\text{m}^3$ Spill
Figure 9.6.16	Benzene – Average Ground Level Concentration in Air ( $\mu\text{g}/\text{m}^3$ ) 4-5 Hours Following the Spill - 160 $\text{m}^3$ Spill
Figure 9.6.17	Benzene – Average Ground Level Concentration in Air ( $\mu\text{g}/\text{m}^3$ ) 5-6 Hours Following the Spill - 160 $\text{m}^3$ Spill
Figure 9.6.18	Benzene – Average Ground Level Concentration in Air ( $\mu\text{g}/\text{m}^3$ ) 6-7 Hours Following the Spill - 160 $\text{m}^3$ Spill
Figure 9.6.19	Benzene – Average Ground Level Concentration in Air ( $\mu\text{g}/\text{m}^3$ ) 12-13 Hours Following the Spill - 160 $\text{m}^3$ Spill
Figure 9.6.20	Benzene – Average Ground Level Concentration in Air ( $\mu\text{g}/\text{m}^3$ ) 24-25 Hours Following the Spill - 160 $\text{m}^3$ Spill
Figure 9.6.21	Benzene – Average Ground Level Concentration in Air ( $\mu\text{g}/\text{m}^3$ ) 48-49 Hours Following the Spill - 160 $\text{m}^3$ Spill
Figure 9.6.22	Volatiles – Maximum 1-hour Average Ground Level Concentration in Air ( $\mu\text{g}/\text{m}^3$ ) - 10 $\text{m}^3$ Spill
Figure 9.6.23	Benzene – Maximum 1-hour Average Ground Level Concentration in Air ( $\mu\text{g}/\text{m}^3$ ) - 10 $\text{m}^3$ Spill
Figure 9.6.24	TEX – Maximum 1-hour Average Ground Level Concentration in Air ( $\mu\text{g}/\text{m}^3$ ) - 10 $\text{m}^3$ Spill
Figure 9.6.25	Aromatics > C8-10 – Maximum 1-hour Average Ground Level Concentration in Air ( $\mu\text{g}/\text{m}^3$ ) - 10 $\text{m}^3$ Spill
Figure 9.6.26	Aromatics > C10-12 – Maximum 1-hour Average Ground Level Concentration in Air ( $\mu\text{g}/\text{m}^3$ ) - 10 $\text{m}^3$ Spill
Figure 9.6.27	Aromatics > C12-16 – Maximum 1-hour Average Ground Level Concentration in Air ( $\mu\text{g}/\text{m}^3$ ) - 10 $\text{m}^3$ Spill
Figure 9.6.28	Aliphatics > C6-8 – Maximum 1-hour Average Ground Level Concentration in Air ( $\mu\text{g}/\text{m}^3$ ) - 10 $\text{m}^3$ Spill
Figure 9.6.29	Aliphatics > C8-10 – Maximum 1-hour Average Ground Level Concentration in Air ( $\mu\text{g}/\text{m}^3$ ) - 10 $\text{m}^3$ Spill
Figure 9.6.30	Aliphatics > C10-12 – Maximum 1-hour Average Ground Level Concentration in Air ( $\mu\text{g}/\text{m}^3$ ) - 10 $\text{m}^3$ Spill
Figure 9.6.31	Aliphatics > C12-16 – Maximum 1-hour Average Ground Level Concentration in Air ( $\mu\text{g}/\text{m}^3$ ) - 10 $\text{m}^3$ Spill
Figure 9.6.32	Aliphatics > C16-21 – Maximum 1-hour Average Ground Level Concentration in Air ( $\mu\text{g}/\text{m}^3$ ) - 10 $\text{m}^3$ Spill





## NOTES

- Sites A, D, E, G and H are based on the DNV Quantitative Risk Assessment.  
Site FR is based on the Dynamic Risk Assessment.

STATUS  
ISSUED FOR USE

CLIENT



## TRANS MOUNTAIN OIL SPILL STUDY

### Spill Locations for the Stochastic Simulations

PROJECT NO.  
V13203022

DWN  
AH

CKD  
JAS

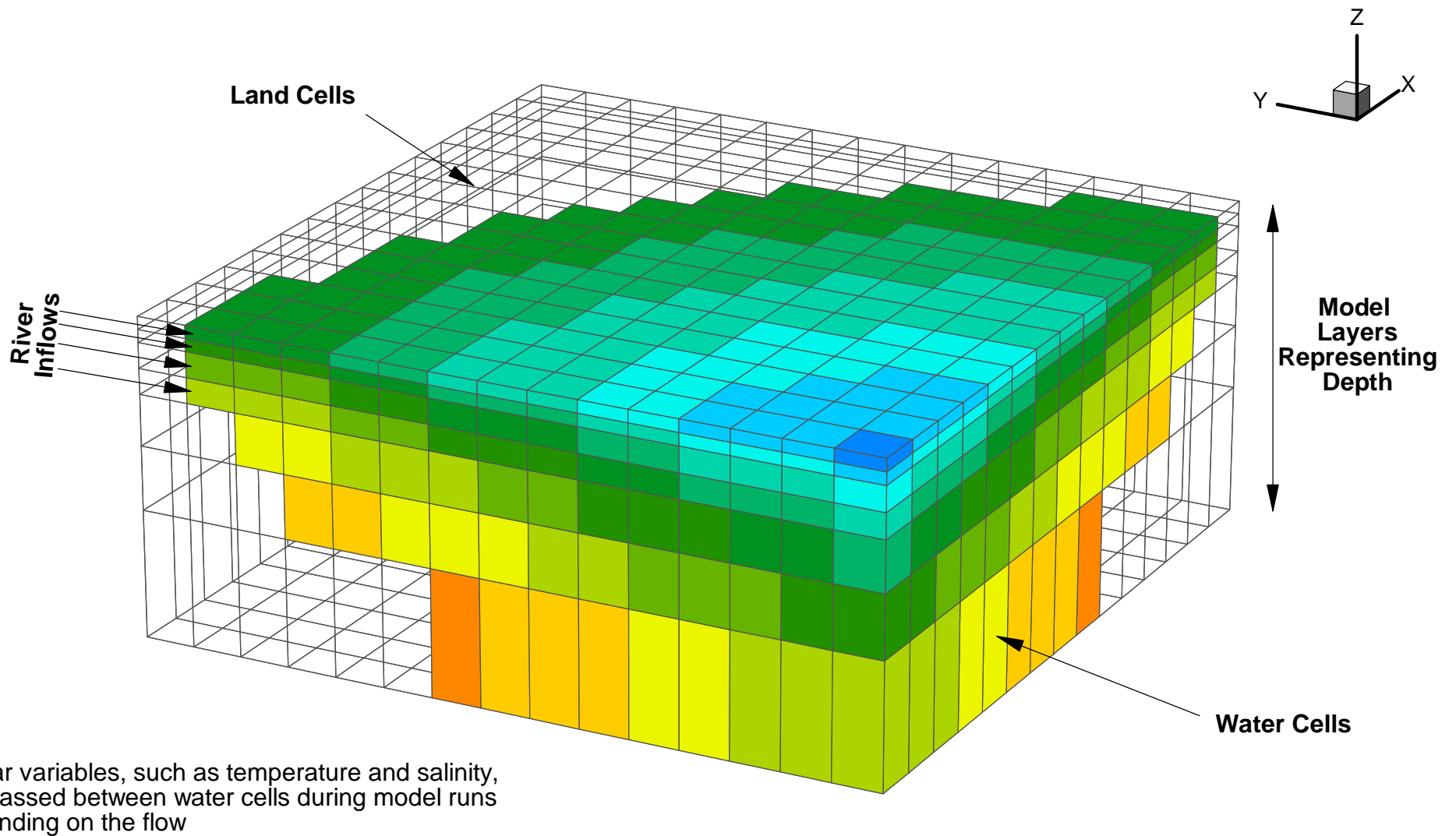
APVD  
JAS

REV  
0

OFFICE  
EBA-VANC

DATE  
October 28, 2013

Figure 2.1.1



## NOTES

Schematic does not represent any particular location

CLIENT



TRANS MOUNTAIN OIL SPILL STUDY

Typical Grid Mesh



PROJECT NO.  
V13203022

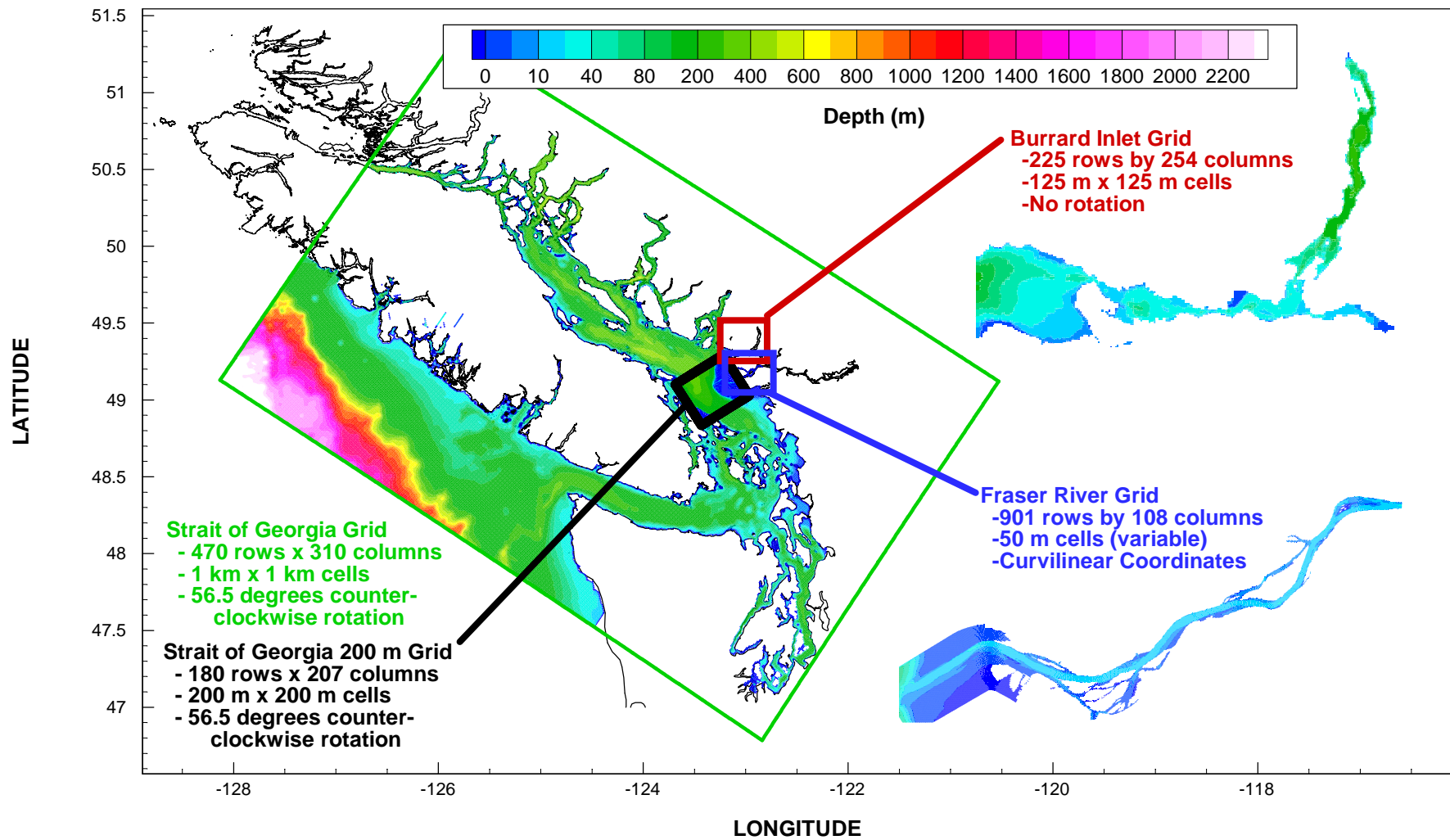
DWN JMR CKD JAS APVD JAS REV 0

OFFICE  
EBA-VANC

DATE  
November 7, 2013

Figure 3.1.1

STATUS  
ISSUED FOR USE



## NOTES

- Model grid was created in a Mercator projection true at 48 degrees 12 minutes N.

STATUS  
ISSUED FOR USE

CLIENT



## TRANS MOUNTAIN OIL SPILL STUDY

### Hydrodynamic Model Grid Domains

PROJECT NO.  
V13203022

OFFICE  
EBA-VANC

DWN  
DP

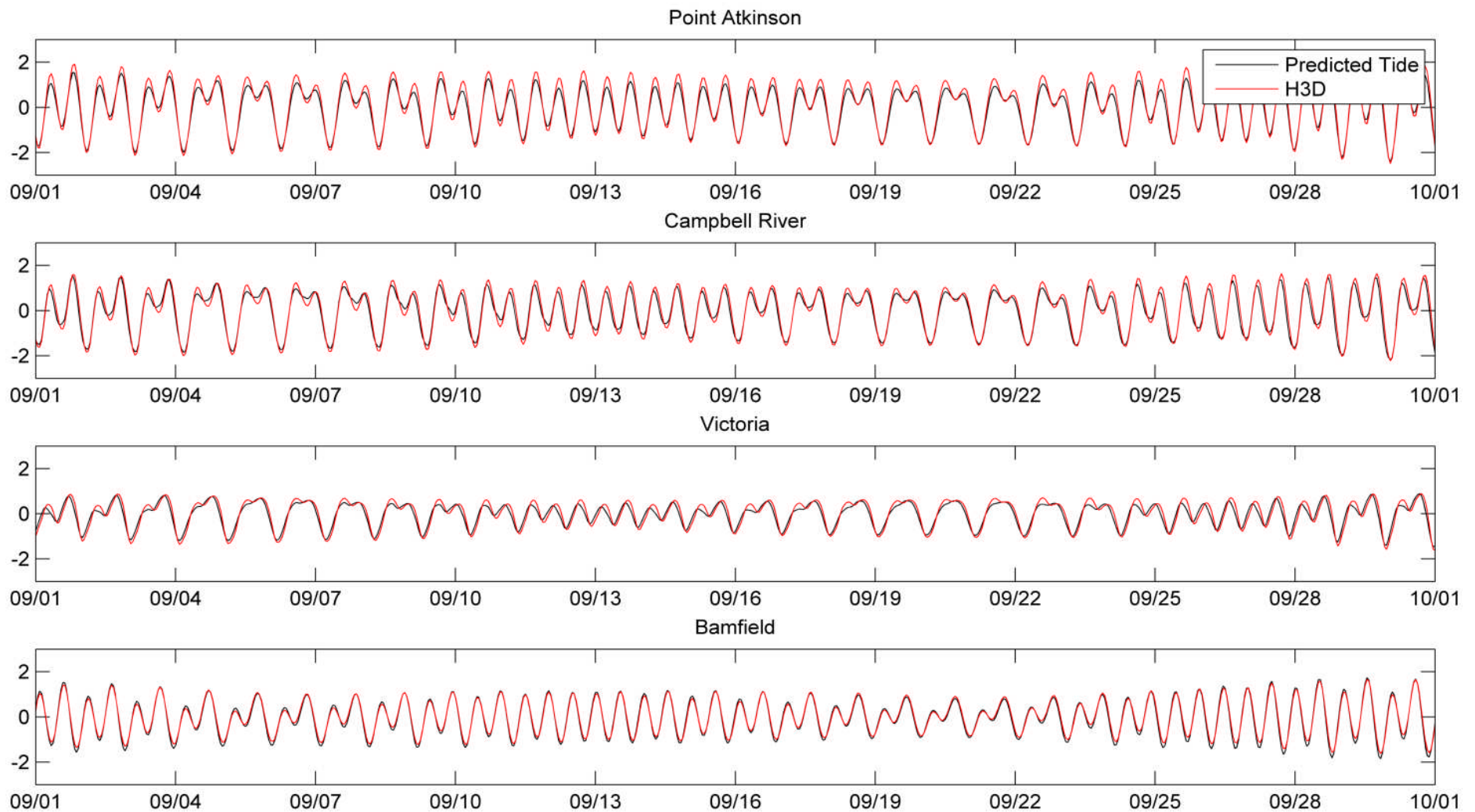
CKD  
AH

APVD  
JAS

REV  
0

DATE  
November 7, 2013

Figure 3.1.2



## NOTES

Modelled water levels are taken from the H3D grid cell closest to the tide gauge  
 Predicted water levels are based on published CHS astronomical tidal constituents

STATUS  
ISSUED FOR USE

CLIENT

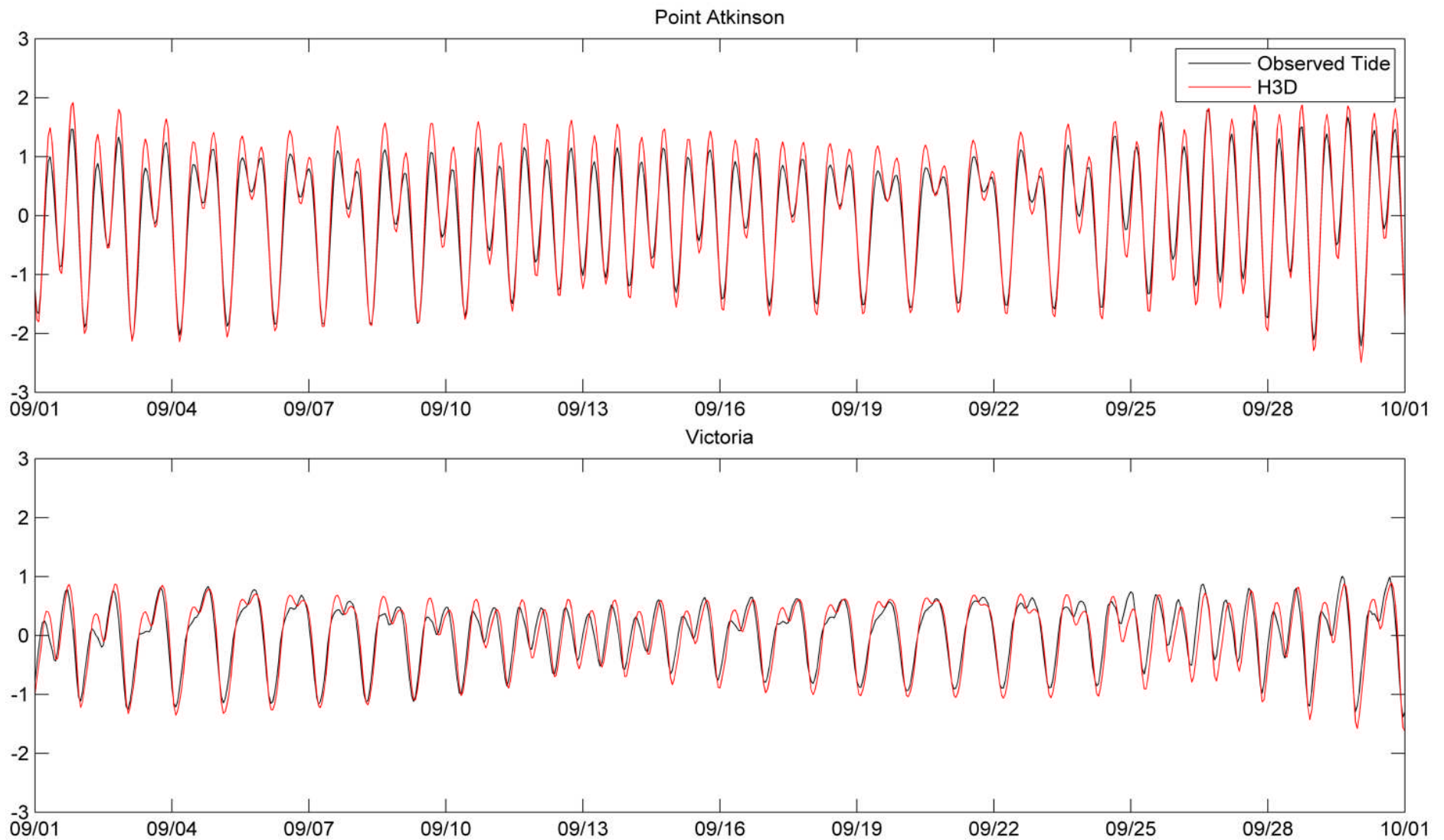


## WESTRIDGE MARINE TERMINAL 2013 OCEANOGRAPHIC DATA REPORT

### Modelled and Predicted Water Levels September 2011

PROJECT NO. V13203022	DWN JMR	CKD JAS	APVD JAS	REV 0	Figure 3.2.1
OFFICE EBA-VANC	DATE October 2013				





## NOTES

Modelled water levels are taken from the H3D grid cell closest to the tide gauge

Observed water levels data source: DFO

STATUS  
ISSUED FOR USE

CLIENT



## WESTRIDGE MARINE TERMINAL 2013 OCEANOGRAPHIC DATA REPORT

### Modelled and Observed Water Levels September 2011

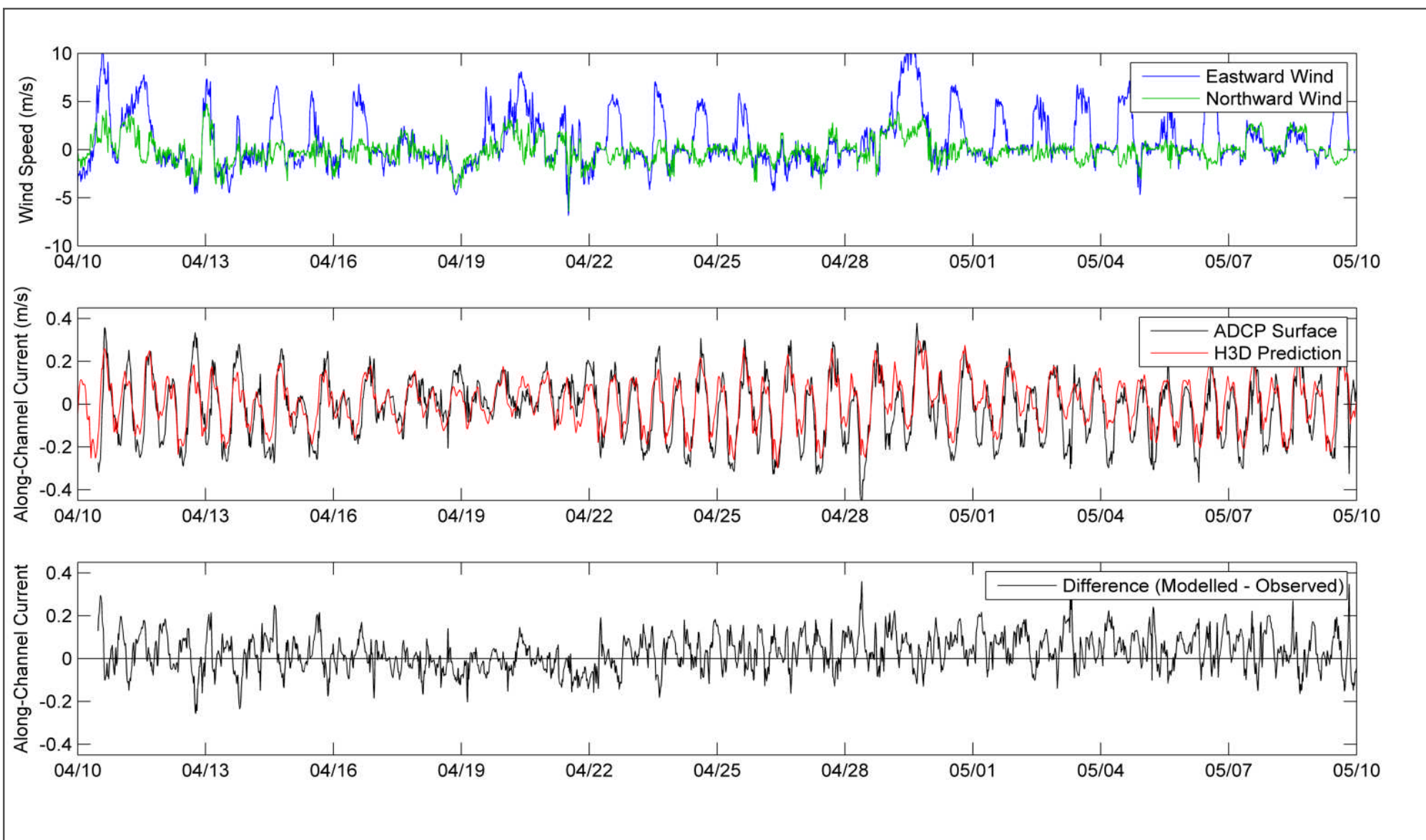
PROJECT NO.  
V13203022

OFFICE  
EBA-VANC

DWN JMR CKD JAS APVD JAS REV 0

DATE  
October 2013

Figure 3.2.2



## NOTES

Observed currents are the along-channel component of the top two metres of available current data. Positive currents are eastward (flood tide).

Modelled water levels are taken from the H3D grid cell closest to the ADCP.

Winds from the Trans Mountain meteorological station were used in the model run.

STATUS  
ISSUED FOR USE

CLIENT



## WESTRIDGE MARINE TERMINAL 2013 OCEANOGRAPHIC DATA REPORT

### Modelled and Observed Surface Currents April 2013

PROJECT NO. V13203022	DWN JMR	CKD JAS	APVD JAS	REV 0
OFFICE EBA-VANC	DATE October 2013			

Figure 3.2.3



Figure 3.2.4: Bob Lord's Drift Path



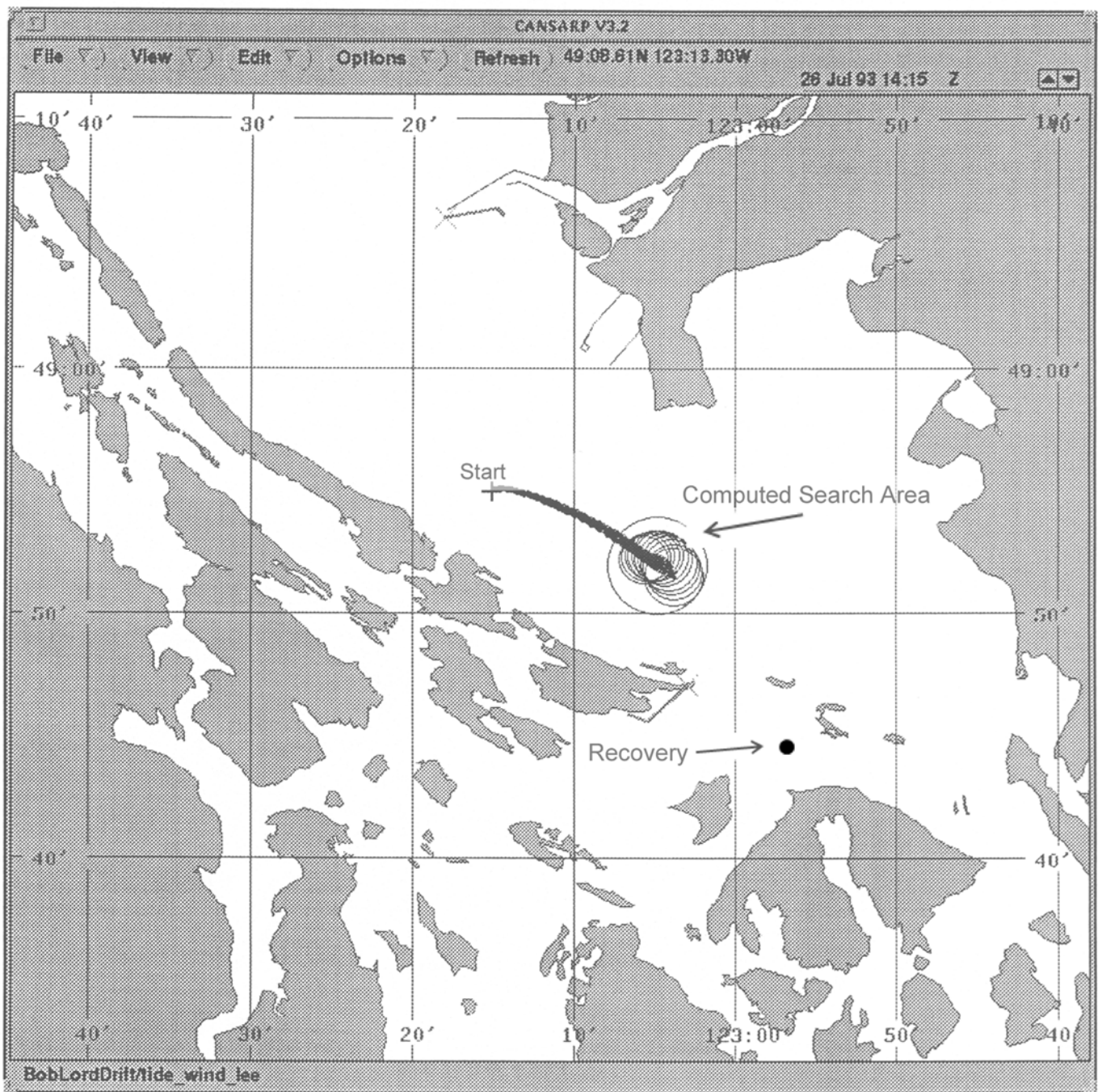


Figure 3.2.5: Bob Lord's Drift Path computed by CANSARP

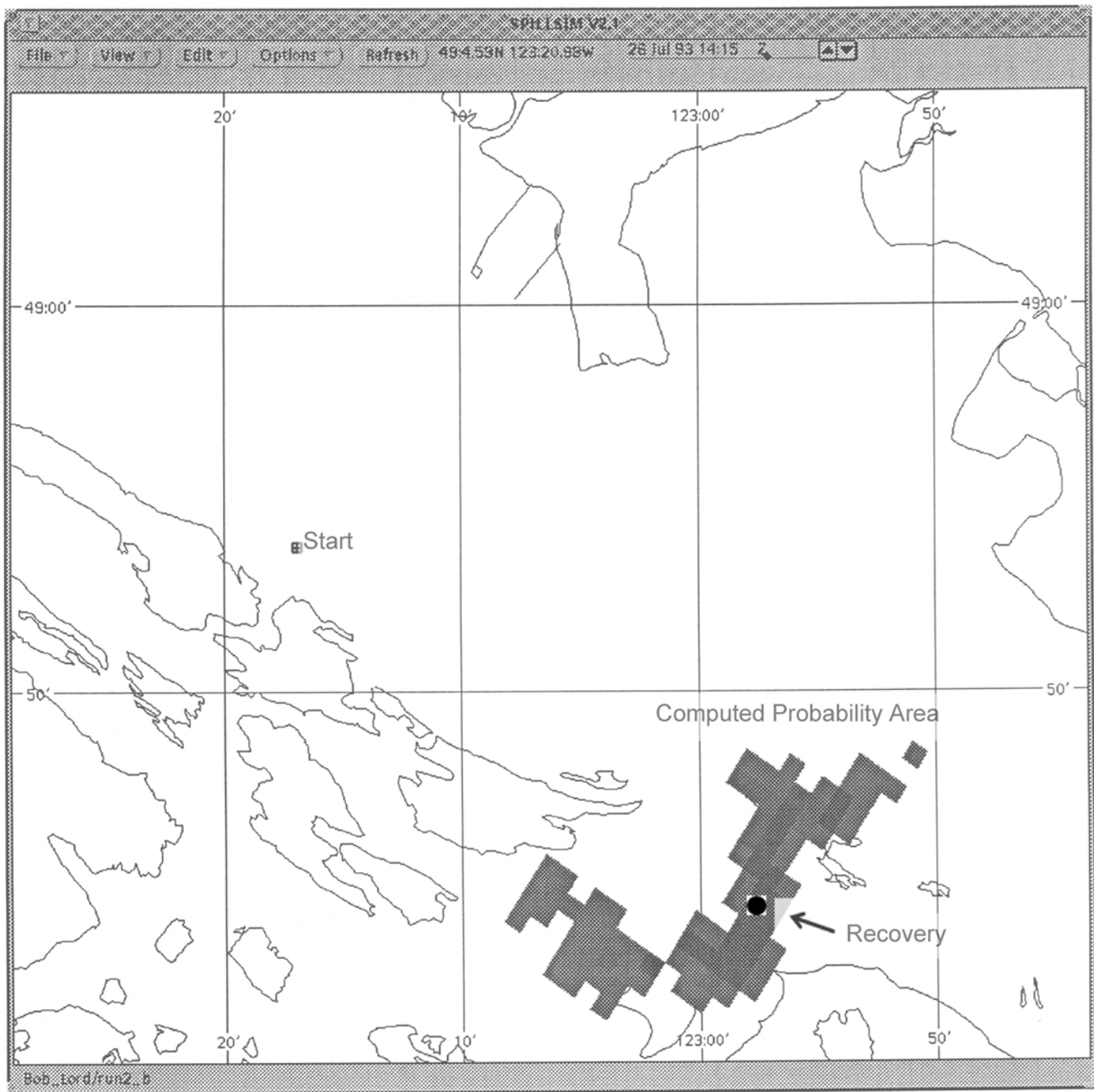
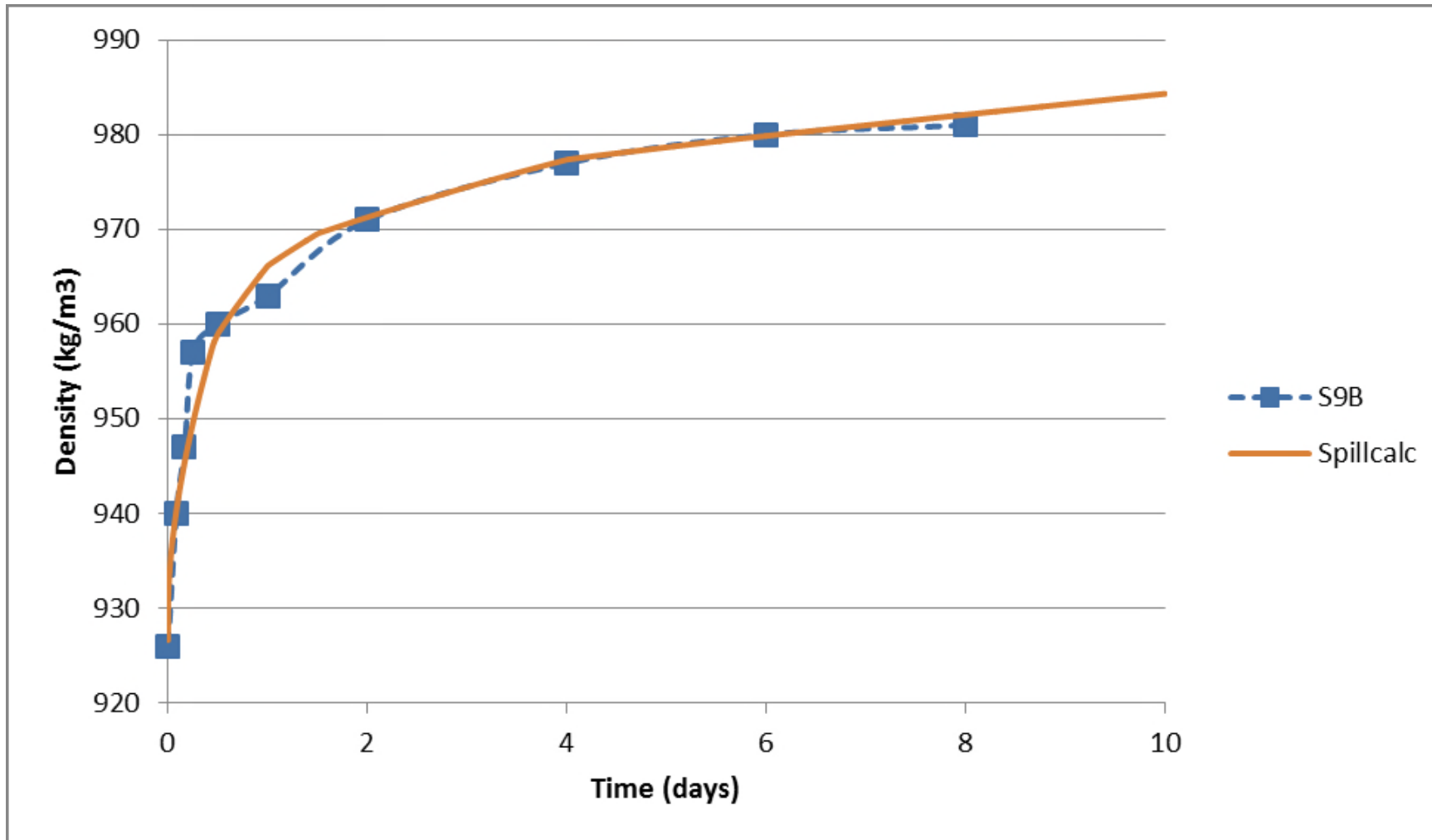


Figure 3.2.6: Bob Lord's Drift Path computed by SPILLCALC



## NOTES

- Conditions from the Gainford Study were reproduced into the oil spill model SPILLCALC.

STATUS  
ISSUED FOR USE

CLIENT

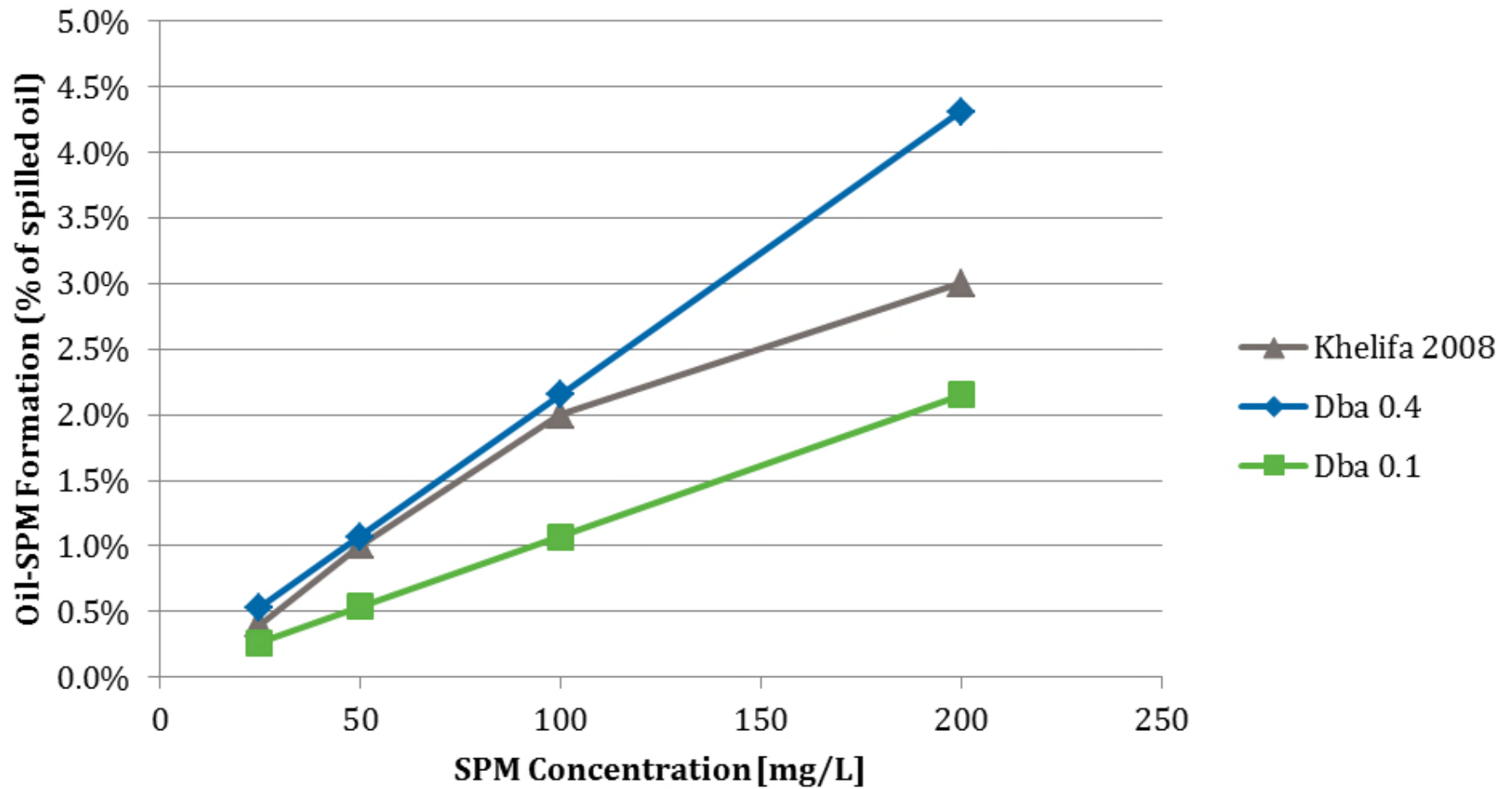


## TRANS MOUNTAIN OIL SPILL STUDY

### Observed and Hindcast Density Time-Series

PROJECT NO. V13203022	DWN AH	CKD JAS	APVD JAS	REV 0
OFFICE EBA-VANC	DATE October 28, 2013			

Figure 5.2.1



## NOTES

- Conditions from Khelifa's experiment were reproduced to the best extent into the oil spill model SPILLCALC.

STATUS  
ISSUED FOR USE

CLIENT



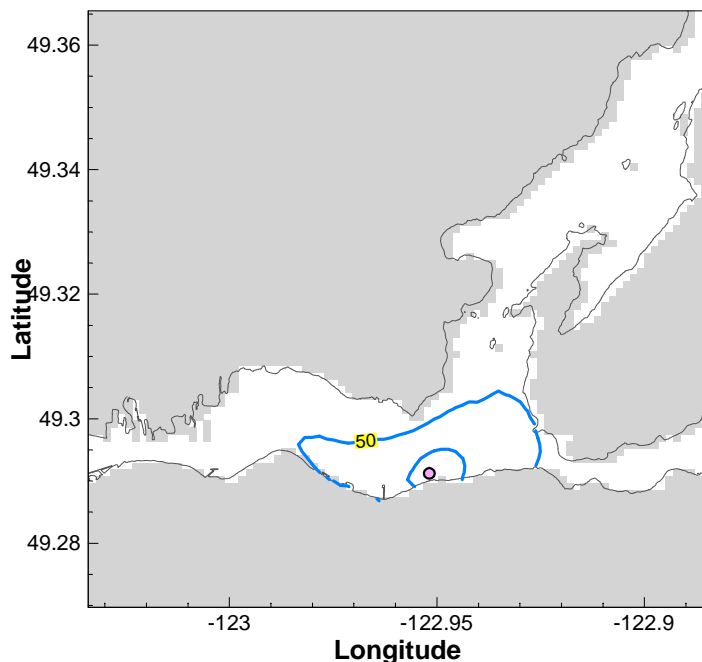
## TRANS MOUNTAIN OIL SPILL STUDY

### Percentage of Oil-SPM Interaction

PROJECT NO. V13203022	DWN AH	CKD JAS	APVD JAS	REV 0
OFFICE EBA-VANC	DATE October 28, 2013			

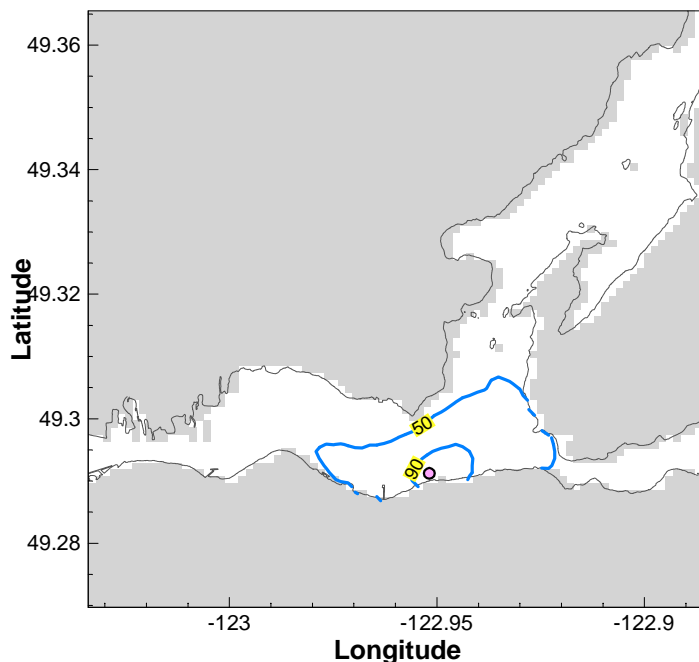
Figure 5.2.2





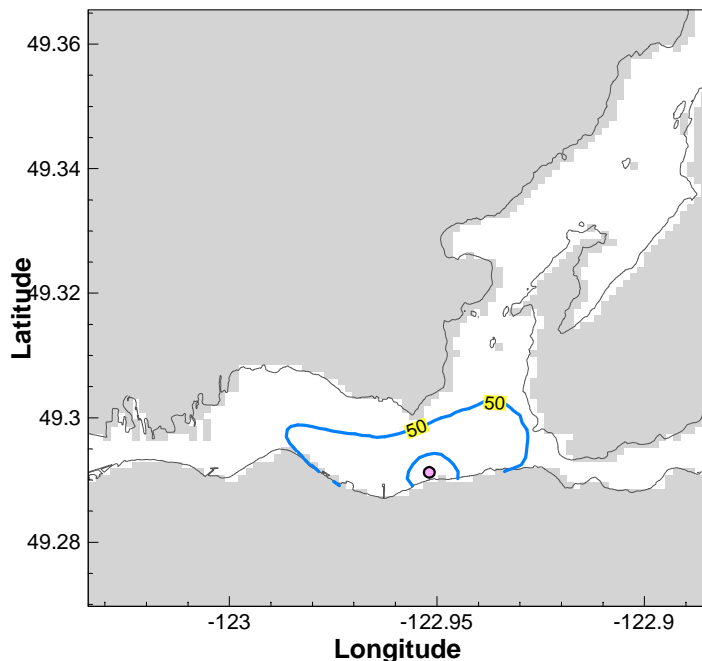
### Winter 2012

Area within the  $P_{50}$  Contour Line: 4.5 km<sup>2</sup>  
 Area within the  $P_{90}$  Contour Line: 0.5 km<sup>2</sup>  
 Average Thickness within the  $P_{50}$  Contour Line: < 1  $\mu$ m  
 Average Thickness within the  $P_{90}$  Contour Line: < 1  $\mu$ m  
 Average Shore Oiled: 5 km



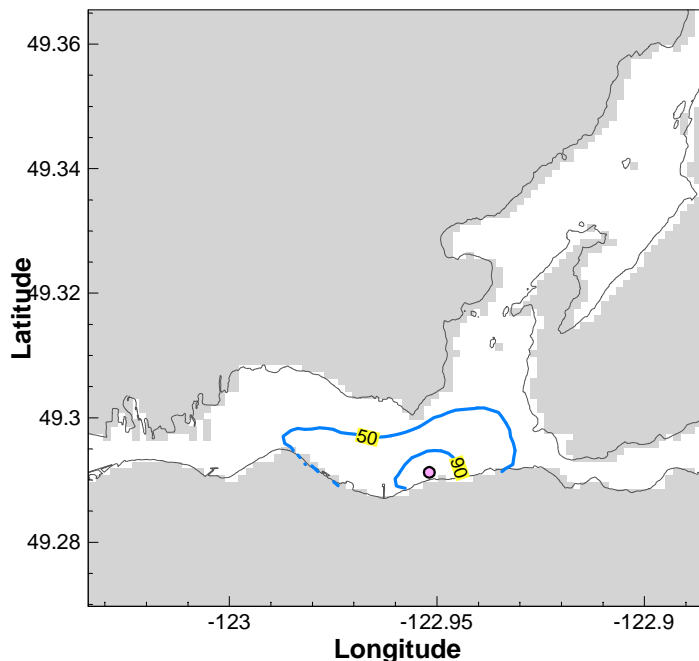
### Spring 2012

Area within the  $P_{50}$  Contour Line: 4.7 km<sup>2</sup>  
 Area within the  $P_{90}$  Contour Line: 0.6 km<sup>2</sup>  
 Average Thickness within the  $P_{50}$  Contour Line: < 0.1  $\mu$ m  
 Average Thickness within the  $P_{90}$  Contour Line: < 0.1  $\mu$ m  
 Average Shore Oiled: 5 km



### Summer 2012

Area within the  $P_{50}$  Contour Line: 4.3 km<sup>2</sup>  
 Area within the  $P_{90}$  Contour Line: 0.4 km<sup>2</sup>  
 Average Thickness within the  $P_{50}$  Contour Line: < 0.1  $\mu$ m  
 Average Thickness within the  $P_{90}$  Contour Line: < 0.1  $\mu$ m  
 Average Shore Oiled: 5 km



### Fall 2011

Area within the  $P_{50}$  Contour Line: 4.1 km<sup>2</sup>  
 Area within the  $P_{90}$  Contour Line: 0.6 km<sup>2</sup>  
 Average Thickness within the  $P_{50}$  Contour Line: < 0.1  $\mu$ m  
 Average Thickness within the  $P_{90}$  Contour Line: < 0.1  $\mu$ m  
 Average Shore Oiled: 5 km

## NOTES

○ Release Location

Probability of oil presence is the percentage of simulations in which oil was present at a given location.  
 $P_{50}$ : after 6 hours, there is 50% or greater probability for the area within the  $P_{50}$  contour line to have been contacted.  
 $P_{90}$ : after 6 hours, there is 90% or greater probability for the area within the  $P_{90}$  contour line to have been contacted.  
 Statistical results for each season based on independent spills occurring every 6 hours for three months.  
 Tracking time for each spill was 6 hours.  
 The average thickness is based on a full coverage of each grid cell that contains oil and lies within the contour line.

STATUS  
ISSUED FOR USE

## CLIENT



TRANSMOUNTAIN



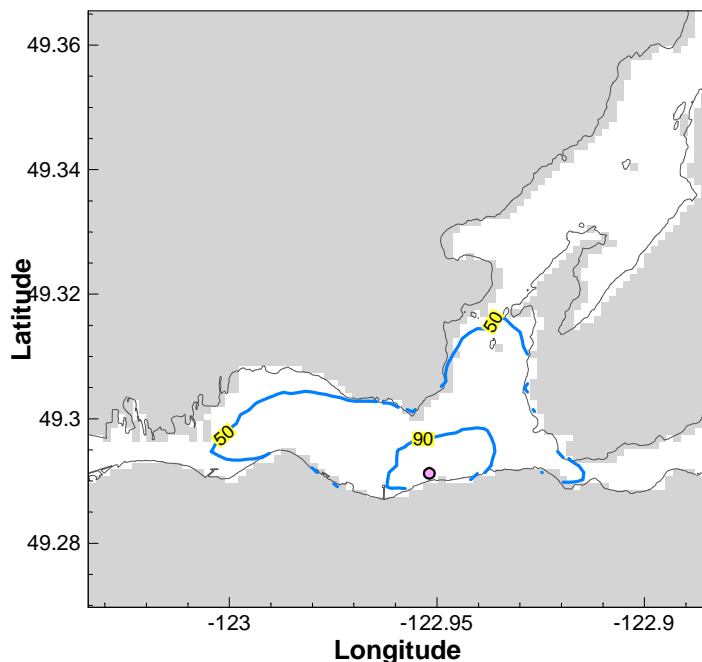
A TETRA TECH COMPANY

## TRANS MOUNTAIN OIL SPILL STUDY

Stochastic Simulation  
 Site A (160 m<sup>3</sup>)  
 $P_{50}$  and  $P_{90}$  after 6 Hours

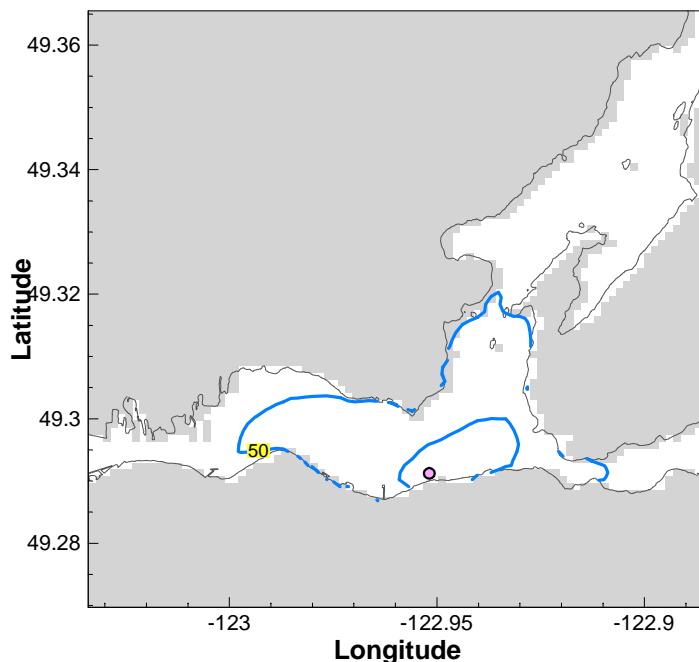
PROJECT NO. V13203022	DWN AH	CKD JAS	APVD -	REV 0
OFFICE EBA-VANC	DATE November 27, 2013			

Figure 8.1.1



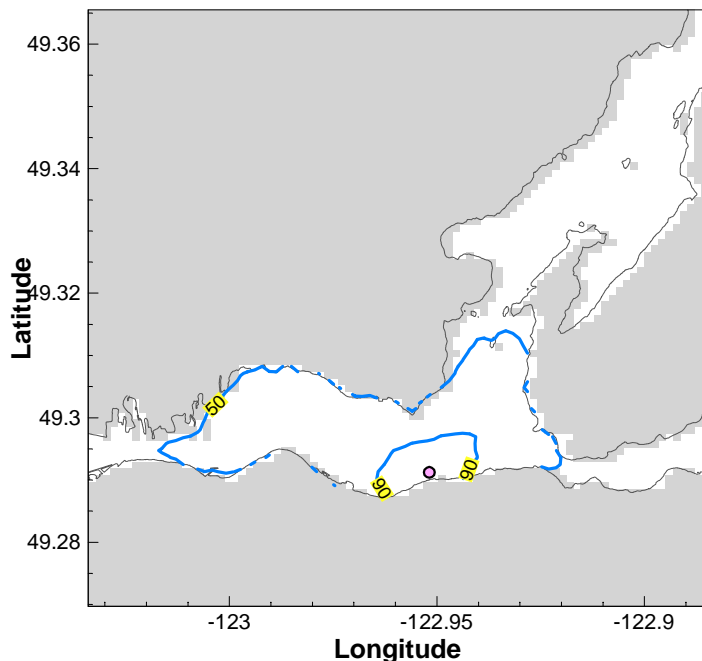
### Winter 2012

Area within the  $P_{50}$  Contour Line: 9.8 km<sup>2</sup>  
 Area within the  $P_{90}$  Contour Line: 1.5 km<sup>2</sup>  
 Average Thickness within the  $P_{50}$  Contour Line: < 1  $\mu$ m  
 Average Thickness within the  $P_{90}$  Contour Line: < 1  $\mu$ m  
 Average Shore Oiled: 9 km



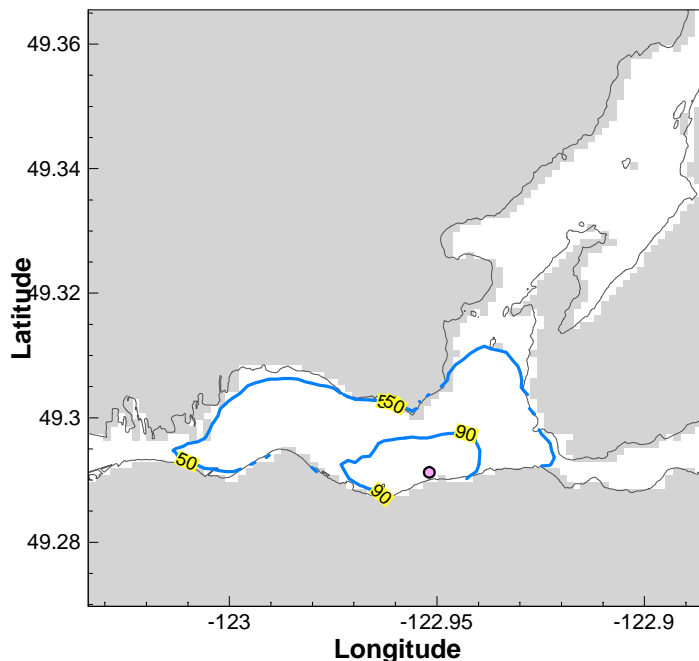
### Spring 2012

Area within the  $P_{50}$  Contour Line: 9.9 km<sup>2</sup>  
 Area within the  $P_{90}$  Contour Line: 1.6 km<sup>2</sup>  
 Average Thickness within the  $P_{50}$  Contour Line: < 0.1  $\mu$ m  
 Average Thickness within the  $P_{90}$  Contour Line: < 0.1  $\mu$ m  
 Average Shore Oiled: 10 km



### Summer 2012

Area within the  $P_{50}$  Contour Line: 11.0 km<sup>2</sup>  
 Area within the  $P_{90}$  Contour Line: 1.3 km<sup>2</sup>  
 Average Thickness within the  $P_{50}$  Contour Line: < 0.1  $\mu$ m  
 Average Thickness within the  $P_{90}$  Contour Line: < 0.1  $\mu$ m  
 Average Shore Oiled: 10 km



### Fall 2011

Area within the  $P_{50}$  Contour Line: 9.9 km<sup>2</sup>  
 Area within the  $P_{90}$  Contour Line: 1.8 km<sup>2</sup>  
 Average Thickness within the  $P_{50}$  Contour Line: < 0.1  $\mu$ m  
 Average Thickness within the  $P_{90}$  Contour Line: < 0.1  $\mu$ m  
 Average Shore Oiled: 9 km

## NOTES

○ Release Location

Probability of oil presence is the percentage of simulations in which oil was present at a given location.  
 $P_{50}$ : after 12 hours, there is 50% or greater probability for the area within the  $P_{50}$  contour line to have been contacted.  
 $P_{90}$ : after 12 hours, there is 90% or greater probability for the area within the  $P_{90}$  contour line to have been contacted.  
 Statistical results for each season based on independent spills occurring every 6 hours for three months.  
 Tracking time for each spill was 12 hours.  
 The average thickness is based on a full coverage of each grid cell that contains oil and lies within the contour line.

STATUS  
ISSUED FOR USE

CLIENT



TRANSMOUNTAIN



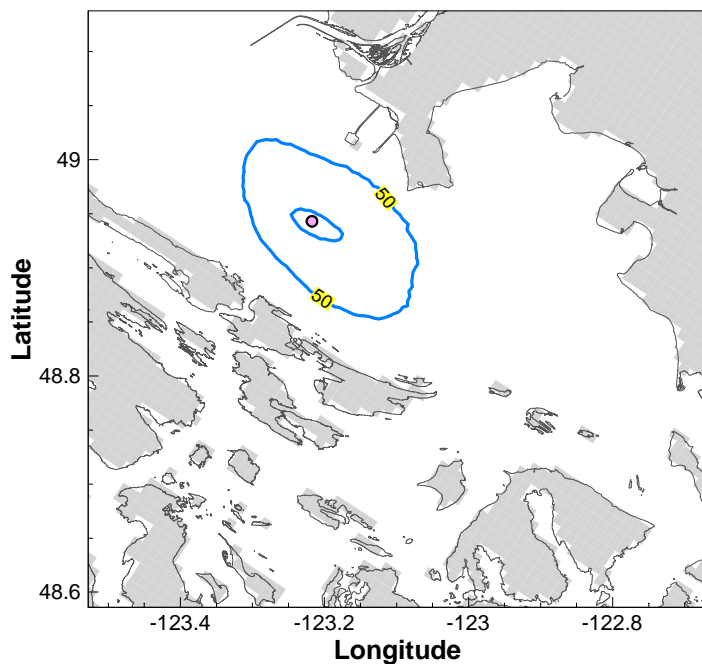
A TETRA TECH COMPANY

## TRANS MOUNTAIN OIL SPILL STUDY

Stochastic Simulation  
 Site A (160 m<sup>3</sup>)  
 $P_{50}$  and  $P_{90}$  after 12 Hours

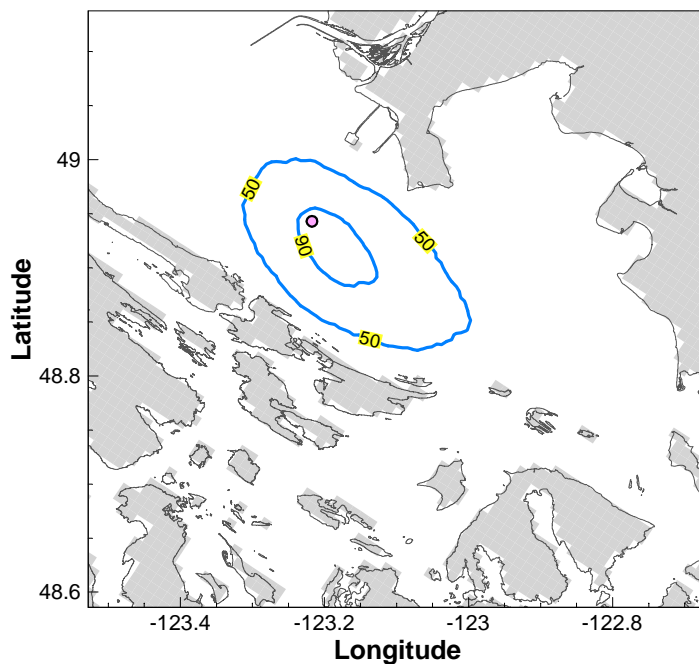
PROJECT NO. V13203022	DWN AH	CKD JAS	APVD -	REV 0
OFFICE EBA-VANC	DATE November 27, 2013			

Figure 8.1.2



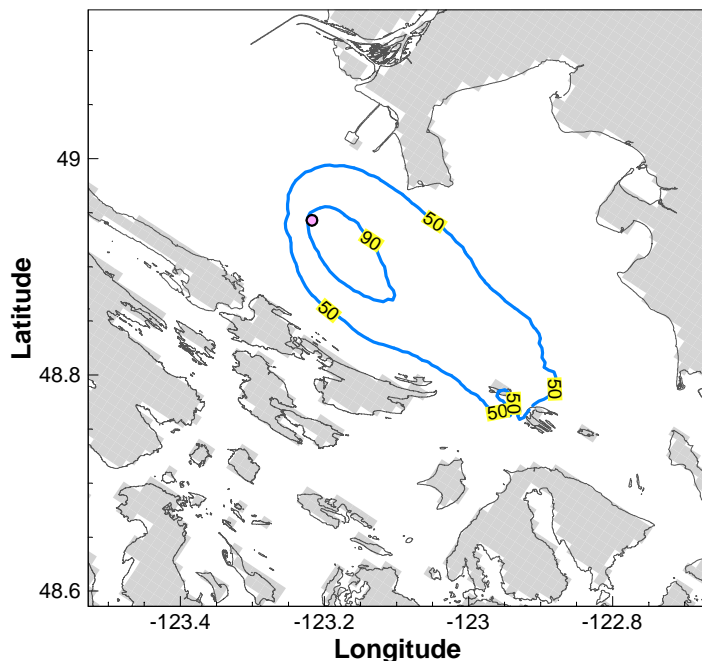
### Winter 2012

Area within the P<sub>50</sub> Contour Line: 217.5 km<sup>2</sup>  
 Area within the P<sub>90</sub> Contour Line: 9.8 km<sup>2</sup>  
 Average Thickness within the P<sub>50</sub> Contour Line: 48 µm  
 Average Thickness within the P<sub>90</sub> Contour Line: 100 µm  
 Average Shore Oiled: 9.5 km



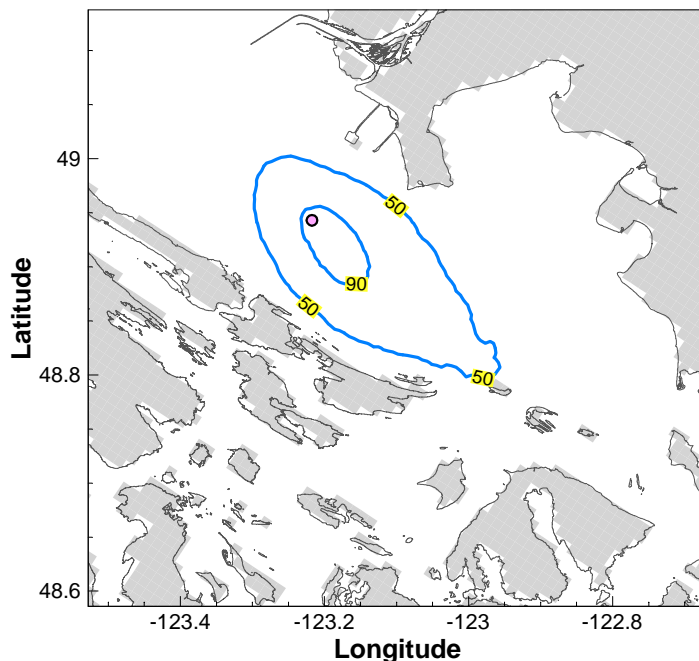
### Spring 2012

Area within the P<sub>50</sub> Contour Line: 285.0 km<sup>2</sup>  
 Area within the P<sub>90</sub> Contour Line: 41.8 km<sup>2</sup>  
 Average Thickness within the P<sub>50</sub> Contour Line: 42 µm  
 Average Thickness within the P<sub>90</sub> Contour Line: 63 µm  
 Average Shore Oiled: 13 km



### Summer 2012

Area within the P<sub>50</sub> Contour Line: 364.2 km<sup>2</sup>  
 Area within the P<sub>90</sub> Contour Line: 48.8 km<sup>2</sup>  
 Average Thickness within the P<sub>50</sub> Contour Line: 34 µm  
 Average Thickness within the P<sub>90</sub> Contour Line: 57 µm  
 Average Shore Oiled: 14.7 km



### Fall 2011

Area within the P<sub>50</sub> Contour Line: 308.0 km<sup>2</sup>  
 Area within the P<sub>90</sub> Contour Line: 36.3 km<sup>2</sup>  
 Average Thickness within the P<sub>50</sub> Contour Line: 37 µm  
 Average Thickness within the P<sub>90</sub> Contour Line: 62 µm  
 Average Shore Oiled: 13 km

## NOTES

○ Release Location

Probability of oil presence is the percentage of simulations in which oil was present at a given location.  
 P<sub>50</sub>: after 24 hours, there is 50% or greater probability for the area within the P<sub>50</sub> contour line to have been contacted.  
 P<sub>90</sub>: after 24 hours, there is 90% or greater probability for the area within the P<sub>90</sub> contour line to have been contacted.  
 Statistical results for each season based on independent spills occurring every 6 hours for three months.  
 Tracking time for each spill was 24 hours.  
 The average thickness is based on a full coverage of each grid cell that contains oil and lies within the contour line.

STATUS  
ISSUED FOR USE

CLIENT



TRANSMOUNTAIN



A TETRA TECH COMPANY

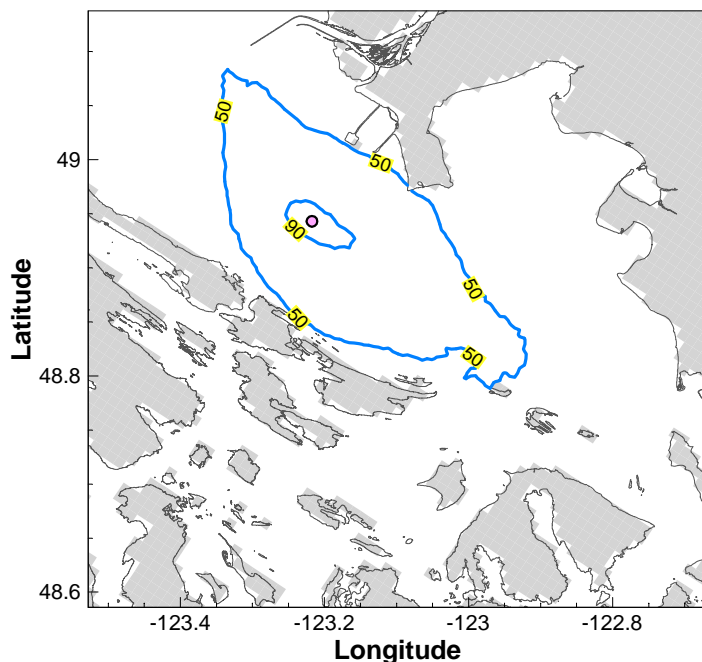
## TRANS MOUNTAIN OIL SPILL STUDY

Stochastic Simulation  
 Site D (16,500 m<sup>3</sup>)  
 P<sub>50</sub> and P<sub>90</sub> after 24 Hours

PROJECT NO.	DWN	CKD	APVD	REV
V13203022	DP	JAS	-	0
OFFICE	DATE			
EBA-VANC	October 25, 2013			

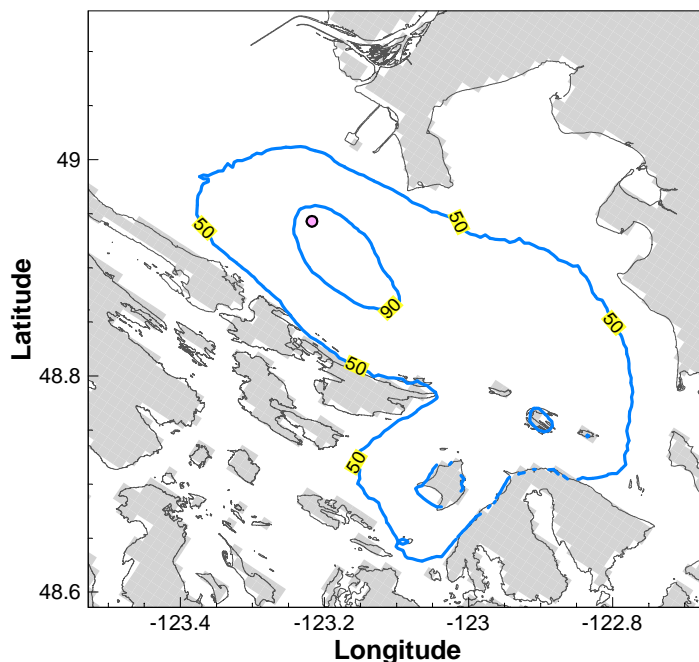
Figure 8.2.1





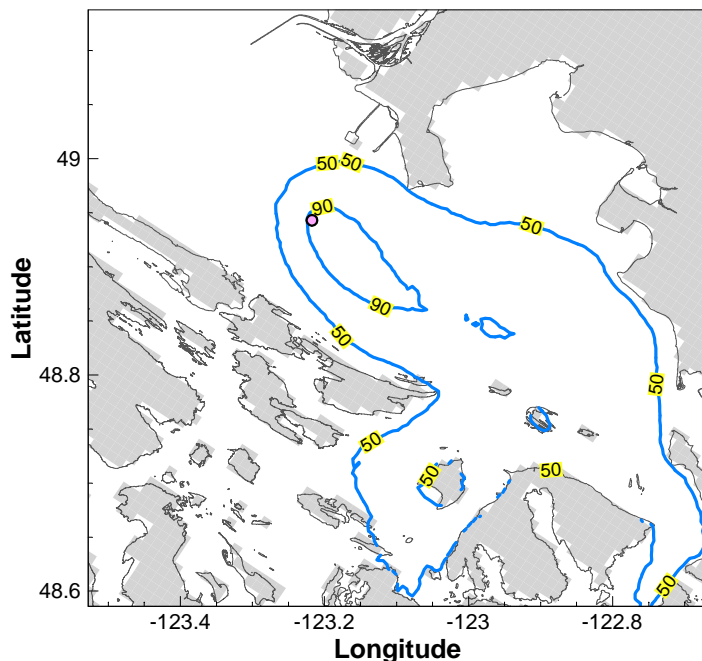
### Winter 2012

Area within the  $P_{50}$  Contour Line: 495.2 km<sup>2</sup>  
 Area within the  $P_{90}$  Contour Line: 19.8 km<sup>2</sup>  
 Average Thickness within the  $P_{50}$  Contour Line: 25 um  
 Average Thickness within the  $P_{90}$  Contour Line: 67 um  
 Average Shore Oiled: 39 km



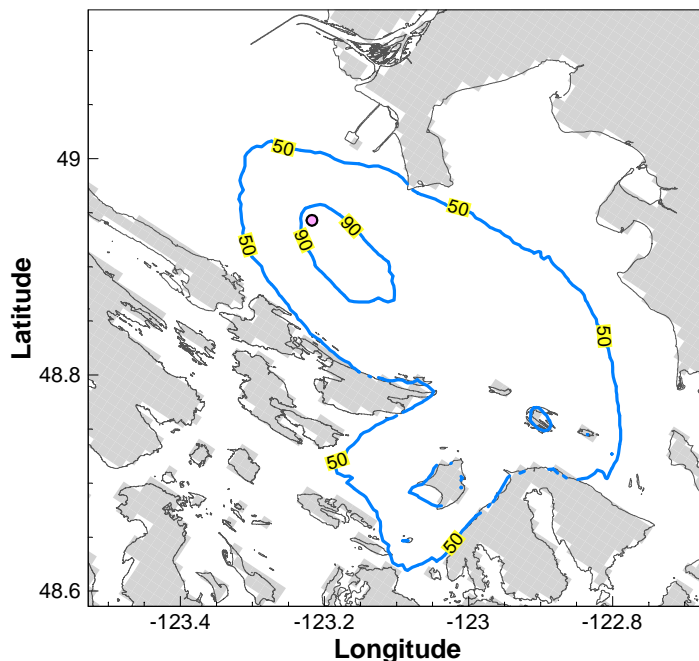
### Spring 2012

Area within the  $P_{50}$  Contour Line: 957.5 km<sup>2</sup>  
 Area within the  $P_{90}$  Contour Line: 66.8 km<sup>2</sup>  
 Average Thickness within the  $P_{50}$  Contour Line: 15 um  
 Average Thickness within the  $P_{90}$  Contour Line: 44 um  
 Average Shore Oiled: 63 km



### Summer 2012

Area within the  $P_{50}$  Contour Line: 1032.7 km<sup>2</sup>  
 Area within the  $P_{90}$  Contour Line: 65.8 km<sup>2</sup>  
 Average Thickness within the  $P_{50}$  Contour Line: 15 um  
 Average Thickness within the  $P_{90}$  Contour Line: 46 um  
 Average Shore Oiled: 77.5 km



### Fall 2011

Area within the  $P_{50}$  Contour Line: 929.7 km<sup>2</sup>  
 Area within the  $P_{90}$  Contour Line: 58.8 km<sup>2</sup>  
 Average Thickness within the  $P_{50}$  Contour Line: 14 um  
 Average Thickness within the  $P_{90}$  Contour Line: 43 um  
 Average Shore Oiled: 63 km

## NOTES

● Release Location

Probability of oil presence is the percentage of simulations in which oil was present at a given location.

$P_{50}$ : after 48 hours, there is 50% or greater probability for the area within the  $P_{50}$  contour line to have been contacted.

$P_{90}$ : after 48 hours, there is 90% or greater probability for the area within the  $P_{90}$  contour line to have been contacted.

Statistical results for each season based on independent spills occurring every 6 hours for three months.

Tracking time for each spill was 48 hours.

The average thickness is based on a full coverage of each grid cell that contains oil and lies within the contour line.

STATUS  
ISSUED FOR USE

CLIENT

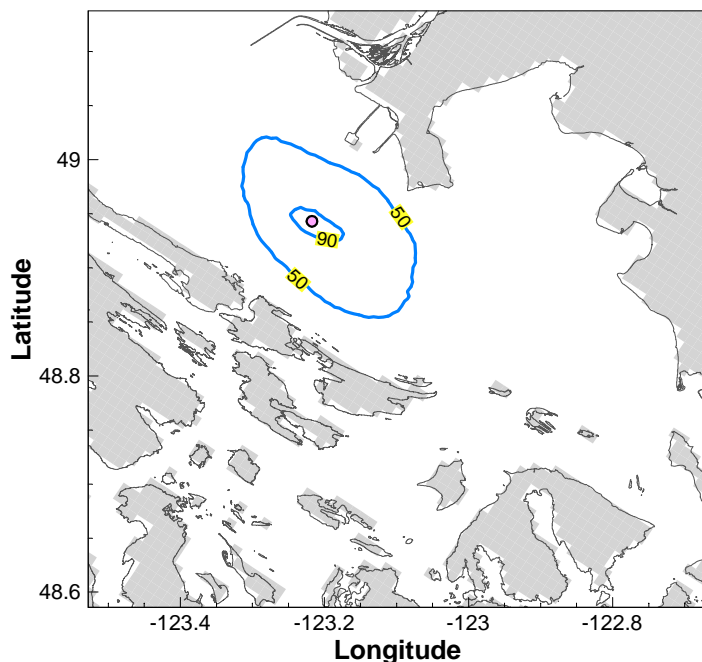


## TRANS MOUNTAIN OIL SPILL STUDY

Stochastic Simulation  
 Site D (16,500 m<sup>3</sup>)  
 $P_{50}$  and  $P_{90}$  after 48 Hours

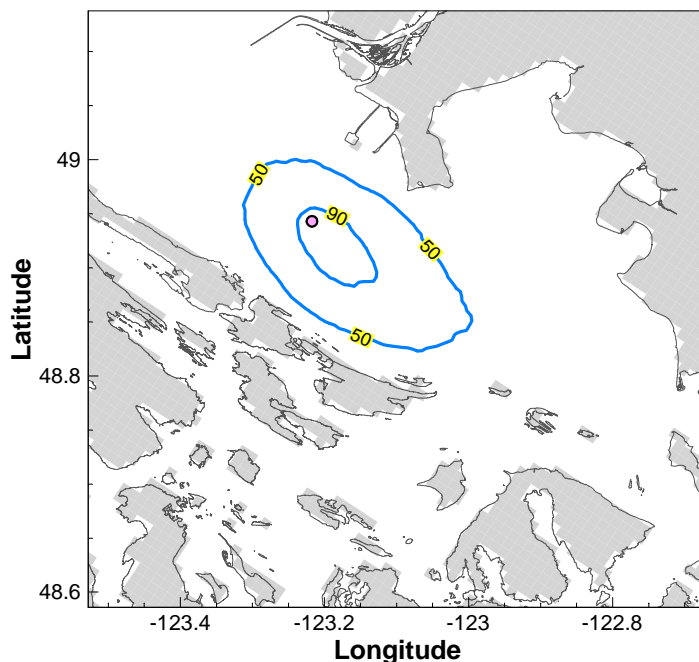
PROJECT NO.	DWN	CKD	APVD	REV
V13203022	DP	JAS	-	0
OFFICE	DATE			
EBA-VANC	October 25, 2013			

Figure 8.2.2



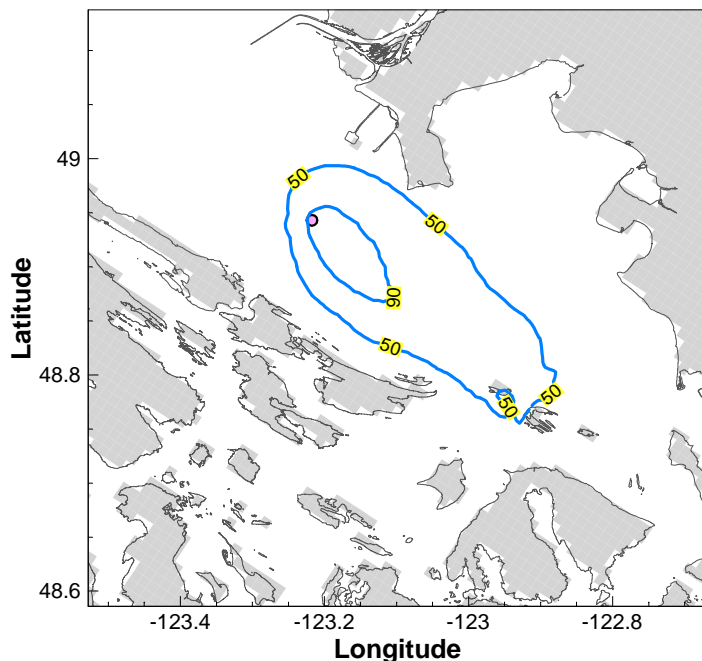
### Winter 2012

Area within the P<sub>50</sub> Contour Line: 216.8 km<sup>2</sup>  
 Area within the P<sub>90</sub> Contour Line: 10.8 km<sup>2</sup>  
 Average Thickness within the P<sub>50</sub> Contour Line: 24 µm  
 Average Thickness within the P<sub>90</sub> Contour Line: 49 µm  
 Average Shore Oiled: 9 km



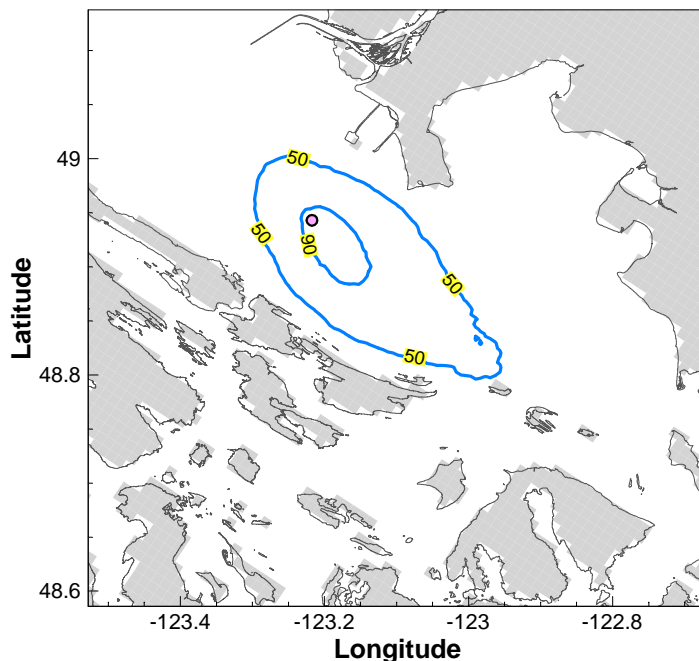
### Spring 2012

Area within the P<sub>50</sub> Contour Line: 286.7 km<sup>2</sup>  
 Area within the P<sub>90</sub> Contour Line: 41.3 km<sup>2</sup>  
 Average Thickness within the P<sub>50</sub> Contour Line: 21 µm  
 Average Thickness within the P<sub>90</sub> Contour Line: 32 µm  
 Average Shore Oiled: 13 km



### Summer 2012

Area within the P<sub>50</sub> Contour Line: 364.7 km<sup>2</sup>  
 Area within the P<sub>90</sub> Contour Line: 49.8 km<sup>2</sup>  
 Average Thickness within the P<sub>50</sub> Contour Line: 17 µm  
 Average Thickness within the P<sub>90</sub> Contour Line: 28 µm  
 Average Shore Oiled: 14 km



### Fall 2011

Area within the P<sub>50</sub> Contour Line: 310.5 km<sup>2</sup>  
 Area within the P<sub>90</sub> Contour Line: 35.5 km<sup>2</sup>  
 Average Thickness within the P<sub>50</sub> Contour Line: 18 µm  
 Average Thickness within the P<sub>90</sub> Contour Line: 31 µm  
 Average Shore Oiled: 12 km

## NOTES

○ Release Location

Probability of oil presence is the percentage of simulations in which oil was present at a given location.  
 P<sub>50</sub>: after 24 hours, there is 50% or greater probability for the area within the P<sub>50</sub> contour line to have been contacted.  
 P<sub>90</sub>: after 24 hours, there is 90% or greater probability for the area within the P<sub>90</sub> contour line to have been contacted.  
 Statistical results for each season based on independent spills occurring every 6 hours for three months.  
 Tracking time for each spill was 24 hours.  
 The average thickness is based on a full coverage of each grid cell that contains oil and lies within the contour line.

STATUS  
ISSUED FOR USE

## CLIENT



TRANSMOUNTAIN



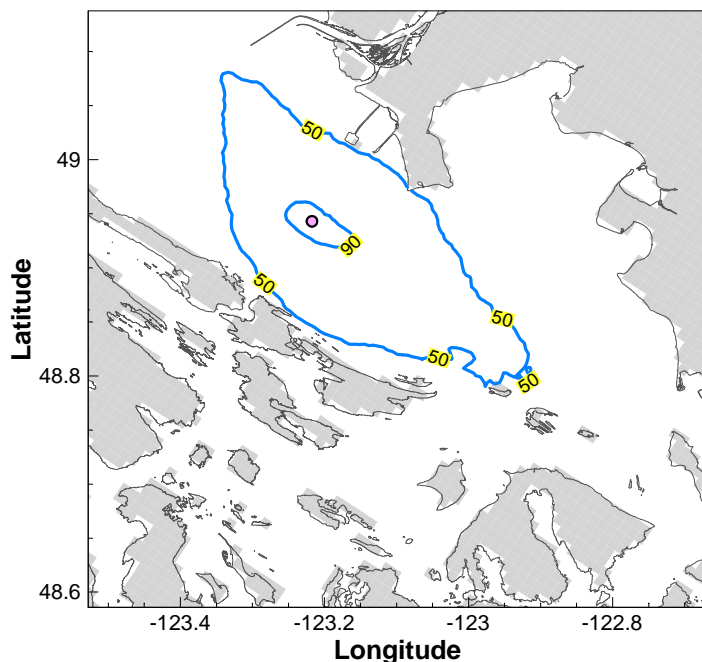
A TETRA TECH COMPANY

## TRANS MOUNTAIN OIL SPILL STUDY

Stochastic Simulation  
 Site D (8,250 m<sup>3</sup>)  
 P<sub>50</sub> and P<sub>90</sub> after 24 Hours

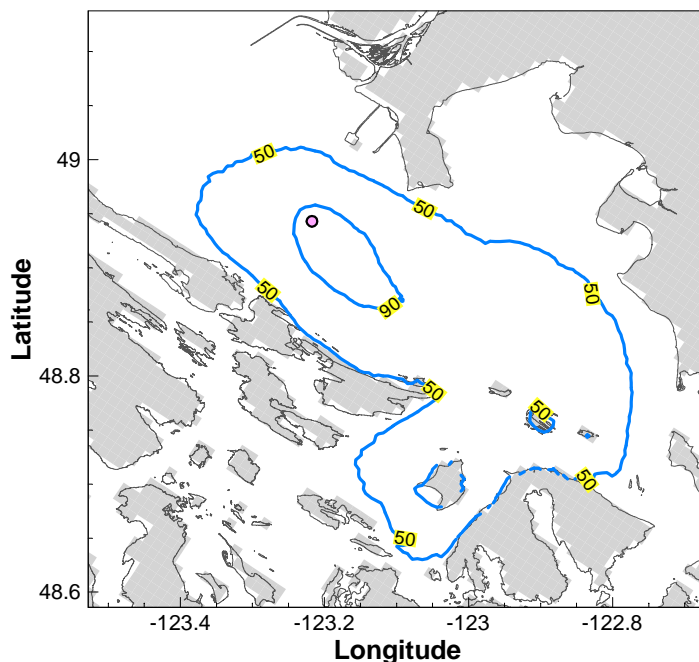
PROJECT NO.	DWN	CKD	APVD	REV
V13203022	DP	JAS	-	0
OFFICE	DATE			
EBA-VANC	October 25, 2013			

Figure 8.2.3



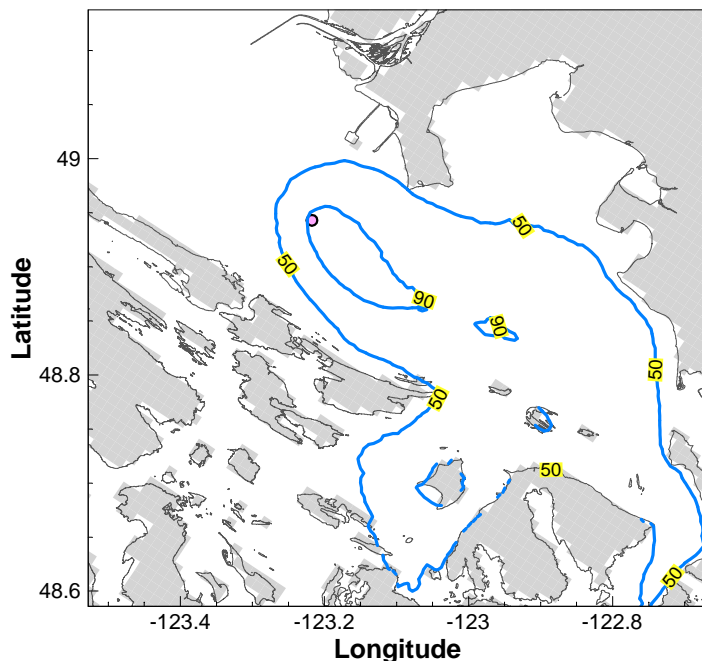
### Winter 2012

Area within the  $P_{50}$  Contour Line: 493.5 km<sup>2</sup>  
 Area within the  $P_{90}$  Contour Line: 18.5 km<sup>2</sup>  
 Average Thickness within the  $P_{50}$  Contour Line: 12  $\mu$ m  
 Average Thickness within the  $P_{90}$  Contour Line: 34  $\mu$ m  
 Average Shore Oiled: 36 km



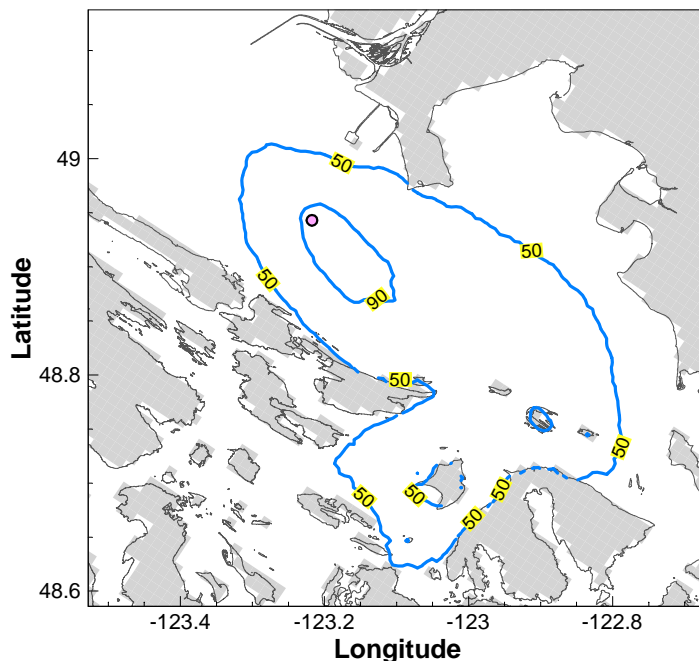
### Spring 2012

Area within the  $P_{50}$  Contour Line: 946.7 km<sup>2</sup>  
 Area within the  $P_{90}$  Contour Line: 66.8 km<sup>2</sup>  
 Average Thickness within the  $P_{50}$  Contour Line: 8  $\mu$ m  
 Average Thickness within the  $P_{90}$  Contour Line: 22  $\mu$ m  
 Average Shore Oiled: 60 km



### Summer 2012

Area within the  $P_{50}$  Contour Line: 1022.7 km<sup>2</sup>  
 Area within the  $P_{90}$  Contour Line: 66.0 km<sup>2</sup>  
 Average Thickness within the  $P_{50}$  Contour Line: 8  $\mu$ m  
 Average Thickness within the  $P_{90}$  Contour Line: 23  $\mu$ m  
 Average Shore Oiled: 72 km



### Fall 2011

Area within the  $P_{50}$  Contour Line: 924.0 km<sup>2</sup>  
 Area within the  $P_{90}$  Contour Line: 57.5 km<sup>2</sup>  
 Average Thickness within the  $P_{50}$  Contour Line: 7  $\mu$ m  
 Average Thickness within the  $P_{90}$  Contour Line: 22  $\mu$ m  
 Average Shore Oiled: 59 km

## NOTES

○ Release Location

Probability of oil presence is the percentage of simulations in which oil was present at a given location.

$P_{50}$ : after 48 hours, there is 50% or greater probability for the area within the  $P_{50}$  contour line to have been contacted.

$P_{90}$ : after 48 hours, there is 90% or greater probability for the area within the  $P_{90}$  contour line to have been contacted.

Statistical results for each season based on independent spills occurring every 6 hours for three months.

Tracking time for each spill was 48 hours.

The average thickness is based on a full coverage of each grid cell that contains oil and lies within the contour line.

STATUS  
ISSUED FOR USE

CLIENT



TRANSMOUNTAIN



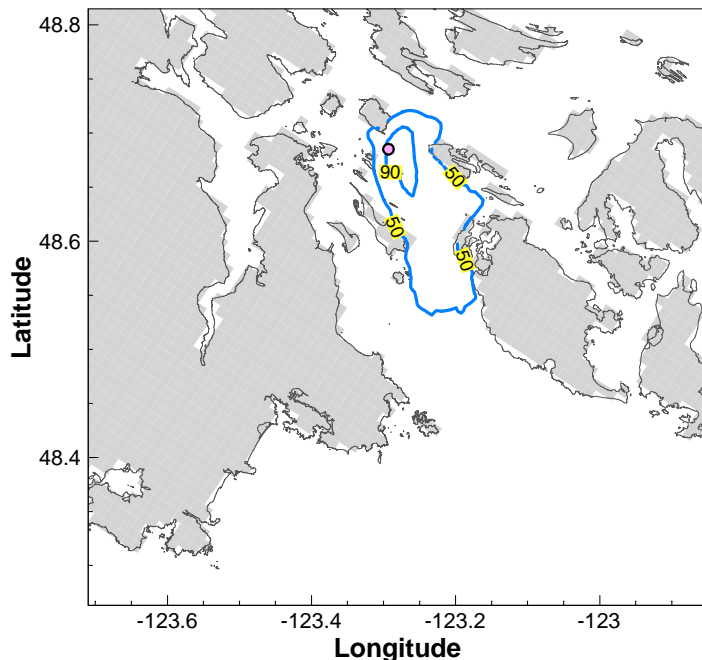
A TETRA TECH COMPANY

## TRANS MOUNTAIN OIL SPILL STUDY

Stochastic Simulation  
 Site D (8,250 m<sup>3</sup>)  
 $P_{50}$  and  $P_{90}$  after 48 Hours

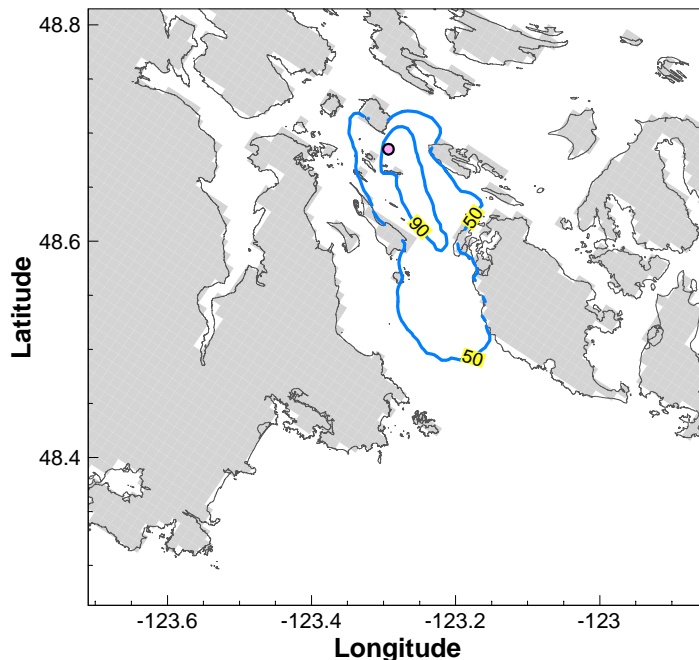
PROJECT NO.	DWN	CKD	APVD	REV
V13203022	DP	JAS	-	0
OFFICE	DATE			
EBA-VANC	October 25, 2013			

Figure 8.2.4



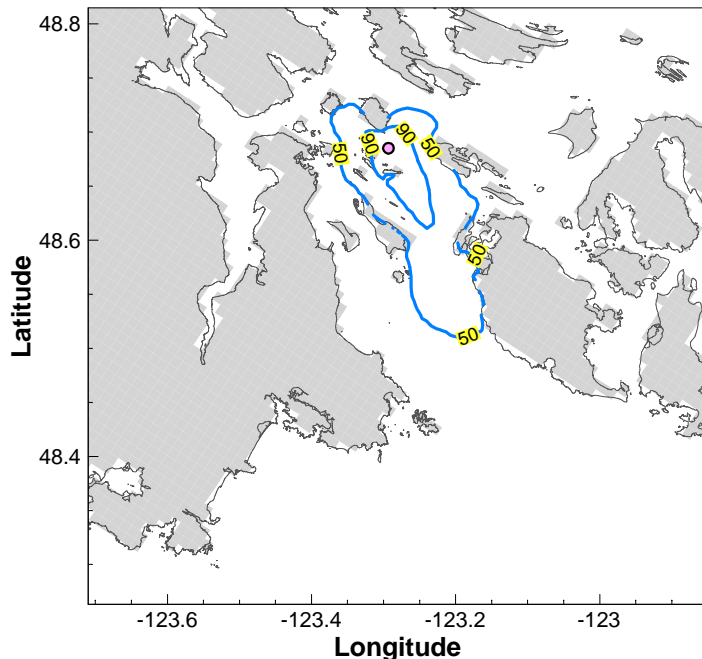
### Winter 2012

Area within the P<sub>50</sub> Contour Line: 139.3 km<sup>2</sup>  
 Area within the P<sub>90</sub> Contour Line: 16.3 km<sup>2</sup>  
 Average Thickness within the P<sub>50</sub> Contour Line: 54 µm  
 Average Thickness within the P<sub>90</sub> Contour Line: 133 µm  
 Average Shore Oiled: 29 km



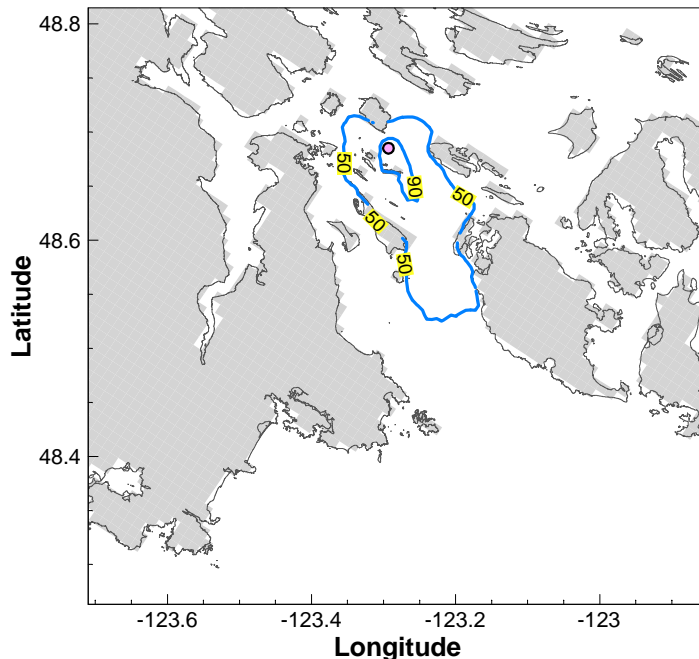
### Spring 2012

Area within the P<sub>50</sub> Contour Line: 210.0 km<sup>2</sup>  
 Area within the P<sub>90</sub> Contour Line: 36.0 km<sup>2</sup>  
 Average Thickness within the P<sub>50</sub> Contour Line: 41 µm  
 Average Thickness within the P<sub>90</sub> Contour Line: 89 µm  
 Average Shore Oiled: 35 km



### Summer 2012

Area within the P<sub>50</sub> Contour Line: 196 km<sup>2</sup>  
 Area within the P<sub>90</sub> Contour Line: 37.8 km<sup>2</sup>  
 Average Thickness within the P<sub>50</sub> Contour Line: 36 µm  
 Average Thickness within the P<sub>90</sub> Contour Line: 78 µm  
 Average Shore Oiled: 36 km



### Fall 2011

Area within the P<sub>50</sub> Contour Line: 167.5 km<sup>2</sup>  
 Area within the P<sub>90</sub> Contour Line: 12.8 km<sup>2</sup>  
 Average Thickness within the P<sub>50</sub> Contour Line: 43 µm  
 Average Thickness within the P<sub>90</sub> Contour Line: 133 µm  
 Average Shore Oiled: 34 km

## NOTES

○ Release Location

Probability of oil presence is the percentage of simulations in which oil was present at a given location.  
 P<sub>50</sub>: after 24 hours, there is 50% or greater probability for the area within the P<sub>50</sub> contour line to have been contacted.  
 P<sub>90</sub>: after 24 hours, there is 90% or greater probability for the area within the P<sub>90</sub> contour line to have been contacted.  
 Statistical results for each season based on independent spills occurring every 6 hours for three months.  
 Tracking time for each spill was 24 hours.  
 The average thickness is based on a full coverage of each grid cell that contains oil and lies within the contour line.

STATUS  
ISSUED FOR USE

CLIENT



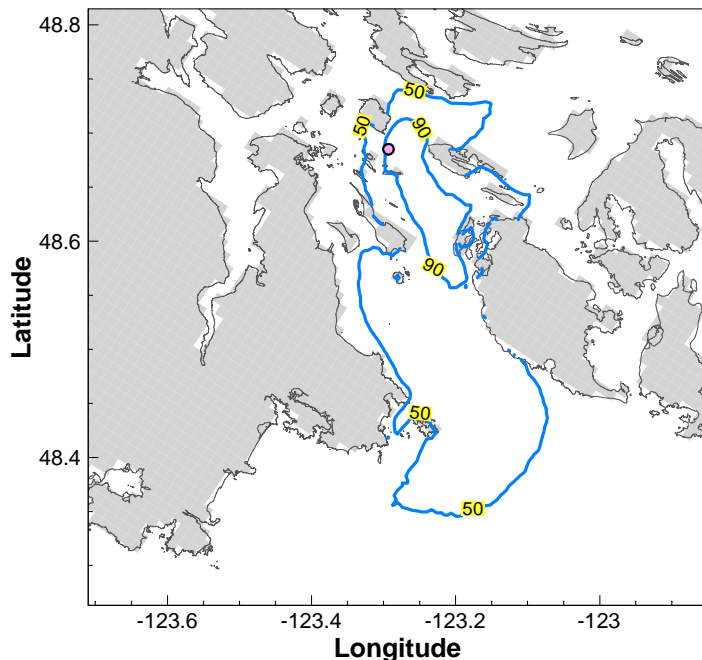
## TRANS MOUNTAIN OIL SPILL STUDY

Stochastic Simulation  
 Site E (16,500 m<sup>3</sup>)  
 P<sub>50</sub> and P<sub>90</sub> after 24 Hours

PROJECT NO.	DWN	CKD	APVD	REV
V13203022	DP	JAS	-	0
OFFICE	DATE			
EBA-VANC	October 25, 2013			

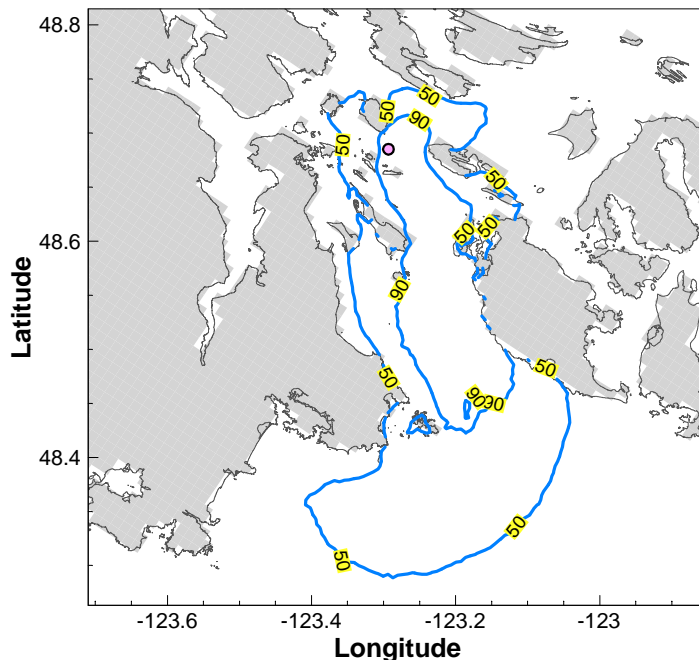
Figure 8.3.1





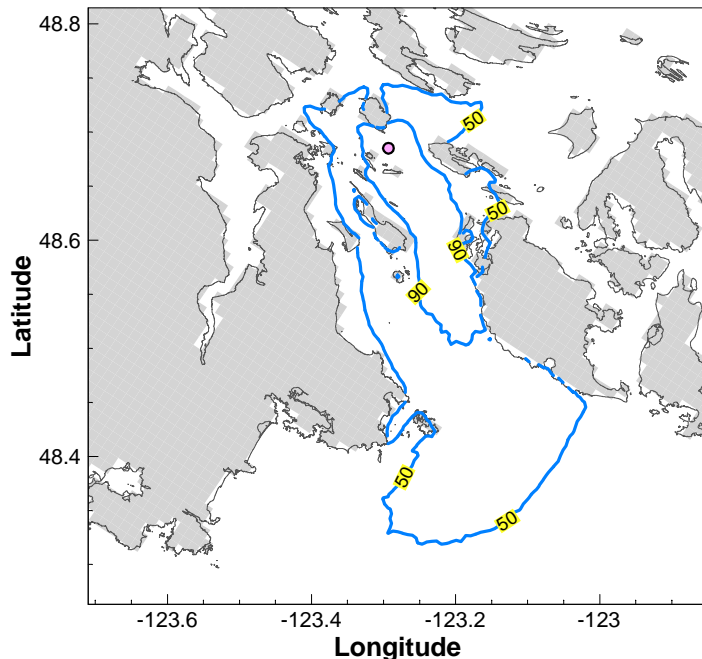
### Winter 2012

Area within the P<sub>50</sub> Contour Line: 516.5 km<sup>2</sup>  
 Area within the P<sub>90</sub> Contour Line: 69.3 km<sup>2</sup>  
 Average Thickness within the P<sub>50</sub> Contour Line: 17 µm  
 Average Thickness within the P<sub>90</sub> Contour Line: 47 µm  
 Average Shore Oiled: 75 km



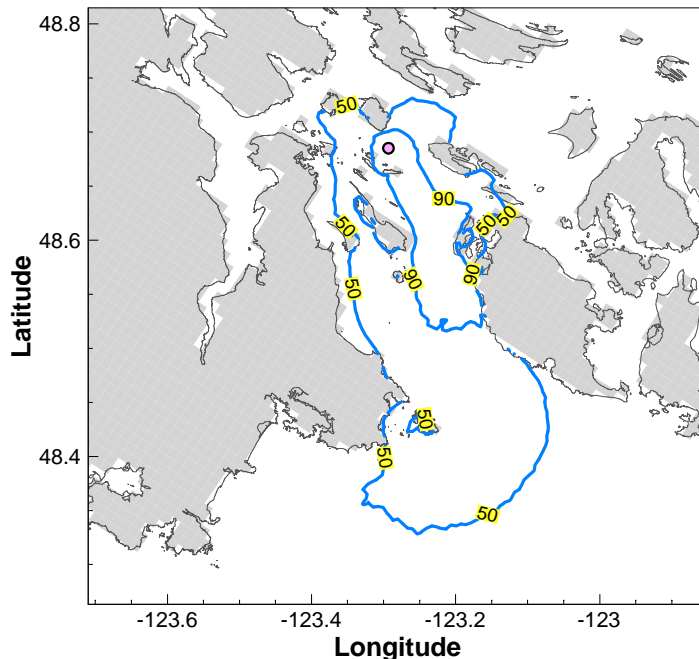
### Spring 2012

Area within the P<sub>50</sub> Contour Line: 767.5 km<sup>2</sup>  
 Area within the P<sub>90</sub> Contour Line: 227.0 km<sup>2</sup>  
 Average Thickness within the P<sub>50</sub> Contour Line: 10 µm  
 Average Thickness within the P<sub>90</sub> Contour Line: 21 µm  
 Average Shore Oiled: 90 km



### Summer 2012

Area within the P<sub>50</sub> Contour Line: 646.0 km<sup>2</sup>  
 Area within the P<sub>90</sub> Contour Line: 132.3 km<sup>2</sup>  
 Average Thickness within the P<sub>50</sub> Contour Line: 11 µm  
 Average Thickness within the P<sub>90</sub> Contour Line: 27 µm  
 Average Shore Oiled: 85 km



### Fall 2011

Area within the P<sub>50</sub> Contour Line: 603.7 km<sup>2</sup>  
 Area within the P<sub>90</sub> Contour Line: 106.8 km<sup>2</sup>  
 Average Thickness within the P<sub>50</sub> Contour Line: 12 µm  
 Average Thickness within the P<sub>90</sub> Contour Line: 28 µm  
 Average Shore Oiled: 83 km

## NOTES

○ Release Location

Probability of oil presence is the percentage of simulations in which oil was present at a given location.  
 P<sub>50</sub>: after 48 hours, there is 50% or greater probability for the area within the P<sub>50</sub> contour line to have been contacted.  
 P<sub>90</sub>: after 48 hours, there is 90% or greater probability for the area within the P<sub>90</sub> contour line to have been contacted.  
 Statistical results for each season based on independent spills occurring every 6 hours for three months.  
 Tracking time for each spill was 48 hours.  
 The average thickness is based on a full coverage of each grid cell that contains oil and lies within the contour line.

STATUS  
ISSUED FOR USE

CLIENT

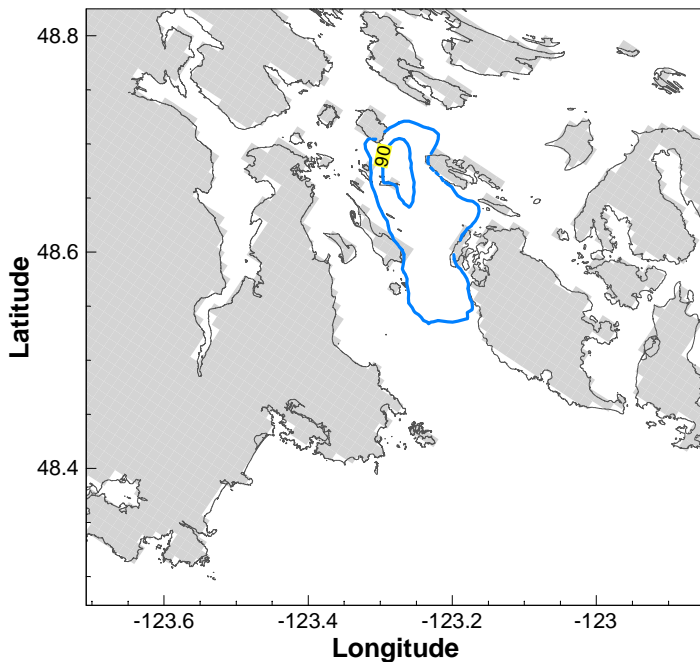


## TRANS MOUNTAIN OIL SPILL STUDY

Stochastic Simulation  
 Site E (16,500 m<sup>3</sup>)  
 P<sub>50</sub> and P<sub>90</sub> after 48 Hours

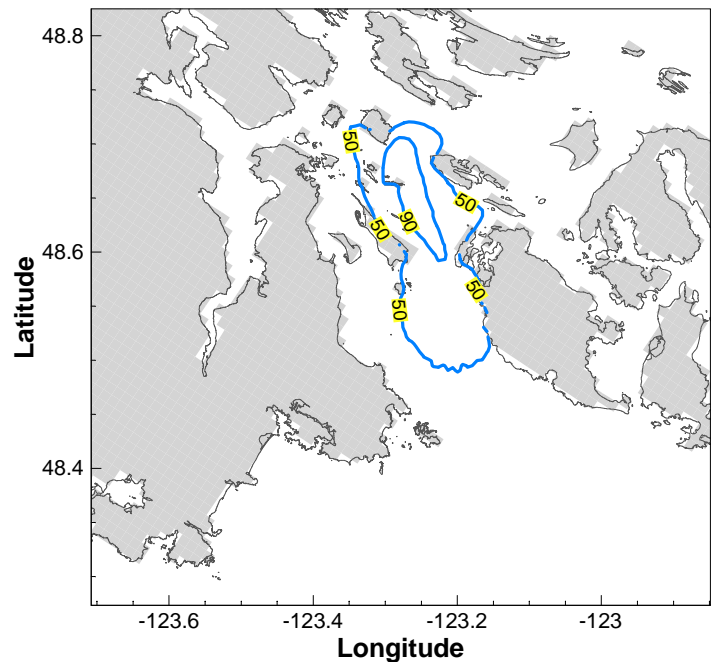
PROJECT NO.	DWN	CKD	APVD	REV
V13203022	DP	JAS	-	0
OFFICE	DATE			
EBA-VANC	October 25, 2013			

Figure 8.3.2



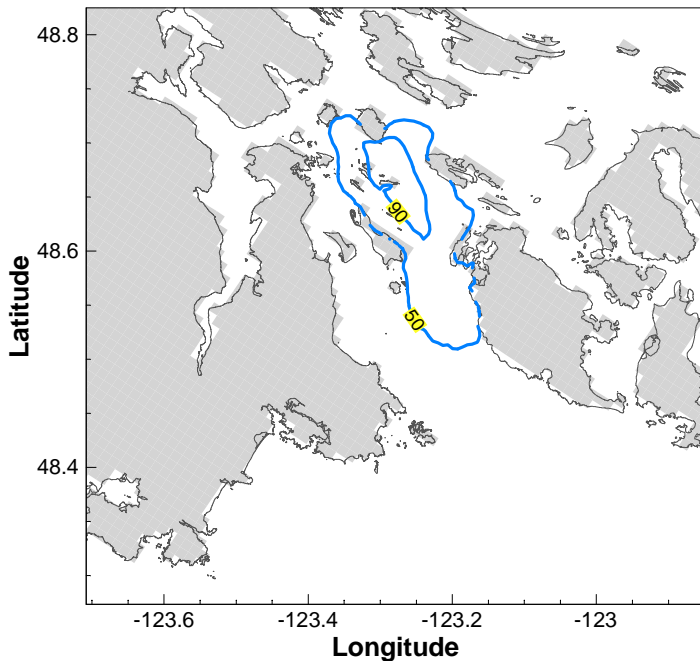
### Winter 2012

Area within the  $P_{50}$  Contour Line: 140.3 km<sup>2</sup>  
 Area within the  $P_{90}$  Contour Line: 16.3 km<sup>2</sup>  
 Average Thickness within the  $P_{50}$  Contour Line: 27  $\mu$ m  
 Average Thickness within the  $P_{90}$  Contour Line: 66  $\mu$ m  
 Average Shore Oiled: 27 km



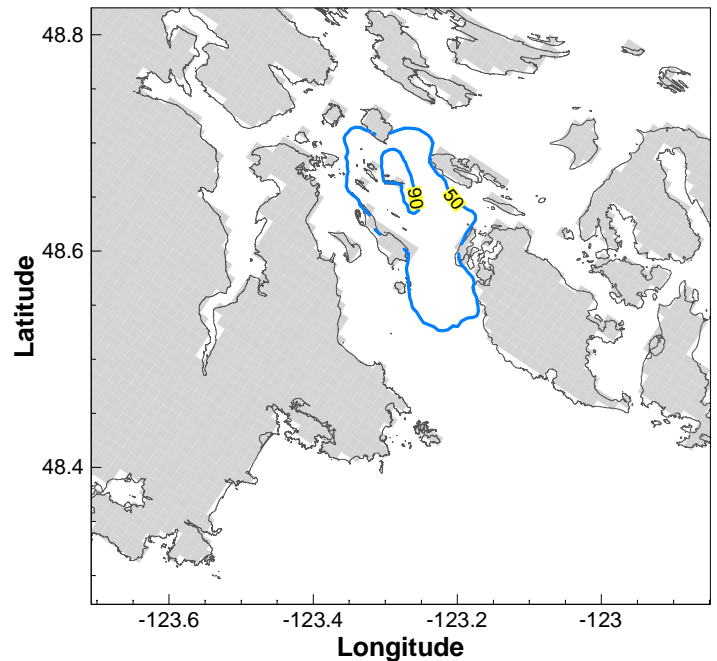
### Spring 2012

Area within the  $P_{50}$  Contour Line: 206.3 km<sup>2</sup>  
 Area within the  $P_{90}$  Contour Line: 34.5 km<sup>2</sup>  
 Average Thickness within the  $P_{50}$  Contour Line: 20  $\mu$ m  
 Average Thickness within the  $P_{90}$  Contour Line: 45  $\mu$ m  
 Average Shore Oiled: 33 km



### Summer 2012

Area within the  $P_{50}$  Contour Line: 194.8 km<sup>2</sup>  
 Area within the  $P_{90}$  Contour Line: 36.3 km<sup>2</sup>  
 Average Thickness within the  $P_{50}$  Contour Line: 18  $\mu$ m  
 Average Thickness within the  $P_{90}$  Contour Line: 40  $\mu$ m  
 Average Shore Oiled: 32 km



### Fall 2011

Area within the  $P_{50}$  Contour Line: 162.8 km<sup>2</sup>  
 Area within the  $P_{90}$  Contour Line: 12.8 km<sup>2</sup>  
 Average Thickness within the  $P_{50}$  Contour Line: 22  $\mu$ m  
 Average Thickness within the  $P_{90}$  Contour Line: 66  $\mu$ m  
 Average Shore Oiled: 32 km

## NOTES

○ Release Location

Probability of oil presence is the percentage of simulations in which oil was present at a given location.  
 $P_{50}$ : after 24 hours, there is 50% or greater probability for the area within the  $P_{50}$  contour line to have been contacted.  
 $P_{90}$ : after 24 hours, there is 90% or greater probability for the area within the  $P_{90}$  contour line to have been contacted.  
 Statistical results for each season based on independent spills occurring every 6 hours for three months.  
 Tracking time for each spill was 24 hours.  
 The average thickness is based on a full coverage of each grid cell that contains oil and lies within the contour line.

STATUS  
ISSUED FOR USE

CLIENT



TRANSMOUNTAIN



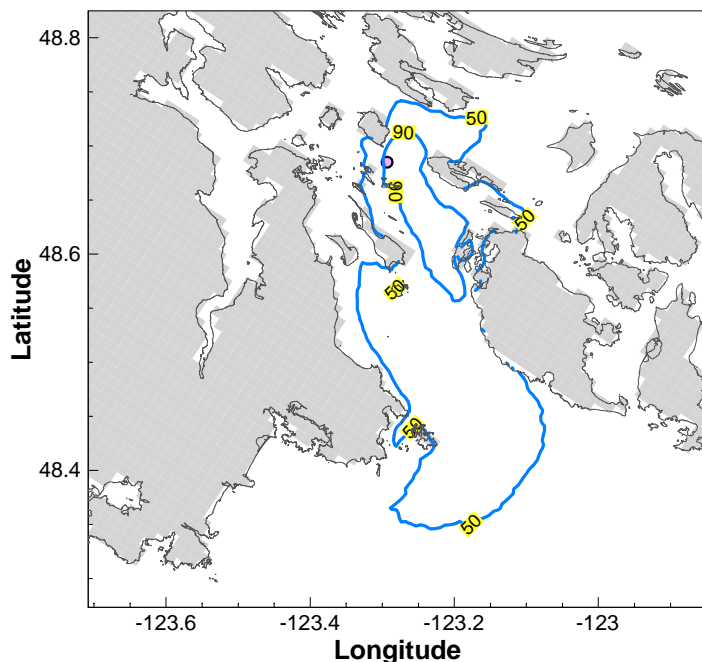
A TETRA TECH COMPANY

## TRANS MOUNTAIN OIL SPILL STUDY

Stochastic Simulation  
 Site E (8,250 m<sup>3</sup>)  
 $P_{50}$  and  $P_{90}$  after 24 Hours

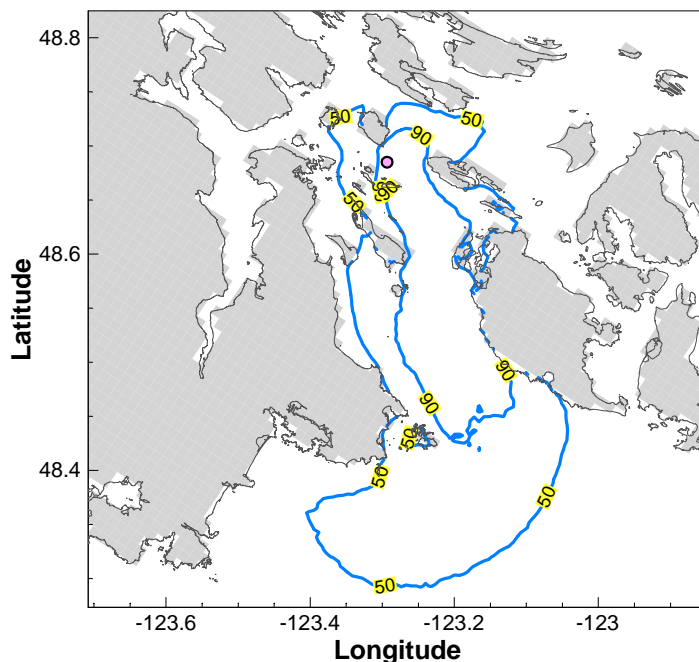
PROJECT NO.	DWN	CKD	APVD	REV
V13203022	DP	JAS	-	0
OFFICE	DATE			
EBA-VANC	October 25, 2013			

Figure 8.3.3



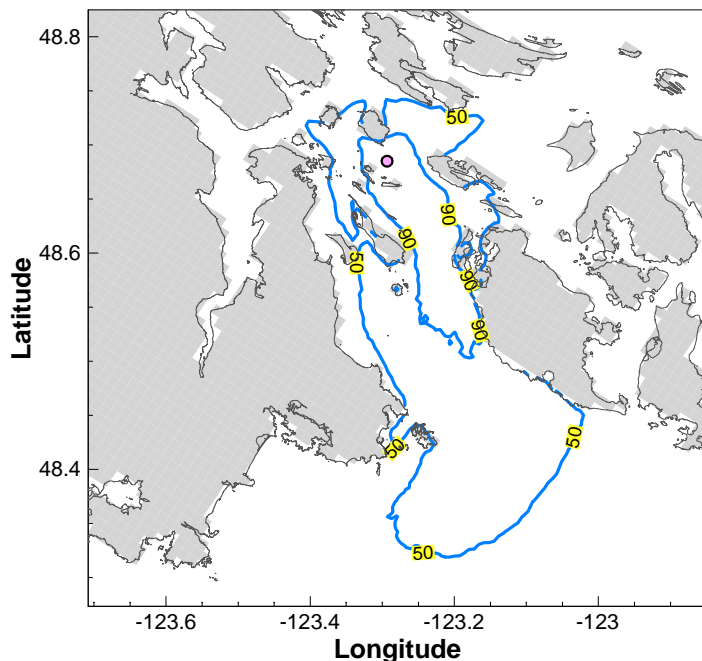
### Winter 2012

Area within the  $P_{50}$  Contour Line: 507.5 km<sup>2</sup>  
 Area within the  $P_{90}$  Contour Line: 66.8 km<sup>2</sup>  
 Average Thickness within the  $P_{50}$  Contour Line: 8  $\mu$ m  
 Average Thickness within the  $P_{90}$  Contour Line: 24  $\mu$ m  
 Average Shore Oiled: 69 km



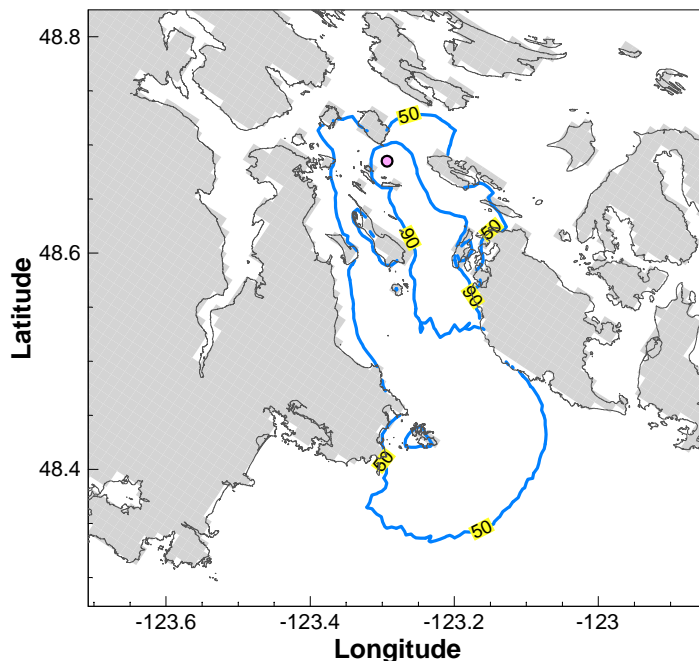
### Spring 2012

Area within the  $P_{50}$  Contour Line: 753.2 km<sup>2</sup>  
 Area within the  $P_{90}$  Contour Line: 221.8 km<sup>2</sup>  
 Average Thickness within the  $P_{50}$  Contour Line: 5  $\mu$ m  
 Average Thickness within the  $P_{90}$  Contour Line: 10  $\mu$ m  
 Average Shore Oiled: 82 km



### Summer 2012

Area within the  $P_{50}$  Contour Line: 628.2 km<sup>2</sup>  
 Area within the  $P_{90}$  Contour Line: 120.0 km<sup>2</sup>  
 Average Thickness within the  $P_{50}$  Contour Line: 5  $\mu$ m  
 Average Thickness within the  $P_{90}$  Contour Line: 14  $\mu$ m  
 Average Shore Oiled: 75 km



### Fall 2011

Area within the  $P_{50}$  Contour Line: 586.0 km<sup>2</sup>  
 Area within the  $P_{90}$  Contour Line: 97.6 km<sup>2</sup>  
 Average Thickness within the  $P_{50}$  Contour Line: 6  $\mu$ m  
 Average Thickness within the  $P_{90}$  Contour Line: 14  $\mu$ m  
 Average Shore Oiled: 76 km

## NOTES

○ Release Location

Probability of oil presence is the percentage of simulations in which oil was present at a given location.  
 $P_{50}$ : after 48 hours, there is 50% or greater probability for the area within the  $P_{50}$  contour line to have been contacted.  
 $P_{90}$ : after 48 hours, there is 90% or greater probability for the area within the  $P_{90}$  contour line to have been contacted.  
 Statistical results for each season based on independent spills occurring every 6 hours for three months.  
 Tracking time for each spill was 48 hours.  
 The average thickness is based on a full coverage of each grid cell that contains oil and lies within the contour line.

STATUS  
ISSUED FOR USE

CLIENT



TRANSMOUNTAIN



A TETRA TECH COMPANY

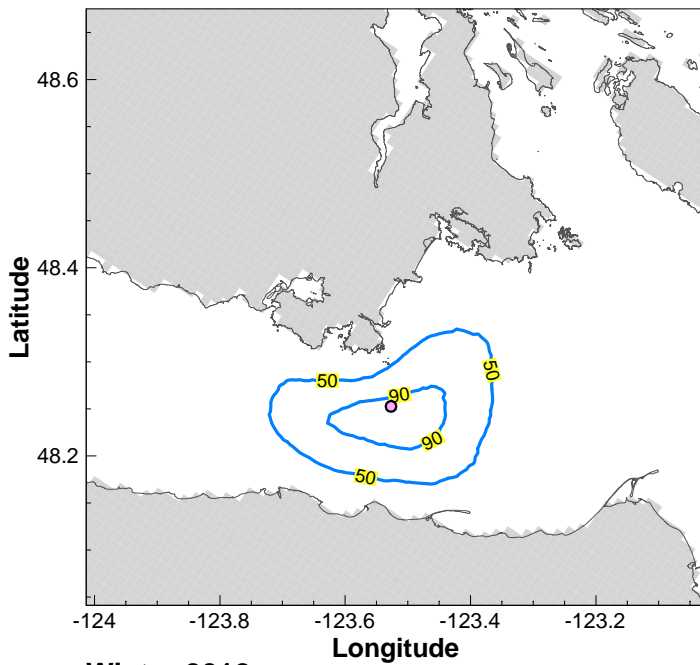
## TRANS MOUNTAIN OIL SPILL STUDY

Stochastic Simulation  
 Site E (8,250 m<sup>3</sup>)  
 $P_{50}$  and  $P_{90}$  after 48 Hours

PROJECT NO.	DWN	CKD	APVD	REV
V13203022	DP	JAS	-	0
OFFICE	DATE			
EBA-VANC	October 25, 2013			

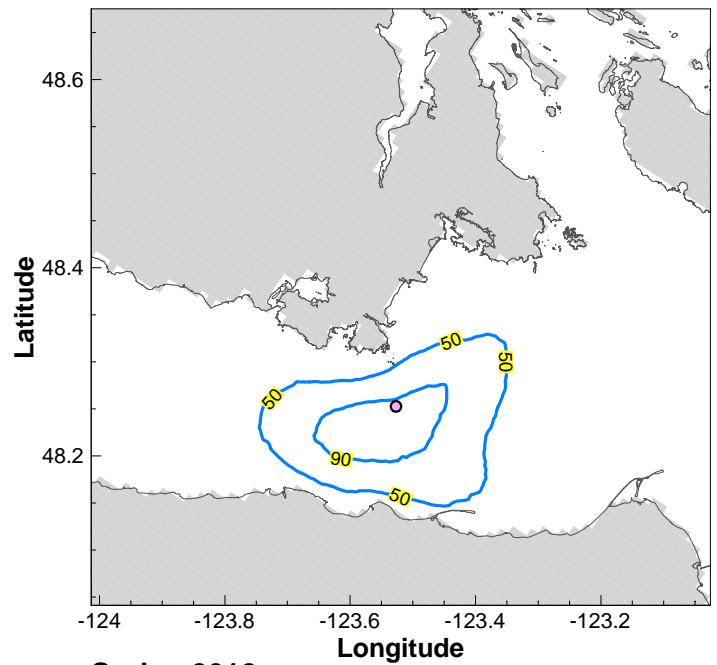
Figure 8.3.4





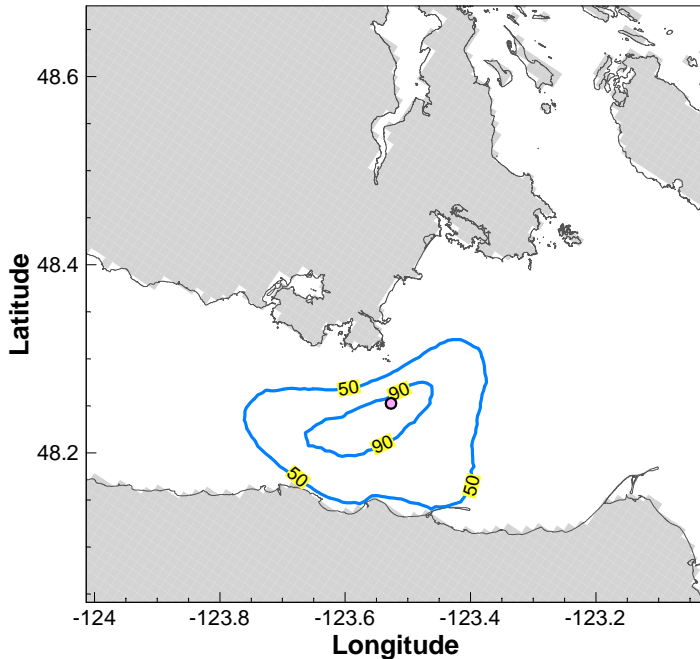
### Winter 2012

Area within the  $P_{50}$  Contour Line: 326.5 km<sup>2</sup>  
 Area within the  $P_{90}$  Contour Line: 68.5 km<sup>2</sup>  
 Average Thickness within the  $P_{50}$  Contour Line: 38  $\mu$ m  
 Average Thickness within the  $P_{90}$  Contour Line: 69  $\mu$ m  
 Average Shore Oiled: 4.3 km



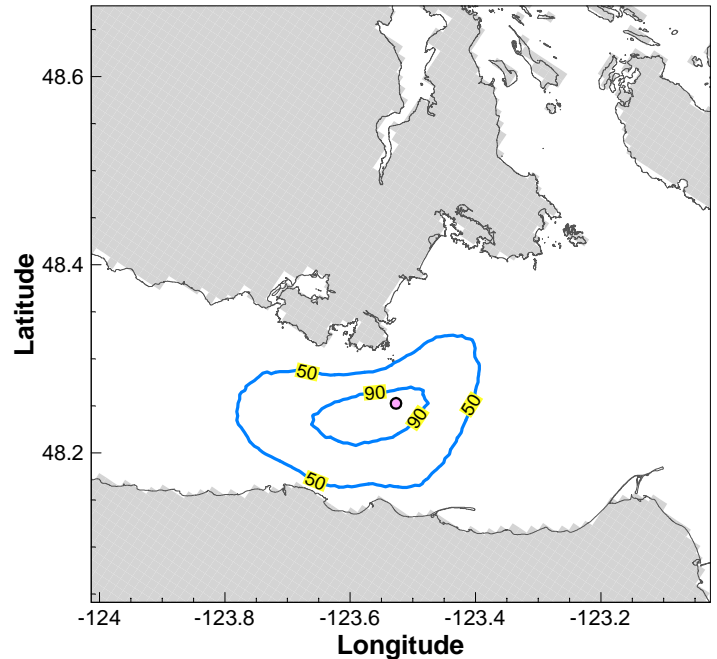
### Spring 2012

Area within the  $P_{50}$  Contour Line: 395.0 km<sup>2</sup>  
 Area within the  $P_{90}$  Contour Line: 95.0 km<sup>2</sup>  
 Average Thickness within the  $P_{50}$  Contour Line: 33  $\mu$ m  
 Average Thickness within the  $P_{90}$  Contour Line: 48  $\mu$ m  
 Average Shore Oiled: 5.6 km



### Summer 2012

Area within the  $P_{50}$  Contour Line: 372.2 km<sup>2</sup>  
 Area within the  $P_{90}$  Contour Line: 64.3 km<sup>2</sup>  
 Average Thickness within the  $P_{50}$  Contour Line: 35  $\mu$ m  
 Average Thickness within the  $P_{90}$  Contour Line: 54  $\mu$ m  
 Average Shore Oiled: 6.8 km



### Fall 2011

Area within the  $P_{50}$  Contour Line: 347.5 km<sup>2</sup>  
 Area within the  $P_{90}$  Contour Line: 61.8 km<sup>2</sup>  
 Average Thickness within the  $P_{50}$  Contour Line: 37  $\mu$ m  
 Average Thickness within the  $P_{90}$  Contour Line: 57  $\mu$ m  
 Average Shore Oiled: 5.3 km

## NOTES

○ Release Location

Probability of oil presence is the percentage of simulations in which oil was present at a given location.

$P_{50}$ : after 24 hours, there is 50% or greater probability for the area within the  $P_{50}$  contour line to have been contacted.

$P_{90}$ : after 24 hours, there is 90% or greater probability for the area within the  $P_{90}$  contour line to have been contacted.

Statistical results for each season based on independent spills occurring every 6 hours for three months.

Tracking time for each spill was 24 hours.

The average thickness is based on a full coverage of each grid cell that contains oil and lies within the contour line.

STATUS  
ISSUED FOR USE

## CLIENT

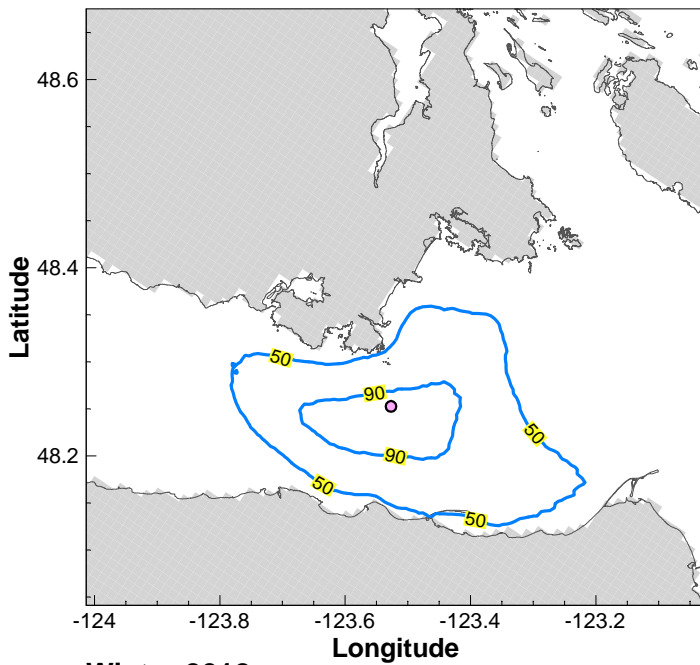


## TRANS MOUNTAIN OIL SPILL STUDY

Stochastic Simulation  
 Site G (16,500 m<sup>3</sup>)  
 $P_{50}$  and  $P_{90}$  after 24 Hours

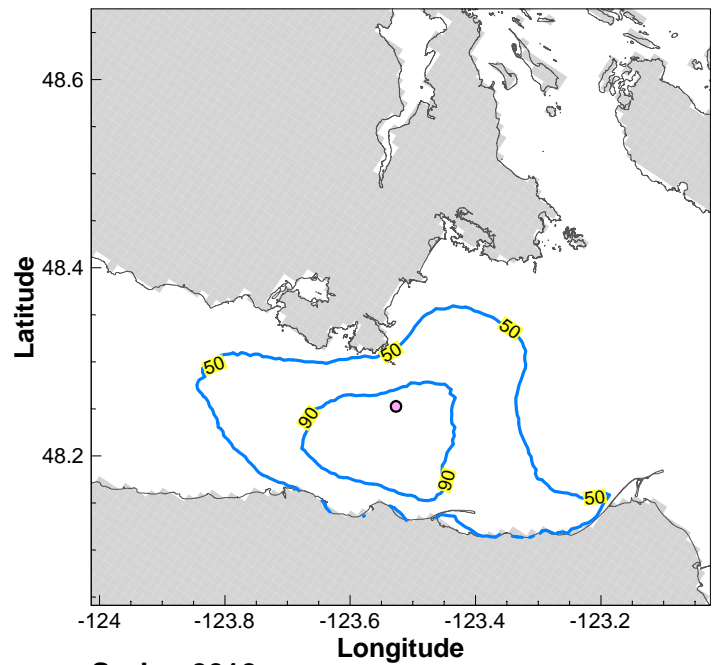
PROJECT NO.	DWN	CKD	APVD	REV
V13203022	DP	JAS	-	0
OFFICE	DATE			
EBA-VANC	October 25, 2013			

Figure 8.4.1



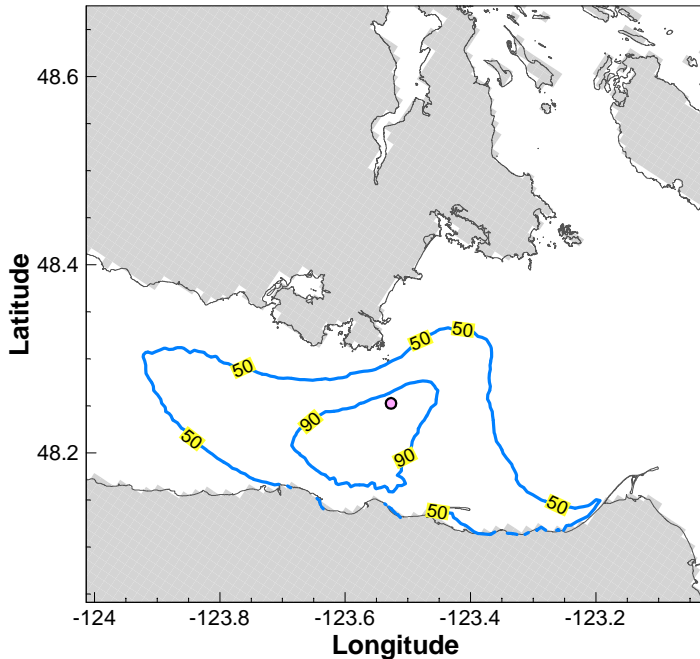
### Winter 2012

Area within the  $P_{50}$  Contour Line: 639.3 km<sup>2</sup>  
 Area within the  $P_{90}$  Contour Line: 122.8 km<sup>2</sup>  
 Average Thickness within the  $P_{50}$  Contour Line: 21 um  
 Average Thickness within the  $P_{90}$  Contour Line: 35 um  
 Average Shore Oiled: 23.5 km



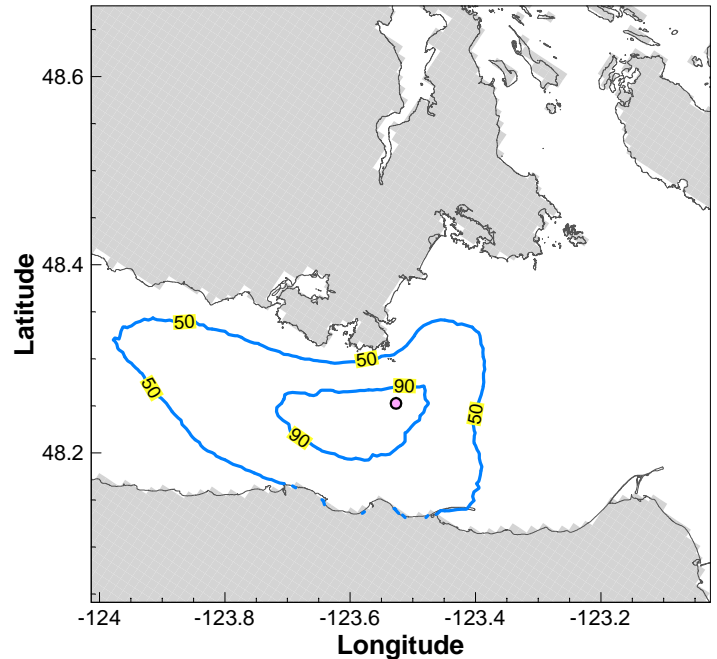
### Spring 2012

Area within the  $P_{50}$  Contour Line: 748.2 km<sup>2</sup>  
 Area within the  $P_{90}$  Contour Line: 182.8 km<sup>2</sup>  
 Average Thickness within the  $P_{50}$  Contour Line: 18 um  
 Average Thickness within the  $P_{90}$  Contour Line: 29 um  
 Average Shore Oiled: 27.4 km



### Summer 2012

Area within the  $P_{50}$  Contour Line: 674.0 km<sup>2</sup>  
 Area within the  $P_{90}$  Contour Line: 128.3 km<sup>2</sup>  
 Average Thickness within the  $P_{50}$  Contour Line: 20 um  
 Average Thickness within the  $P_{90}$  Contour Line: 33 um  
 Average Shore Oiled: 29.4 km



### Fall 2011

Area within the  $P_{50}$  Contour Line: 675.2 km<sup>2</sup>  
 Area within the  $P_{90}$  Contour Line: 38.7 km<sup>2</sup>  
 Average Thickness within the  $P_{50}$  Contour Line: 21 um  
 Average Thickness within the  $P_{90}$  Contour Line: 39 um  
 Average Shore Oiled: 25.9 km

## NOTES

○ Release Location

Probability of oil presence is the percentage of simulations in which oil was present at a given location.  
 $P_{50}$ : after 48 hours, there is 50% or greater probability for the area within the  $P_{50}$  contour line to have been contacted.  
 $P_{90}$ : after 48 hours, there is 90% or greater probability for the area within the  $P_{90}$  contour line to have been contacted.  
 Statistical results for each season based on independent spills occurring every 6 hours for three months.  
 Tracking time for each spill was 48 hours.  
 The average thickness is based on a full coverage of each grid cell that contains oil and lies within the contour line.

STATUS  
ISSUED FOR USE

## CLIENT

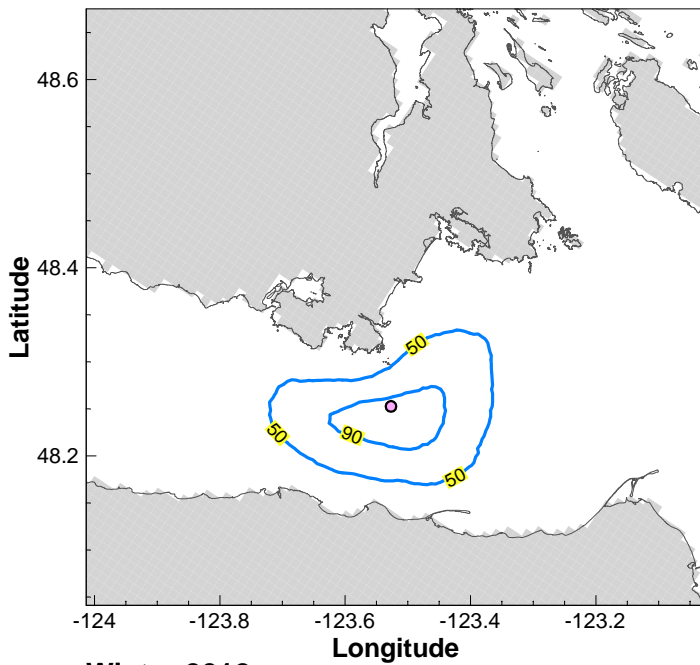


## TRANS MOUNTAIN OIL SPILL STUDY

Stochastic Simulation  
 Site G (16,500 m<sup>3</sup>)  
 $P_{50}$  and  $P_{90}$  after 48 Hours

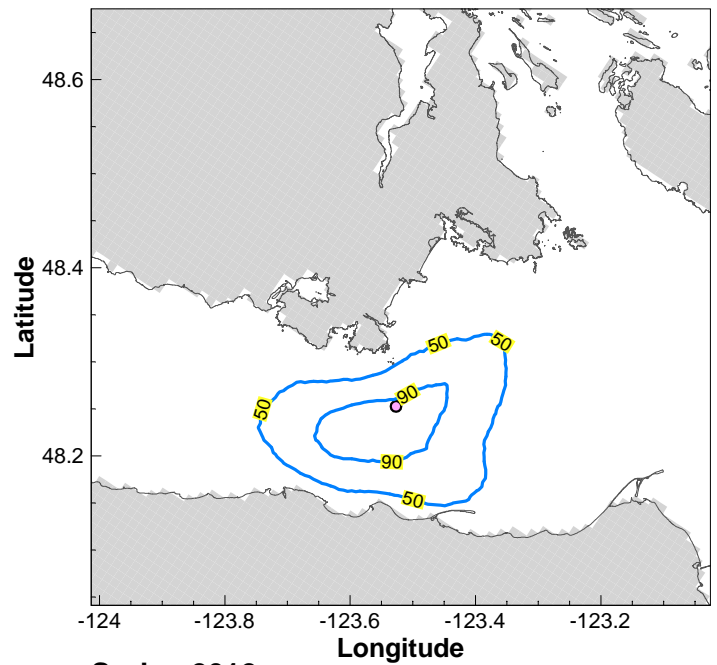
PROJECT NO.	DWN	CKD	APVD	REV
V13203022	DP	JAS	-	0
OFFICE	DATE			
EBA-VANC	October 25, 2013			

Figure 8.4.2



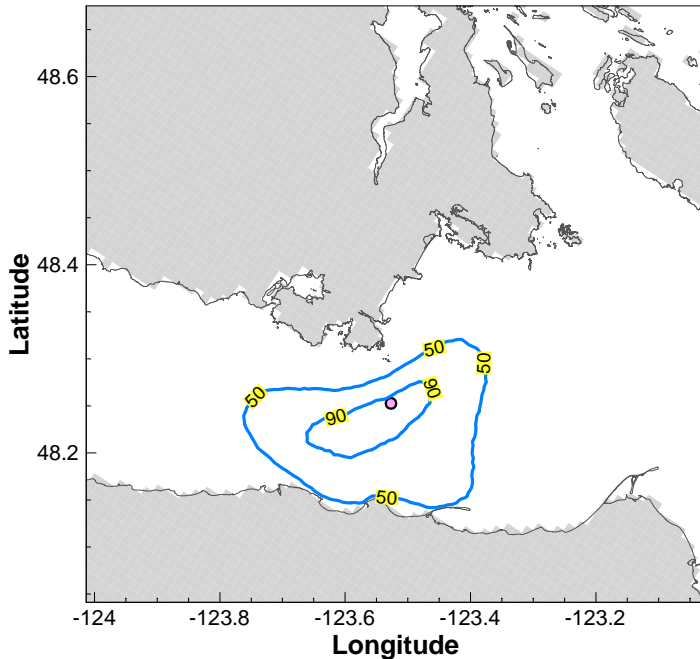
### Winter 2012

Area within the P<sub>50</sub> Contour Line: 327 km<sup>2</sup>  
 Area within the P<sub>90</sub> Contour Line: 68.5 km<sup>2</sup>  
 Average Thickness within the P<sub>50</sub> Contour Line: 19 µm  
 Average Thickness within the P<sub>90</sub> Contour Line: 26 µm  
 Average Shore Oiled: 4 km



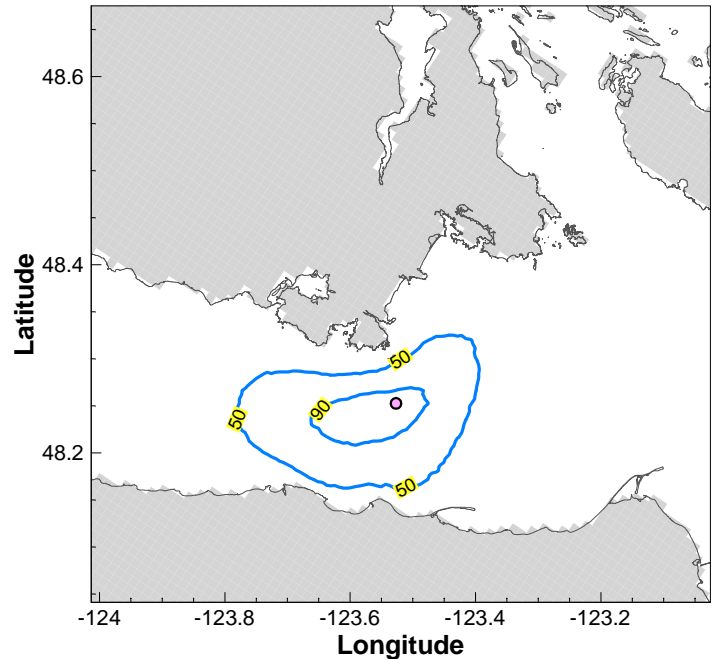
### Spring 2012

Area within the P<sub>50</sub> Contour Line: 397 km<sup>2</sup>  
 Area within the P<sub>90</sub> Contour Line: 96 km<sup>2</sup>  
 Average Thickness within the P<sub>50</sub> Contour Line: 16 µm  
 Average Thickness within the P<sub>90</sub> Contour Line: 24 µm  
 Average Shore Oiled: 6 km



### Summer 2012

Area within the P<sub>50</sub> Contour Line: 373 km<sup>2</sup>  
 Area within the P<sub>90</sub> Contour Line: 65 km<sup>2</sup>  
 Average Thickness within the P<sub>50</sub> Contour Line: 17 µm  
 Average Thickness within the P<sub>90</sub> Contour Line: 27 µm  
 Average Shore Oiled: 7 km



### Fall 2011

Area within the P<sub>50</sub> Contour Line: 352 km<sup>2</sup>  
 Area within the P<sub>90</sub> Contour Line: 62 km<sup>2</sup>  
 Average Thickness within the P<sub>50</sub> Contour Line: 18 µm  
 Average Thickness within the P<sub>90</sub> Contour Line: 28 µm  
 Average Shore Oiled: 5 km

## NOTES

○ Release Location

Probability of oil presence is the percentage of simulations in which oil was present at a given location.  
 P<sub>50</sub>: after 24 hours, there is 50% or greater probability for the area within the P<sub>50</sub> contour line to have been contacted.  
 P<sub>90</sub>: after 24 hours, there is 90% or greater probability for the area within the P<sub>90</sub> contour line to have been contacted.  
 Statistical results for each season based on independent spills occurring every 6 hours for three months.  
 Tracking time for each spill was 24 hours.  
 The average thickness is based on a full coverage of each grid cell that contains oil and lies within the contour line.

STATUS  
ISSUED FOR USE

## CLIENT

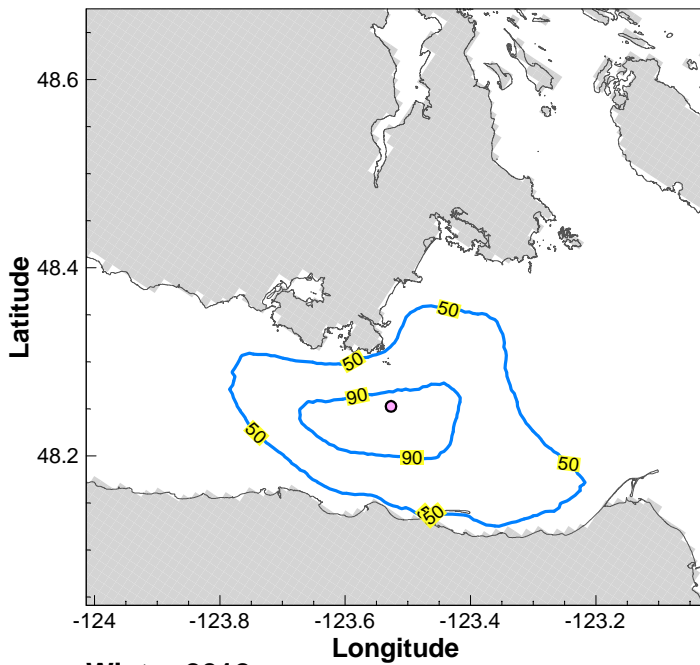


## TRANS MOUNTAIN OIL SPILL STUDY

Stochastic Simulation  
 Site G (8,250 m<sup>3</sup>)  
 P<sub>50</sub> and P<sub>90</sub> after 24 Hours

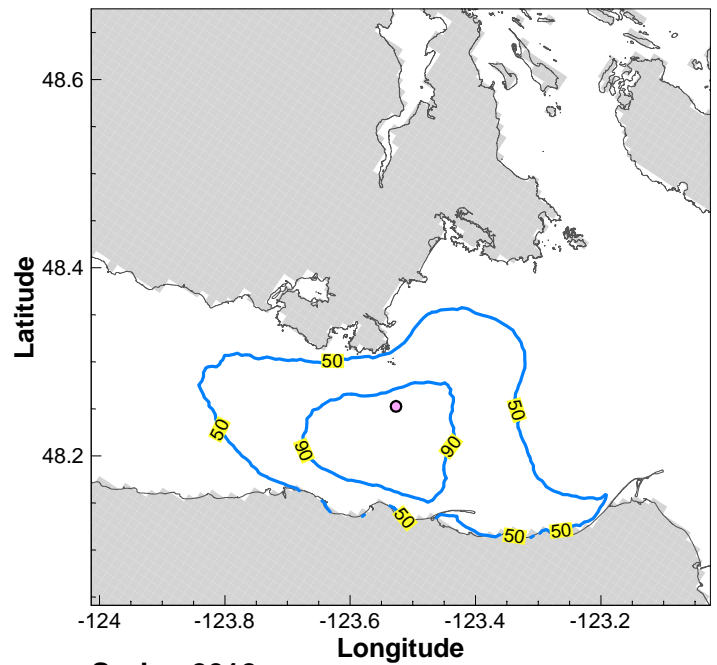
PROJECT NO.	DWN	CKD	APVD	REV
V13203022	DP	JAS	-	0
OFFICE	DATE			
EBA-VANC	October 25, 2013			

Figure 8.4.3



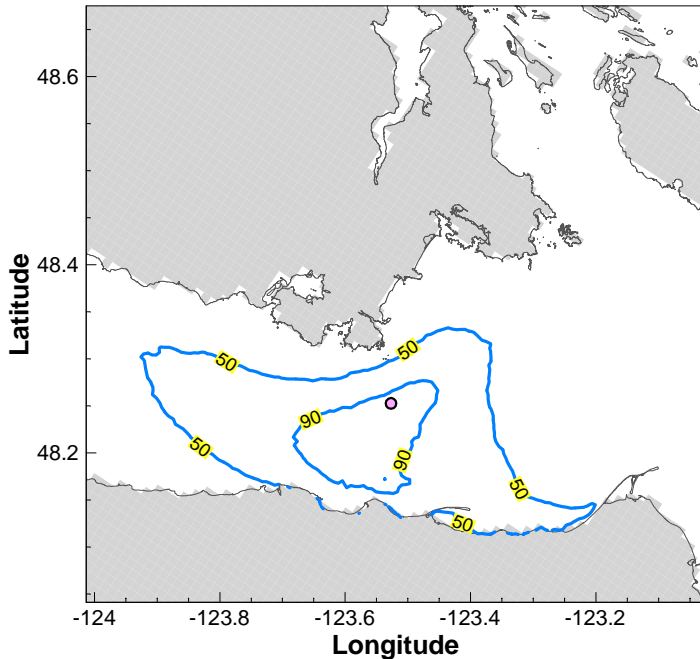
### Winter 2012

Area within the  $P_{50}$  Contour Line: 642 km<sup>2</sup>  
 Area within the  $P_{90}$  Contour Line: 123 km<sup>2</sup>  
 Average Thickness within the  $P_{50}$  Contour Line: 10  $\mu$ m  
 Average Thickness within the  $P_{90}$  Contour Line: 17  $\mu$ m  
 Average Shore Oiled: 23 km



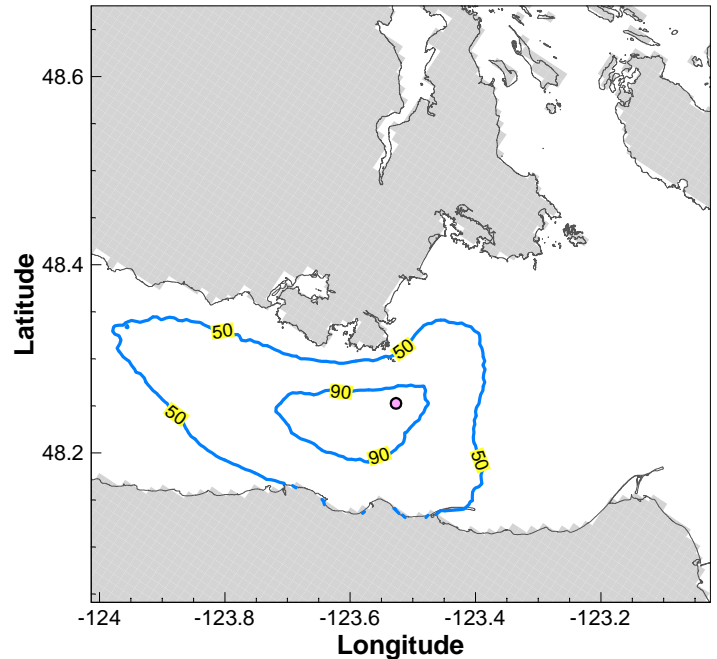
### Spring 2012

Area within the  $P_{50}$  Contour Line: 744 km<sup>2</sup>  
 Area within the  $P_{90}$  Contour Line: 184 km<sup>2</sup>  
 Average Thickness within the  $P_{50}$  Contour Line: 9  $\mu$ m  
 Average Thickness within the  $P_{90}$  Contour Line: 14  $\mu$ m  
 Average Shore Oiled: 26 km



### Summer 2012

Area within the  $P_{50}$  Contour Line: 670 km<sup>2</sup>  
 Area within the  $P_{90}$  Contour Line: 133 km<sup>2</sup>  
 Average Thickness within the  $P_{50}$  Contour Line: 10  $\mu$ m  
 Average Thickness within the  $P_{90}$  Contour Line: 16  $\mu$ m  
 Average Shore Oiled: 29 km



### Fall 2011

Area within the  $P_{50}$  Contour Line: 680 km<sup>2</sup>  
 Area within the  $P_{90}$  Contour Line: 111 km<sup>2</sup>  
 Average Thickness within the  $P_{50}$  Contour Line: 10  $\mu$ m  
 Average Thickness within the  $P_{90}$  Contour Line: 19  $\mu$ m  
 Average Shore Oiled: 25 km

## NOTES

○ Release Location

Probability of oil presence is the percentage of simulations in which oil was present at a given location.  
 $P_{50}$ : after 48 hours, there is 50% or greater probability for the area within the  $P_{50}$  contour line to have been contacted.  
 $P_{90}$ : after 48 hours, there is 90% or greater probability for the area within the  $P_{90}$  contour line to have been contacted.  
 Statistical results for each season based on independent spills occurring every 6 hours for three months.  
 Tracking time for each spill was 48 hours.  
 The average thickness is based on a full coverage of each grid cell that contains oil and lies within the contour line.

STATUS  
ISSUED FOR USE

## CLIENT

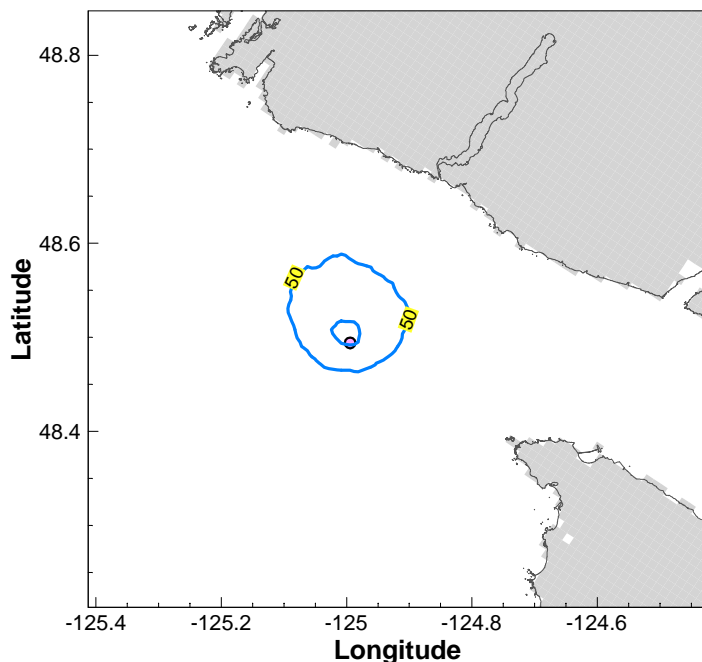


## TRANS MOUNTAIN OIL SPILL STUDY

Stochastic Simulation  
 Site G (8,250 m<sup>3</sup>)  
 $P_{50}$  and  $P_{90}$  after 48 Hours

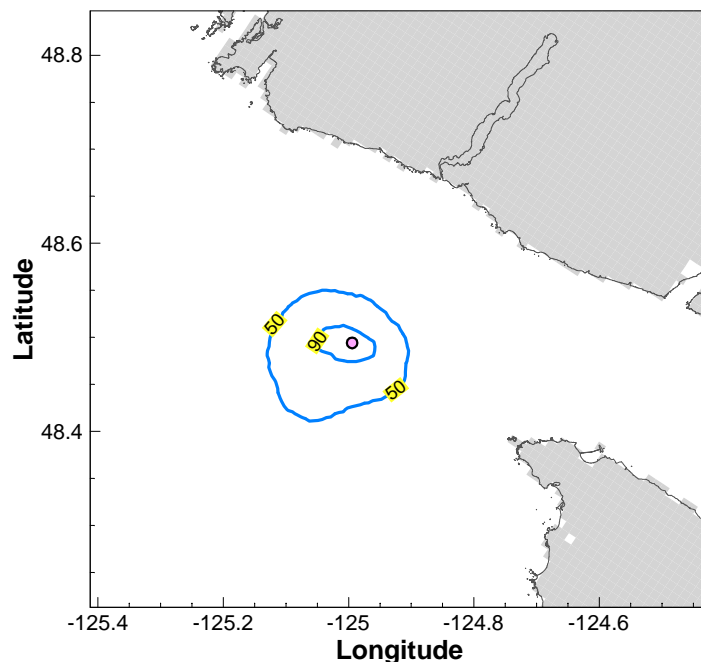
PROJECT NO.	DWN	CKD	APVD	REV
V13203022	DP	JAS	-	0
OFFICE	DATE			
EBA-VANC	October 25, 2013			

Figure 8.4.4



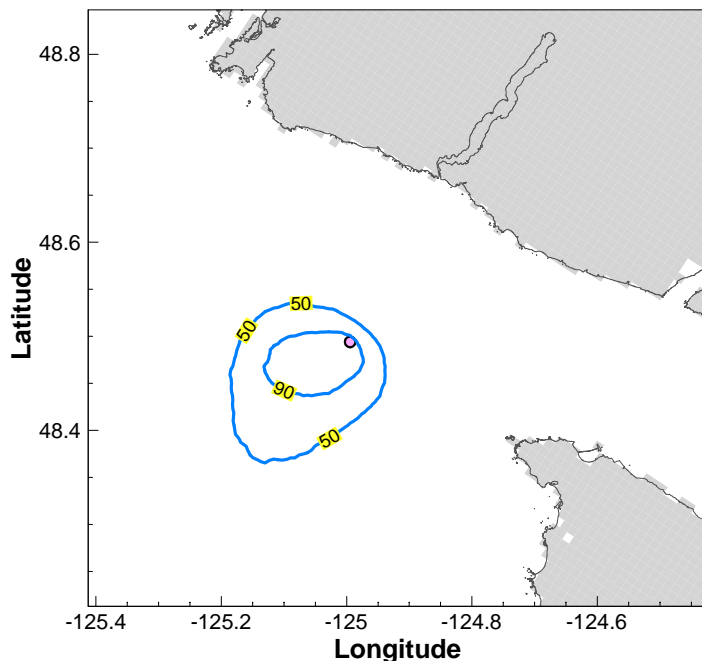
### Winter 2012

Area within the P<sub>50</sub> Contour Line: 146.3 km<sup>2</sup>  
 Area within the P<sub>90</sub> Contour Line: 7.5 km<sup>2</sup>  
 Average Thickness within the P<sub>50</sub> Contour Line: 59 um  
 Average Thickness within the P<sub>90</sub> Contour Line: 108 um  
 Average Shore Oiled: 10 km



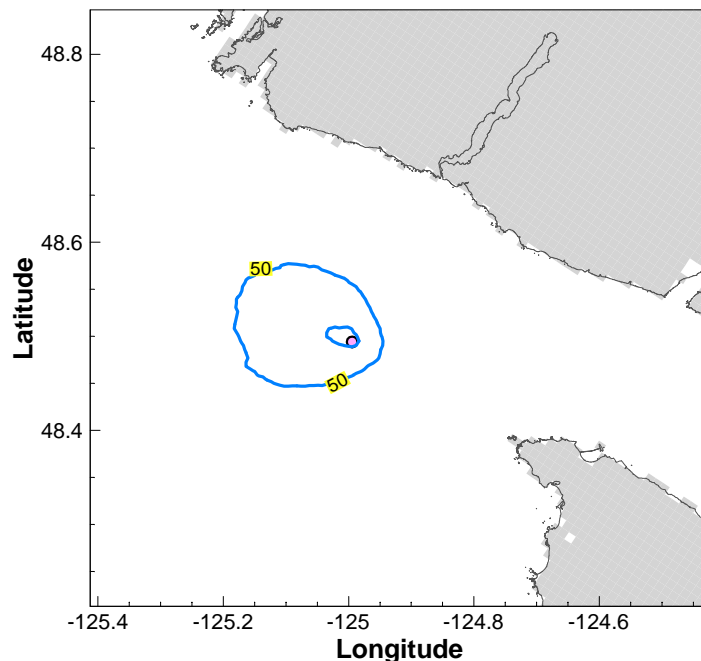
### Spring 2012

Area within the P<sub>50</sub> Contour Line: 195.0 km<sup>2</sup>  
 Area within the P<sub>90</sub> Contour Line: 22.0 km<sup>2</sup>  
 Average Thickness within the P<sub>50</sub> Contour Line: 53 um  
 Average Thickness within the P<sub>90</sub> Contour Line: 87 um  
 Average Shore Oiled: 2 km



### Summer 2012

Area within the P<sub>50</sub> Contour Line: 260.8 km<sup>2</sup>  
 Area within the P<sub>90</sub> Contour Line: 69.3 km<sup>2</sup>  
 Average Thickness within the P<sub>50</sub> Contour Line: 48 um  
 Average Thickness within the P<sub>90</sub> Contour Line: 61 um  
 Average Shore Oiled: 0 km



### Fall 2011

Area within the P<sub>50</sub> Contour Line: 200.5 km<sup>2</sup>  
 Area within the P<sub>90</sub> Contour Line: 6.5 km<sup>2</sup>  
 Average Thickness within the P<sub>50</sub> Contour Line: 54 um  
 Average Thickness within the P<sub>90</sub> Contour Line: 115 um  
 Average Shore Oiled: 7 km

## NOTES

○ Release Location

Probability of oil presence is the percentage of simulations in which oil was present at a given location.

P<sub>50</sub>: after 24 hours, there is 50% or greater probability for the area within the P<sub>50</sub> contour line to have been contacted.

P<sub>90</sub>: after 24 hours, there is 90% or greater probability for the area within the P<sub>90</sub> contour line to have been contacted.

Statistical results for each season based on independent spills occurring every 6 hours for three months.

Tracking time for each spill was 24 hours.

The average thickness is based on a full coverage of each grid cell that contains oil and lies within the contour line.

STATUS  
ISSUED FOR USE

## CLIENT



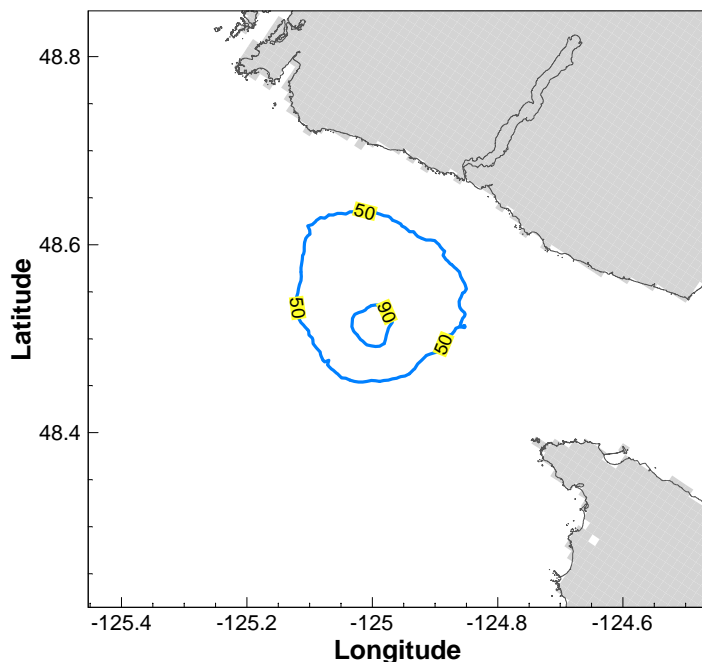
## TRANS MOUNTAIN OIL SPILL STUDY

Stochastic Simulation  
 Site H (16,500 m<sup>3</sup>)  
 P<sub>50</sub> and P<sub>90</sub> after 24 Hours

PROJECT NO.	DWN	CKD	APVD	REV
V13203022	DP	JAS	-	0
OFFICE	DATE			
EBA-VANC	November 7, 2013			

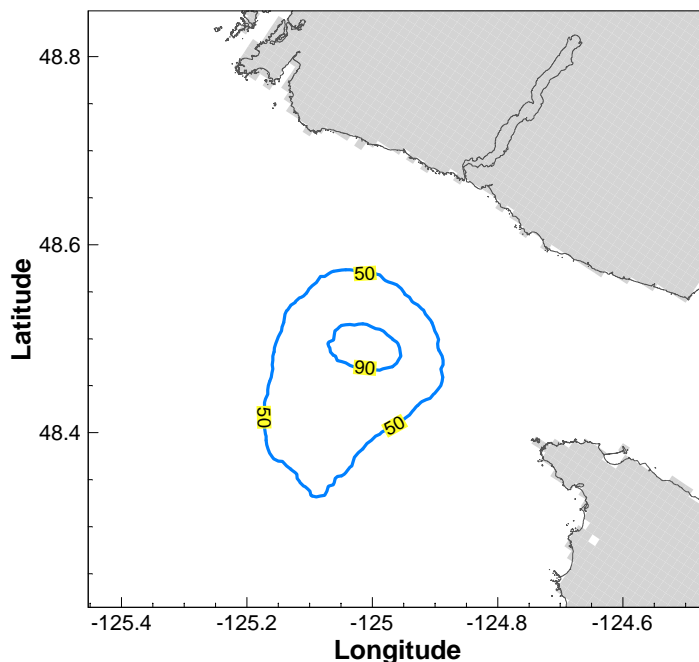
Figure 8.5.1





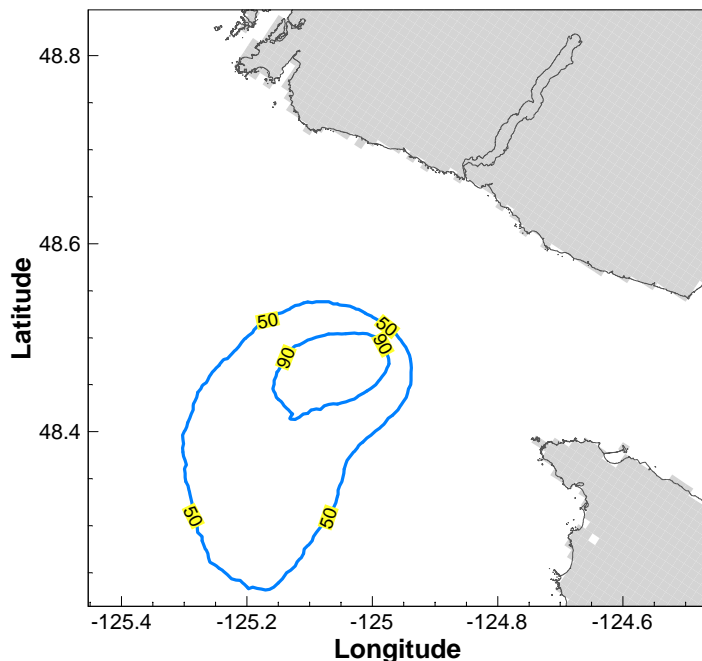
### Winter 2012

Area within the  $P_{50}$  Contour Line: 308.5 km<sup>2</sup>  
 Area within the  $P_{90}$  Contour Line: 17.3 km<sup>2</sup>  
 Average Thickness within the  $P_{50}$  Contour Line: 40 µm  
 Average Thickness within the  $P_{90}$  Contour Line: 74 µm  
 Average Shore Oiled: 24 km



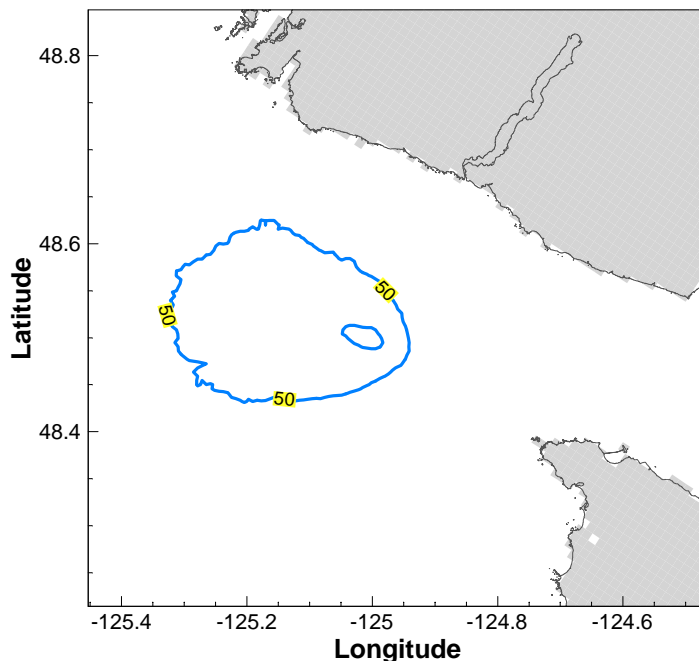
### Spring 2012

Area within the  $P_{50}$  Contour Line: 378.7 km<sup>2</sup>  
 Area within the  $P_{90}$  Contour Line: 34.5 km<sup>2</sup>  
 Average Thickness within the  $P_{50}$  Contour Line: 32 µm  
 Average Thickness within the  $P_{90}$  Contour Line: 64 µm  
 Average Shore Oiled: 7 km



### Summer 2012

Area within the  $P_{50}$  Contour Line: 591.7 km<sup>2</sup>  
 Area within the  $P_{90}$  Contour Line: 95.78 km<sup>2</sup>  
 Average Thickness within the  $P_{50}$  Contour Line: 29 µm  
 Average Thickness within the  $P_{90}$  Contour Line: 50 µm  
 Average Shore Oiled: 2 km



### Fall 2011

Area within the  $P_{50}$  Contour Line: 440.7 km<sup>2</sup>  
 Area within the  $P_{90}$  Contour Line: 9.5 km<sup>2</sup>  
 Average Thickness within the  $P_{50}$  Contour Line: 34 µm  
 Average Thickness within the  $P_{90}$  Contour Line: 99 µm  
 Average Shore Oiled: 18 km

## NOTES

○ Release Location

Probability of oil presence is the percentage of simulations in which oil was present at a given location.

$P_{50}$ : after 48 hours, there is 50% or greater probability for the area within the  $P_{50}$  contour line to have been contacted.

$P_{90}$ : after 48 hours, there is 90% or greater probability for the area within the  $P_{90}$  contour line to have been contacted.

Statistical results for each season based on independent spills occurring every 6 hours for three months.

Tracking time for each spill was 48 hours.

The average thickness is based on a full coverage of each grid cell that contains oil and lies within the contour line.

STATUS  
ISSUED FOR USE

CLIENT



TRANSMOUNTAIN



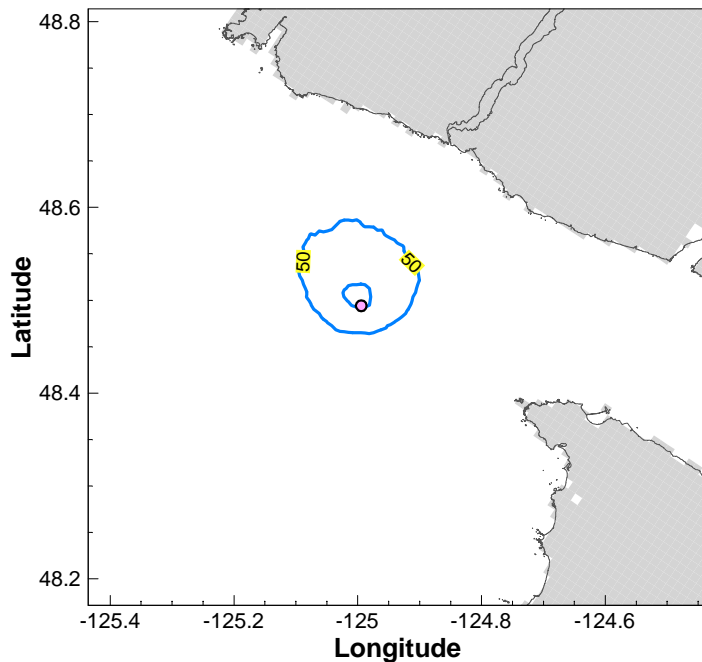
A TETRA TECH COMPANY

## TRANS MOUNTAIN OIL SPILL STUDY

Stochastic Simulation  
 Site H (16,500 m<sup>3</sup>)  
 $P_{50}$  and  $P_{90}$  after 48 Hours

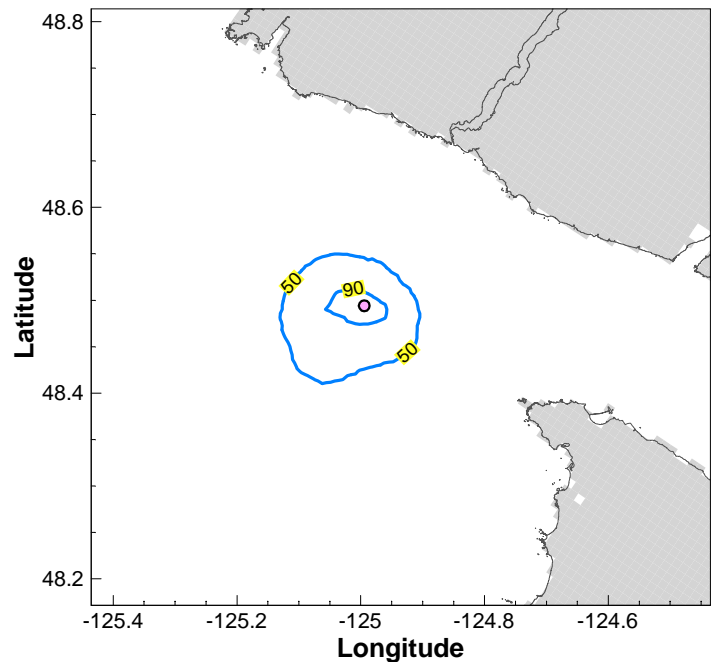
PROJECT NO.	DWN	CKD	APVD	REV
V13203022	DP	JAS	-	0
OFFICE	DATE			
EBA-VANC	November 7, 2013			

Figure 8.5.2



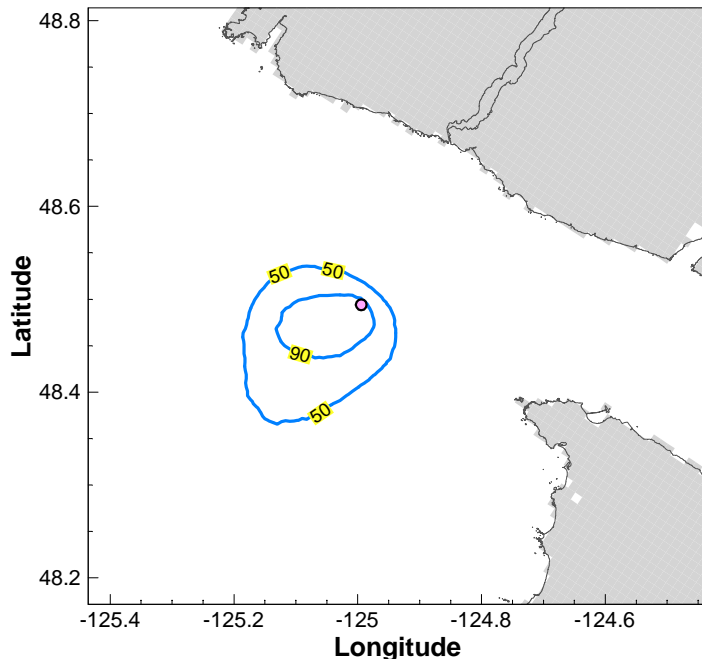
### Winter 2012

Area within the  $P_{50}$  Contour Line: 145.0 km<sup>2</sup>  
 Area within the  $P_{90}$  Contour Line: 8.0 km<sup>2</sup>  
 Average Thickness within the  $P_{50}$  Contour Line: 29 um  
 Average Thickness within the  $P_{90}$  Contour Line: 53 um  
 Average Shore Oiled: 4.3 km



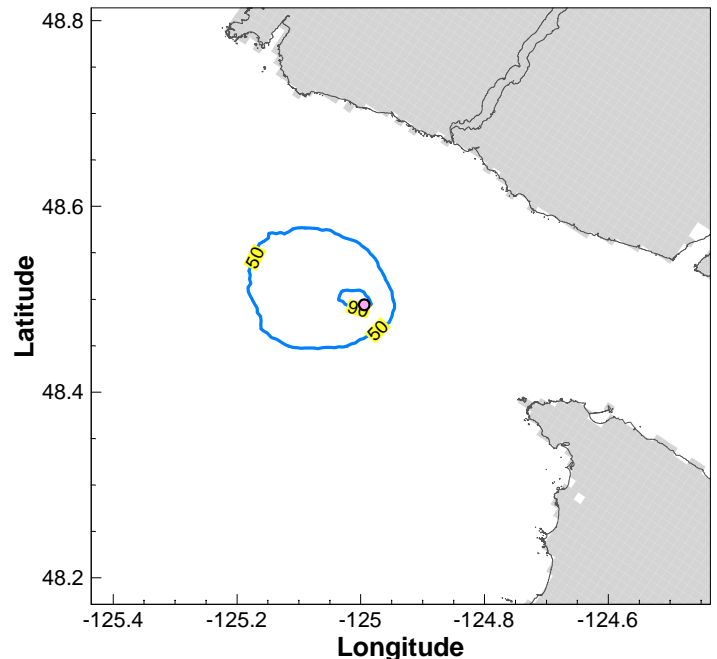
### Spring 2012

Area within the  $P_{50}$  Contour Line: 195.0 km<sup>2</sup>  
 Area within the  $P_{90}$  Contour Line: 21.8 km<sup>2</sup>  
 Average Thickness within the  $P_{50}$  Contour Line: 26 um  
 Average Thickness within the  $P_{90}$  Contour Line: 44 um  
 Average Shore Oiled: 2 km



### Summer 2012

Area within the  $P_{50}$  Contour Line: 260.3 km<sup>2</sup>  
 Area within the  $P_{90}$  Contour Line: 69.0 km<sup>2</sup>  
 Average Thickness within the  $P_{50}$  Contour Line: 24 um  
 Average Thickness within the  $P_{90}$  Contour Line: 30 um  
 Average Shore Oiled: 0 km



### Fall 2011

Area within the  $P_{50}$  Contour Line: 199.5 km<sup>2</sup>  
 Area within the  $P_{90}$  Contour Line: 6.8 km<sup>2</sup>  
 Average Thickness within the  $P_{50}$  Contour Line: 27 um  
 Average Thickness within the  $P_{90}$  Contour Line: 57 um  
 Average Shore Oiled: 6.8 km

## NOTES

○ Release Location

Probability of oil presence is the percentage of simulations in which oil was present at a given location.  
 $P_{50}$ : after 24 hours, there is 50% or greater probability for the area within the  $P_{50}$  contour line to have been contacted.  
 $P_{90}$ : after 24 hours, there is 90% or greater probability for the area within the  $P_{90}$  contour line to have been contacted.  
 Statistical results for each season based on independent spills occurring every 6 hours for three months.  
 Tracking time for each spill was 24 hours.  
 The average thickness is based on a full coverage of each grid cell that contains oil and lies within the contour line.

STATUS  
ISSUED FOR USE

## CLIENT



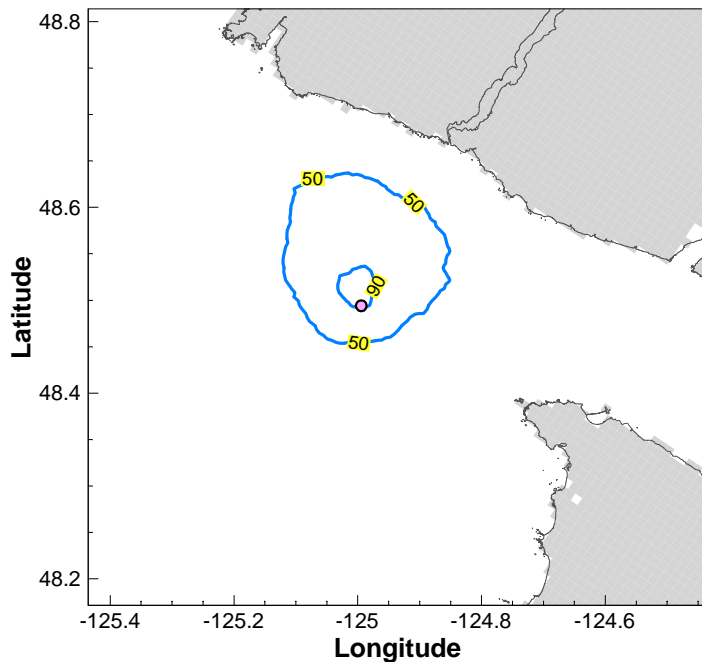
## TRANS MOUNTAIN OIL SPILL STUDY

Stochastic Simulation  
 Site H (8,250 m<sup>3</sup>)  
 $P_{50}$  and  $P_{90}$  after 24 Hours

PROJECT NO.	DWN	CKD	APVD	REV
V13203022	DP	JAS	-	0
OFFICE	DATE			
EBA-VANC	October 25, 2013			

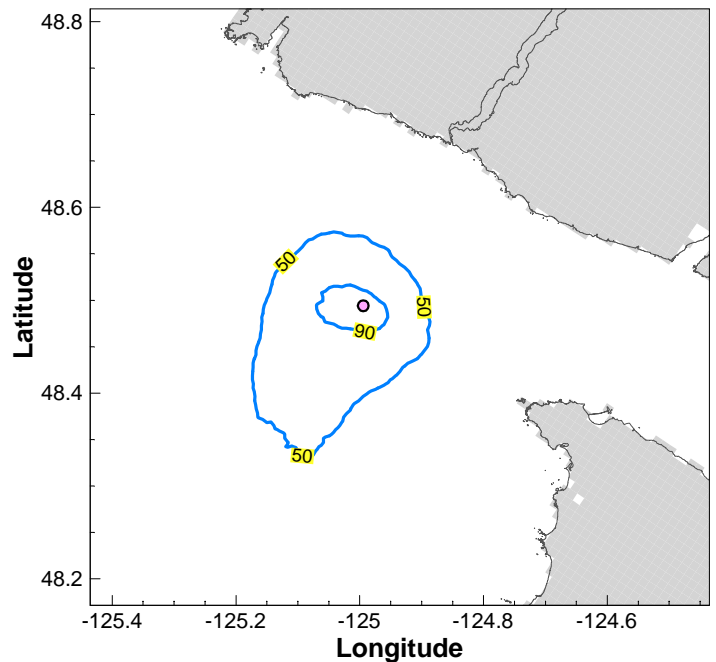
Figure 8.5.3





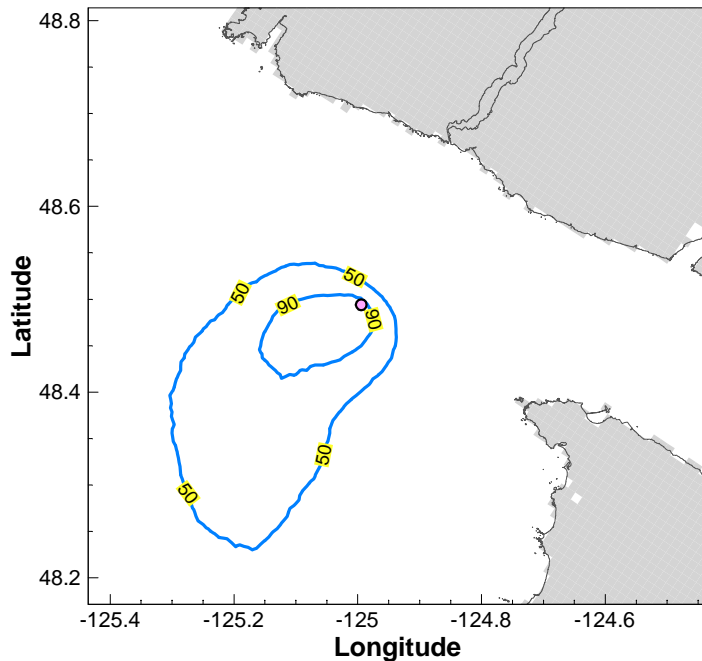
### Winter 2012

Area within the  $P_{50}$  Contour Line: 311.5 km<sup>2</sup>  
 Area within the  $P_{90}$  Contour Line: 17.3 km<sup>2</sup>  
 Average Thickness within the  $P_{50}$  Contour Line: 20  $\mu$ m  
 Average Thickness within the  $P_{90}$  Contour Line: 37  $\mu$ m  
 Average Shore Oiled: 23.5 km



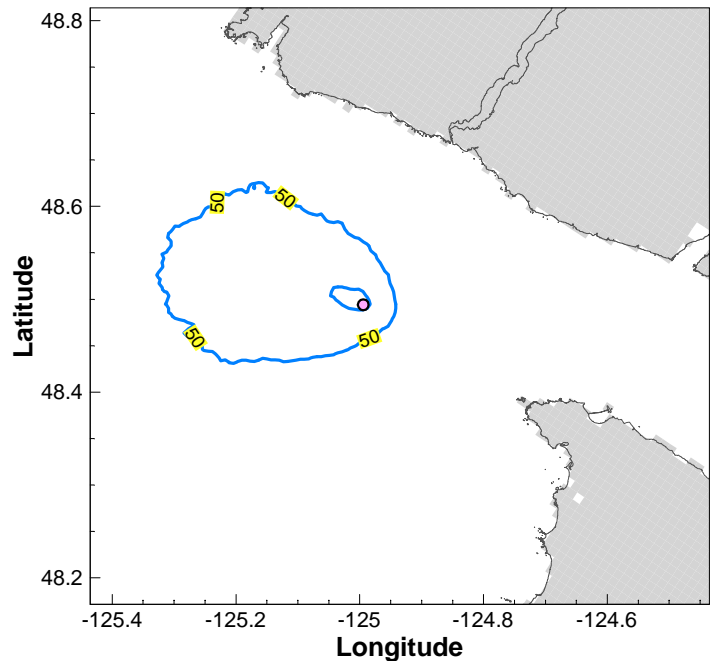
### Spring 2012

Area within the  $P_{50}$  Contour Line: 378.0 km<sup>2</sup>  
 Area within the  $P_{90}$  Contour Line: 34.8 km<sup>2</sup>  
 Average Thickness within the  $P_{50}$  Contour Line: 15.8  $\mu$ m  
 Average Thickness within the  $P_{90}$  Contour Line: 32  $\mu$ m  
 Average Shore Oiled: 7 km



### Summer 2012

Area within the  $P_{50}$  Contour Line: 590.0 km<sup>2</sup>  
 Area within the  $P_{90}$  Contour Line: 95.5 km<sup>2</sup>  
 Average Thickness within the  $P_{50}$  Contour Line: 14  $\mu$ m  
 Average Thickness within the  $P_{90}$  Contour Line: 25  $\mu$ m  
 Average Shore Oiled: 0.1 km



### Fall 2011

Area within the  $P_{50}$  Contour Line: 435.2 km<sup>2</sup>  
 Area within the  $P_{90}$  Contour Line: 9.5 km<sup>2</sup>  
 Average Thickness within the  $P_{50}$  Contour Line: 17  $\mu$ m  
 Average Thickness within the  $P_{90}$  Contour Line: 49  $\mu$ m  
 Average Shore Oiled: 16.5 km

## NOTES

○ Release Location

Probability of oil presence is the percentage of simulations in which oil was present at a given location.  
 $P_{50}$ : after 48 hours, there is 50% or greater probability for the area within the  $P_{50}$  contour line to have been contacted.  
 $P_{90}$ : after 48 hours, there is 90% or greater probability for the area within the  $P_{90}$  contour line to have been contacted.  
 Statistical results for each season based on independent spills occurring every 6 hours for three months.  
 Tracking time for each spill was 48 hours.  
 The average thickness is based on a full coverage of each grid cell that contains oil and lies within the contour line.

STATUS  
ISSUED FOR USE

## CLIENT

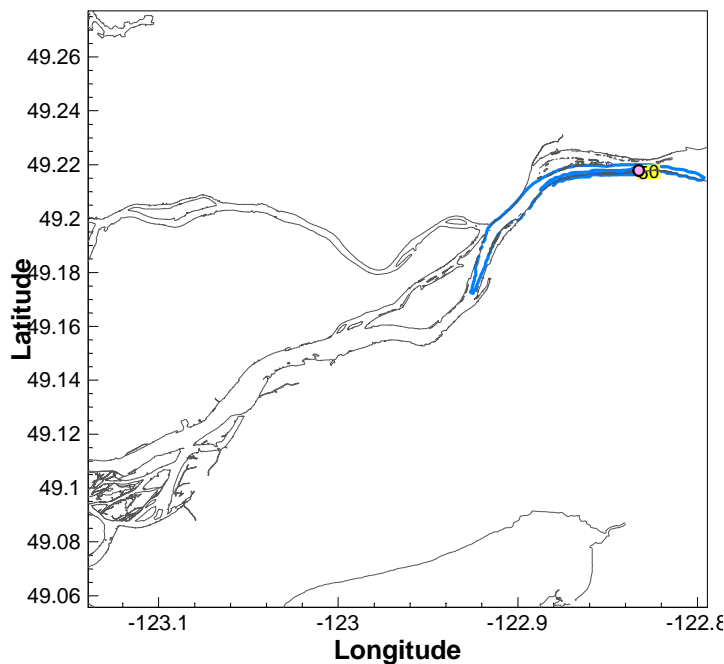


## TRANS MOUNTAIN OIL SPILL STUDY

Stochastic Simulation  
 Site H (8,250 m<sup>3</sup>)  
 $P_{50}$  and  $P_{90}$  after 48 Hours

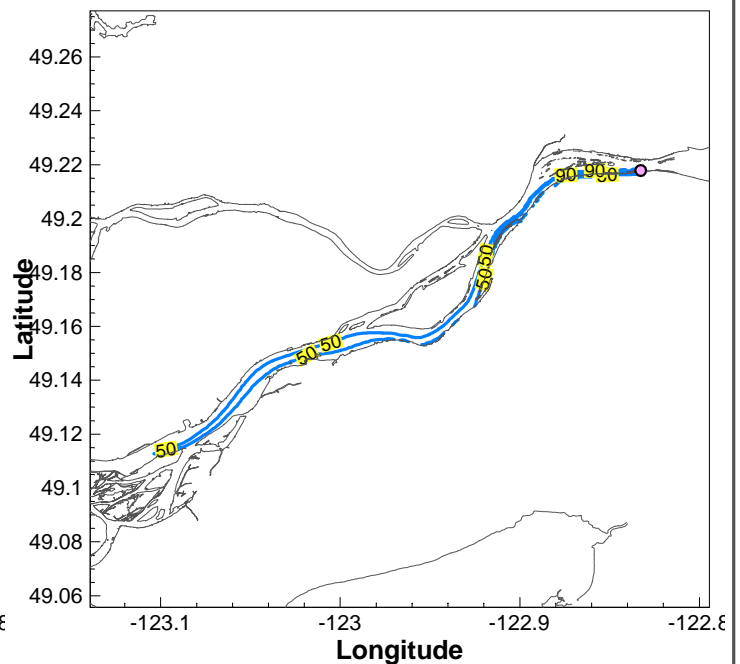
PROJECT NO.	DWN	CKD	APVD	REV
V13203022	DP	JAS	-	0
OFFICE	DATE			
EBA-VANC	October 25, 2013			

Figure 8.5.4



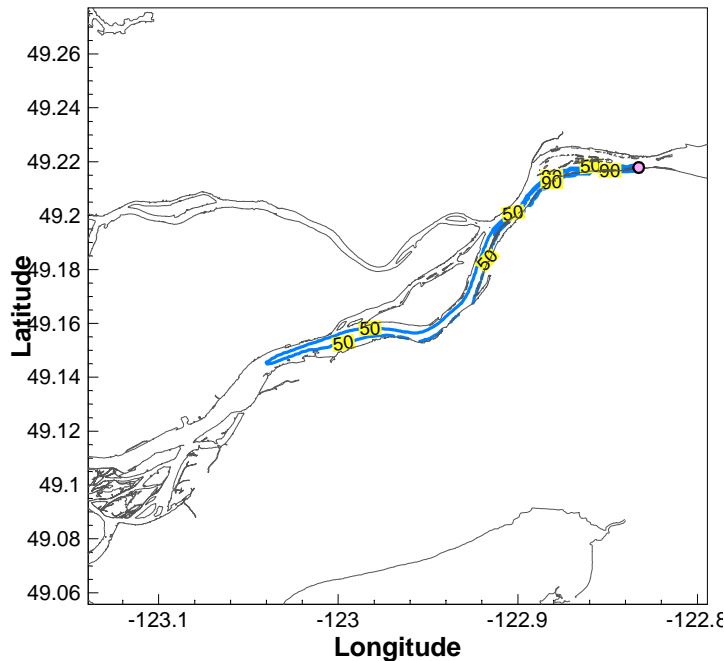
### Winter 2012

Area within the  $P_{50}$  Contour Line: 5.0 km<sup>2</sup>  
 Area within the  $P_{90}$  Contour Line: 1.0 km<sup>2</sup>  
 Average Thickness within the  $P_{50}$  Contour Line: 5  $\mu$ m  
 Average Thickness within the  $P_{90}$  Contour Line: 17  $\mu$ m  
 Average Shore Oiled: 15 km



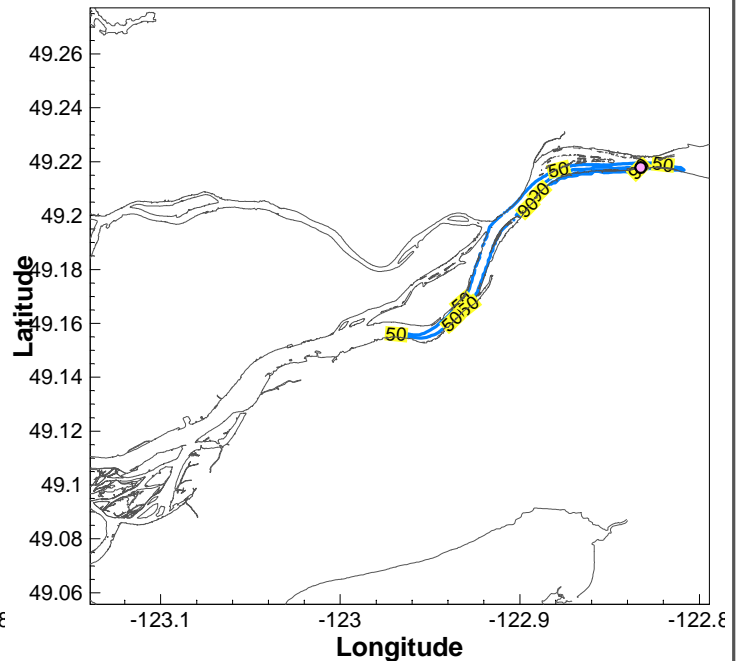
### Spring 2012

Area within the  $P_{50}$  Contour Line: 6.8 km<sup>2</sup>  
 Area within the  $P_{90}$  Contour Line: 1.4 km<sup>2</sup>  
 Average Thickness within the  $P_{50}$  Contour Line: 4  $\mu$ m  
 Average Thickness within the  $P_{90}$  Contour Line: 19  $\mu$ m  
 Average Shore Oiled: 14 km



### Summer 2012

Area within the  $P_{50}$  Contour Line: 5.4 km<sup>2</sup>  
 Area within the  $P_{90}$  Contour Line: 1.3 km<sup>2</sup>  
 Average Thickness within the  $P_{50}$  Contour Line: 5  $\mu$ m  
 Average Thickness within the  $P_{90}$  Contour Line: 17  $\mu$ m  
 Average Shore Oiled: 15 km



### Fall 2011

Area within the  $P_{50}$  Contour Line: 5.6 km<sup>2</sup>  
 Area within the  $P_{90}$  Contour Line: 1.1 km<sup>2</sup>  
 Average Thickness within the  $P_{50}$  Contour Line: 5  $\mu$ m  
 Average Thickness within the  $P_{90}$  Contour Line: 19  $\mu$ m  
 Average Shore Oiled: 14 km

## NOTES

○ Release Location

Probability of oil presence is the percentage of simulations in which oil was present at a given location.  
 $P_{50}$ : after 12 hours, there is 50% or greater probability for the area within the  $P_{50}$  contour line to have been contacted.  
 $P_{90}$ : after 12 hours, there is 90% or greater probability for the area within the  $P_{90}$  contour line to have been contacted.  
 Statistical results for each season based on independent spills occurring every 6 hours for three months.  
 Tracking time for each spill was 12 hours.  
 The average thickness is based on a full coverage of each grid cell that contains oil and lies within the contour line.

STATUS  
ISSUED FOR USE

CLIENT



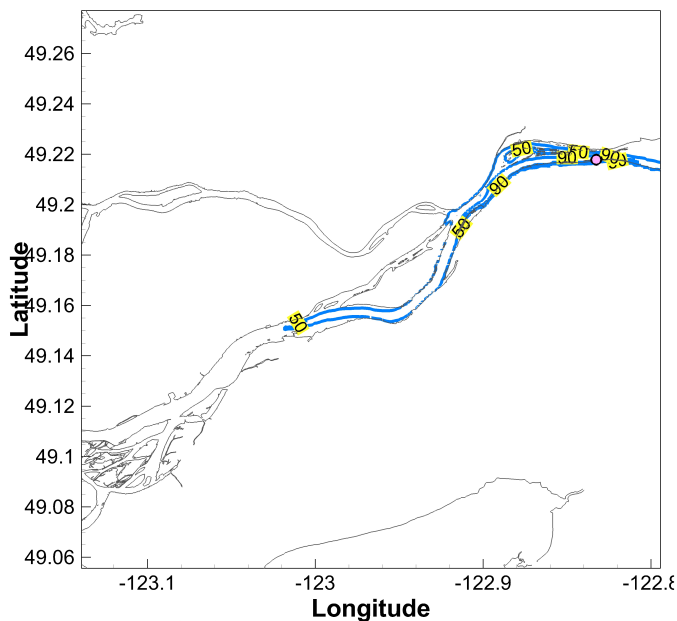
A TETRA TECH COMPANY

## TRANS MOUNTAIN OIL SPILL STUDY

Stochastic Simulation  
 Site FR (1,250 m<sup>3</sup>)  
 $P_{50}$  and  $P_{90}$  after 12 Hours

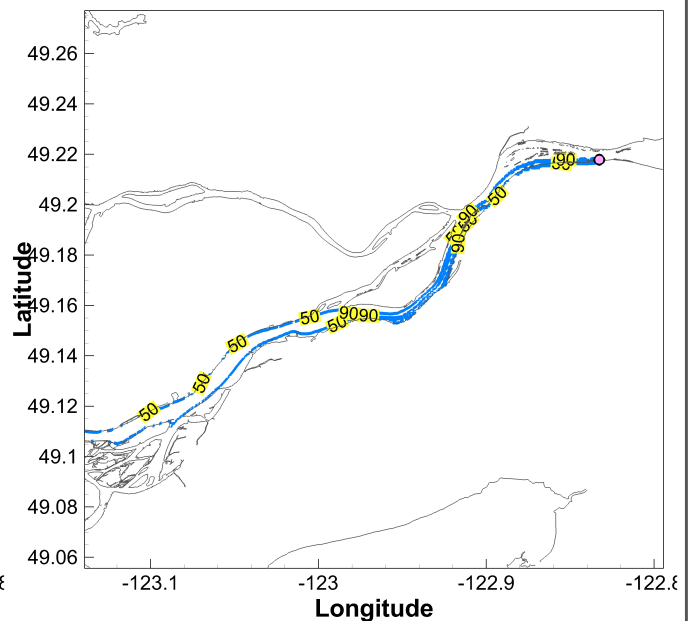
PROJECT NO.	DWN	CKD	APVD	REV
V13203022	AH	JAS	-	0
OFFICE	DATE			
EBA-VANC	November 27, 2013			

Figure 8.6.1



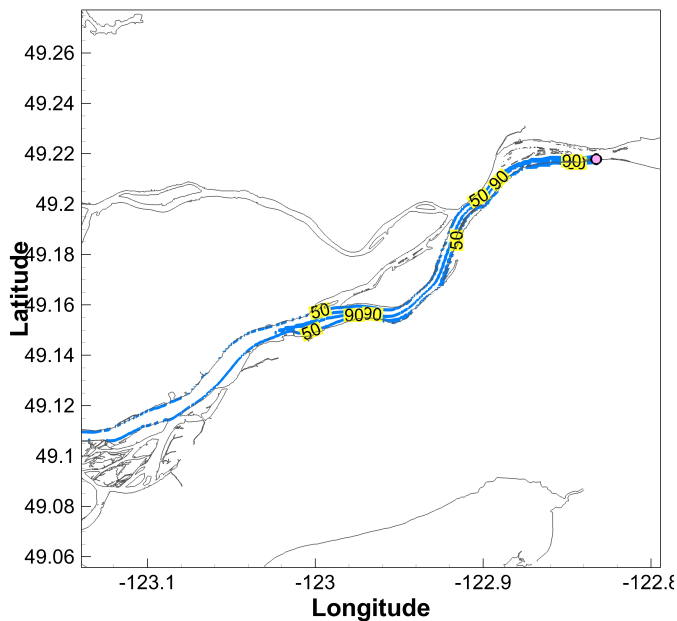
### Winter 2012

Area within the P<sub>50</sub> Contour Line: 10.8 km<sup>2</sup>  
 Area within the P<sub>90</sub> Contour Line: 2.4 km<sup>2</sup>  
 Average Thickness within the P<sub>50</sub> Contour Line: 2 µm  
 Average Thickness within the P<sub>90</sub> Contour Line: 5 µm  
 Average Shore Oiled: 34 km



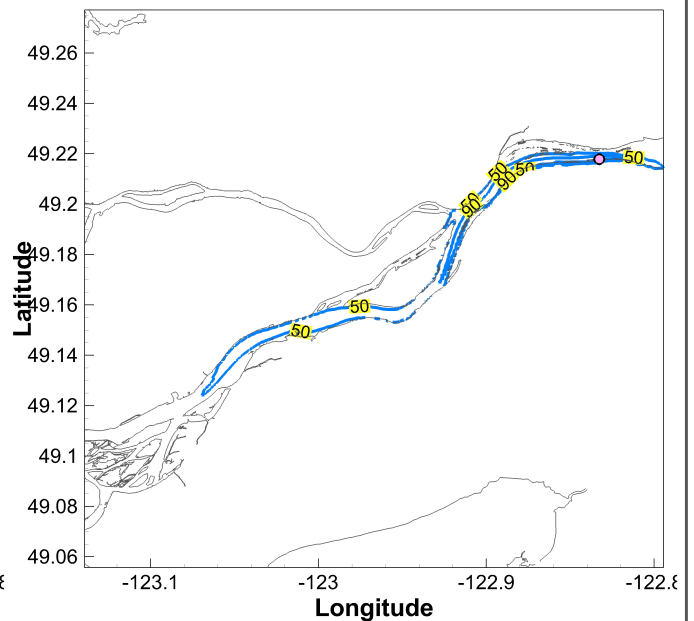
### Spring 2012

Area within the P<sub>50</sub> Contour Line: 16.8 km<sup>2</sup>  
 Area within the P<sub>90</sub> Contour Line: 2.6 km<sup>2</sup>  
 Average Thickness within the P<sub>50</sub> Contour Line: 2 µm  
 Average Thickness within the P<sub>90</sub> Contour Line: 9 µm  
 Average Shore Oiled: 25 km



### Summer 2012

Area within the P<sub>50</sub> Contour Line: 15.6 km<sup>2</sup>  
 Area within the P<sub>90</sub> Contour Line: 3.5 km<sup>2</sup>  
 Average Thickness within the P<sub>50</sub> Contour Line: 2 µm  
 Average Thickness within the P<sub>90</sub> Contour Line: 6 µm  
 Average Shore Oiled: 33 km



### Fall 2011

Area within the P<sub>50</sub> Contour Line: 12.6 km<sup>2</sup>  
 Area within the P<sub>90</sub> Contour Line: 2.7 km<sup>2</sup>  
 Average Thickness within the P<sub>50</sub> Contour Line: 2 µm  
 Average Thickness within the P<sub>90</sub> Contour Line: 8 µm  
 Average Shore Oiled: 36 km

## NOTES

○ Release Location

Probability of oil presence is the percentage of simulations in which oil was present at a given location.  
 P<sub>50</sub>: after 24 hours, there is 50% or greater probability for the area within the P<sub>50</sub> contour line to have been contacted.  
 P<sub>90</sub>: after 24 hours, there is 90% or greater probability for the area within the P<sub>90</sub> contour line to have been contacted.  
 Statistical results for each season based on independent spills occurring every 6 hours for three months.  
 Tracking time for each spill was 24 hours.  
 The average thickness is based on a full coverage of each grid cell that contains oil and lies within the contour line.

STATUS  
ISSUED FOR USE

## CLIENT



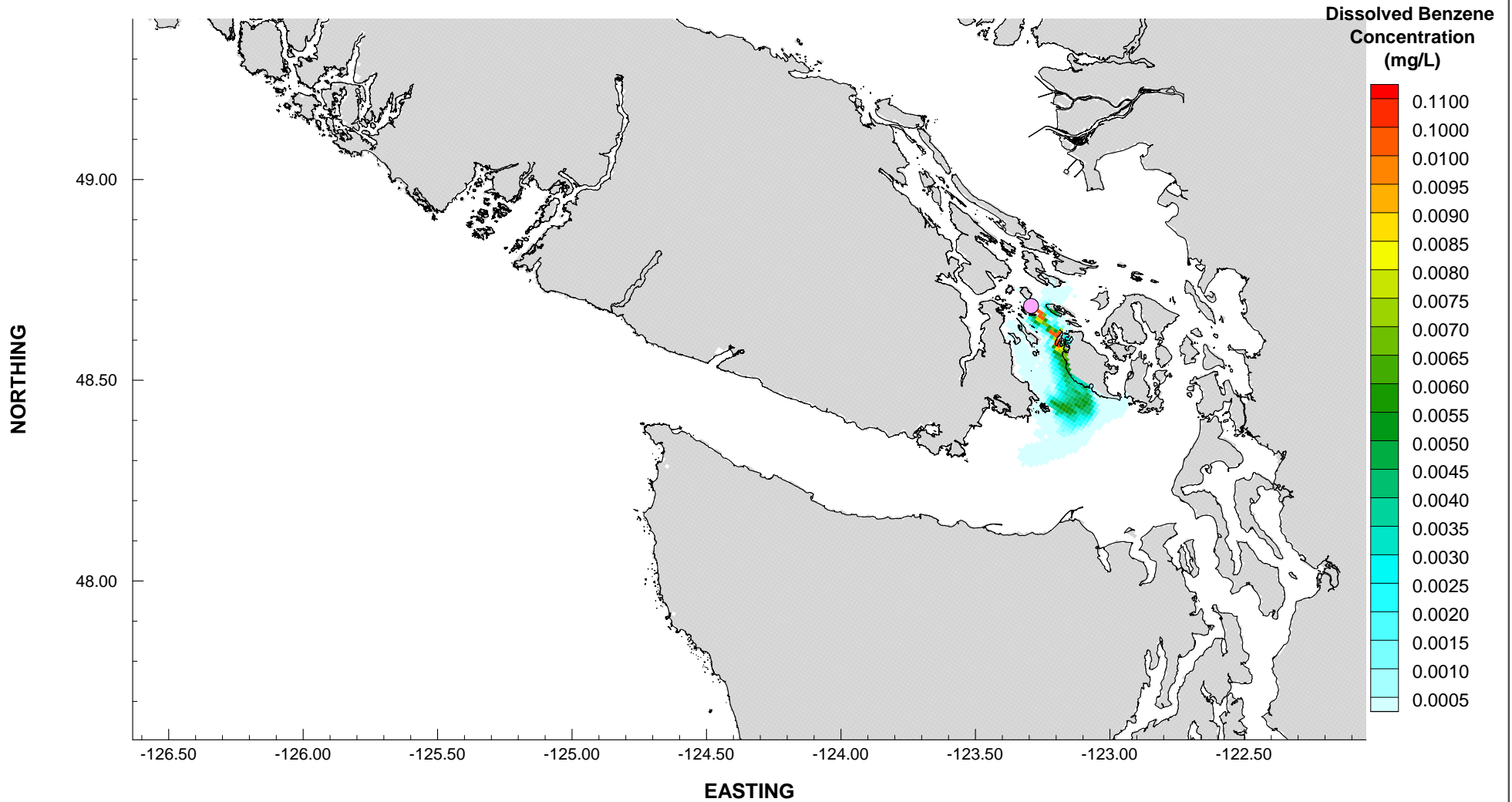
## TRANS MOUNTAIN OIL SPILL STUDY

Stochastic Simulation  
 Site FR (1,250 m<sup>3</sup>)  
 P<sub>50</sub> and P<sub>90</sub> after 24 Hours

PROJECT NO.	DWN	CKD	APVD	REV
V13203022	AH	JAS	-	0
OFFICE	DATE			
EBA-VANC	November 27, 2013			

Figure 8.6.2

201207232000



## NOTES

- The benzene concentration is displayed in mg per litre.
- For comparison purpose, the CCME guideline for the Protection of Aquatic Life is set for benzene at 0.11 mg/L (110 micrograms per litre of water).
- A cut-off value of 1e-8 mg/L was applied.

STATUS  
ISSUED FOR USE

CLIENT



## TRANS MOUNTAIN OIL SPILL STUDY

### Benzene Concentration in the Surface Layer after 13 Hours

PROJECT NO.  
V13203022

OFFICE  
EBA-VANC

DWN  
AH

DATE  
November 18, 2013

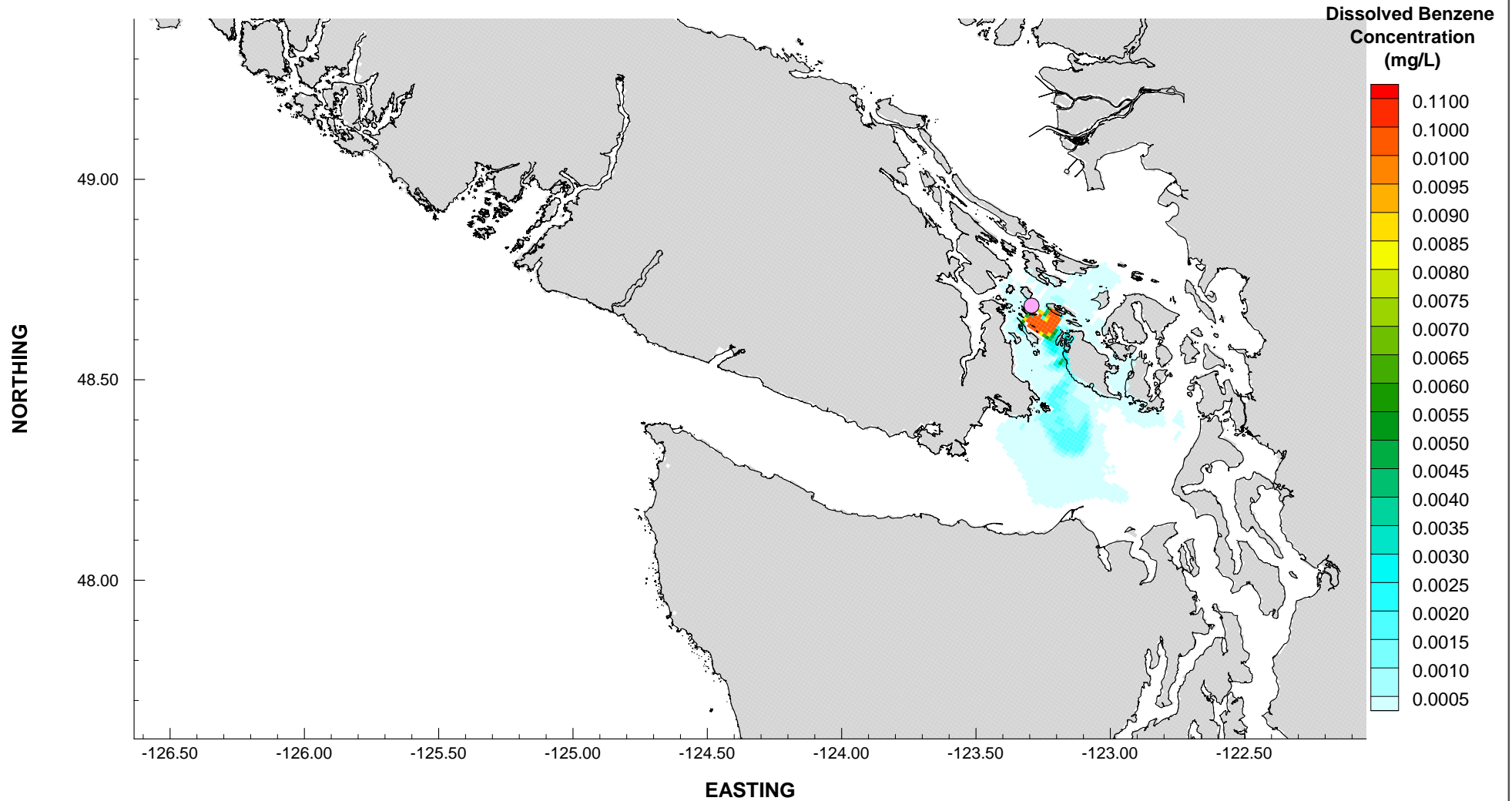
CKD  
JAS

APVD  
JAS

REV  
0

Figure 9.2.1

201207240700



## NOTES

- The benzene concentration is displayed in mg per litre.
- For comparison purpose, the CCME guideline for the Protection of Aquatic Life is set for benzene at 0.11 mg/L (110 micrograms per litre of water).
- A cut-off value of 1e-8 mg/L was applied.

STATUS  
ISSUED FOR USE

CLIENT



## TRANS MOUNTAIN OIL SPILL STUDY

### Benzene Concentration in the Surface Layer after 24 Hours

PROJECT NO.  
V13203022

OFFICE  
EBA-VANC

DWN  
AH

DATE  
November 18, 2013

CKD  
JAS

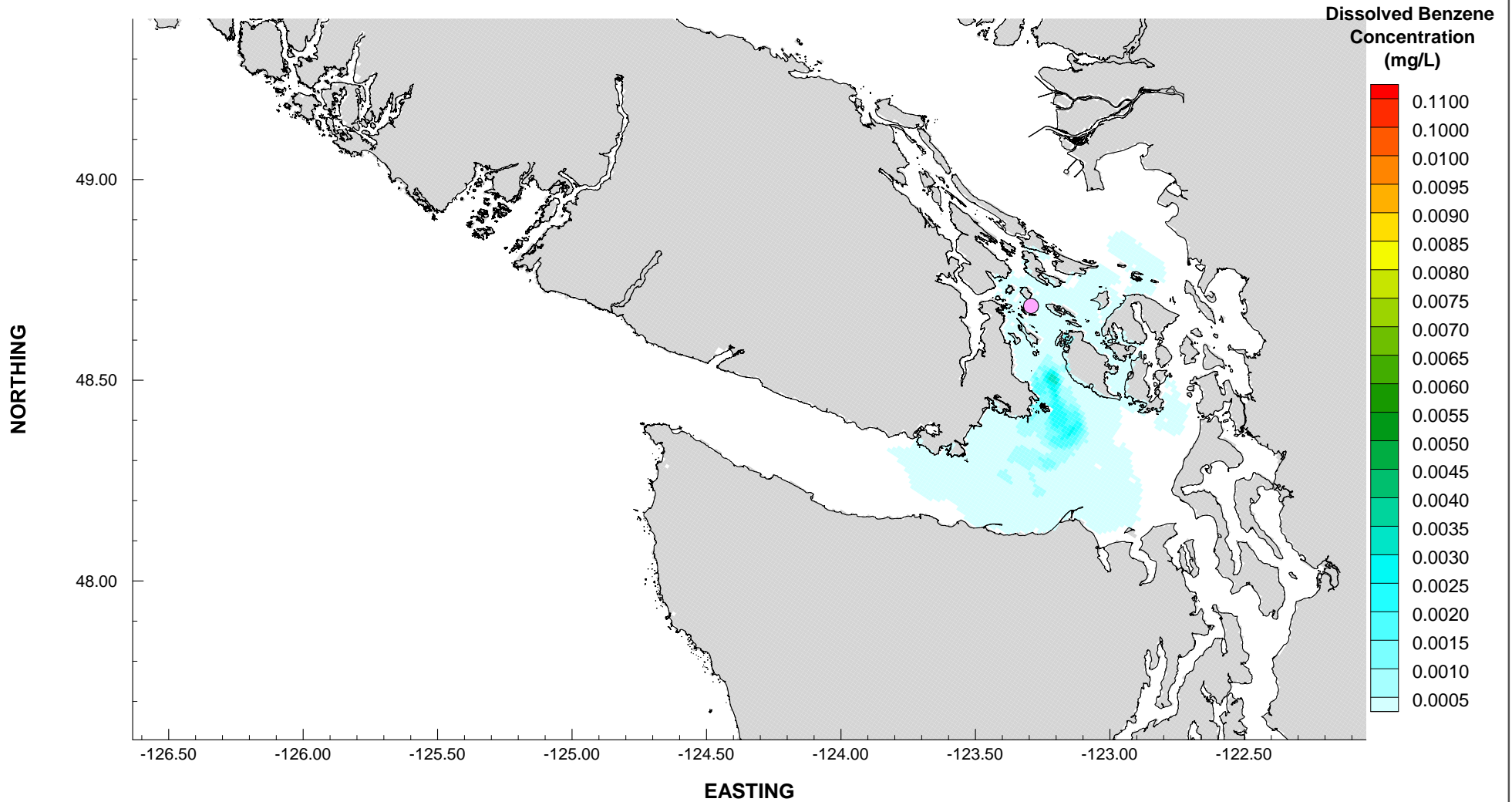
APVD  
JAS

REV  
0

Figure 9.2.2



201207250700



## NOTES

- The benzene concentration is displayed in mg per litre.
- For comparison purpose, the CCME guideline for the Protection of Aquatic Life is set for benzene at 0.11 mg/L (110 micrograms per litre of water).
- A cut-off value of 1e-8 mg/L was applied.

STATUS  
ISSUED FOR USE

CLIENT



## TRANS MOUNTAIN OIL SPILL STUDY

### Benzene Concentration in the Surface Layer after 48 Hours

PROJECT NO.  
V13203022

OFFICE  
EBA-VANC

DWN  
AH

DATE  
November 18, 2013

CKD  
JAS

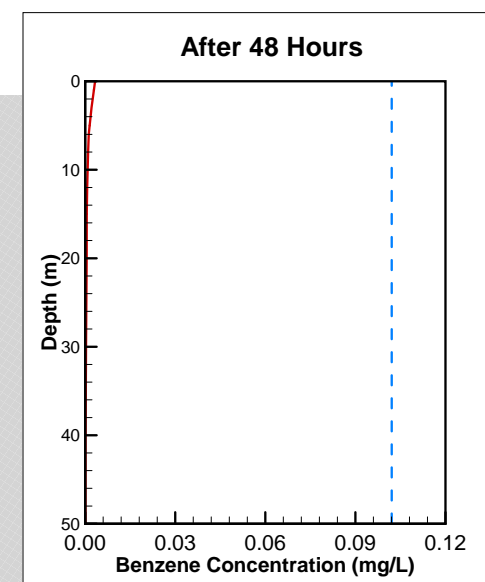
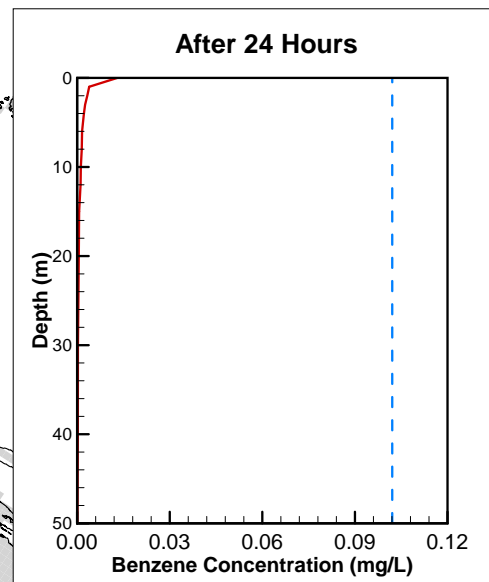
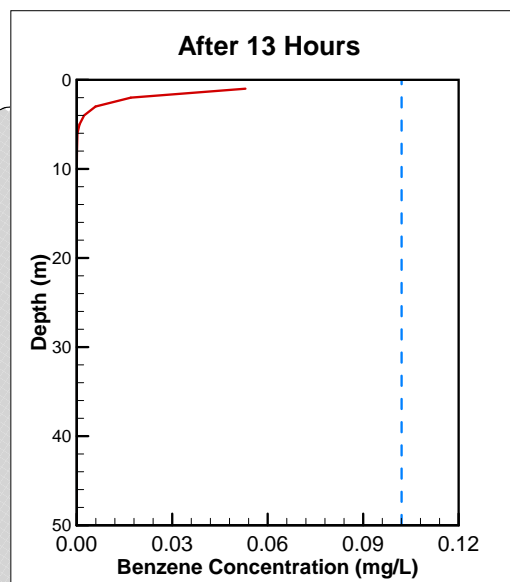
APVD  
JAS

REV  
0

Figure 9.2.3

NORTHING

49.20  
49.00  
48.80  
48.60  
48.40



Release Location

Profile after 13 Hours

Profile after 24 Hours

Profile after 48 Hours

EASTING

-124.60 -124.40 -124.20 -124.00 -123.80 -123.60 -123.40 -123.20 -123.00 -122.80 -122.60 -122.40 -122.20 -122.00

## NOTES

- The CCME guideline for the Protection of Aquatic Life in marine environment is set for benzene at 0.11 mg/L (110 micrograms per litre of water).
- Three benzene concentration profiles corresponding to the maximum surface concentration after 13, 24, 48 hours were plotted. The red line represents the benzene concentration. The dashed blue line represents the CCME threshold value.

STATUS  
ISSUED FOR USE

CLIENT



## TRANS MOUNTAIN OIL SPILL STUDY

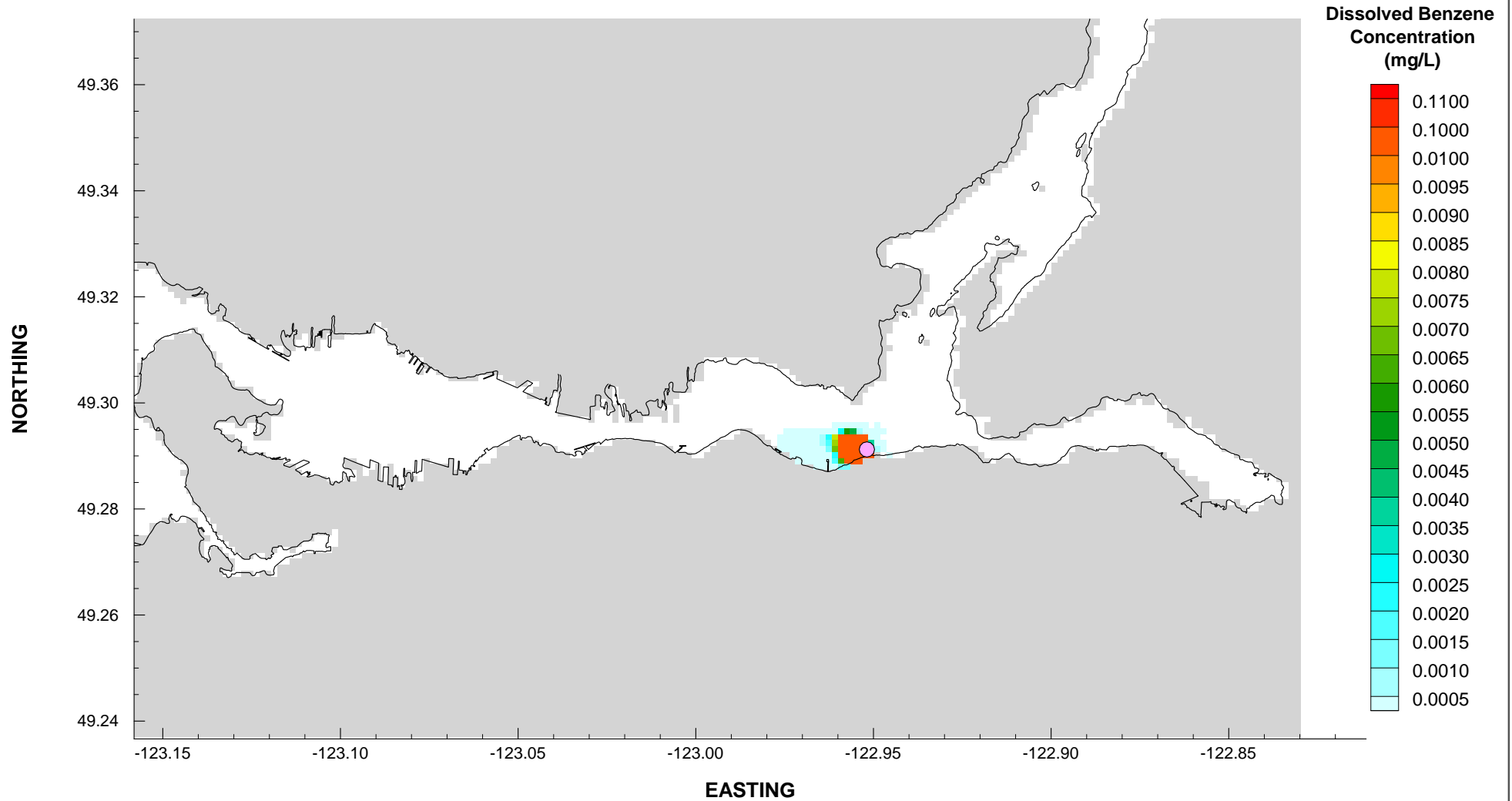
### Profile of Benzene Concentration

PROJECT NO. V13203022	DWN AH	CKD JAS	APVD JAS	REV 0
OFFICE EBA-VANC	DATE November 18, 2013			

Figure 9.2.4



201208212300



## NOTES

- The benzene concentration is displayed in mg per litre.
- For comparison purpose, the CCME guideline for the Protection of Aquatic Life is set for benzene at 0.11 mg/L (110 micrograms per litre of water).
- A cut-off value of 1e-8 mg/L was applied.

STATUS  
ISSUED FOR USE

CLIENT



## TRANS MOUNTAIN OIL SPILL STUDY

### Benzene Concentration in the Surface Layer after 1 Hour

PROJECT NO.  
V13203022

OFFICE  
EBA-VANC

DWN  
AH

DATE  
November 20, 2013

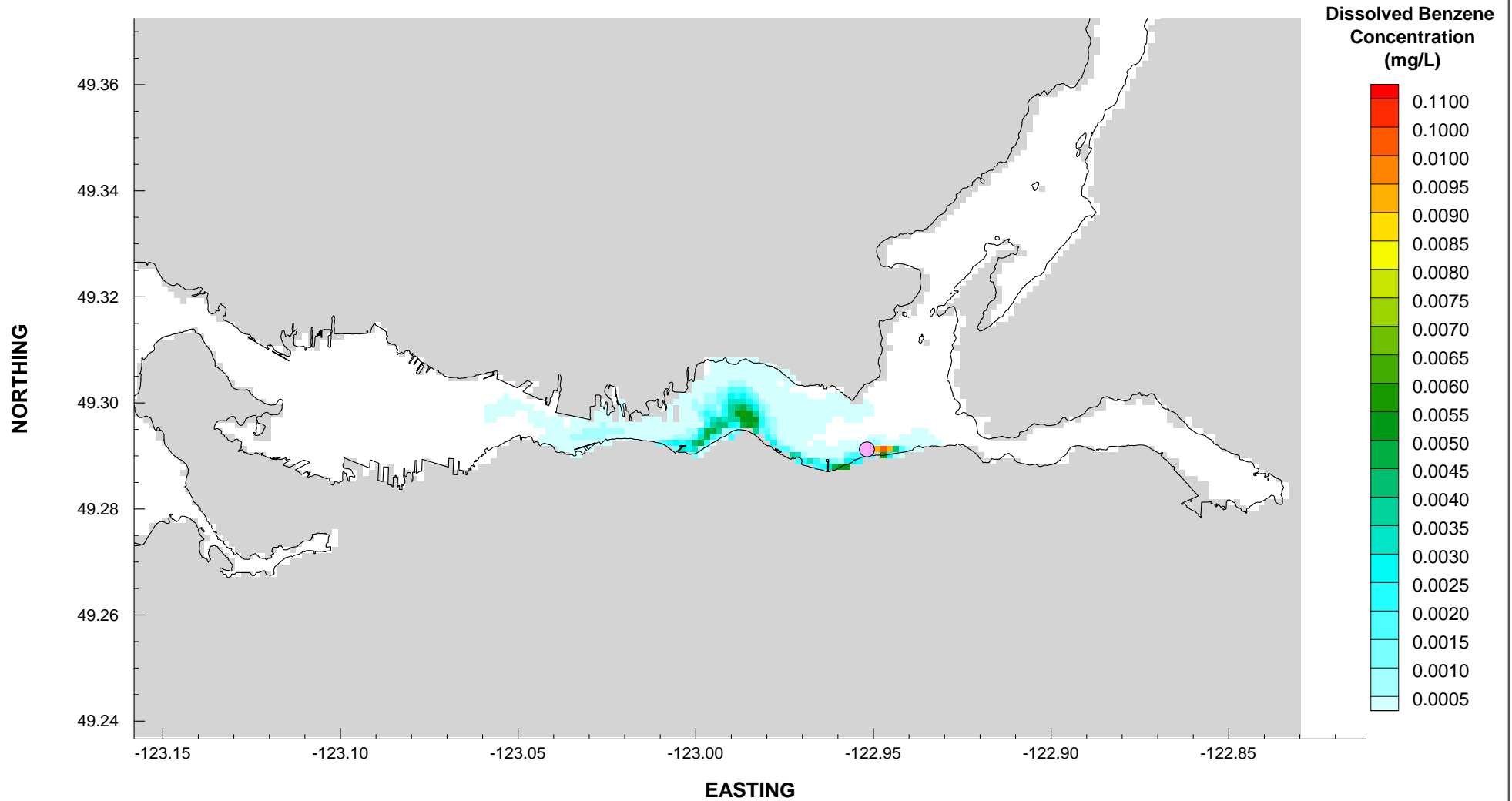
CKD  
JAS

APVD  
JAS

REV  
0

Figure 9.5.1

201208220400



## NOTES

- The benzene concentration is displayed in mg per litre.
- For comparison purpose, the CCME guideline for the Protection of Aquatic Life is set for benzene at 0.11 mg/L (110 micrograms per litre of water).
- A cut-off value of 1e-8 mg/L was applied.

STATUS  
ISSUED FOR USE

CLIENT



## TRANS MOUNTAIN OIL SPILL STUDY

### Benzene Concentration in the Surface Layer after 6 Hours

PROJECT NO.  
V13203022

OFFICE  
EBA-VANC

DWN  
AH

DATE  
November 20, 2013

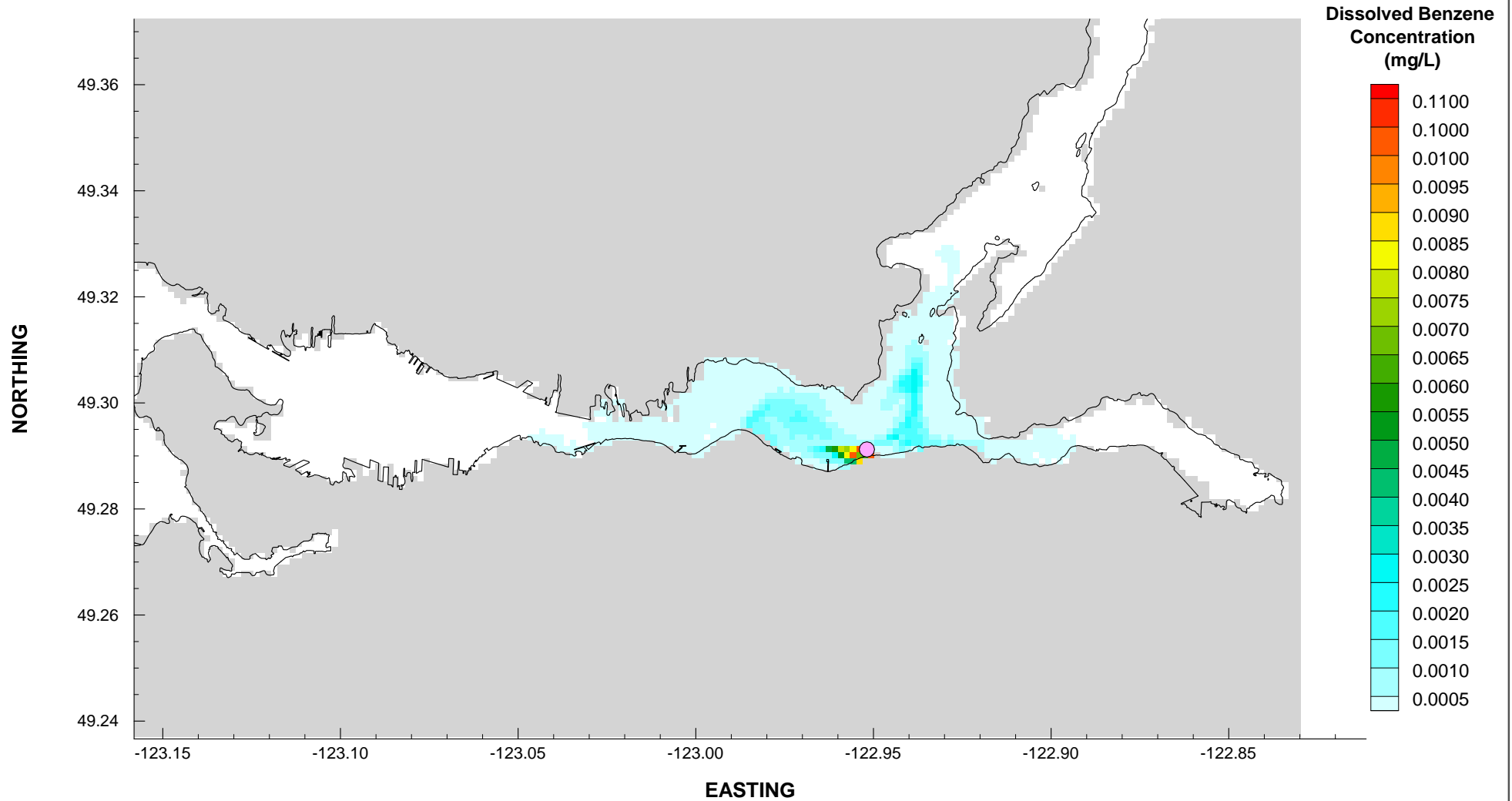
CKD  
JAS

APVD  
JAS

REV  
0

Figure 9.5.2

201208221000



## NOTES

- The benzene concentration is displayed in mg per litre.
- For comparison purpose, the CCME guideline for the Protection of Aquatic Life is set for benzene at 0.11 mg/L (110 micrograms per litre of water).
- A cut-off value of 1e-8 mg/L was applied.

STATUS  
ISSUED FOR USE

CLIENT



## TRANS MOUNTAIN OIL SPILL STUDY

### Benzene Concentration in the Surface Layer after 12 Hours

PROJECT NO.  
V13203022

OFFICE  
EBA-VANC

DWN  
AH

DATE  
November 20, 2013

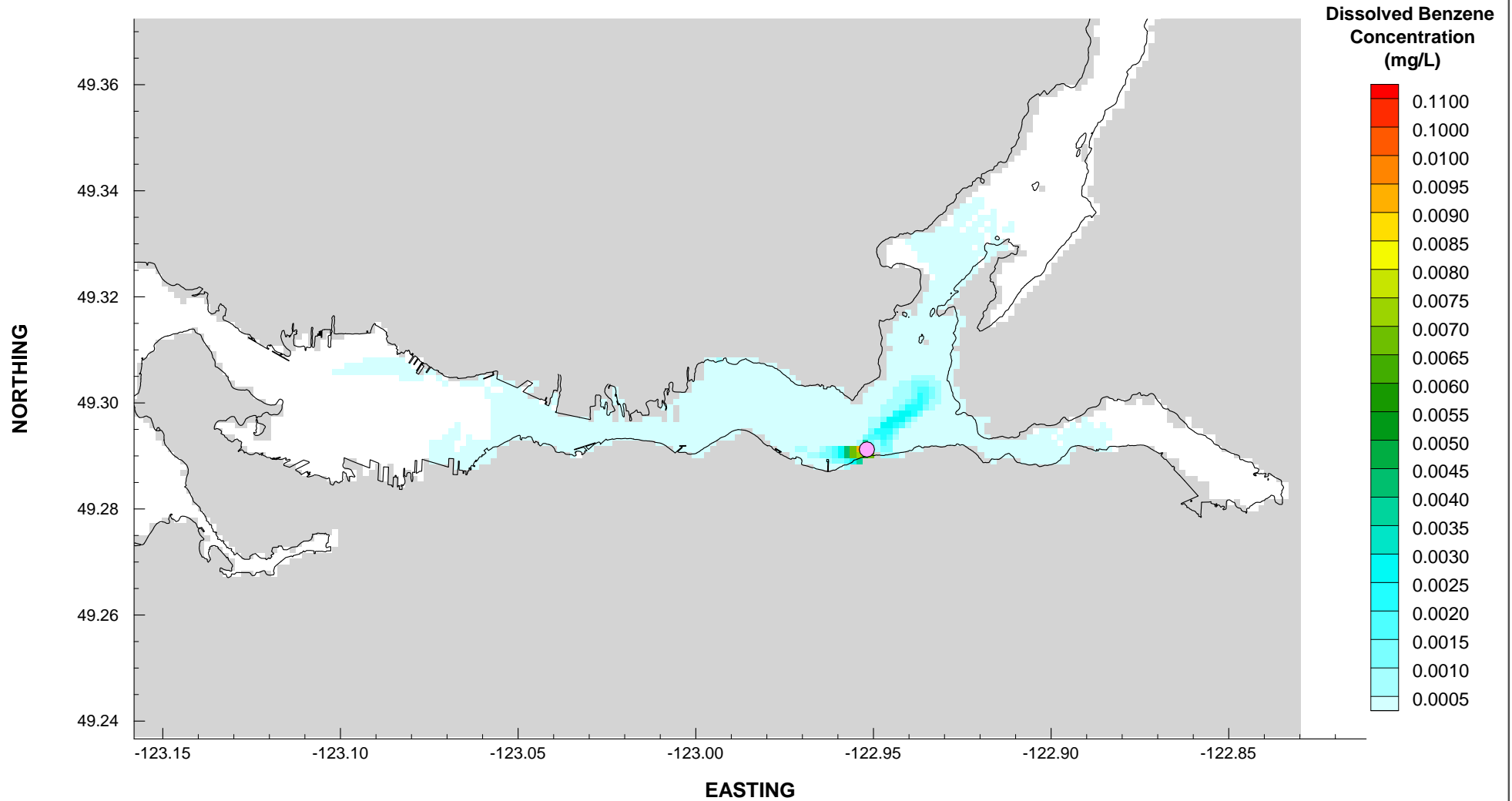
CKD  
JAS

APVD  
JAS

REV  
0

Figure 9.5.3

201208222200



## NOTES

- The benzene concentration is displayed in mg per litre.
- For comparison purpose, the CCME guideline for the Protection of Aquatic Life is set for benzene at 0.11 mg/L (110 micrograms per litre of water).
- A cut-off value of 1e-8 mg/L was applied.

STATUS  
ISSUED FOR USE

CLIENT



## TRANS MOUNTAIN OIL SPILL STUDY

### Benzene Concentration in the Surface Layer after 24 Hours

PROJECT NO.  
V13203022

OFFICE  
EBA-VANC

DWN  
AH

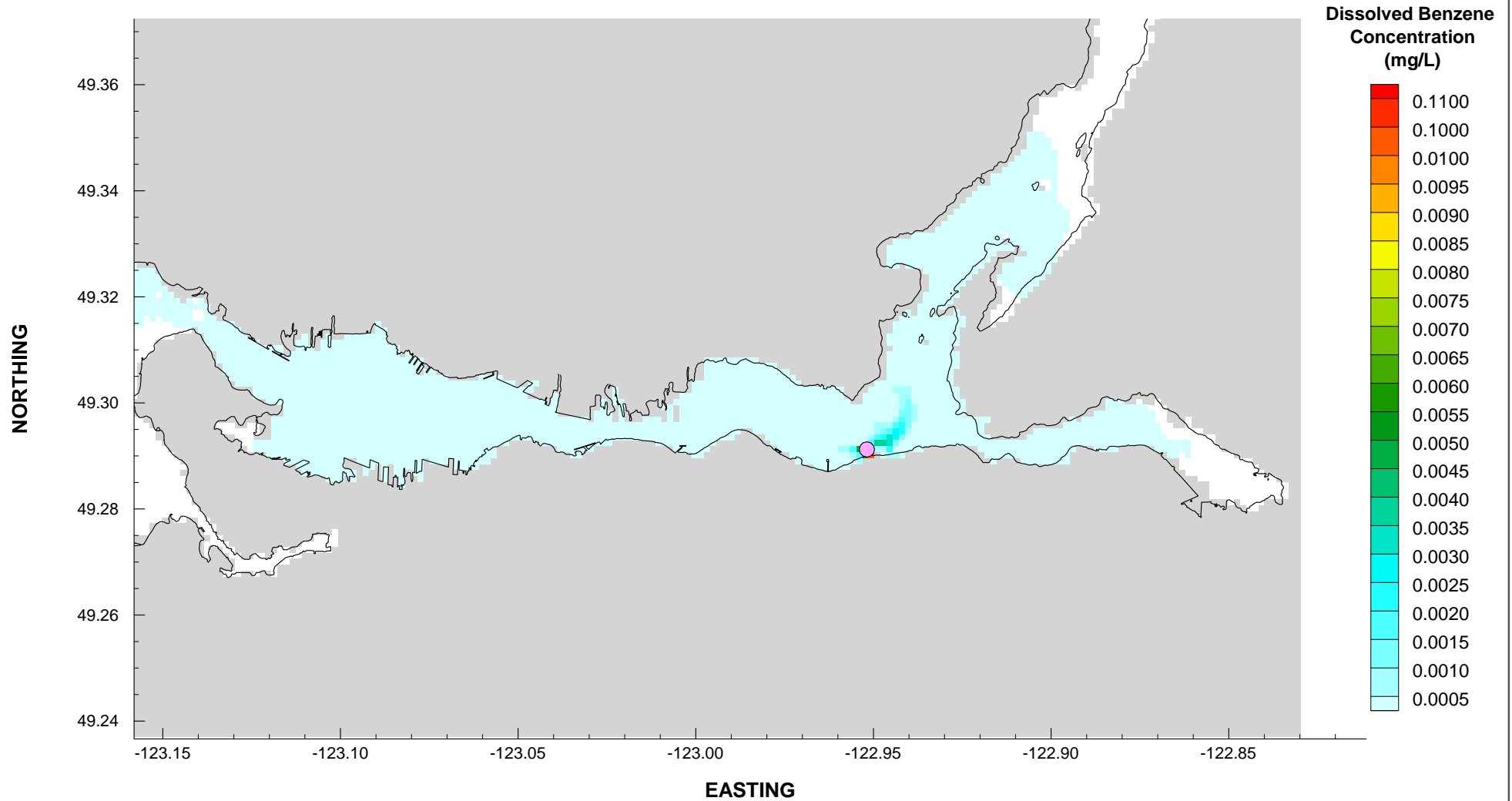
DATE  
November 20, 2013

CKD  
JAS

APVD  
JAS

REV  
0

Figure 9.5.4



## NOTES

- The benzene concentration is displayed in mg per litre.
- For comparison purpose, the CCME guideline for the Protection of Aquatic Life is set for benzene at 0.11 mg/L (110 micrograms per litre of water).
- A cut-off value of 1e-8 mg/L was applied.

STATUS  
ISSUED FOR USE

CLIENT



## TRANS MOUNTAIN OIL SPILL STUDY

### Benzene Concentration in the Surface Layer after 48 Hours

PROJECT NO.  
V13203022

OFFICE  
EBA-VANC

DWN  
AH

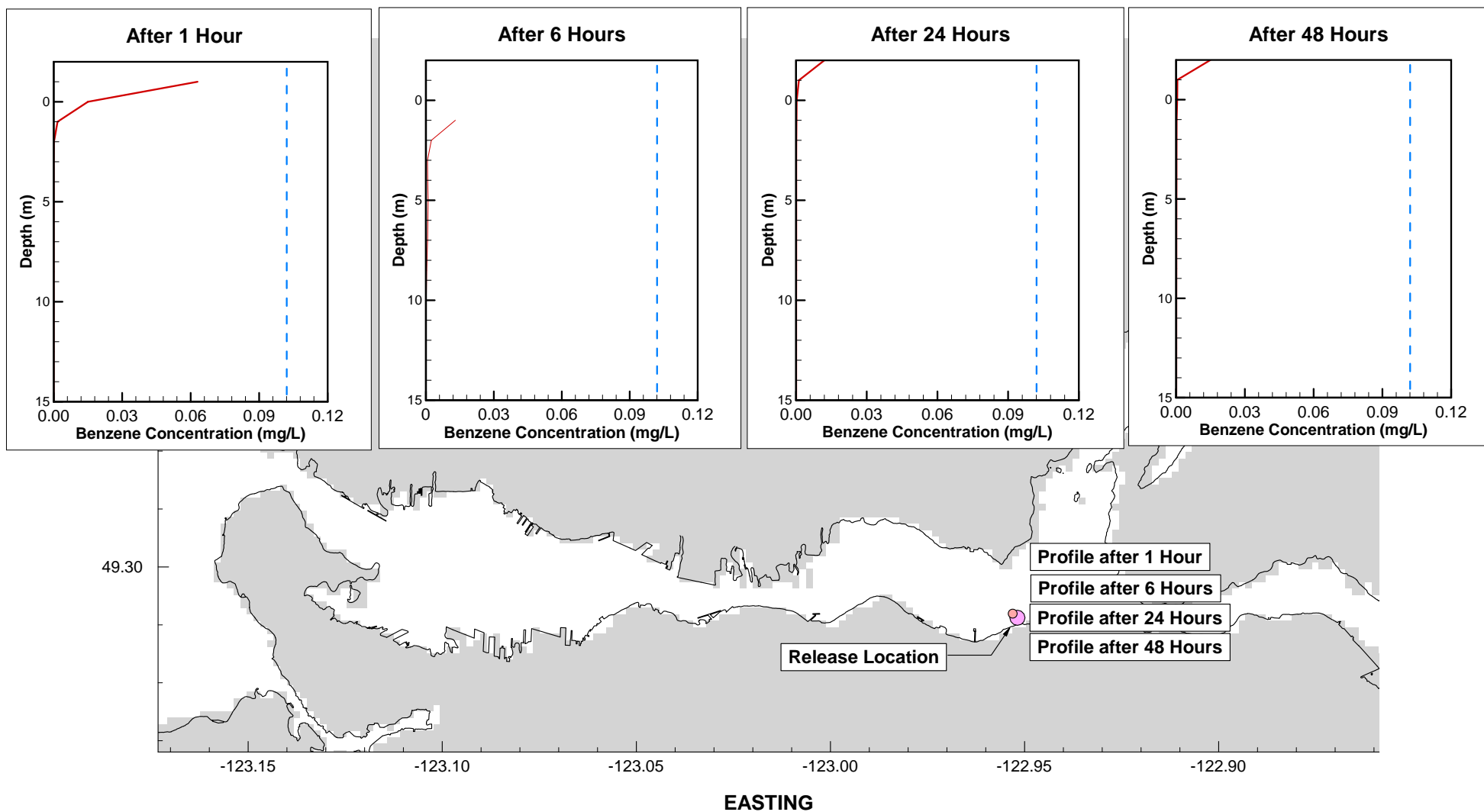
DATE  
November 20, 2013

CKD  
JAS

APVD  
JAS

REV  
0

Figure 9.5.5



## NOTES

- The CCME guideline for the Protection of Aquatic Life in marine environment is set for benzene at 0.11 mg/L (110 micrograms per litre of water).
- Three benzene concentration profiles corresponding to the maximum surface concentration after 13, 24, 48 hours were plotted. The red line represents the benzene concentration. The dashed blue line represents the CCME threshold value.

STATUS  
ISSUED FOR USE

CLIENT

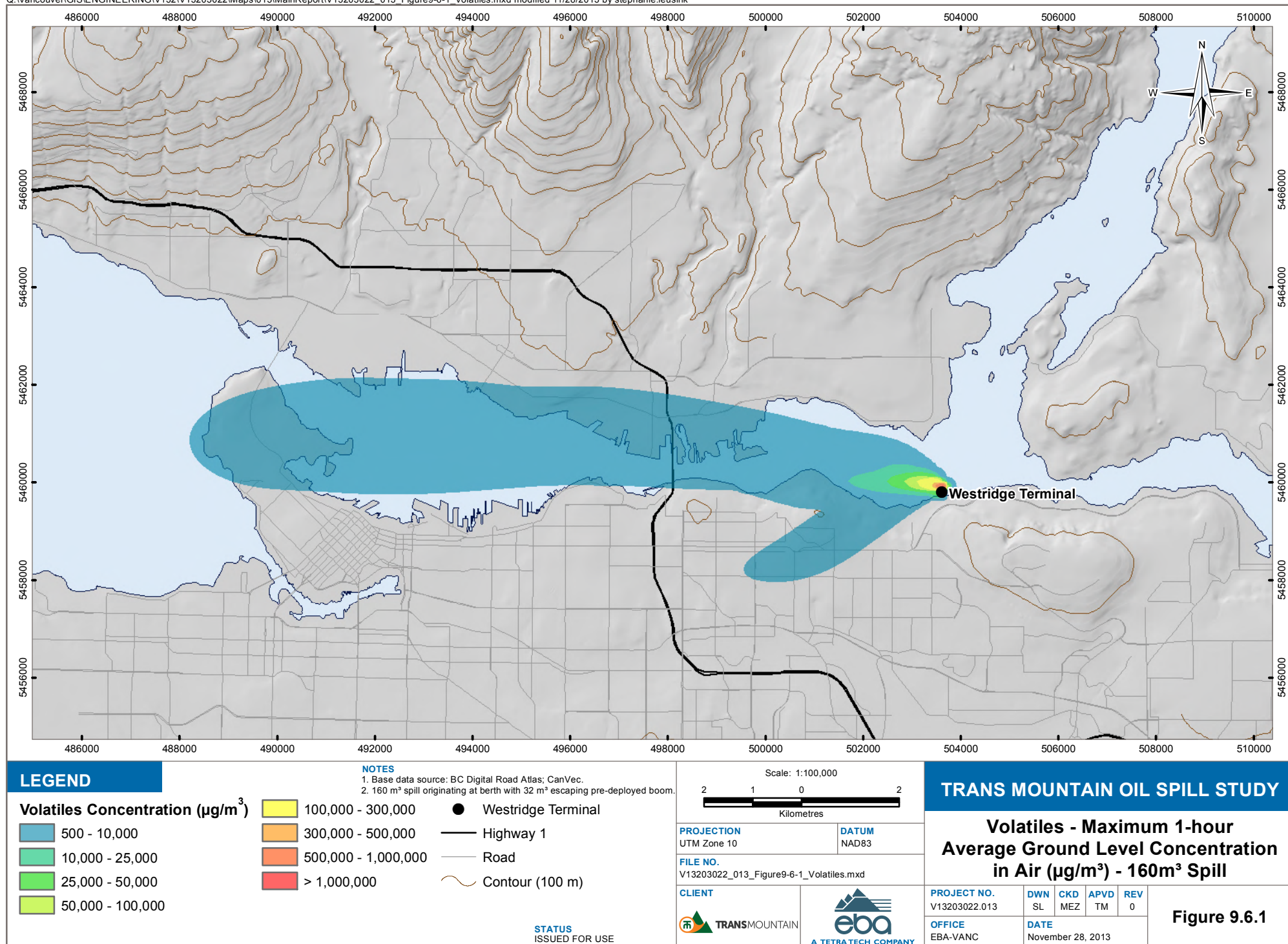


## TRANS MOUNTAIN OIL SPILL STUDY

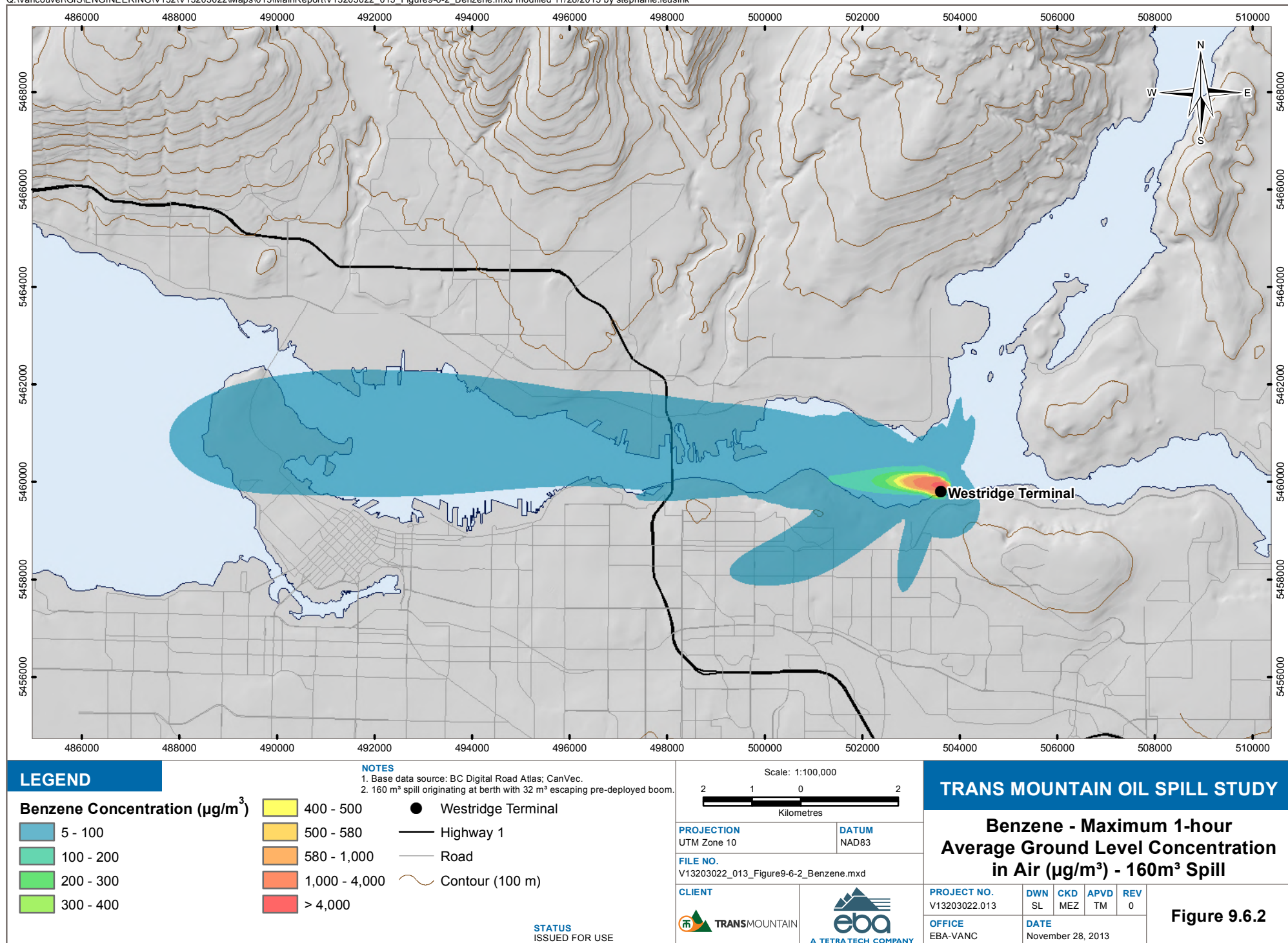
### Profile of Benzene Concentration

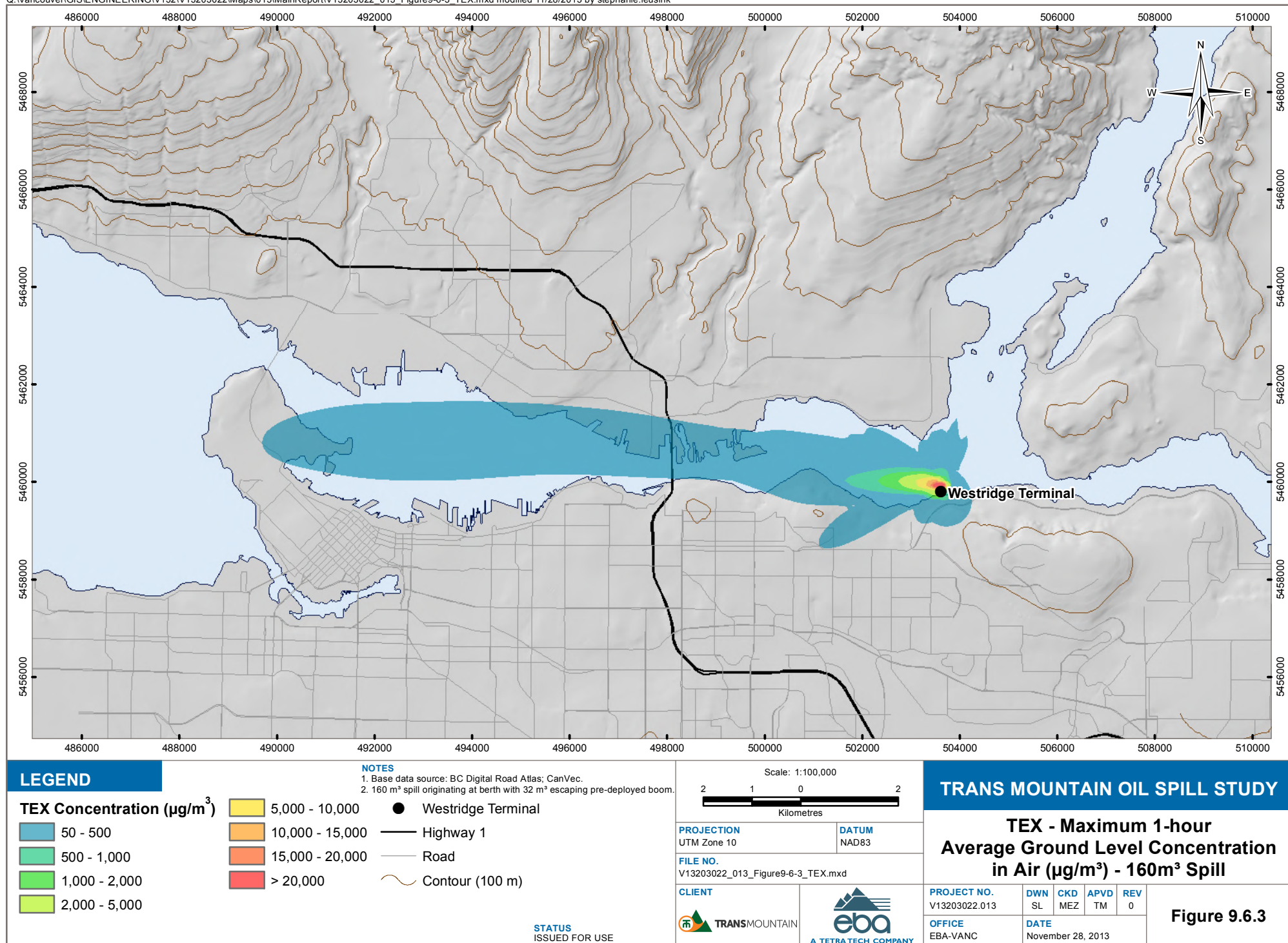
PROJECT NO. V13203022	DWN AH	CKD JAS	APVD JAS	REV 0
OFFICE EBA-VANC	DATE November 20, 2013			

Figure 9.5.6

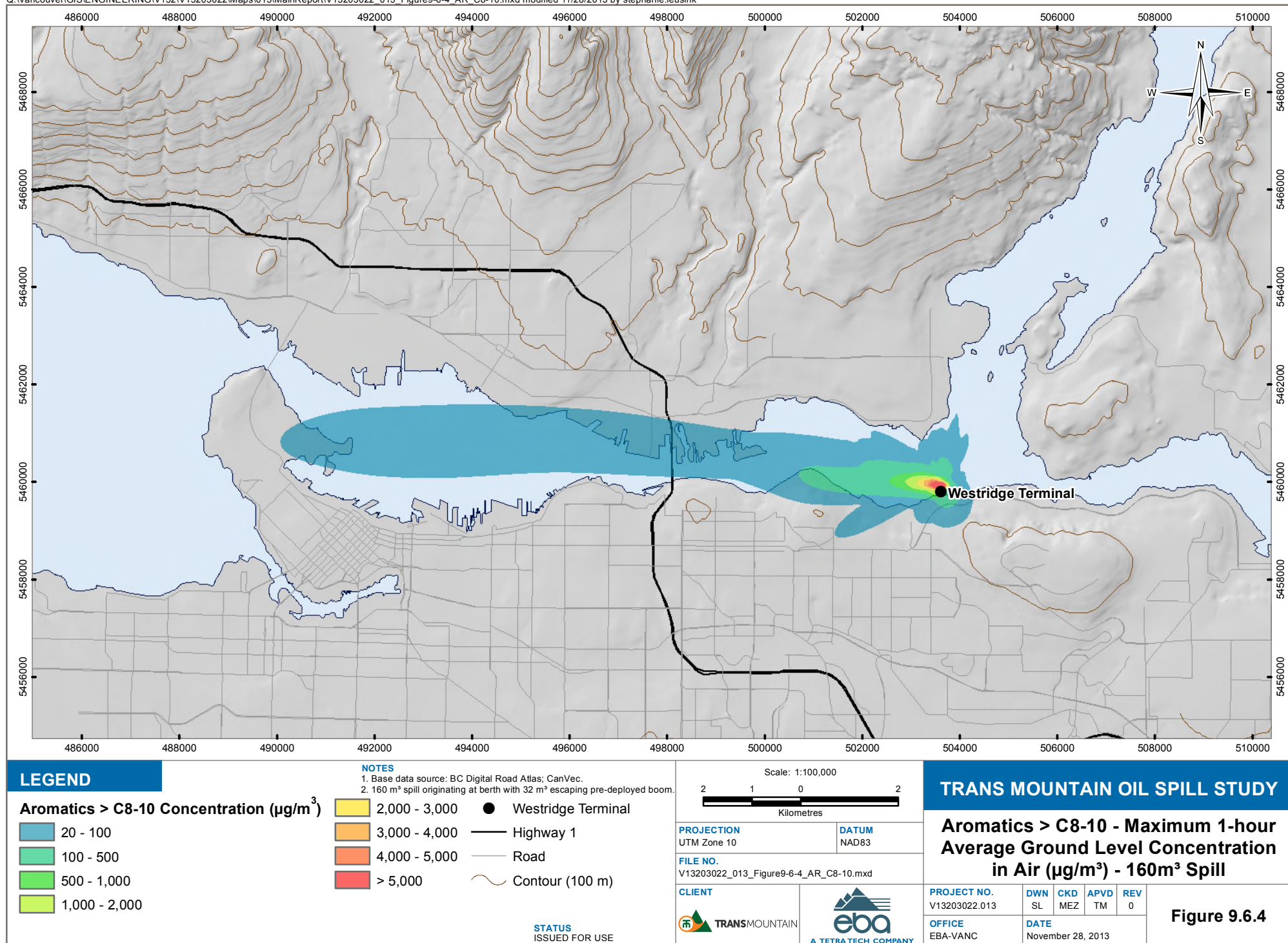


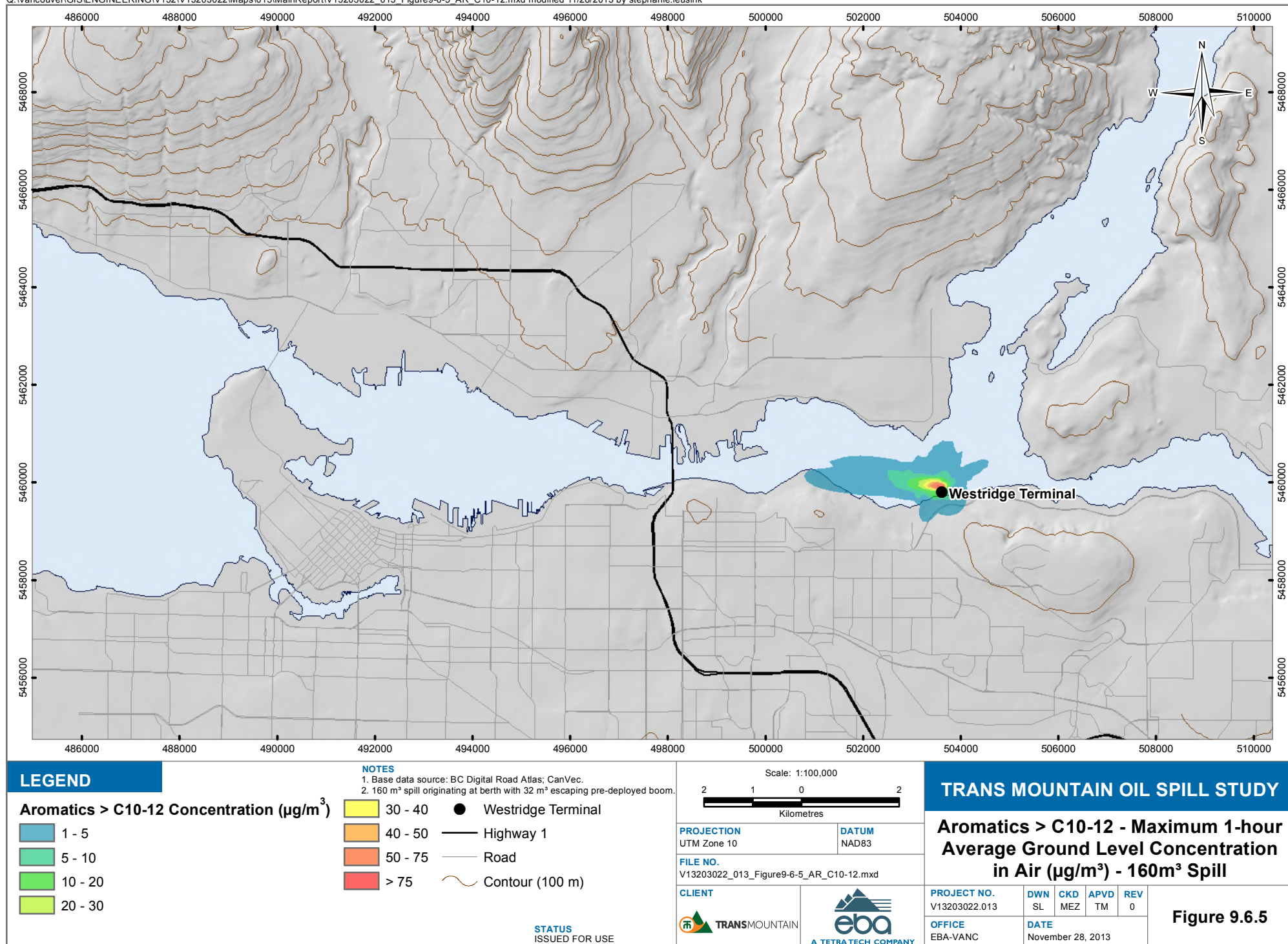




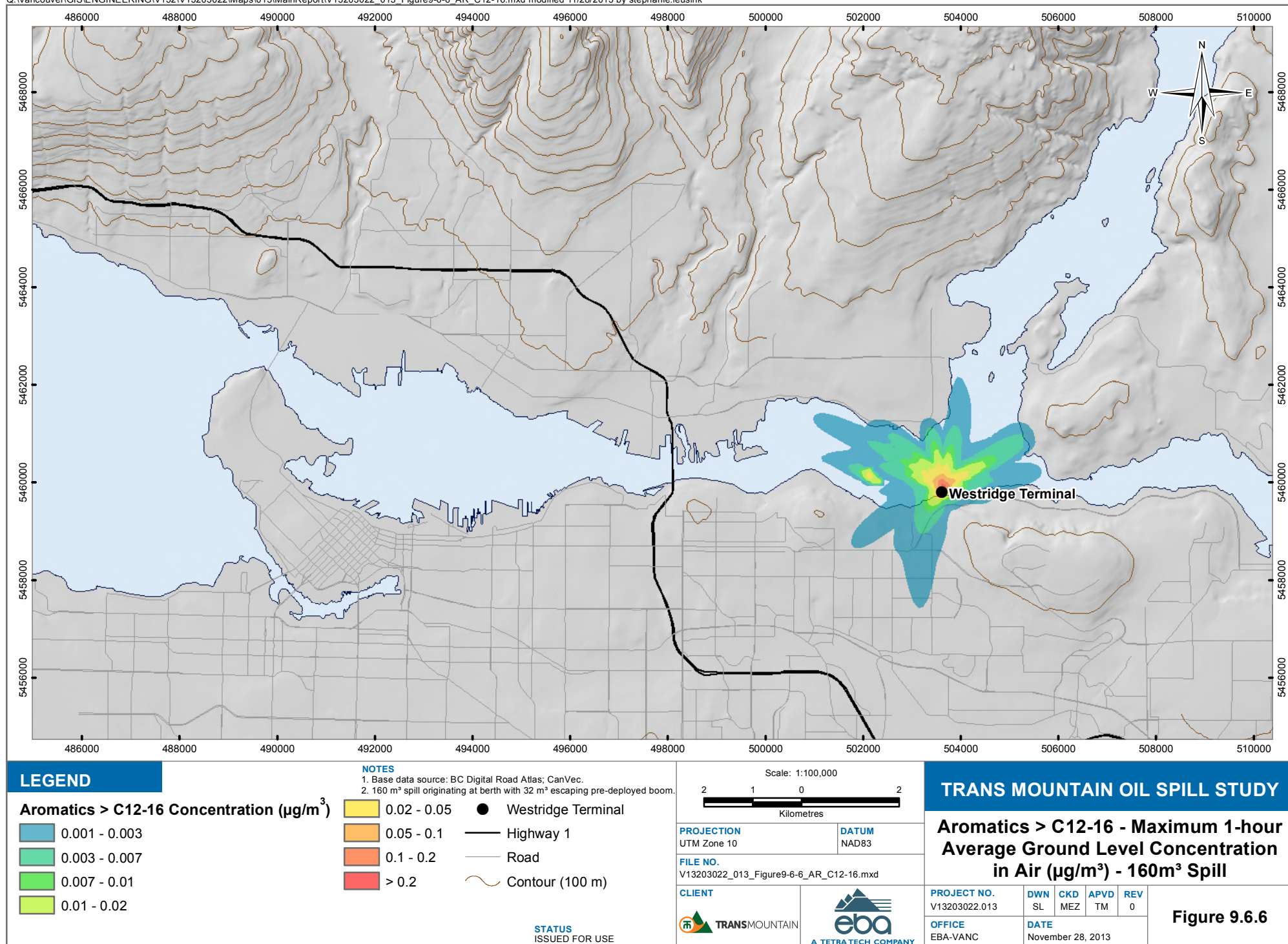


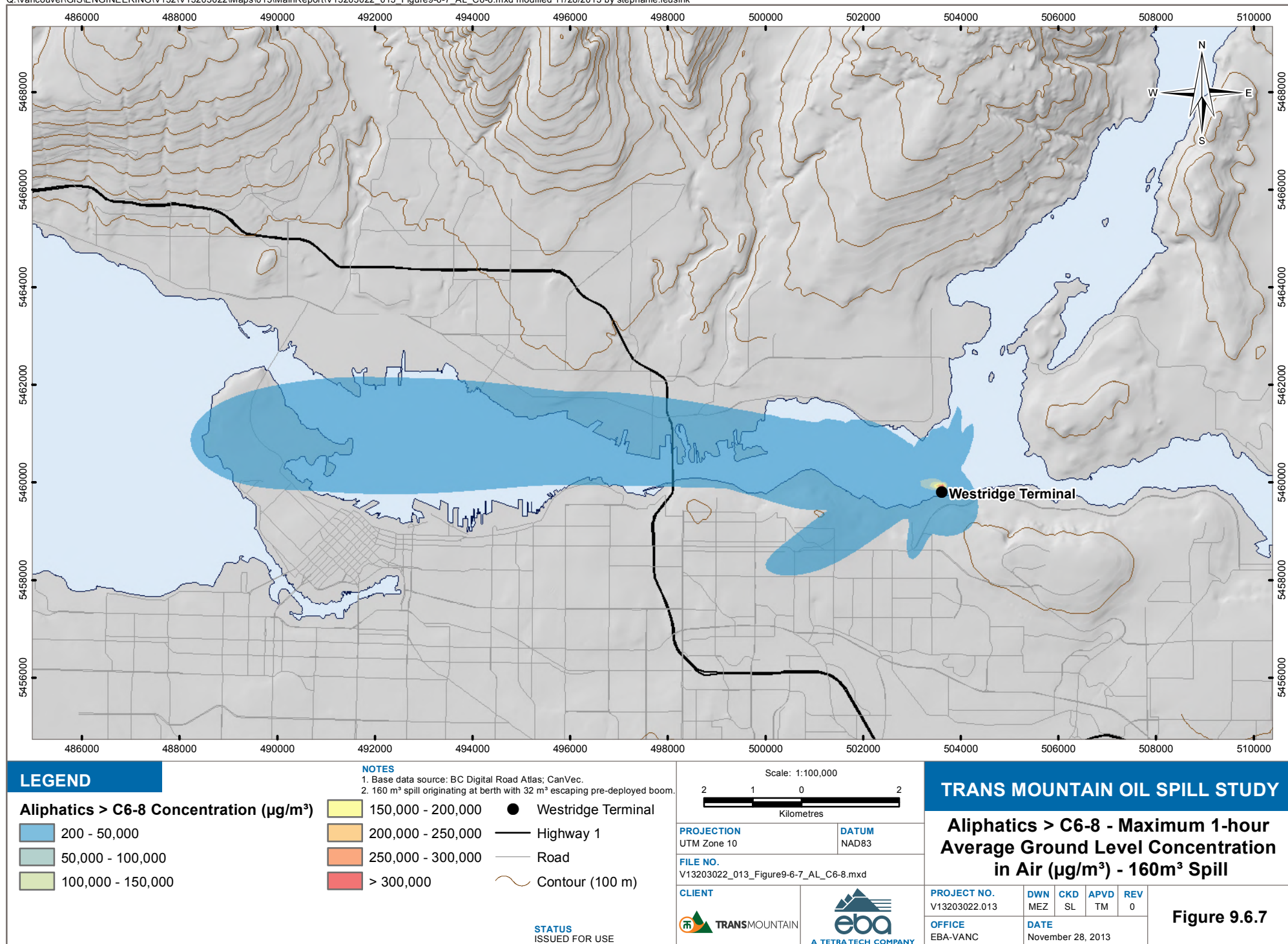




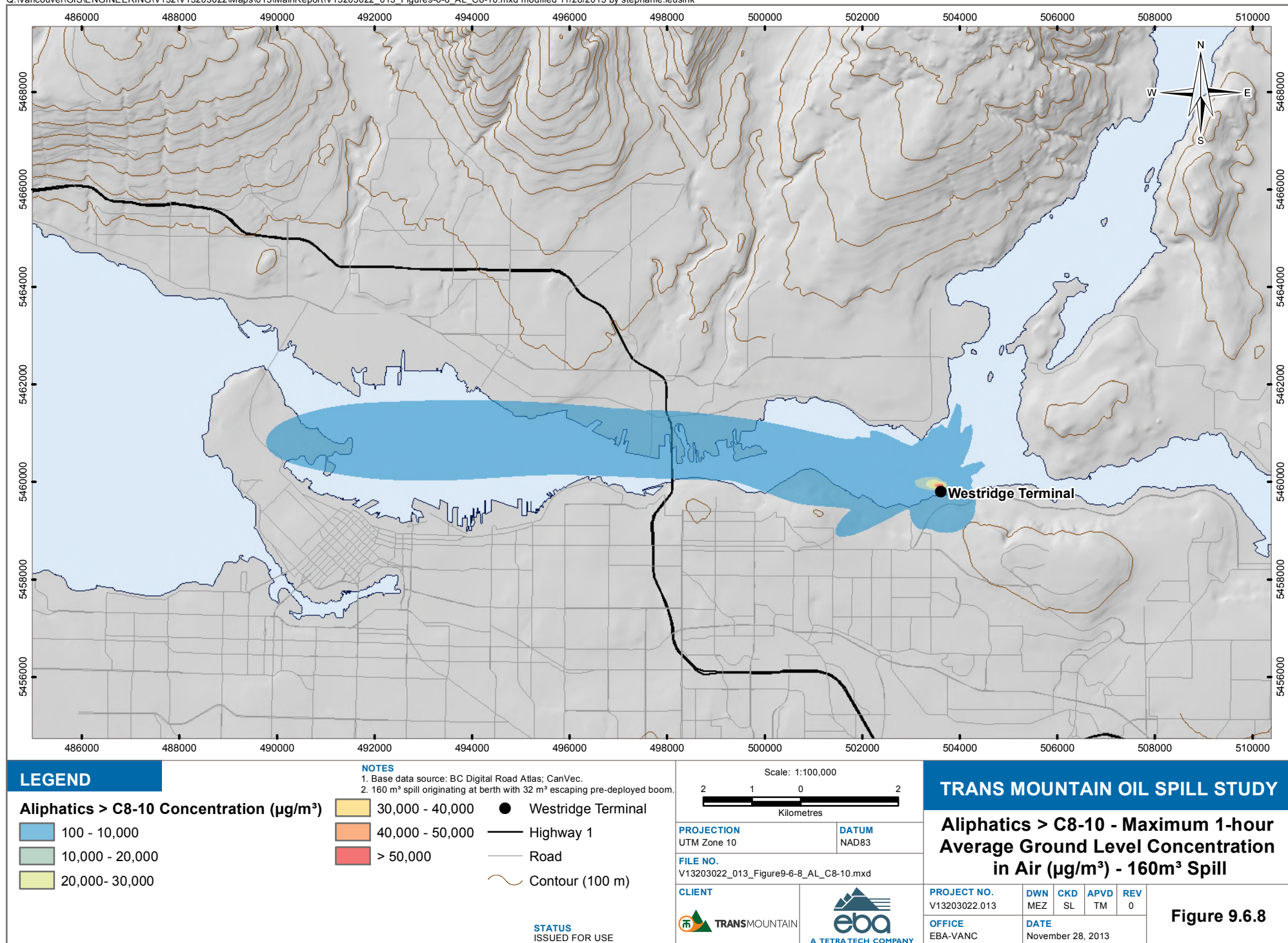


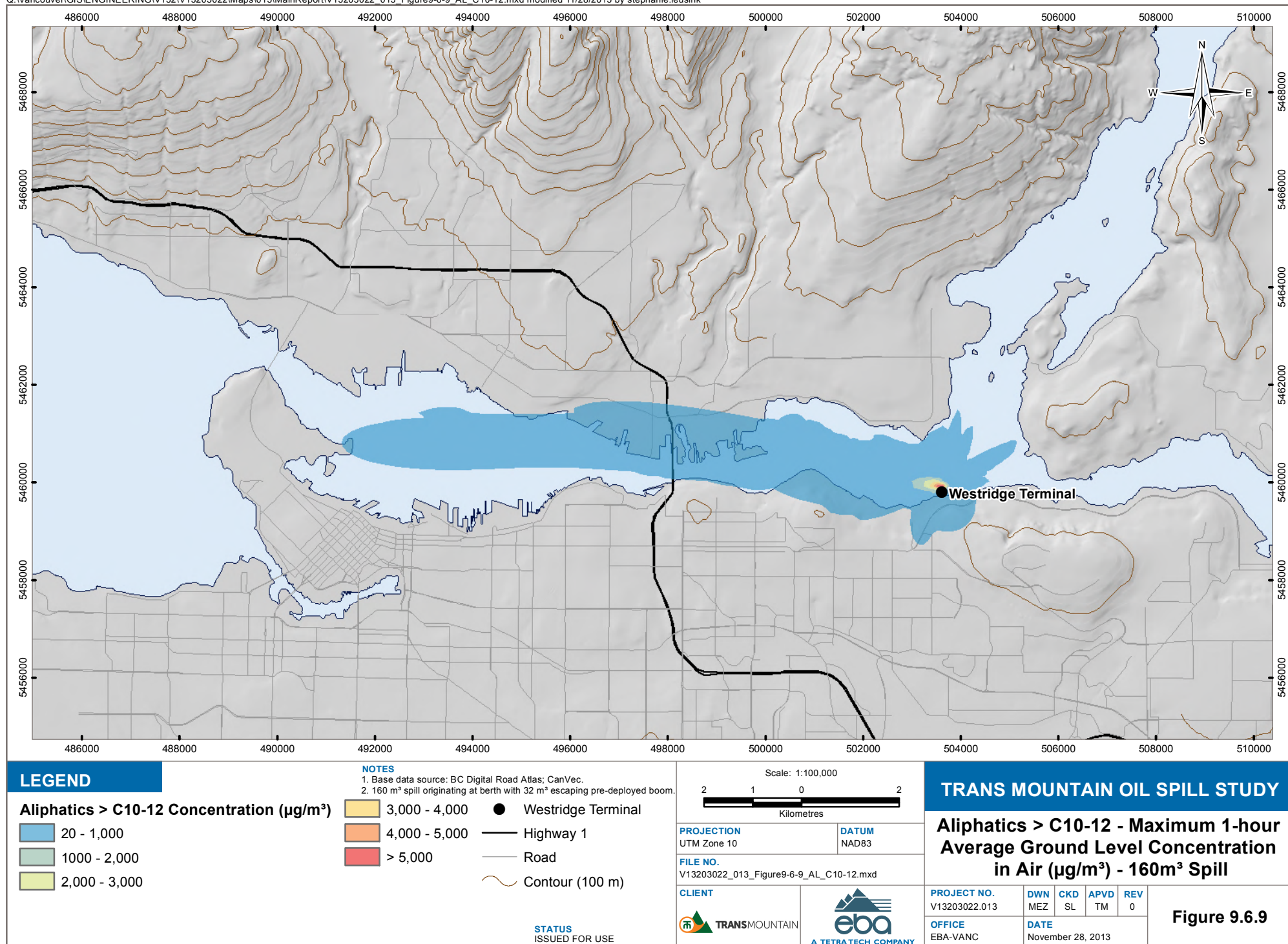




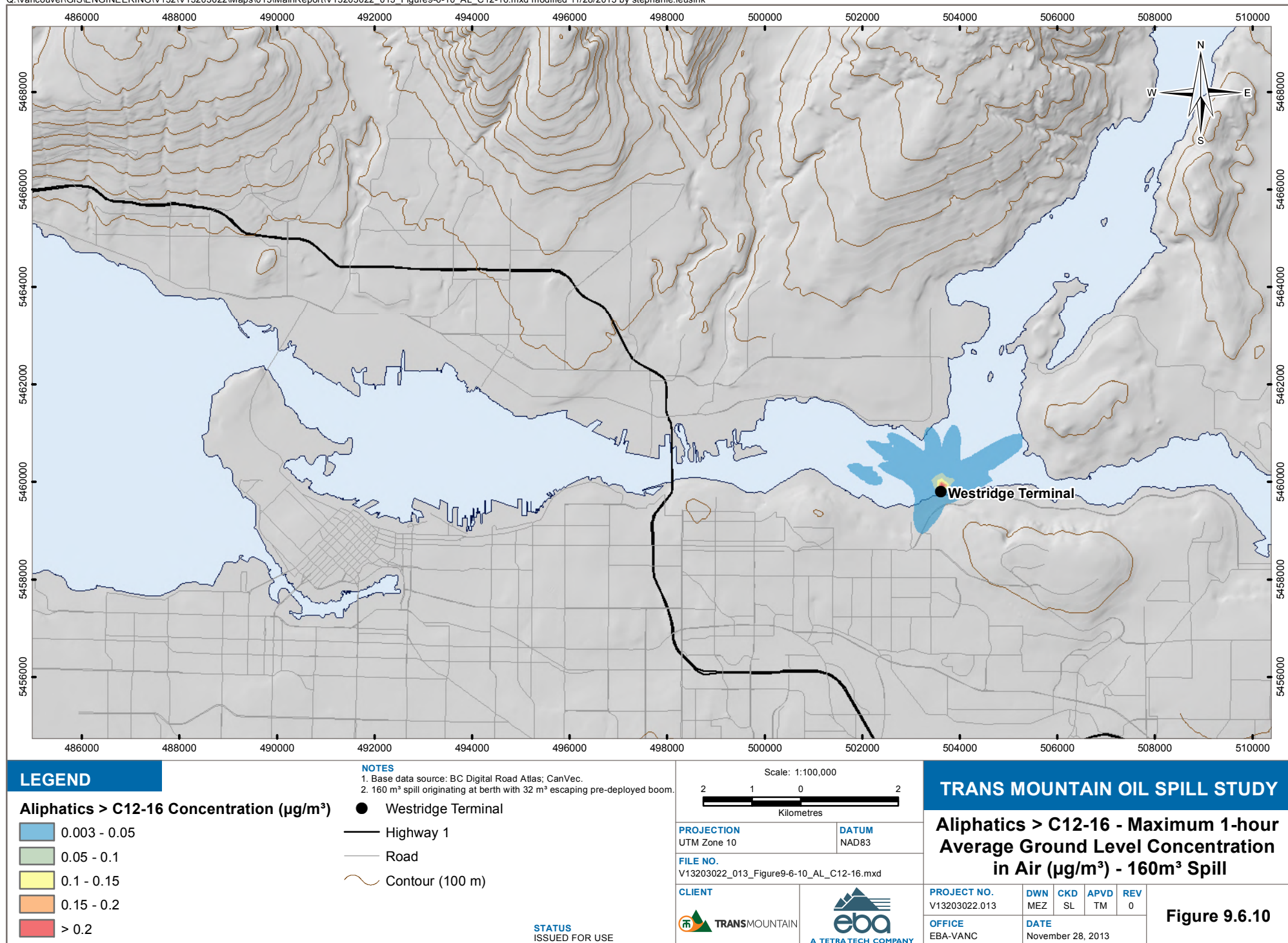


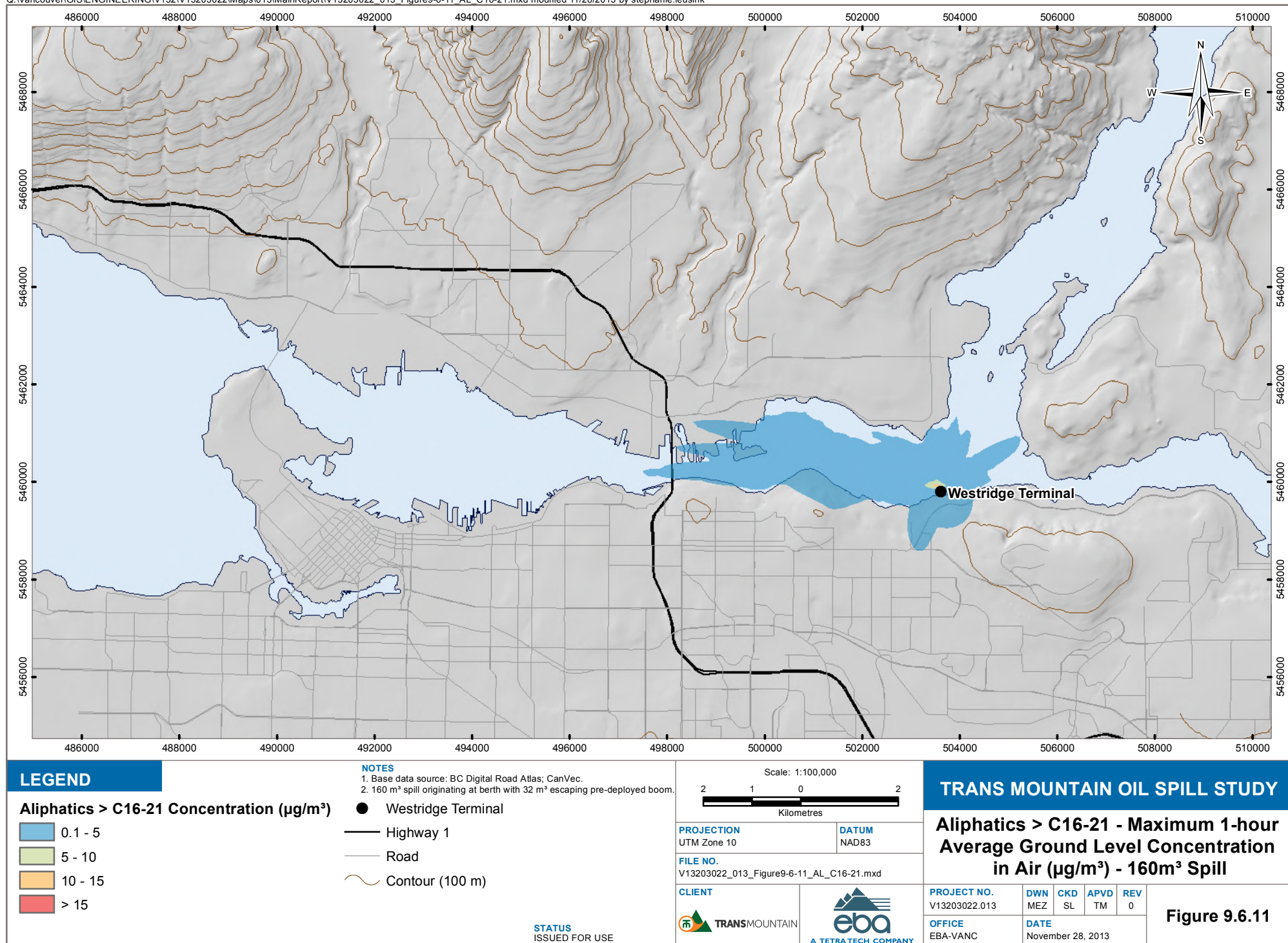




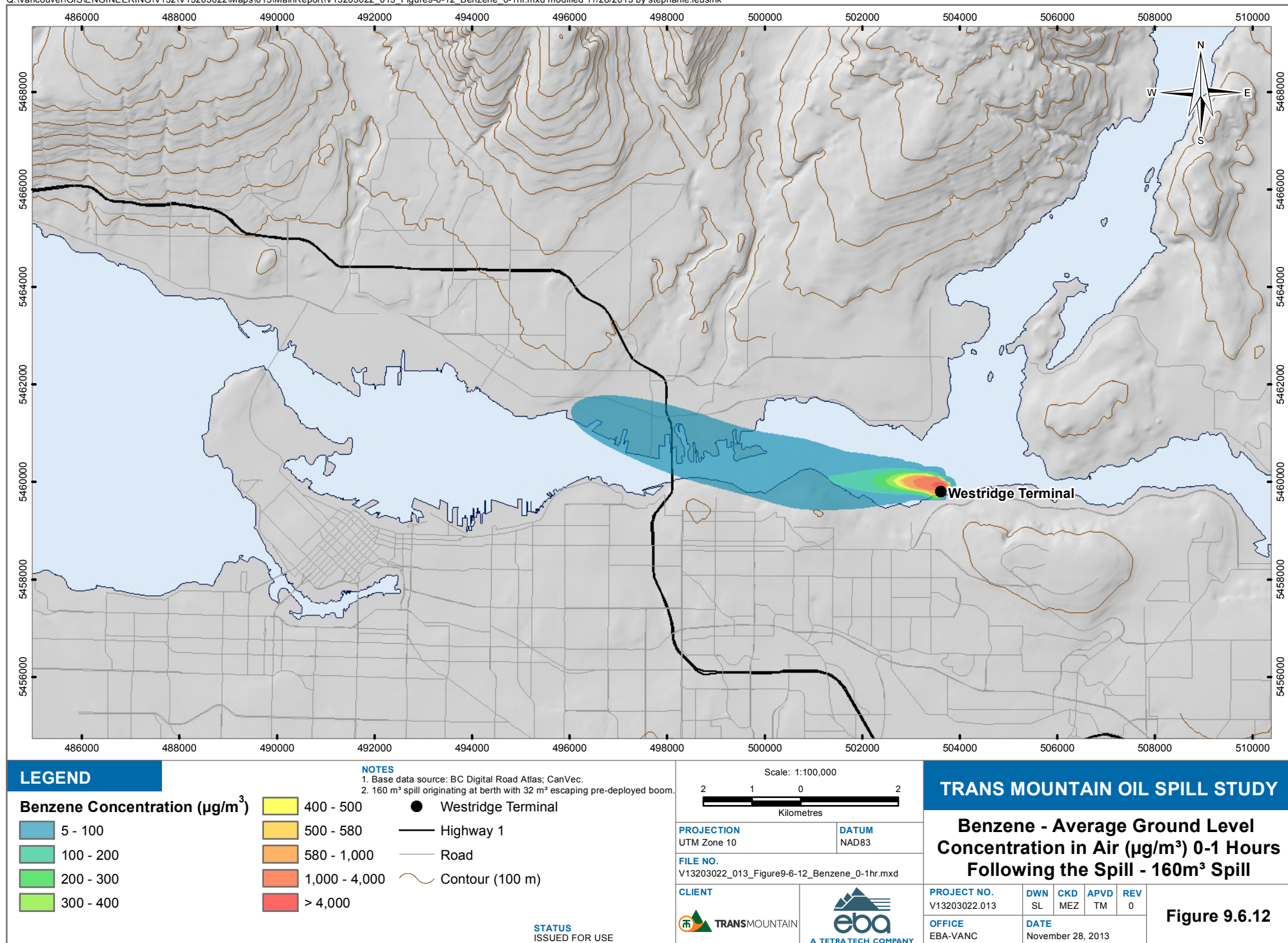




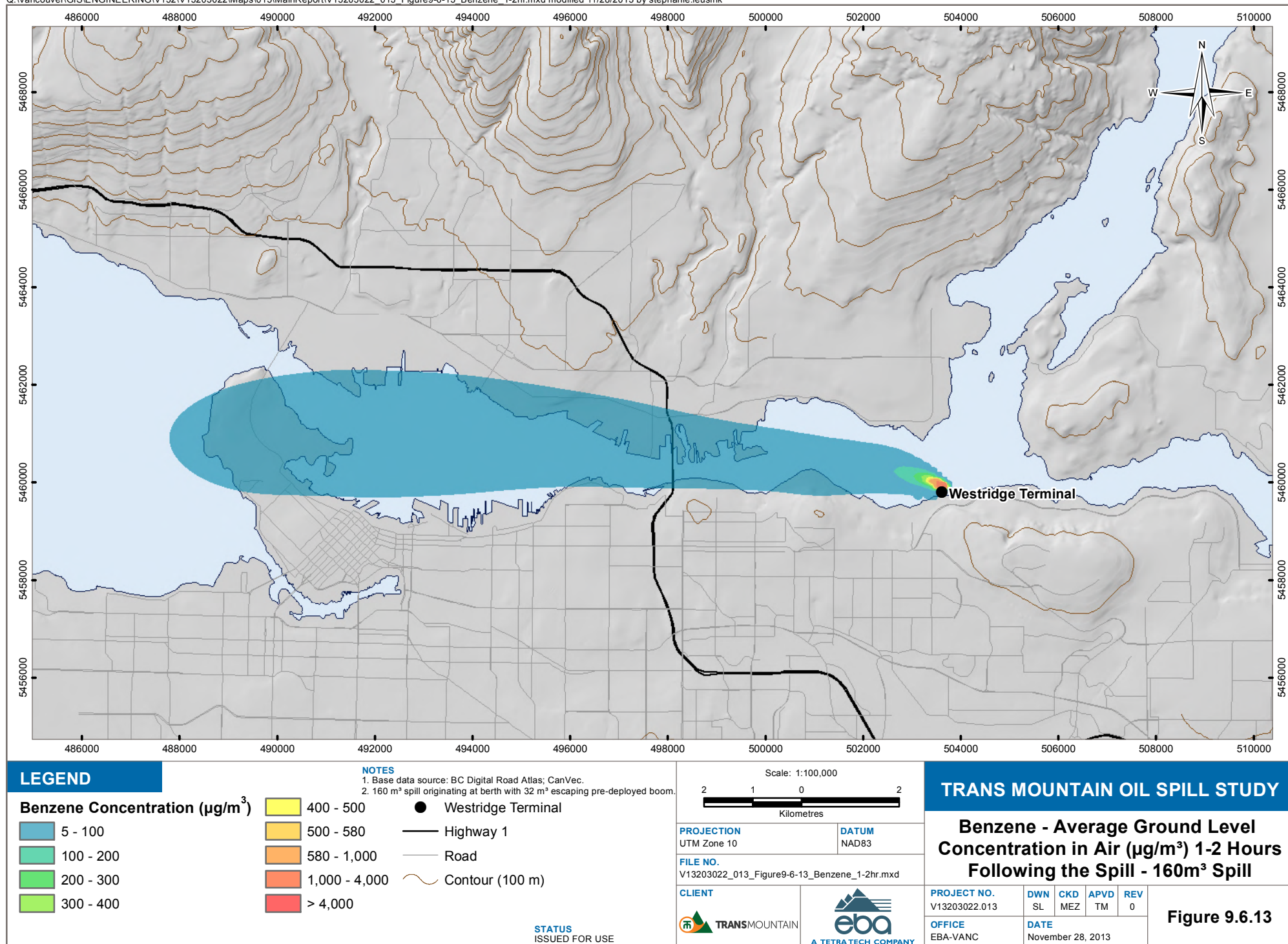


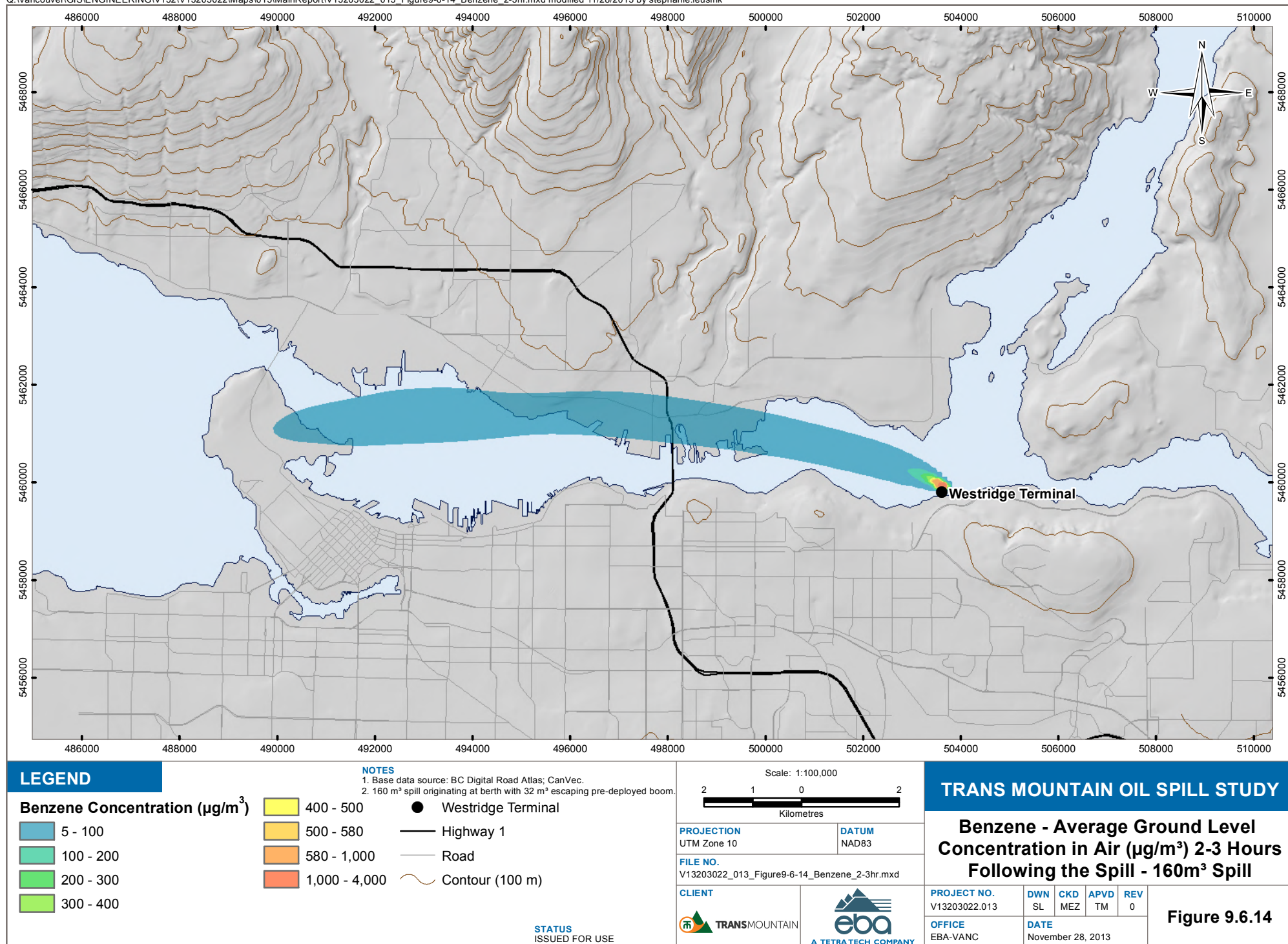




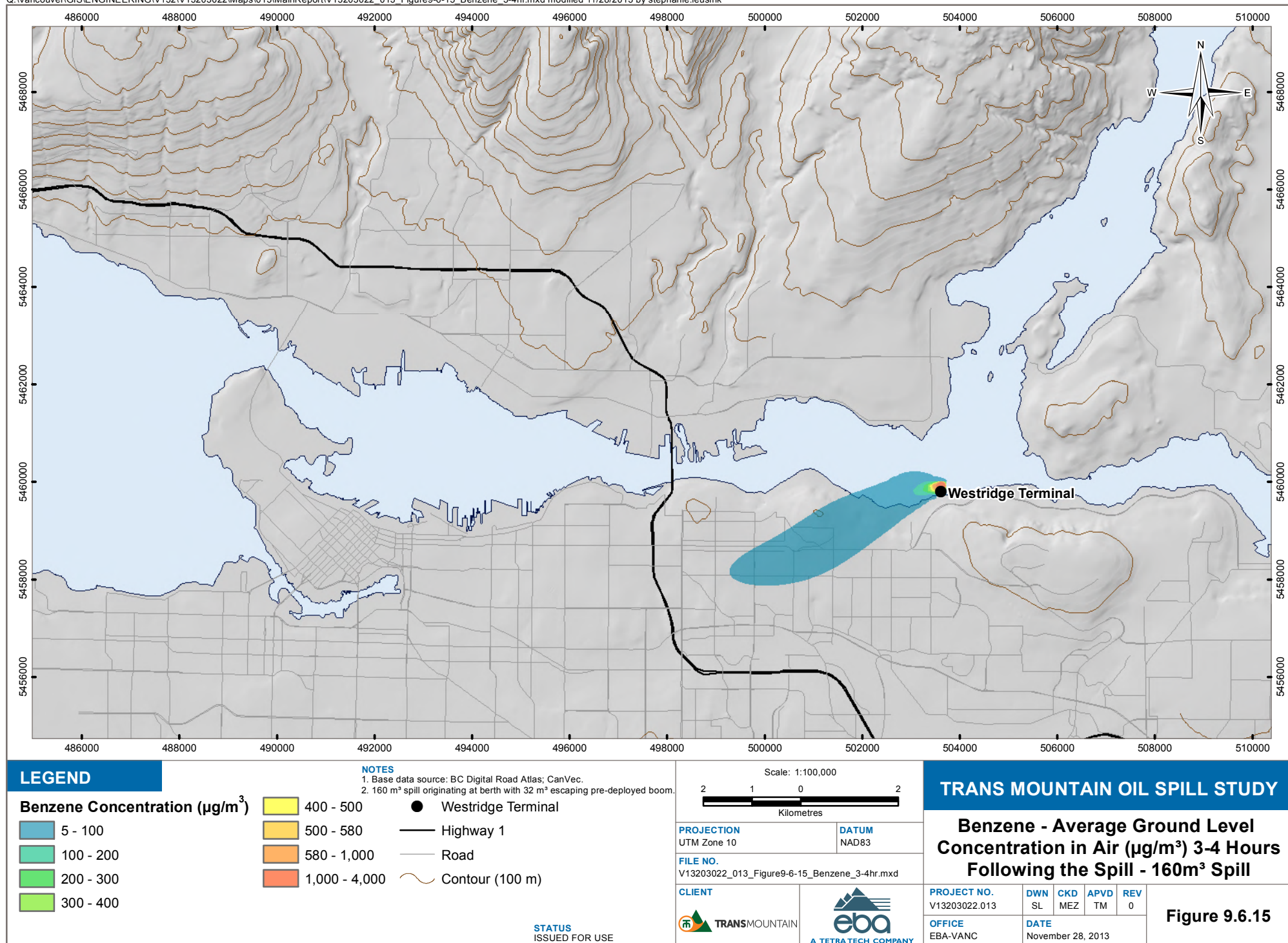


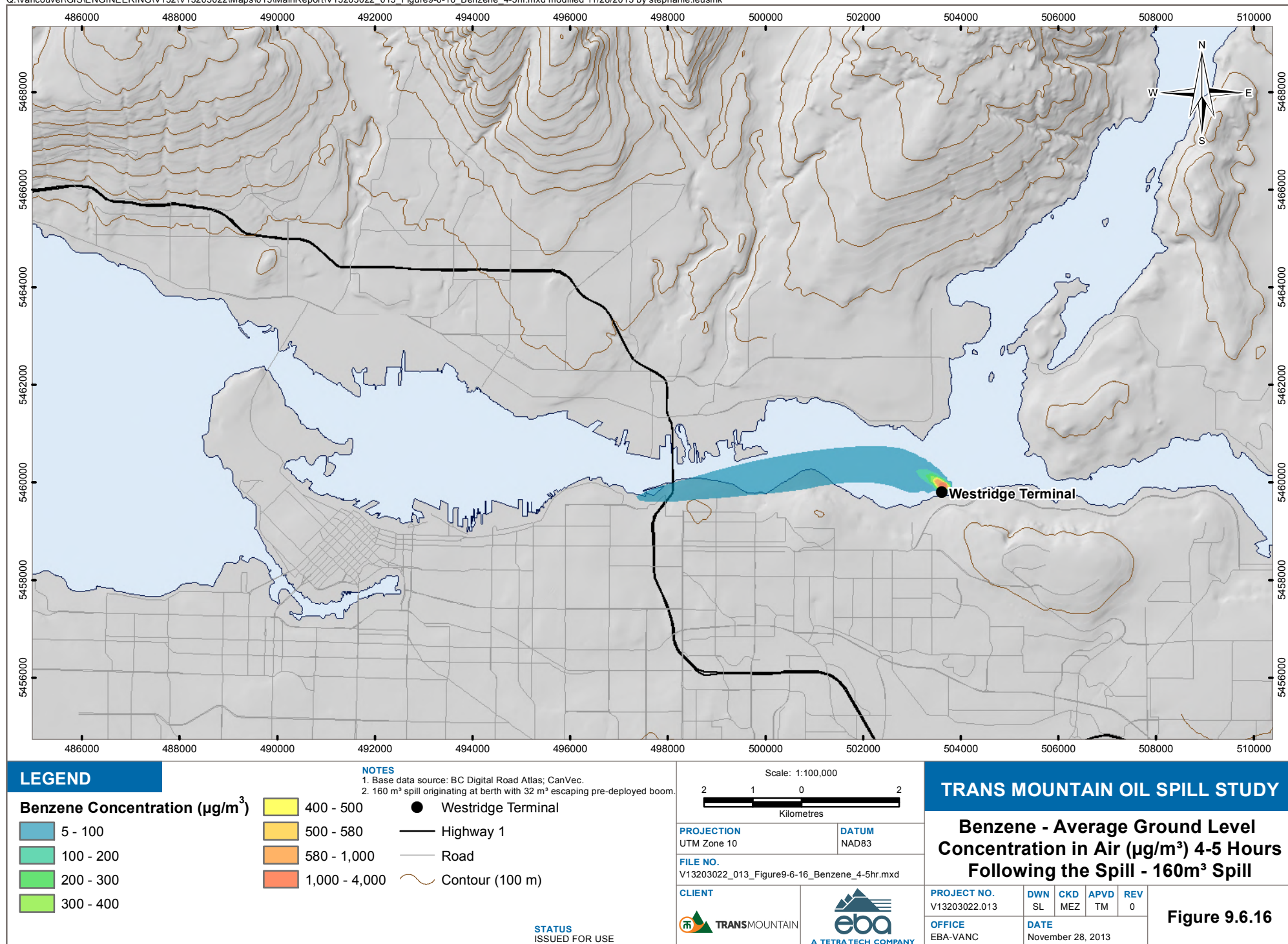




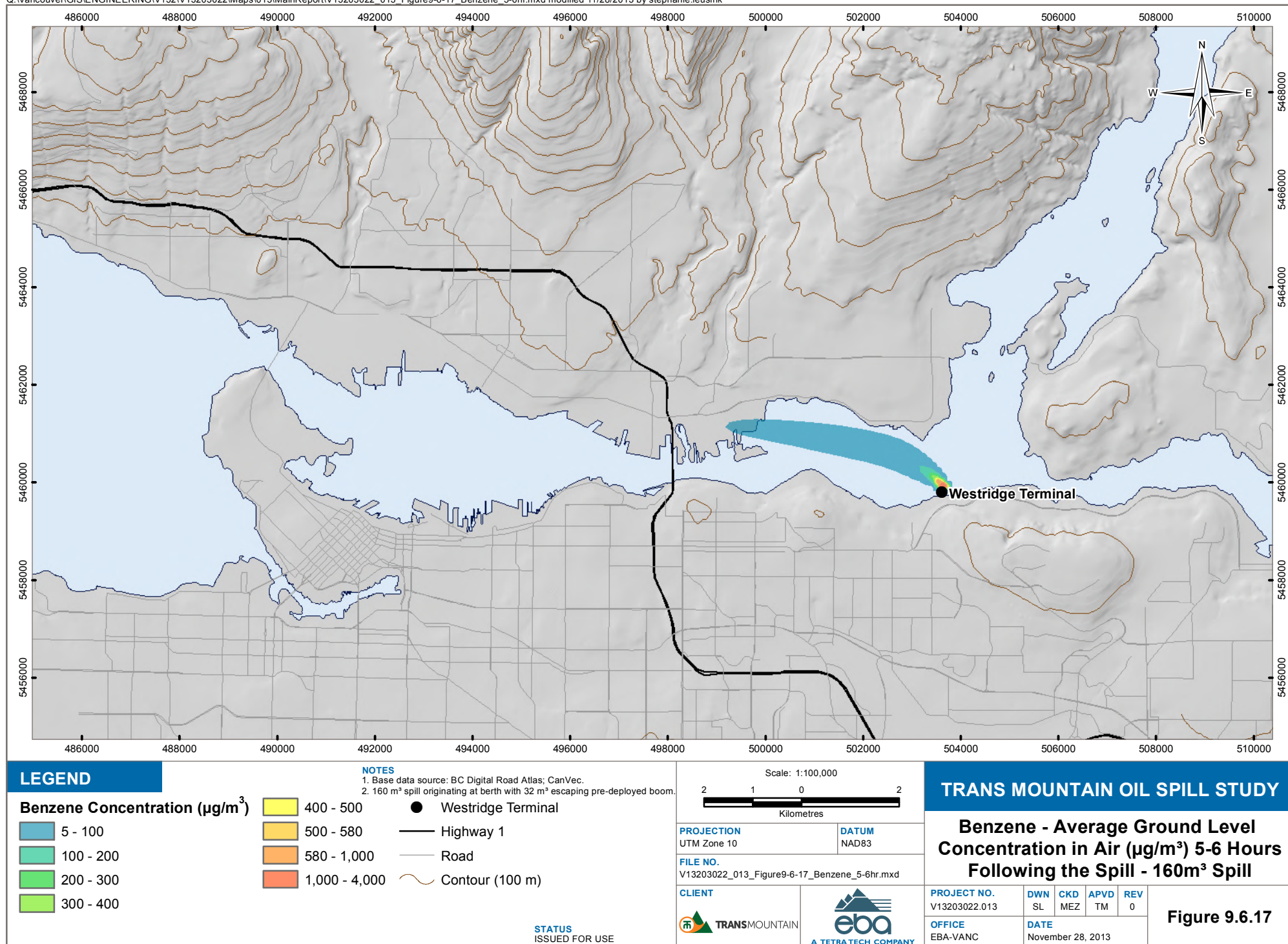




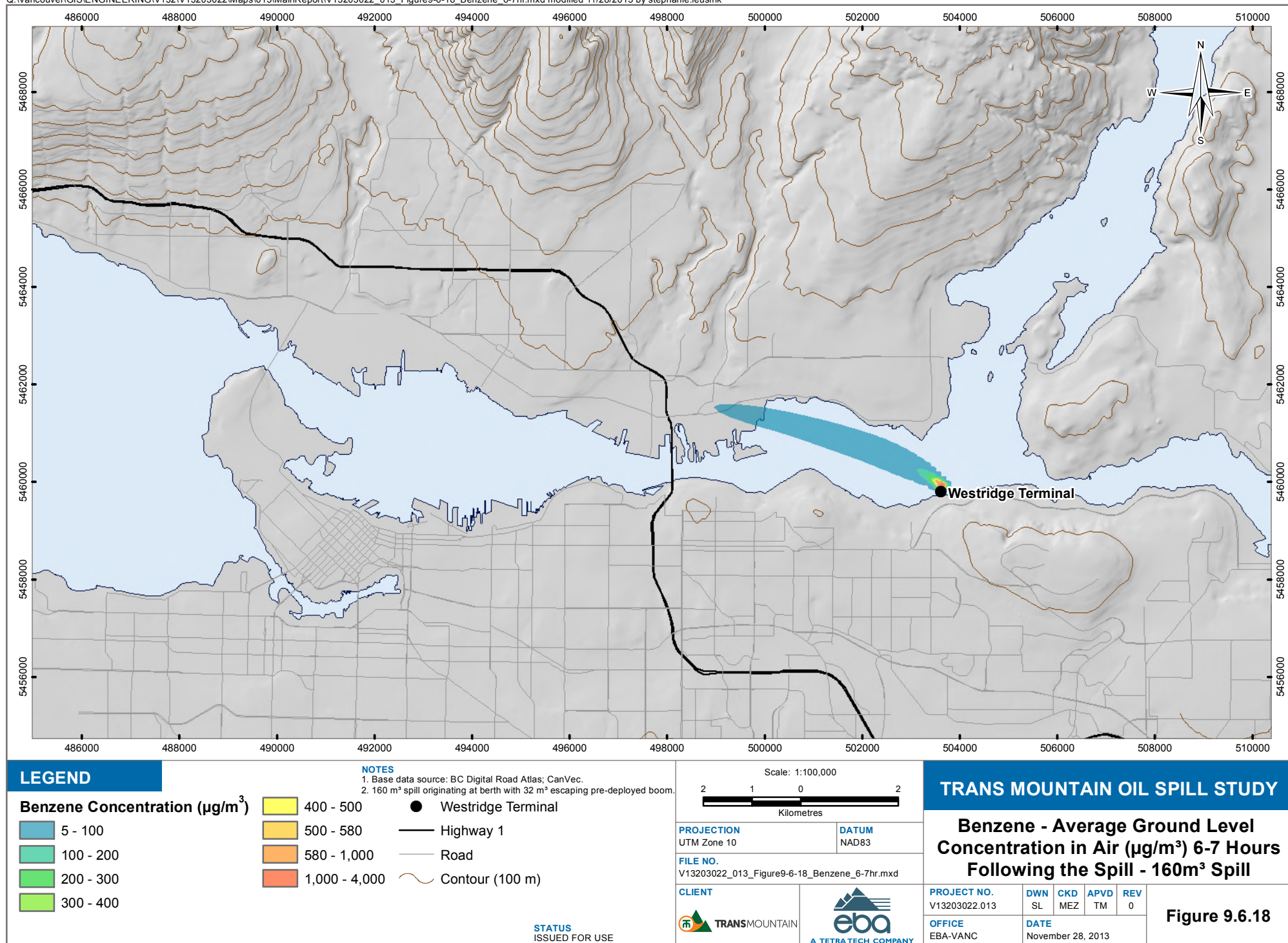


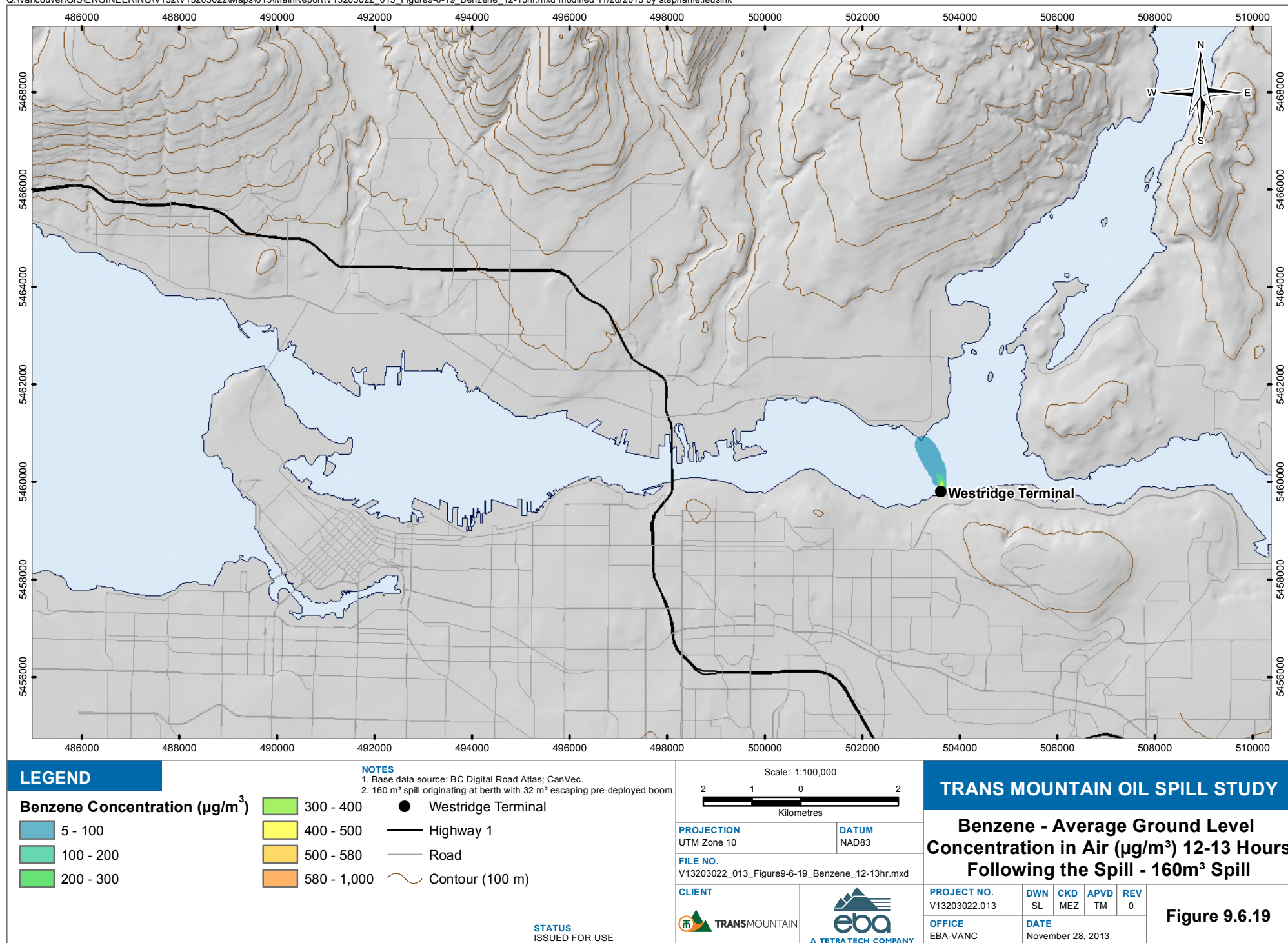




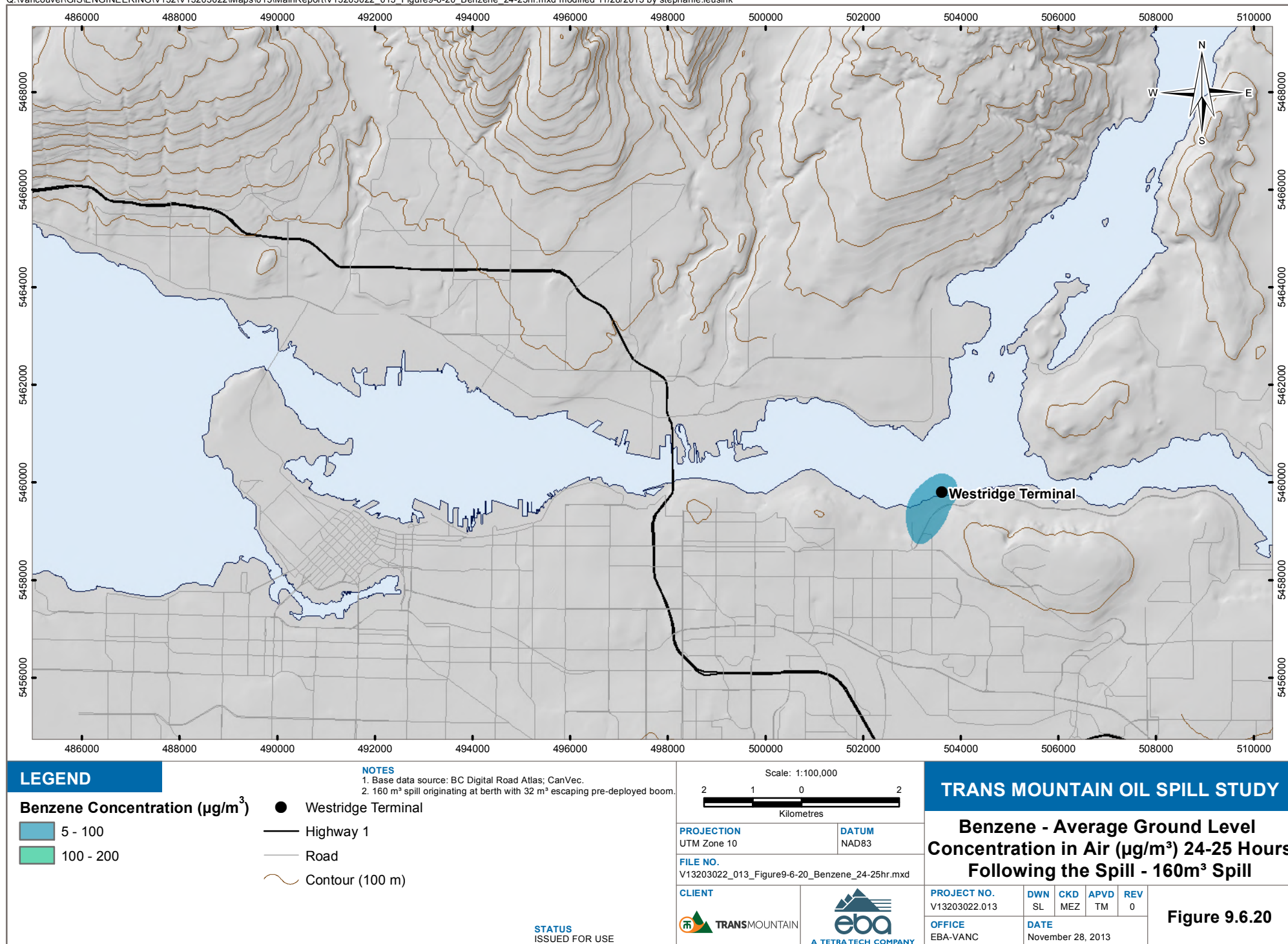


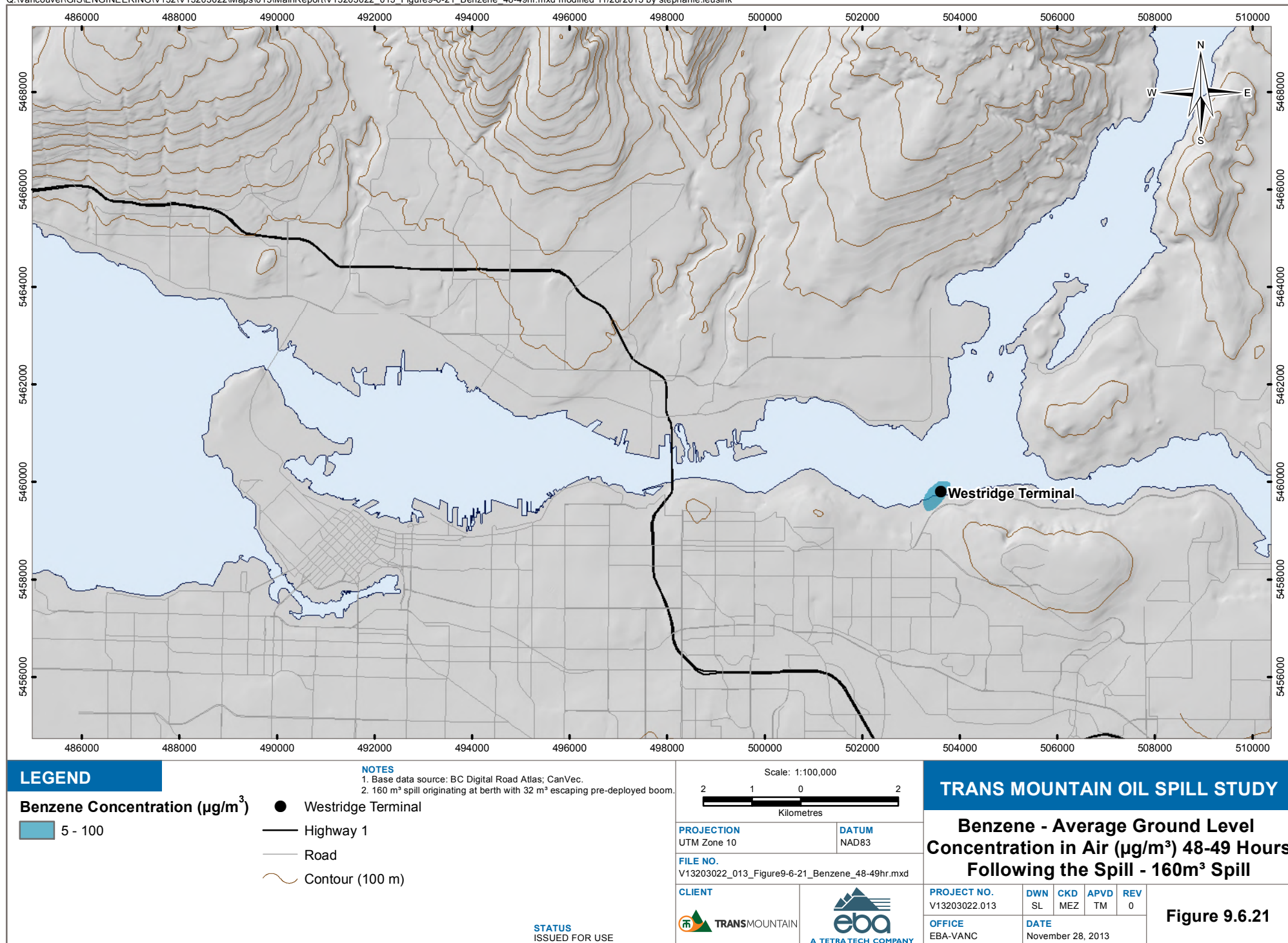




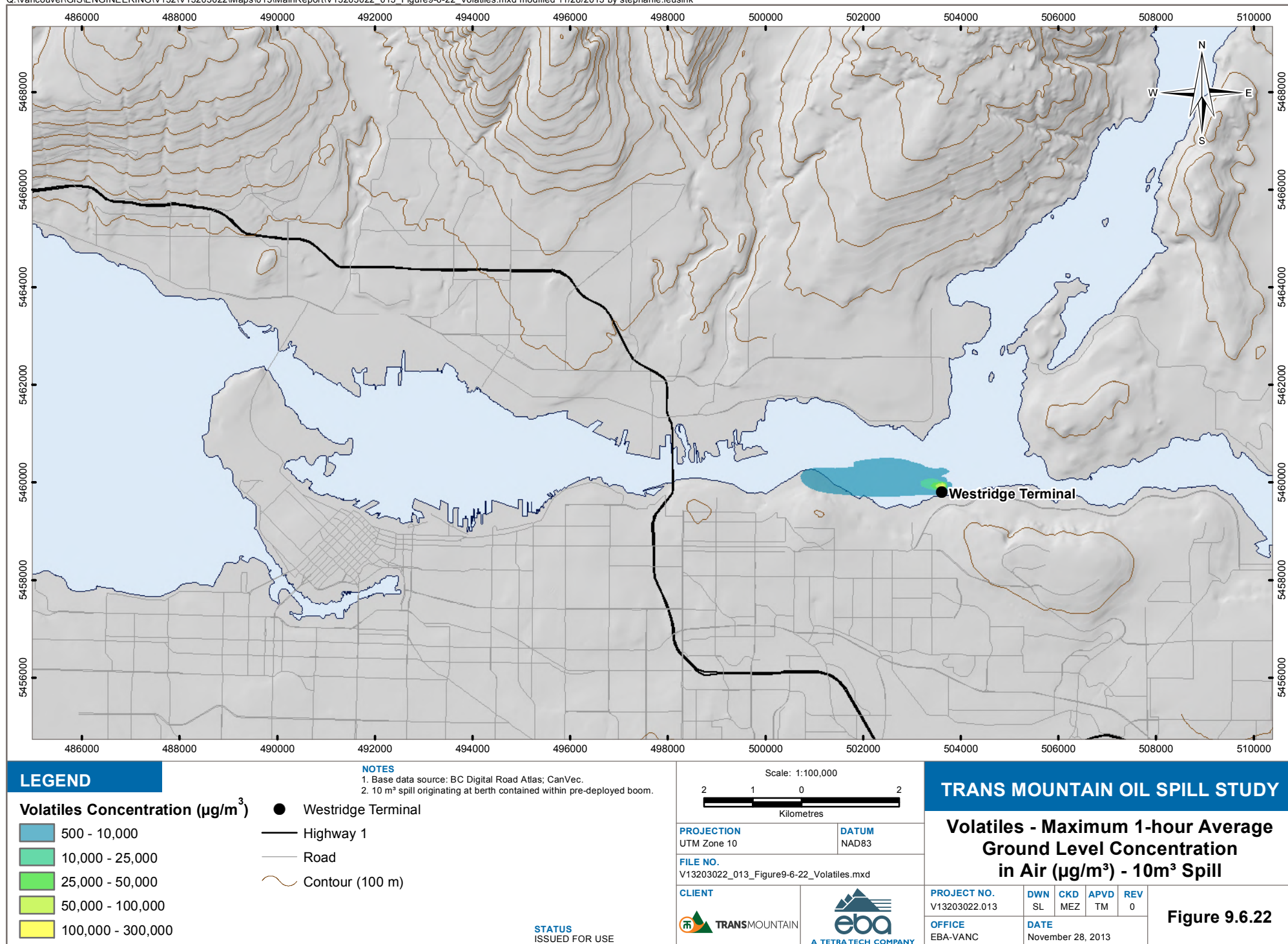




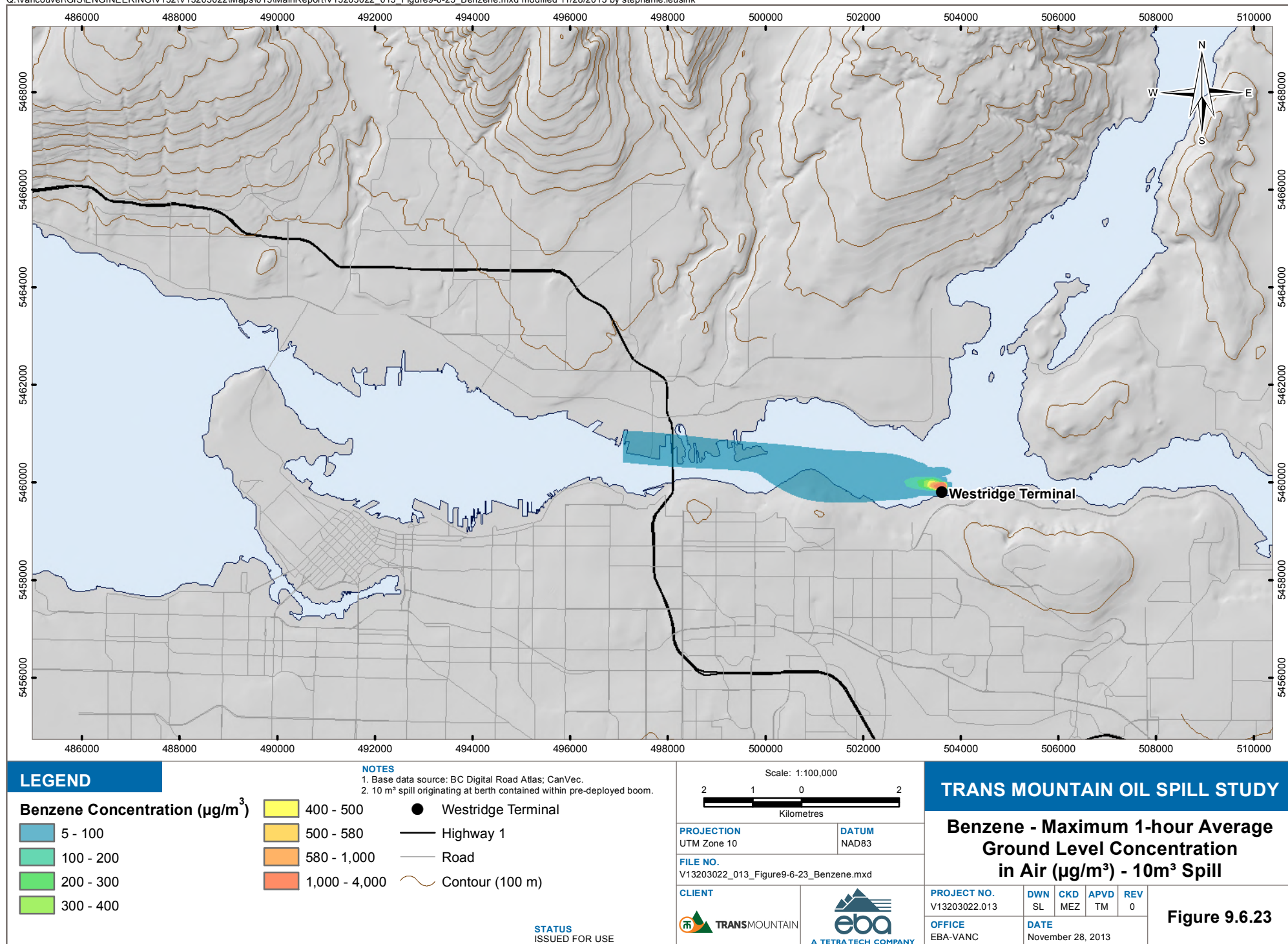


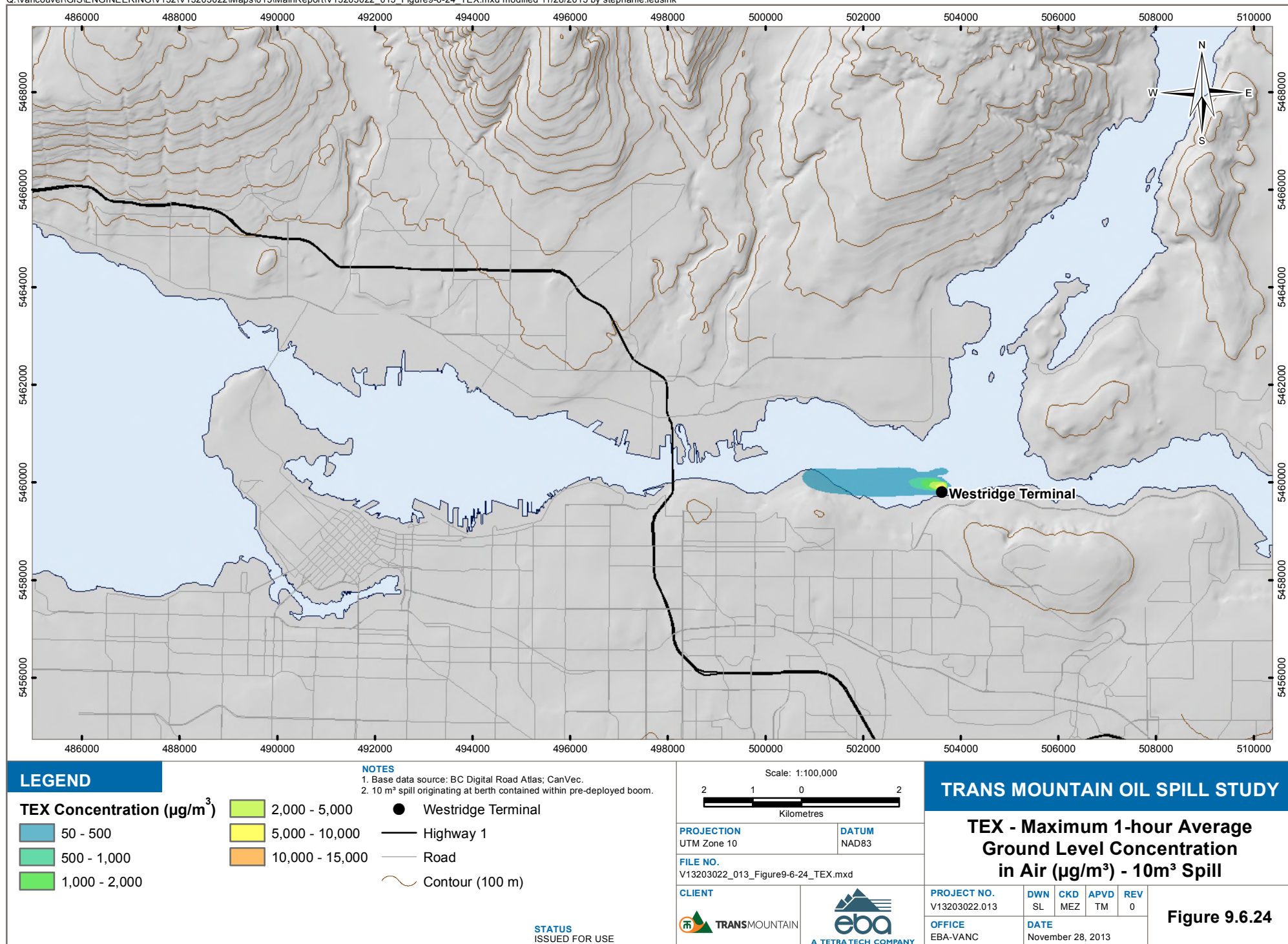




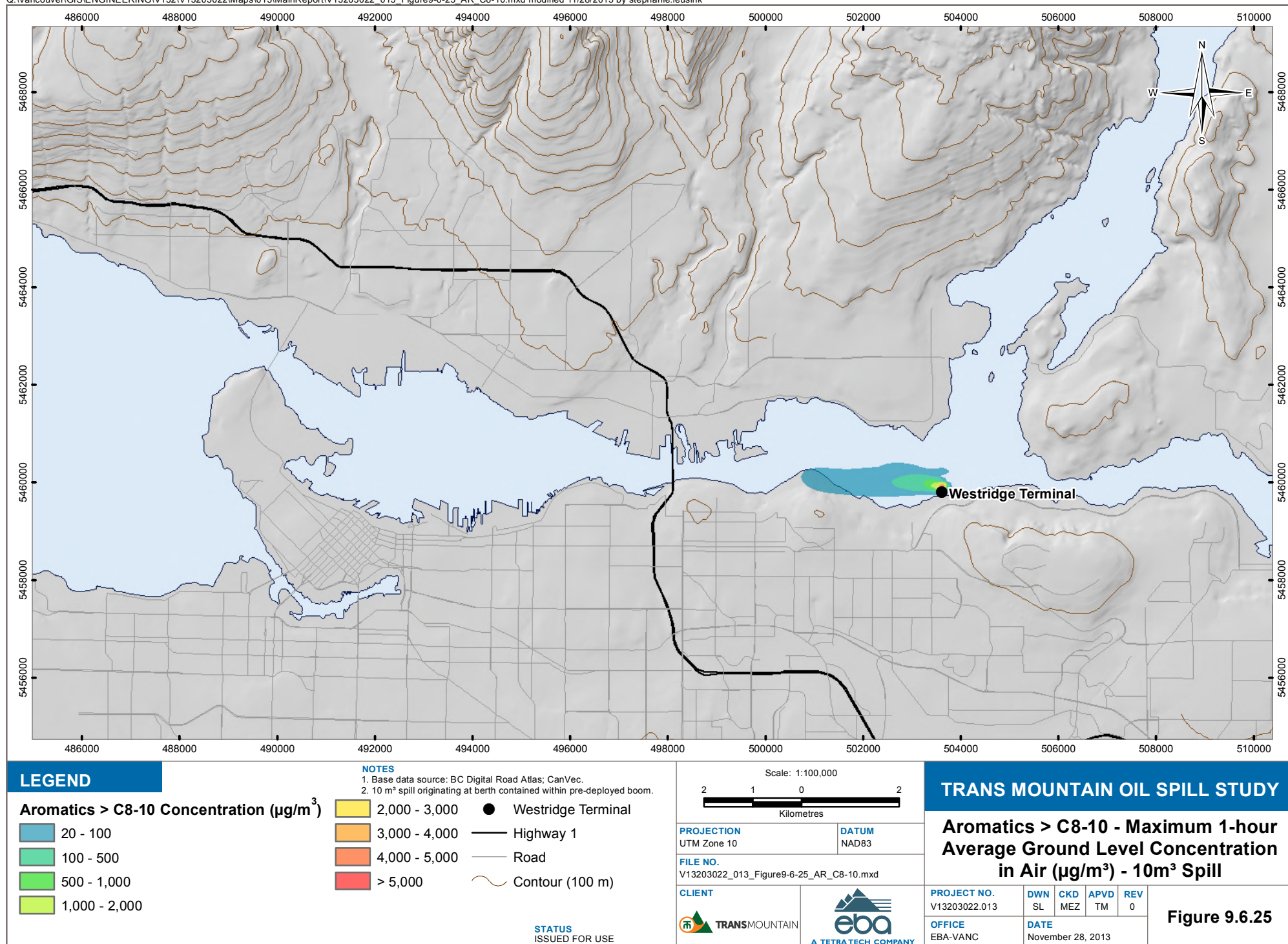


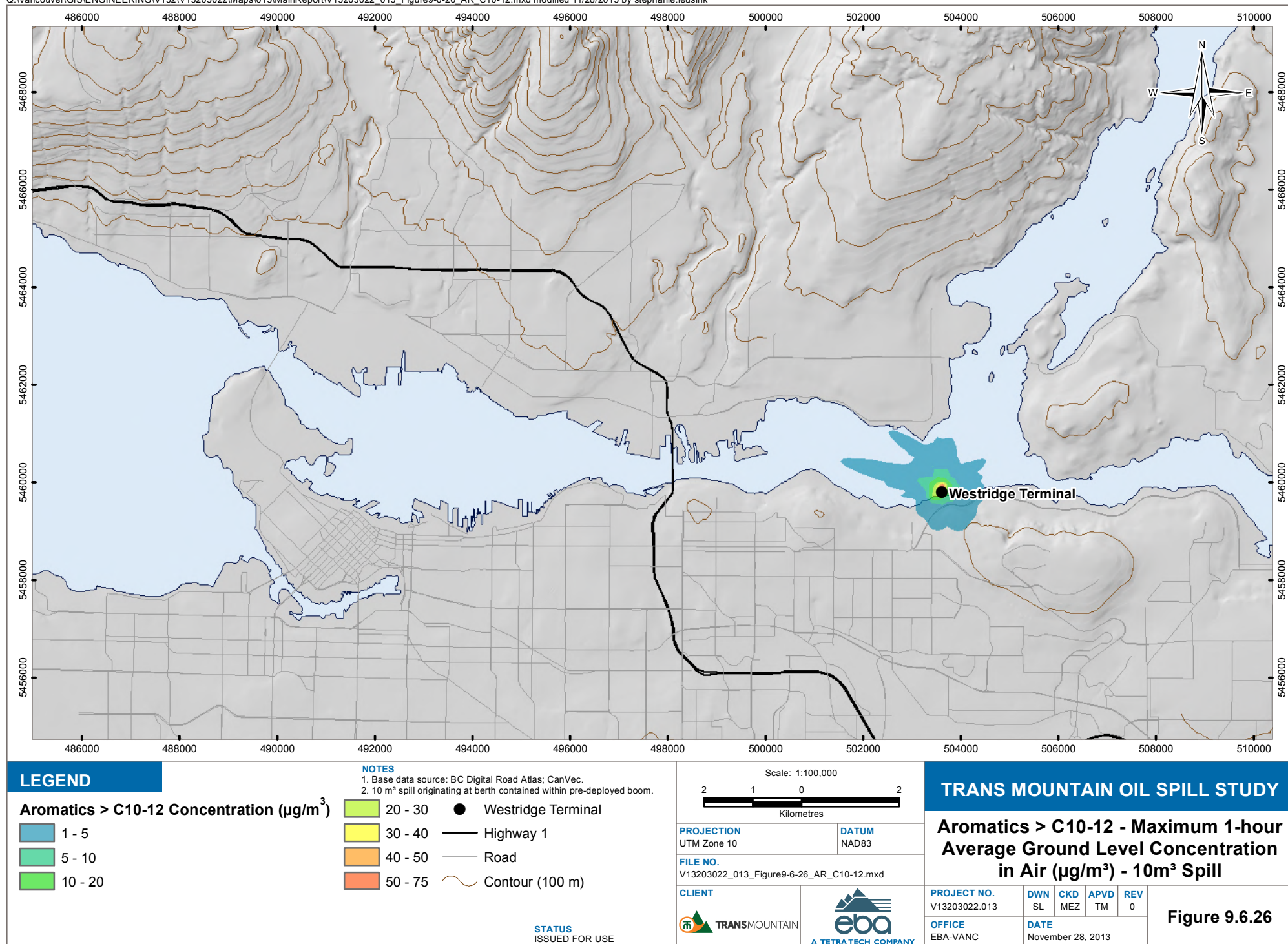




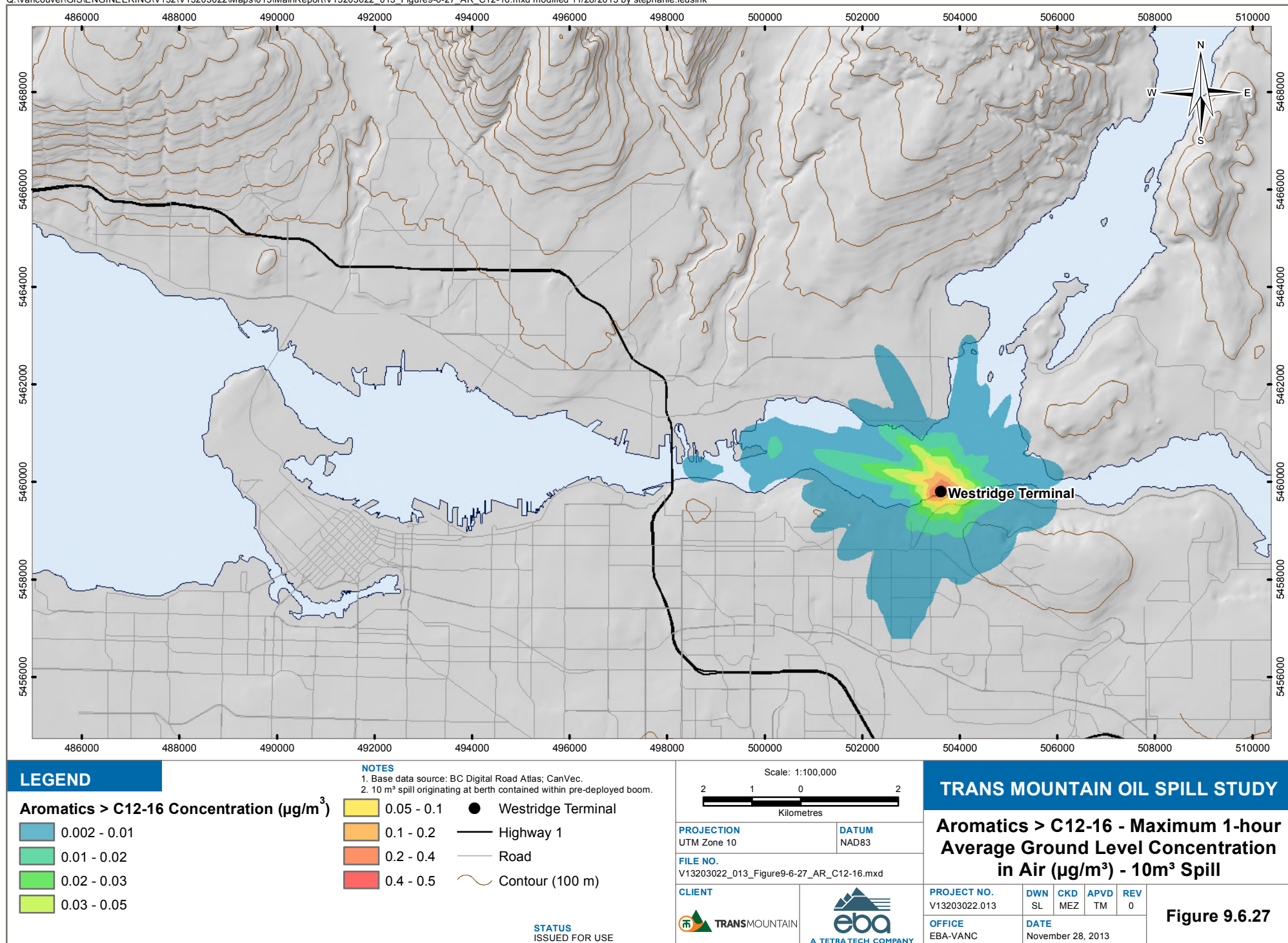




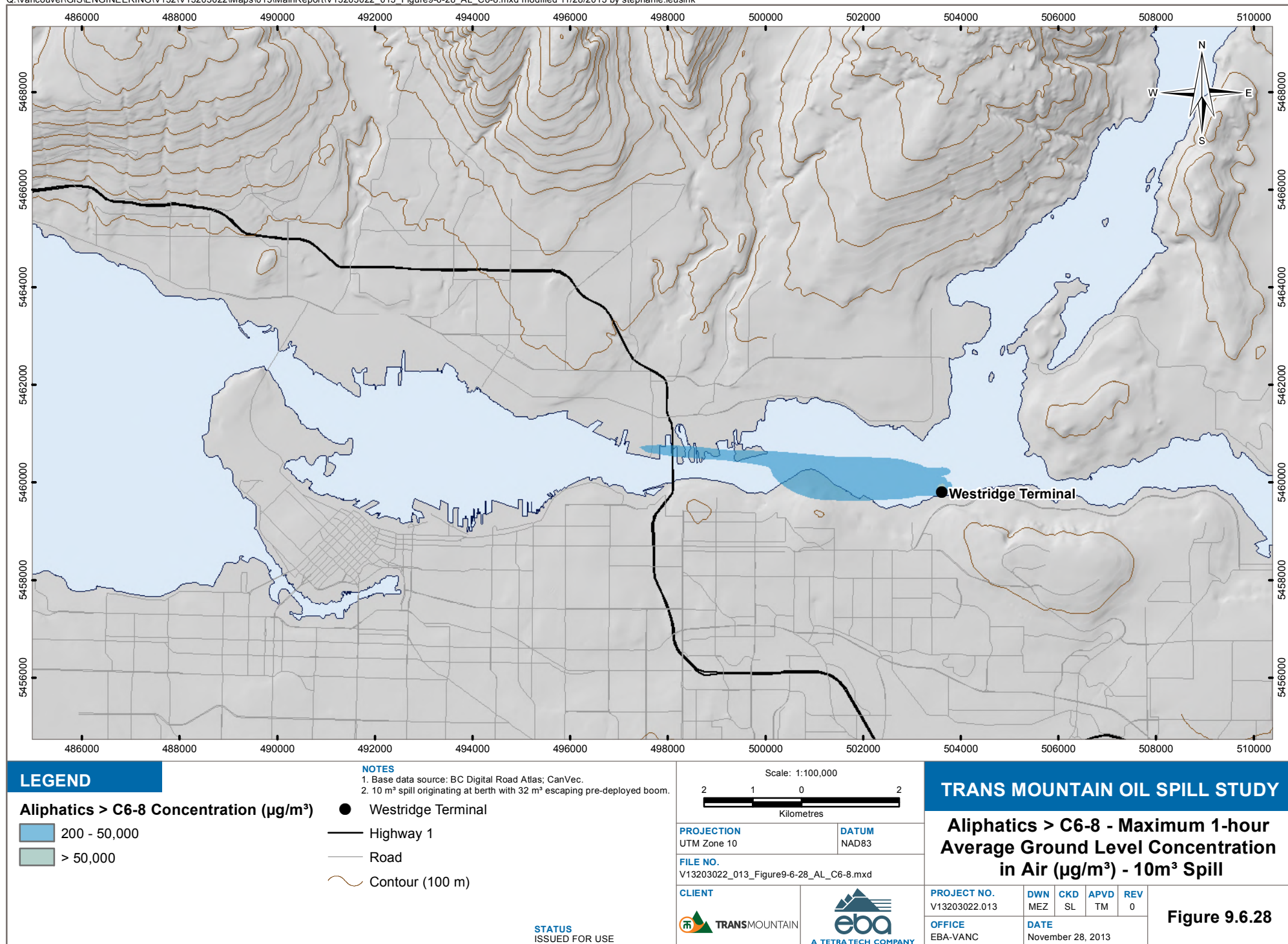


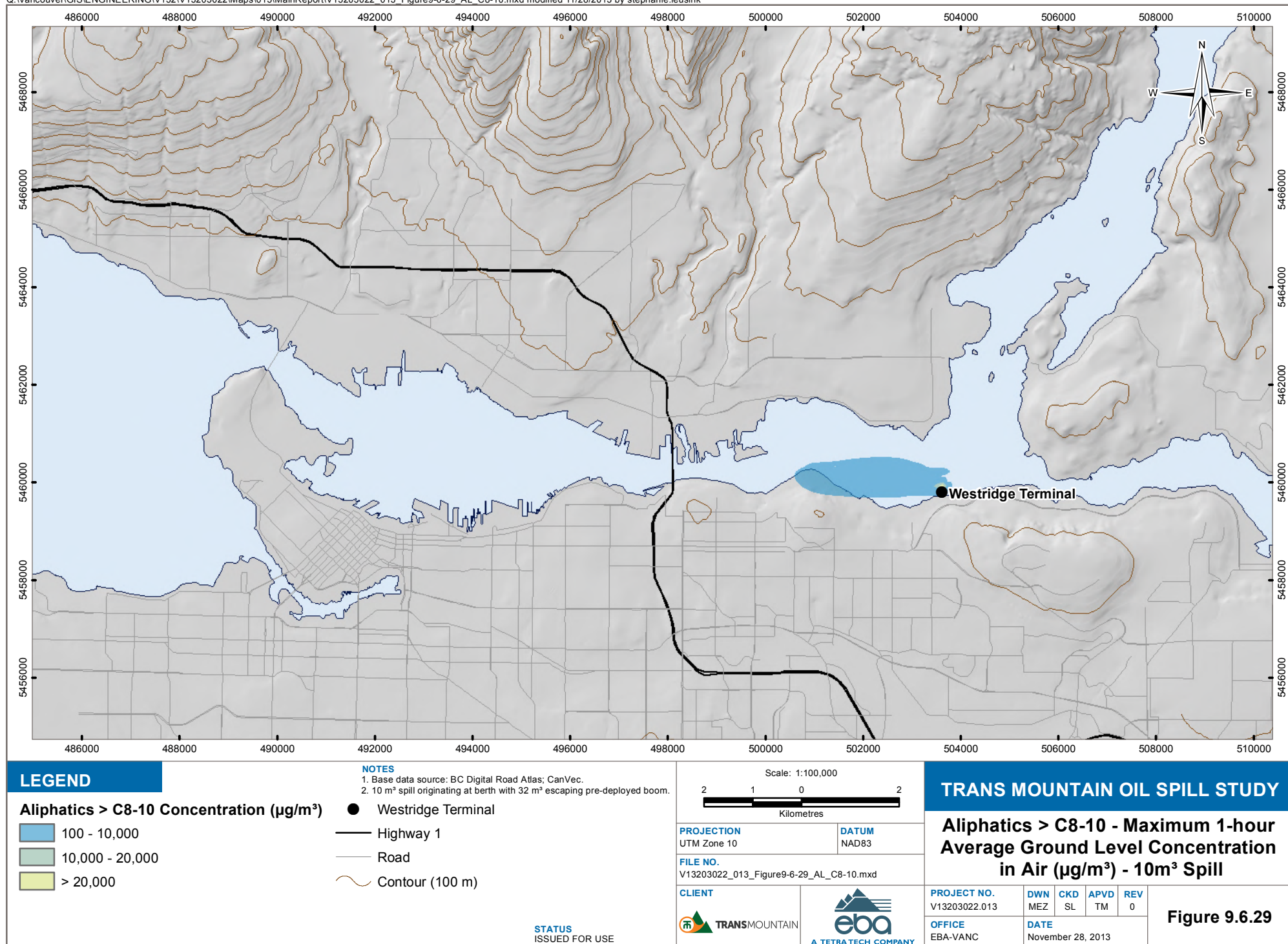




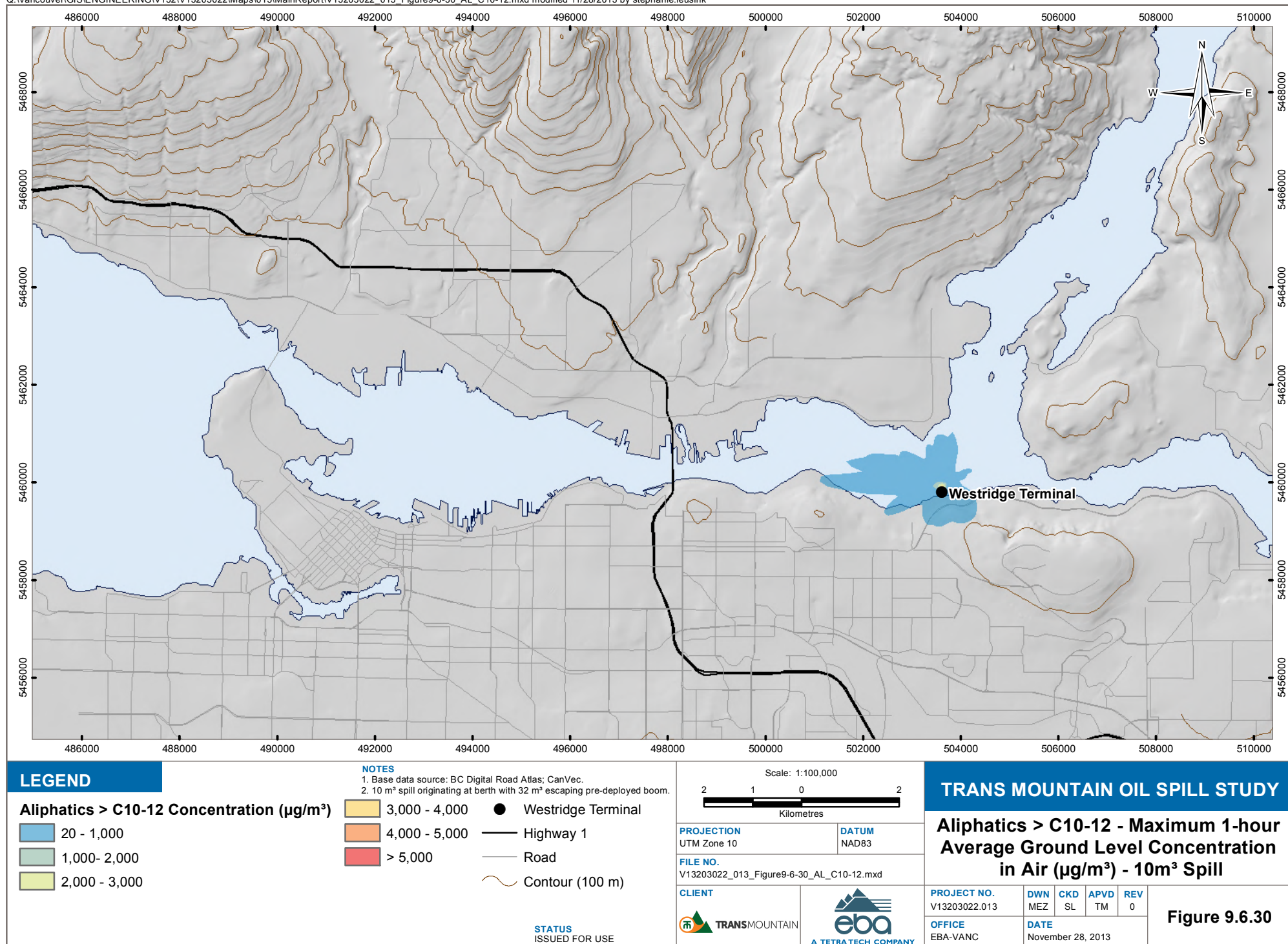


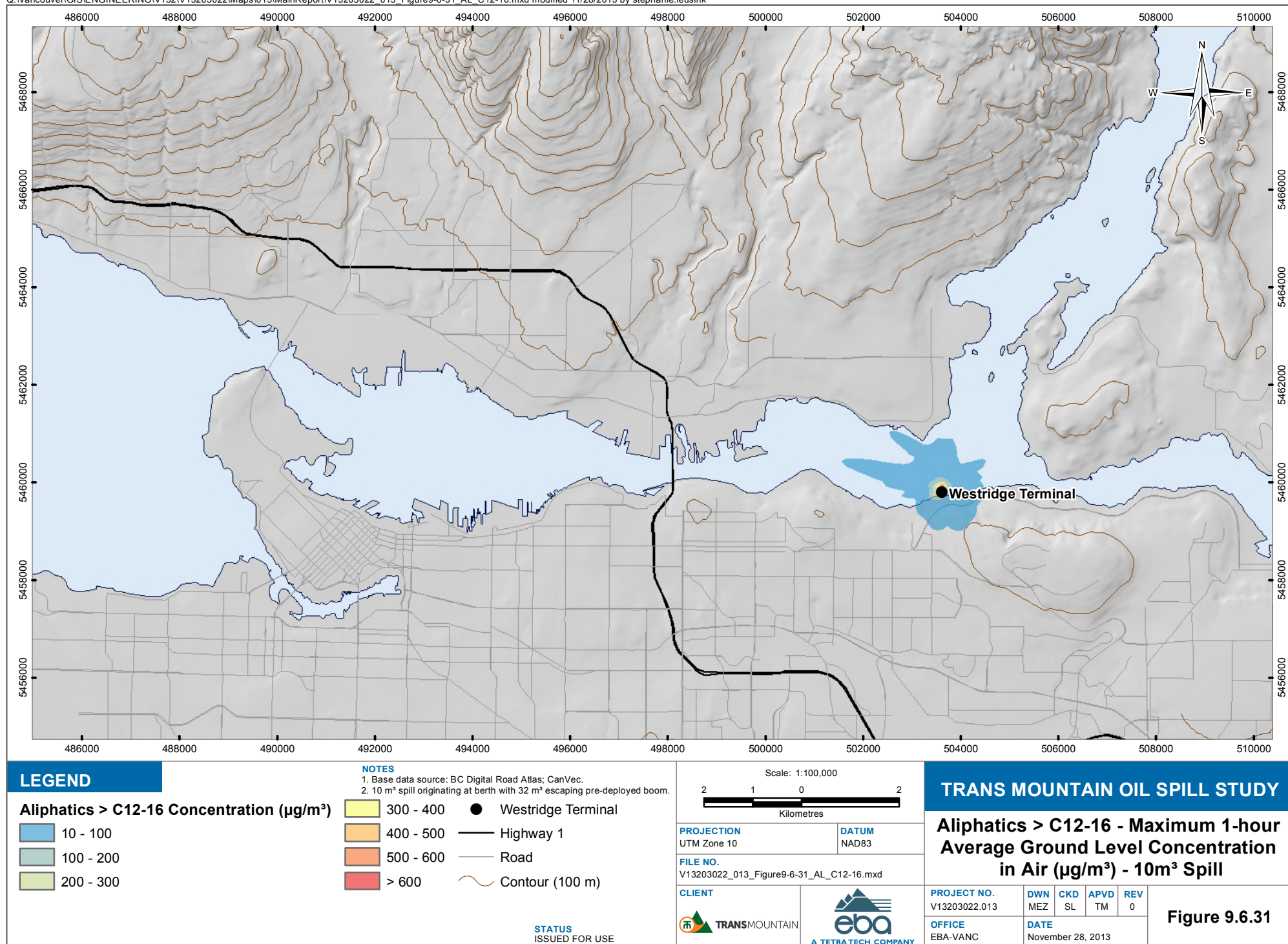




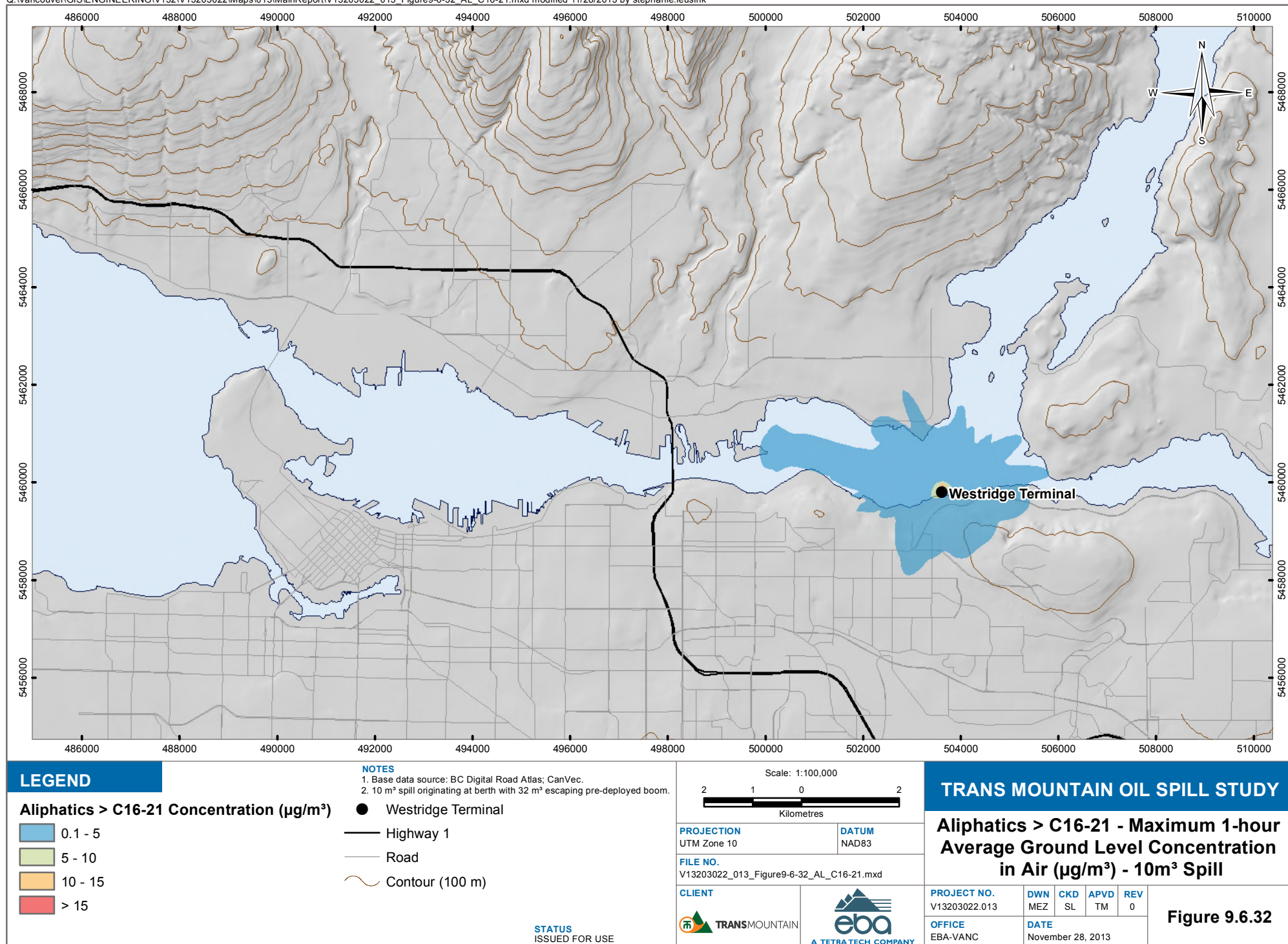












# APPENDIX A

## H3D THEORY

---

## APPENDIX A: H3D TECHNICAL DESCRIPTION

### 1.0 INTRODUCTION

H3D is an implementation of the numerical model developed by Backhaus (1983; 1985) which has had numerous applications to the European continental shelf, (Duwe et al., 1983; Backhaus and Meir Reimer, 1983), Arctic waters (Kampf and Backhaus, 1999; Backhaus and Kampf, 1999) and deep estuarine waters, (Stronach et al., 1993). Locally, H3D has been used to model the temperature structure of Okanagan Lake (Stronach et al., 2002), the transport of scalar contaminants in Okanagan Lake, (Wang and Stronach, 2005), sediment movement and scour / deposition in the Fraser River, circulation and wave propagation in Seymour and Capilano dams, and salinity movement in the lower Fraser River. H3D forms the basis of the model developed by Saucier and co-workers for the Gulf of St. Lawrence (Saucier et al., 2003), and has been applied to the Gulf of Mexico (Rego et al., 2010). H3D and its hydrocarbon transport and weathering module have been used in three recent environmental assessment applications currently before the appropriate regulatory agencies. H3D was used to simulate an existing and proposed reservoir for BC Hydro's Site C Clean Energy Project. Temperature, ice cover, and sedimentation characteristics of the proposed reservoir were predicted, supported by model validations in existing Dinosaur Reservoir. Two reports are available at the provincial Environmental Assessment Office. H3D was used to do oil spill modelling for the environmental and engineering assessments for the proposed Gateway project involving oil shipment out of Kitimat. The modelling work forms part of the information package submitted to the National Energy Board which is currently under review. Similarly, H3D was used to assess the fate of accidental fuel spills arising from a proposed jet fuel terminal in the Fraser River. This modelling work is part of the information package submitted to the provincial Environmental Assessment Office.

### 2.0 THEORETICAL BASIS

H3D is a three-dimensional time-stepping numerical model which computes the three components of velocity ( $u,v,w$ ) on a regular grid in three dimensions ( $x,y,z$ ), as well as scalar fields such as temperature and contaminant concentrations. The model uses the Arakawa C-grid (Arakawa and Lamb, 1977) in space, and uses a two level semi-implicit scheme in the time domain. H3D bears many similarities to the well-known Princeton Ocean Model (POM) (Blumberg and Mellor, 1987) in terms of the equations it solves, but differs in how the time-domain aspects are implemented. H3D uses a semi-implicit scheme, allowing relatively large time steps, and does not separately solve the internal and external models as POM does. It also uses a considerably simpler turbulence scheme in the vertical. These considerations combined allow H3D to execute complex problems relatively quickly.

The equations to be solved are:

Mass Conservation:

$$\frac{\partial u}{\partial x} + \frac{\partial v}{\partial y} + \frac{\partial w}{\partial z} = 0 \quad (A1)$$

At the end of each timestep equation, (A1) is used to diagnostically determine the vertical component of velocity ( $w$ ) once the two horizontal components of velocity ( $u$  and  $v$ ) have been calculated by the model.

X-directed momentum:

$$\frac{\partial u}{\partial t} + u \frac{\partial u}{\partial x} + v \frac{\partial u}{\partial y} + w \frac{\partial u}{\partial z} + g \frac{\partial \eta}{\partial x} + \frac{1}{\rho_o} \frac{\partial}{\partial x} \int_z^\eta (\rho_w - \rho_o) g dz - f v \frac{\partial}{\partial x} A_H \frac{\partial u}{\partial x} - \frac{\partial}{\partial y} A_H \frac{\partial u}{\partial y} - \frac{\partial}{\partial z} A_v \frac{\partial u}{\partial z} = 0. \quad (A2)$$

Y-directed momentum:

$$\frac{\partial v}{\partial t} + u \frac{\partial v}{\partial x} + v \frac{\partial v}{\partial y} + w \frac{\partial v}{\partial z} + g \frac{\partial \eta}{\partial y} + \frac{1}{\rho_o} \frac{\partial}{\partial y} \int_z^\eta (\rho_w - \rho_o) g dz + f u \frac{\partial}{\partial x} A_H \frac{\partial v}{\partial x} - \frac{\partial}{\partial y} A_H \frac{\partial v}{\partial y} - \frac{\partial}{\partial z} A_v \frac{\partial v}{\partial z} = 0. \quad (A3)$$

Water surface elevation determined from the vertically-integrated continuity equation:

$$\frac{\partial \eta}{\partial t} = - \frac{\partial}{\partial x} \int_{-H}^\eta u dz - \frac{\partial}{\partial y} \int_{-H}^\eta v dz. \quad (A4)$$

The effect of wind forcing introduced by means of the surface wind-stress boundary condition:

$$\left( A_v \frac{\partial u}{\partial z}, A_v \frac{\partial v}{\partial z} \right)_{z=\eta} = \frac{\rho_a}{\rho_w} C_{D,air} \vec{U}_{wind} \left| \vec{U}_{wind} \right|. \quad (A5)$$

The effect of bottom friction introduced by the bottom boundary condition:

$$\left( A_v \frac{\partial u}{\partial z}, A_v \frac{\partial v}{\partial z} \right)_{z=-H} = K_{bottom} \vec{U}_{bottom} \left| \vec{U}_{bottom} \right|. \quad (A6)$$

The bottom friction coefficient is usually understood to apply to currents at an elevation of one metre above the bottom. The bottom-most vector in H3D will, in general, be at a different elevation, i.e., at the midpoint of the lowest computational cell. H3D uses the 'law of the wall' to estimate the flow velocity at one metre above the bottom from the modelled near-bottom velocity.

The evolution of scalars, such as salinity, temperature, or suspended sediment, is given by the scalar transport/diffusion equation:

$$\frac{\partial S}{\partial t} + u \frac{\partial S}{\partial x} + v \frac{\partial S}{\partial y} + w \frac{\partial S}{\partial z} - \frac{\partial}{\partial x} N_H \frac{\partial S}{\partial x} - \frac{\partial}{\partial y} N_H \frac{\partial S}{\partial y} - \frac{\partial}{\partial z} N_v \frac{\partial S}{\partial z} = Q. \quad (A7)$$



In the above equations:

- $u(x,y,z,t)$ : component of velocity in the  $x$  direction;
- $v(x,y,z,t)$ : component of velocity in the  $y$  direction;
- $w(x,y,z,t)$ : component of velocity in the  $z$  direction;
- $S(x,y,z,t)$ : scalar concentration;
- $Q(x,y,z,t)$ : source term for each scalar species
- $f$ : Coriolis parameter, determined by the earth's rotation and the local latitude;
- $A_H(\partial u / \partial x, \partial u / \partial y, \partial v / \partial x, \partial v / \partial y)$ : horizontal eddy viscosity;
- $A_V(\partial u / \partial z, \partial v / \partial z, \partial \rho_{water} / \partial z)$ : vertical eddy viscosity;
- $N_H$ : horizontal eddy diffusivity;
- $N_V(\partial u / \partial z, \partial v / \partial z, \partial \rho_{water} / \partial z)$ : vertical eddy diffusivity;
- $C_{D,air}$ : drag coefficient at the air-water interface;
- $C_{D,bottom}$ : drag coefficient at the water/sea bottom interface;
- $\rho_a$ : density of air;
- $\rho_w(x,y,z,t)$ : density of water;
- $\rho_o$ : reference density of water;
- $\eta(x,y,t)$ : water surface elevation;
- $H(x,y)$ : local depth of water.

The above equations are formally integrated over the small volumes defined by the computational grid, and a set of algebraic equations results, for which an appropriate time-stepping methodology must be found. Backhaus (1983, 1985) presents such a procedure, referred to as a semi-implicit method. The spatially-discretized version of the continuity equation is written as:

$$\eta^{(1)} = \eta^{(0)} - \alpha \frac{\Delta t}{\Delta l} (\delta_x U^{(1)} + \delta_y V^{(1)}) - (1-\alpha) \frac{\Delta t}{\Delta l} (\delta_x U^{(0)} + \delta_y V^{(0)}) \quad (A8)$$

where superscript  $(0)$  and  $(1)$  refer to the present and the advanced time,  $\delta_x$  and  $\delta_y$  are spatial differencing operators, and  $U$  and  $V$  are vertically integrated velocities. The factor  $\alpha$  represents an implicit weighting, which must be greater than 0.5 for numerical stability.  $U^{(0)}$  and  $V^{(0)}$  are known at the start of each computational cycle.  $U^{(1)}$ , and similarly  $V^{(1)}$ , can be expressed as:

$$U^{(1)} = U^{(0)} - g\alpha\Delta t\eta_x^{(1)} - g(1-\alpha)\Delta t\eta_x^{(0)} + \Delta tX^{(0)} \quad (A9)$$

where  $X^{(0)}$  symbolically represents all other terms in the equation of motion for the  $u$ - or  $v$ -component, which are evaluated at time level  $(0)$ : Coriolis force, internal pressure gradients, non-linear terms, and top and bottom stresses,. When these expressions are substituted into the continuity equation (A4), after some further manipulations, there results an elliptic equation for  $\delta_{i,k}$ , the change in water level over one timestep at grid cell  $i,k$  (respectively the  $y$  and  $x$  directions):

$$\delta_{i,k} - (ce\delta_{i,k+1} + cw\delta_{i,k-1} + cn\delta_{i-1,k} + cs\delta_{i+1,k}) = Z_{i,k} \quad (A10)$$

where  $ce$ ,  $cw$ ,  $cn$ , and  $cs$  are coefficients depending on local depths and the weighting factor ( $\alpha$ ), and  $Z_{i,k}$  represents the sum of the divergence formed from velocities at time level ( $0$ ) plus a weighted sum of adjacent water levels at time level ( $0$ ).

Once equation (A10) is solved for  $\delta_{i,k}$ , the water level can be updated:

$$\eta_{i,k}^{(1)} = \eta_{i,k}^{(0)} + \delta_{i,k} \quad (A11)$$

and equation (A9) can be completed.

At the end of each timestep, volume conservation is used to diagnostically compute the vertical velocity  $w(j,i,k)$  from the two horizontal components  $u$  and  $v$ .

## 2.1 Vertical Grid Geometry

In the vertical, the levels near the surface are typically closely spaced to assist with resolving near-surface dynamics. In addition, the model is capable of dealing with relatively large excursions in overall water level as the water level rises and falls in response to varying inflows and outflows, by allowing the number of near-surface layers to change as the water level varies. That is, as water levels rise in a particular cell, successive layers above the original layer are turned on and become part of the computational mesh. Similarly, as water levels fall, layers are turned off. This procedure has proven to be quite robust, and allows for any reasonable vertical resolution in near-surface waters. When modelling thin river plumes in areas of large tidal range, the variable number of layers approach allows for much better control over vertical resolution than does the  $\sigma$ -coordinate method.

In addition to tides, the model is able to capture the important response, in terms of enhanced currents and vertical mixing, to wind-driven events. This is achieved by applying wind stress to each surface grid point on each time step. Vertical mixing in the model then re-distributes this horizontal momentum throughout the water column. Similarly, heat flux through the water surface is re-distributed by turbulence and currents in temperature simulations.

## 2.2 Turbulence Closure

Turbulence modelling is important in determining the correct distribution of velocity and scalars in the model. The diffusion coefficients for momentum ( $A_H$  and  $A_V$ ) and scalars ( $N_H$  and  $N_V$ ) at each computational cell are dependent on the level of turbulence at that point. H3D uses a shear-dependent turbulence formulation in the horizontal, (Smagorinsky, 1963). The basic form is:

$$A_H = A_{H0} dx dy \sqrt{\left(\frac{du}{dx}\right)^2 + \left(\frac{dv}{dy}\right)^2 + \frac{1}{2}\left(\frac{\partial v}{\partial x} + \frac{\partial u}{\partial y}\right)^2} \quad (A12)$$

The parameter  $A_{H0}$  is a dimensionless tuning variable, and experience has shown it to lie in the range of 0.25 to 0.45 for most water bodies such as rivers, lakes and estuaries.

A shear and stratification dependent formulation, the Level 2 model of Mellor and Yamada (1982), is used for the vertical eddy diffusivity. The basic theory for the vertical viscosity formulation is taken from an early paper, Mellor and Durbin (1975). The evaluation of length scale is based on a methodology presented in Mellor and Yamada (1982).

For scalars, both horizontal and vertical eddy diffusivity are taken to be similar to their eddy viscosity counterparts, but scaled by a fixed ratio from the eddy viscosity values. Different ratios are used for the horizontal and vertical diffusivities. If data is available for calibration, these ratios can be adjusted based on comparisons between modelled and observed data. Otherwise, standard values based on experience with similar previously modelled water bodies are used. In a recent reservoir simulation, the ratio of vertical eddy diffusivity to vertical eddy viscosity was 0.75 and the ratio between horizontal eddy diffusivity and horizontal eddy viscosity was 1.0.

### 2.3 Scalar Transport

The scalar transport equation implements a form of the flux-corrected algorithm (Zalesak, 1979), in which all fluxes through the sides of each computational cell are first calculated using a second-order method. Although generally more accurate than a first order method, second order flux calculations can sometimes lead to unwanted high frequency oscillations in the numerical solution. To determine if such a situation is developing, the model examines each cell to see if the computed second order flux would cause a local minimum or maximum to develop. If so, then all fluxes into or out of that cell are replaced by first order fluxes, and the calculation is completed. As noted, the method is not a strict implementation of the Zalesak method, but is much faster and achieves very good performance with respect to propagation of a Gaussian distribution through a computational mesh. It does not propagate box-car distributions as well as the full Zalesak method, but achieves realistic simulations of the advection of scalars in lakes, rivers and estuaries, which is the goal of the model. This scheme as implemented is thus a good tradeoff between precision and execution time, important since in many situations, where more than one scalar is involved, the transport-diffusion algorithm can take up more than half the execution time.

### 2.4 Heat Flux at the Air-Water Interface

The contribution of heat flux to the evolution of the water temperature field can be schematized as:

$$\frac{dT}{dt} = \frac{\Delta Q}{\rho * c_p * h}$$

where  $\Delta Q$  is the net heat flux per unit area retained in a particular layer,  $\rho$  is the density of water,  $c_p$  is the heat capacity of water and  $h$  is the layer thickness.

Heat flux at the air-water interface incorporates the following terms:

$Q_{in}$ : incident short wave radiation. Generally, this is not known from direct observations. Generally, it is estimated from the cloud cover and opacity observations at nearby stations, a theoretical calculation of radiation at the top of the atmosphere based on the geometry of the earth/sun system, and an empirical adjustment based on radiation measurements at Vancouver Airport and UBC respectively for the period 1974-1977. This procedure has worked well for many water bodies, notably Okanagan Lake and the waters of

the north coast of British Columbia, in terms of allowing H3D to reproduce the observed temperature distributions in space and time. Values for albedo as a function of solar height are taken from Kondratyev (1972).

$Q_{back}$ : net long wave radiation, calculated according to Gill (1982), involving the usual fourth power dependence on temperature, a factor of 0.985 to allow for the non-black body behaviour of the ocean, a factor depending on vapor pressure to allow for losses due to back radiation from moisture in the air, and a factor representing backscatter from clouds.

$Q_L$  and  $Q_H$ : latent and sensible heat flux. Latent heat flux ( $Q_L$ ) is the heat carried away by the process of evaporation of water. Sensible heat flux ( $Q_S$ ) is driven by the air-water temperature difference and is similar to conduction, but assisted by turbulence in the air. Latent and sensible heat flux is described by:

$$Q_L = 1.32e^{-3} * L * windspeed * (q_{obs} - q_{sat}) * latent\_factor$$
$$Q_S = 1.46e^{-3} * \rho_{air} * c_p * windspeed * (T_{air} - T_{water}) * sensible\_factor$$

Where  $q_{obs}$  and  $q_{sat}$  are the observed and saturated specific humidities,  $T_{air}$  and  $T_{water}$  are the air and water temperatures,  $L$  is the latent heat of evaporation of water, and  $c_p$  is the heat capacity of water. ' $latent\_factor$ ' and ' $sensible\_factor$ ' are scaling factors introduced to account for local factors, and can be adjusted, when needed, to achieve better calibration of the model. Typically, the only adjustment is that  $Sensible\_factor$  is doubled when the air temperature is less than the water or ice surface temperature to account for increased turbulence in an unstable air column.

Light absorption in the water column. As light passes through the water column it is absorbed and the absorbed energy is a component of the energy balance that drives water temperature. H3D assumes that light attenuation follows an exponential decay law:

$$E(z) = E(z_0) * e^{-k*(z-z_0)}$$

The model computes the energy at the top and bottom of each layer and the difference is applied to the general heat equation in that layer. The extinction coefficient ( $k$ ) is related to the Secchi depth ( $D_s$ ) by

$$k = \frac{2.1}{D_s}$$

Temperature is treated like any other scalar as far as advection and diffusion are concerned. Heat flux at the water-sediment interface is not currently included in H3D.

## 2.5 Ice

The ice model is generally based on processes described in Patterson and Hamblin (1988). The ice cover is characterized by a thickness, a fraction of the cell covered, and an ice surface temperature. The temperature of the bottom of the ice is assumed to be the temperature of melting, usually 0° C. The strategy is to compute the differences in heat flux at the top and bottom of the ice layer and use this difference to determine the growth or decay rate and the change in temperature of the ice. The heat flux at



the bottom of the ice layer is dependent on lake temperature and water velocity. The heat flux at the top is dependent on meteorological processes and the surface temperature of the ice. The surface heat flux to the top of the ice sheet is calculated in a similar way as for open water, except that latent heat flux term ( $Q_L$ ) also includes the heat of fusion. Albedo is also altered to account for ice/snow cover.

In order to start ice formation, once the surface water temperature drops below 3° C in a particular cell, a test ice layer of thickness 1 cm is initialized. If the test thickness melts in one time step, then the system cannot support ice cover in that cell at that time. If it survives, then the amount of ice in that cell is converted to a 1 cm thick region with coverage calculated from the mass of ice formed. In this way, a relatively robust start is made to ice formation.

The frictional interaction between the bottom of the ice and the immediately adjacent water is parameterized according to Nezhihkovskiy (1964).

## **2.6 Validation**

Three validations of H3D's water level and temperature prediction skill are discussed below.

### **2.6.1 Strait of Georgia/Point Atkinson Tide: Wave Propagation**

A fundamental concern with a circulation model such as H3D is how well it propagates waves, the carriers of information through the system. Figure A-1 presents results of a simulation of tides in the Strait of Georgia and Juan de Fuca Strait, with tidal elevations prescribed at the entrance to Juan de Fuca Strait and at a section north of Texada Island in the Strait of Georgia. The complex dynamics of the northern passes, such as Discovery Passage and Seymour Narrows, are thus avoided, allowing a test of H3D's wave propagation capabilities. The figure plots the modelled water level at Point Atkinson in red, and the observed water level in black. There is nearly perfect agreement, with the slight difference resulting from small storm surge events. This validation demonstrates that the selection of grid schematization (Arakawa C-grid) and the semi-implicit time-stepping approach have produced a system that can accurately propagate information through a water body.

### **2.6.2 Okanagan Lake Temperature Profiles**

Obtaining good reproduction of the seasonally-evolving temperature structure of a lake indicates that the heat flux across the air-water interface is accurately parameterized and that the transport-diffusive processes operating in the water column are also accurately reproduced by the model. Figure A-2 presents a comparison of observed and computed temperature profiles at the northern end of Okanagan Lake near Vernon, in April, August, October and December of 1997. The agreement is very good as the model reproduced the transition from a well-mixed condition in the spring to the development of a strong thermocline in the summer, the deepening of the upper layer during the fall cooling period, and a return to isothermal conditions in winter. There is little doubt that H3D can compute accurate temperature distributions in water bodies, as long as adequate meteorological data is available. For this simulation, the meteorological data was obtained from Penticton Airport: winds, rotated to follow the thalweg of the valley; cloud cover, air temperature and relative humidity.

### 2.6.3 Thermistor Response: Okanagan Lake

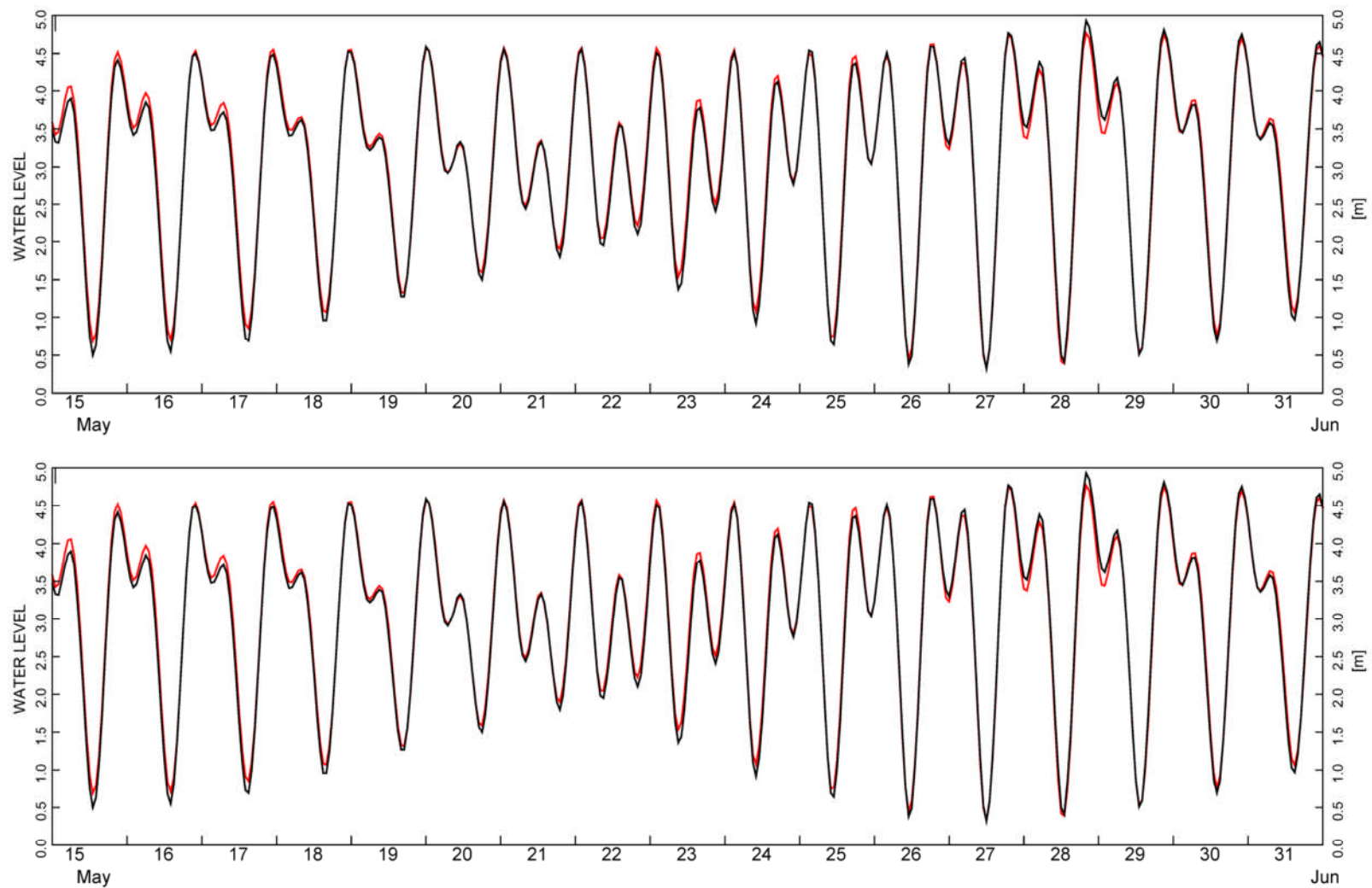
Okanagan Lake is subject to significant fluctuations in the vertical thermal structure during the summer stratified period. Figure A-3 shows a temperature time-series at a site on the north side of the William R. Bennett Bridge which exhibits significant temperature excursions at periods of about 60 hours, or 2.5 days. Figure A-4 shows the modelled time series of temperature at three selected depths, 51 m, 21 m and 9 m. The occurrence and magnitude of the temperature fluctuations is generally predicted by the model, but the reproduction is not perfect: the occurrence and timing of the temperature events is quite good, but the modelled peaks appear to be generally somewhat broader in time. It was found that there were considerable differences in the simulated behaviour depending on whether winds at Kelowna Airport, which is situated in a side-valley, were included in the model or not. It is also clear that H3D can generally reproduce internal seiches in a lake, as long as adequate spatial resolution is used. This is particularly apparent when the coherent internal waves that propagate up and down the lake are examined in a longitudinal section, illustrated in two snapshots from a model simulation of such an event in Figure A-5.

## REFERENCES

- Arakawa, A. and V.R. Lamb. 1977. Computational design of the basic dynamical processes of the UCLA general circulation model. *Methods in Computational Physics*, 17, 173-263.
- Backhaus, J.O. 1983. A semi-implicit scheme for the shallow water equations for applications to shelf sea modelling. *Continental Shelf Research*, 2, 243-254.
- Backhaus, J.O. and E. Meir-Reimer. 1983. On seasonal circulation patterns in the North Sea. In: *North Sea Dynamics*, J. Sundermann and W. Lenz, editors. Springer-Verlag, Heidelberg, pp 63-84.
- Backhaus, J.O., and J. Kampf, 1999. Simulation of sub-mesoscale oceanic convection and ice-ocean interactions in the Greenland Sea. *Deep Sea Research Part II: Topical Studies in Oceanography*, 46, 1427-1455.
- Backhaus, J.O., 1985. A three-dimensional model for the simulation of shelf-sea dynamics. *Deutsche Hydrographische Zeitschrift*, 38, 165-187.
- Blumberg, A. F. and G. L. Mellor, A description of a three-dimensional coastal ocean circulation model, In *Three-Dimensional Coastal Ocean Models*, N. S. Heaps, editor. American Geophysical Union, Washington, DC, 1987, pp 1-16.
- Duwe, K.C., R.R. Hewer, and J.O. Backhaus. 1983. Results of a semi-implicit two-step method for the simulation of markedly non-linear flow in coastal seas. *Continental Shelf Research*, 2, 255-274.
- Friehe C.A. and K.F. Schmitt, 1976. Parameterization of air-sea interface fluxes of sensible heat and moisture by the bulk aerodynamic formulas. *Journal of Physical Oceanography*, 76:801-805.
- Kampf, J. and J.O Backhaus, 1999. Ice-ocean interactions during shallow convection under conditions of steady winds: three-dimensional numerical studies. *Deep Sea Research Part II: Topical Studies in Oceanography*, 46, 1335-1355.
- Kondratyev, K.Y., 1972. *Radiation Processes in the Atmosphere*, WMO No. 309.
- Mellor, G.L. and P.A. Durbin. 1975. The structure and dynamics of the ocean surface mixed layer. *Journal of Physical Oceanography*, 5, 718-728.
- Mellor, G.L. and T. Yamada. 1982. Development of a turbulence closure model for geophysical fluid problems. *Reviews of Geophysics and Space Physics*, 20, 851-875.
- Nezhikhovskiy, R.A. 1964. Coefficients of roughness of bottom surface of slush-ice cover. *Soviet Hydrology: Selected Papers*, 2, 127-150.
- Rego, J.L., E. Meselhe, J. Stronach and E. Habib. Numerical Modeling of the Mississippi-Atchafalaya Rivers' Sediment Transport and Fate: Considerations for Diversion Scenarios. *Journal of Coastal Research*, 26, 212-229.
- Saucier, F.J.; F. Roy, D. Gilbert, P. Pellerin and H. Ritchie. 2003. The formation of water masses and sea ice in the Gulf of St. Lawrence. *Journal of Geophysical Research*, 108 (C8): 3269–3289.
- Smagorinsky, J. 1963. General circulation experiments with primitive equations I. The basic experiment. *Monthly Weather Review*, 91, 91-164.

- Stronach, J.A., J.O. Backhaus, and T.S. Murty. 1993. An update on the numerical simulation of oceanographic processes in the waters between Vancouver Island and the mainland: the G8 model. *Oceanography and Marine Biology: an Annual Review*, 31, 1-86.
- Stronach, J.A., R.P. Mulligan, H. Soderholm, R. Draho, D Degen. 2002. Okanagan Lake Limnology: Helping to Improve Water Quality and Safety. *Innovation, Journal of the Association of Professional Engineers and Geoscientists of B.C.* November 2002.
- Wang, E and J.A. Stronach. 2005. Summerland Water Intake Feasibility Study. In "Water – Our Limiting Resource", *Proceedings of a conference held in Kelowna Feb 23-25, 2005.* BC Branch, Canadian Water Resources Association. pp. 256 – 269.
- Zalesak, S.T. 1979. Fully multidimensional flux-corrected transport algorithms for fluids. *Journal of Computational Physics*, 31, 335-362.





#### LEGEND

- Solid lines represent observed profiles
- Dash lines represent modelled profiles

#### NOTES

#### STATUS

#### CLIENT

-



#### H3D TECHNICAL DESCRIPTION

#### H3D Validation Tidal Reproduction

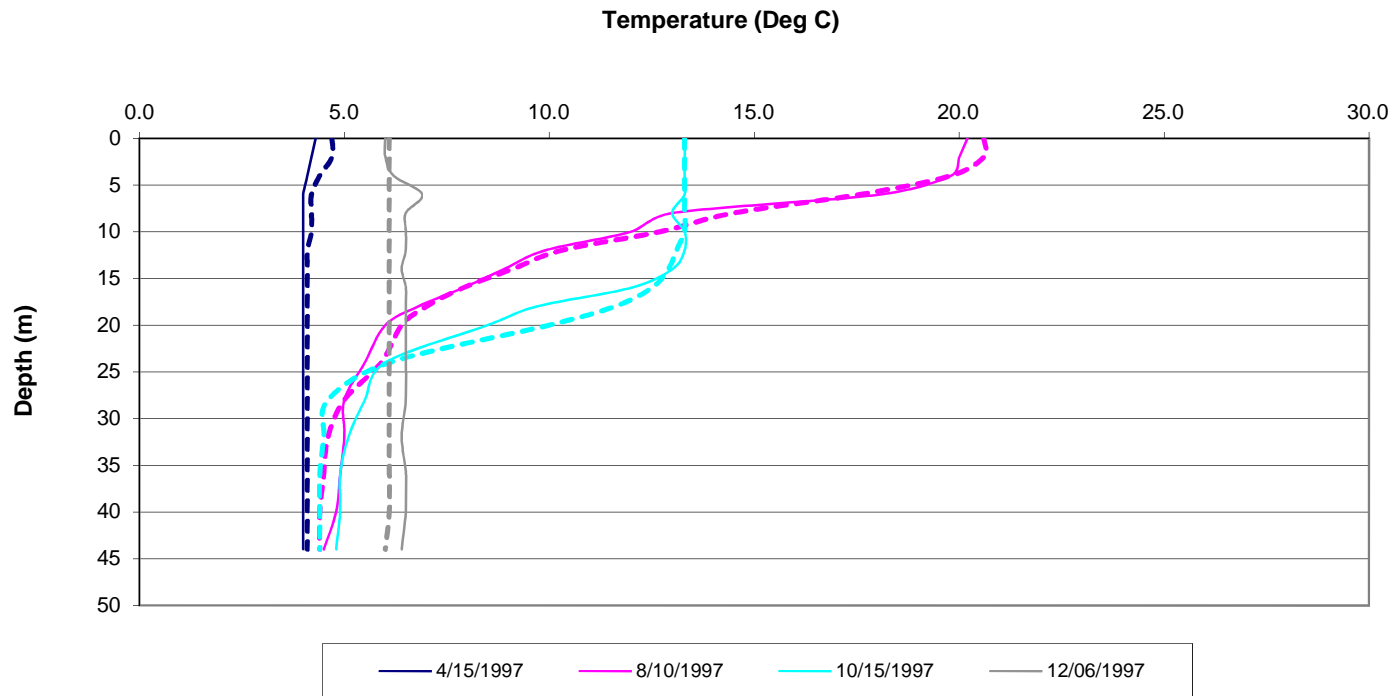
PROJECT NO.  
V132

OFFICE  
EBA-VANC

DWN AL  
CKD JAS  
APVD JAS  
REV 001

DATE  
August 2011

Figure A-1



#### LEGEND

- Solid lines represent observed profiles
- Dash lines represent modelled profiles

#### NOTES

#### STATUS

#### CLIENT

-



A TETRA TECH COMPANY

#### H3D TECHNICAL DESCRIPTION

#### H3D Validation Comparison of Observed and Modelled Temperature Profiles at Vernon

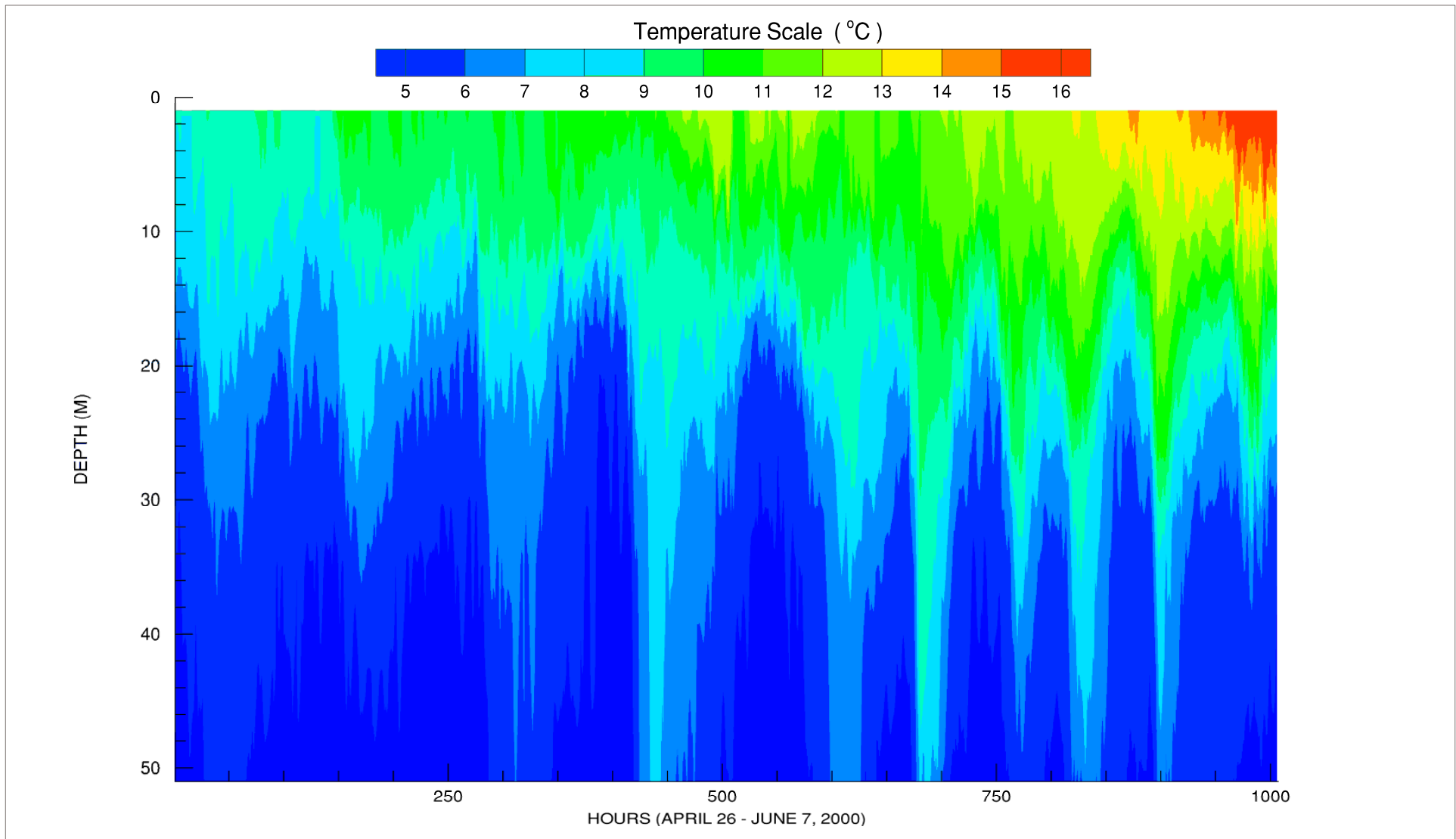
PROJECT NO.  
V132

OFFICE  
EBA-VANC

DWN AL CKD JAS APVD JAS REV 001

DATE  
August , 2011

**Figure A-2**



## LEGEND

## NOTES

## CLIENT

## H3D TECHNICAL DESCRIPTION

### H3D VALIDATION SEICHES IN OKANAGAN LAKE (OBSERVED DATA)

PROJECT NO.  
V132

DWN	CKD	APVD	REV
EW	JAS	JAS	0

OFFICE  
EBA-VANC

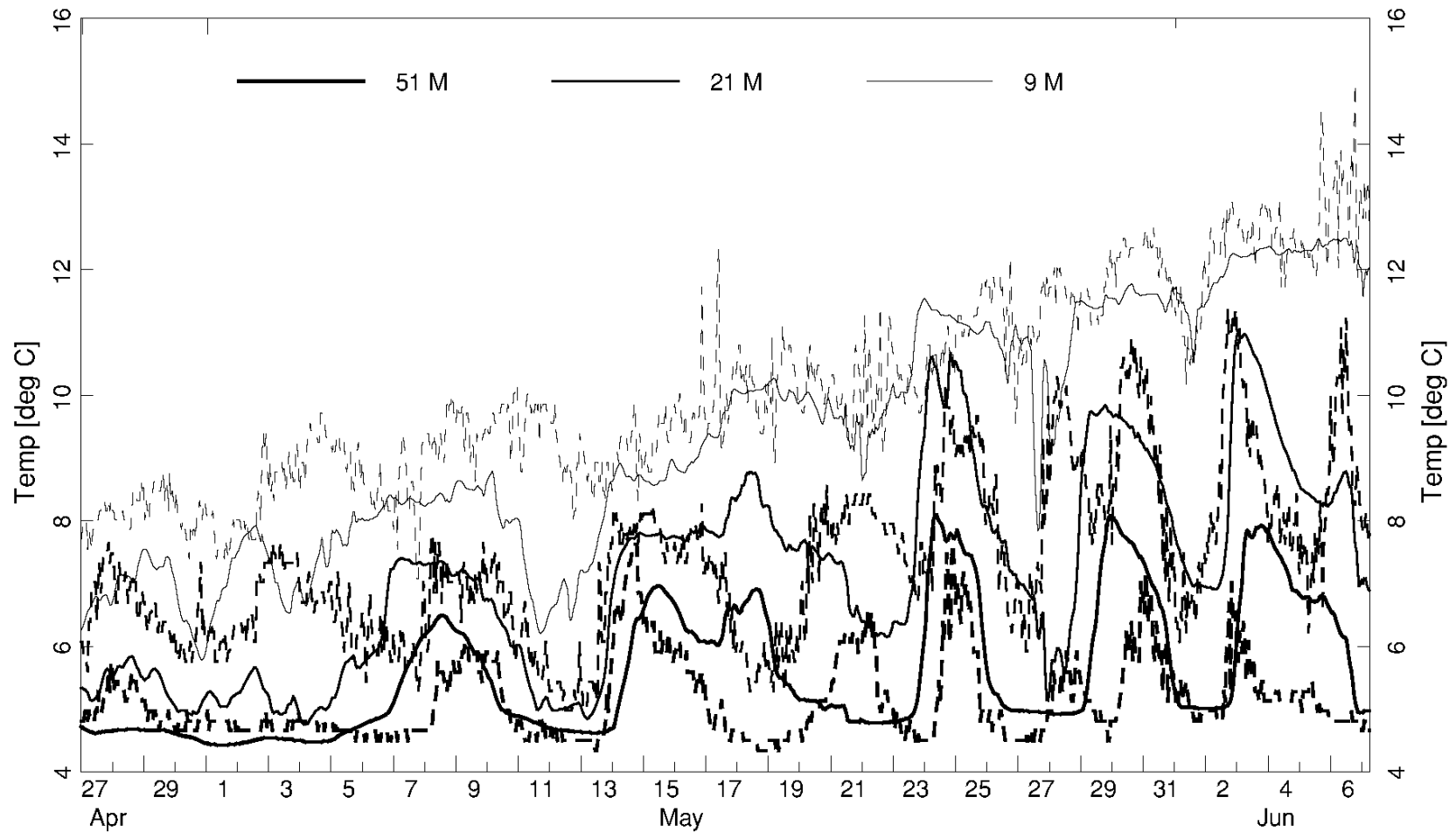
DATE  
August 2, 2011

Figure A-3

STATUS  
ISSUED FOR REVIEW



## TS-A: NORTH STRING



### LEGEND

Dashed Lines: Observed Temperature  
Solid Lines: Modelled Temperature

### NOTES

STATUS  
ISSUED FOR REVIEW

### CLIENT



### H3D TECHNICAL DESCRIPTION

### H3D VALIDATION INTERNAL SEICHE DYNAMICS OKANAGAN LAKE

PROJECT NO.  
V132

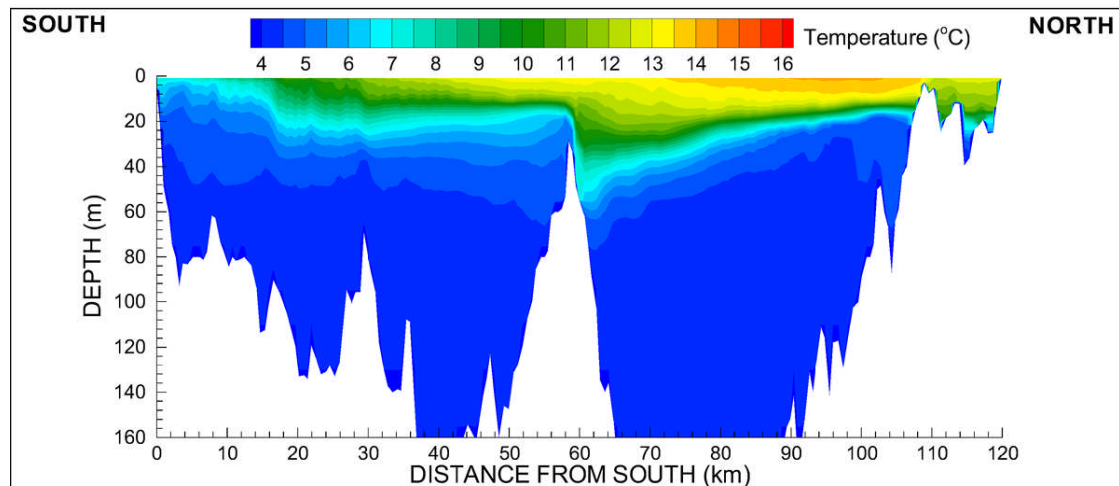
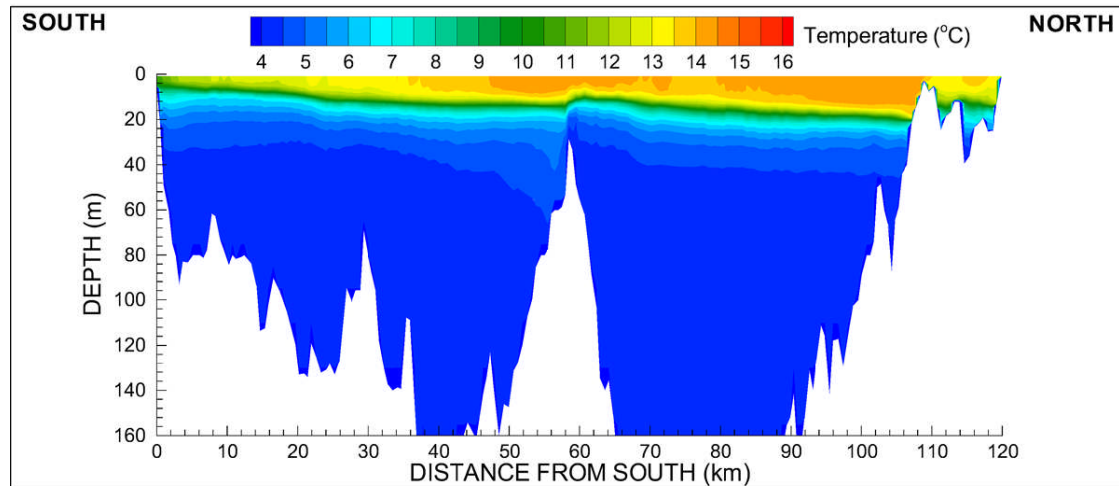
OFFICE  
EBA-VANC

DWN CKD APVD REV  
EW JAS JAS 0

DATE  
August 2, 2011

Figure A-4





LEGEND

NOTES

CLIENT

H3D TECHNICAL DESCRIPTION

H3D VALIDATION  
INTERNAL SEICHE DYNAMICS  
OKANAGAN LAKE

PROJECT NO.  
V132

DWN	CKD	APVD	REV
EW	JAS	JAS	JAS

OFFICE  
EBA-VANC

DATE  
August 2, 2011

Figure A-5

STATUS  
ISSUED FOR REVIEW



# **APPENDIX B**

## **DILUTED BITUMEN WEATHERING MEMOS**

---

# TECHNICAL MEMO

ISSUED FOR USE

<b>TO:</b>	Trans Mountain	<b>DATE:</b>	July 4, 2013
<b>C:</b>		<b>MEMO NO.:</b>	1
<b>FROM:</b>	Jim Stronach and Aurelien Hospital, EBA	<b>EBA FILE:</b>	V13203022
<hr/>			
<b>SUBJECT:</b>	Spreading of Diluted Bitumen		
<hr/>			

## 1.0 INTRODUCTION

This memo describes some exploratory tests that were done at the Western Canada Marine Response Corporation (WCMRC) Kensington Avenue facilities in Burnaby, BC. The purpose of the test was to learn more about the spreading properties of diluted bitumen. Stated simply, the experiment was designed to address the question: how thin can a dil-bit slick become? Alternatively, is there a lower limit to the thickness of a dil-bit slick? That is, dil-bit would not spread till the slick had a thickness of a few microns, but instead, because of its high viscosity, would spread until the thickness was a value of 1 mm, for instance. Tests were done by Aurelien Hospital and Jim Stronach of EBA, assisted by Trevor Davis of WCMRC.

## 2.0 THE TESTS

The test material was diluted bitumen, supplied in a closed 3-L container by Trans Mountain. The oil was obtained from the Trans-Mountain Westridge Terminal. There were two test basins: a 5 gallon (approx.) pail made of white plastic, and a "Fish tank", approximately 1 m x 1 m x 1 m. Both were filled with water to within about 10 cm of their tops. Two syringes were used: a medicine dropper, with a drop size estimate to be 0.03 mL (cm<sup>3</sup>), and a larger syringe with a volume of 30 mL. We first did some practice runs, dropping oil with a medicine dropper into a bucket of water. Then, 30 mL was discharged as one aliquot into the large fish tank. Times and radii of the resulting slicks were recorded, forming the basic measurements conducted. Spill diameters were measured with a ruler, and the measurements for spills in the pail were subject to considerable error because the ruler was longer than the pail diameter, and so had to be held about 10 cm above the slick. Errors also occurred in the fish tank, because the spill was installed in a manner that resulted in a large amount of dispersion at the outset, due to air ingestion, and the resulting slick was larger than the ruler, and developed an asymmetric form. Nevertheless, the results suggest that we can make significant improvements in our modelling based on the observations reported herein. A better-equipped test is certainly recommended for future consideration.

## 2.1 First Test: Drops in a Bucket

Each droplet of oil formed a perfect circle once it contacted the water surface, and spread very little after the initial installation. The perimeter of the circle was very distinct and not diffuse. In fact, one could see the slick sitting very slightly proud of the water surface. We tried using 1, 2, and 5 drops, in different parts of the pail, to determine the relationship between drop size, radius and thickness. Figure 1 shows the resulting relationship between drop volume and slick thickness.

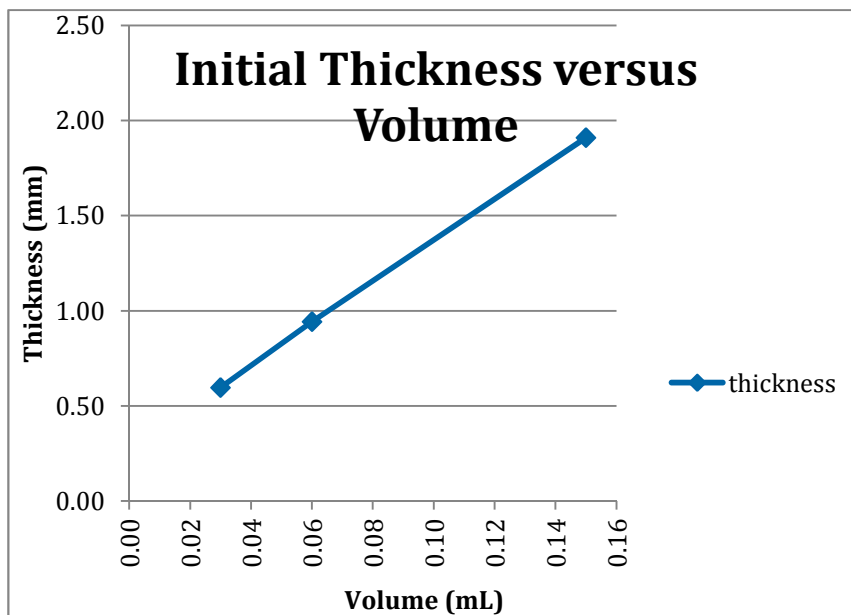
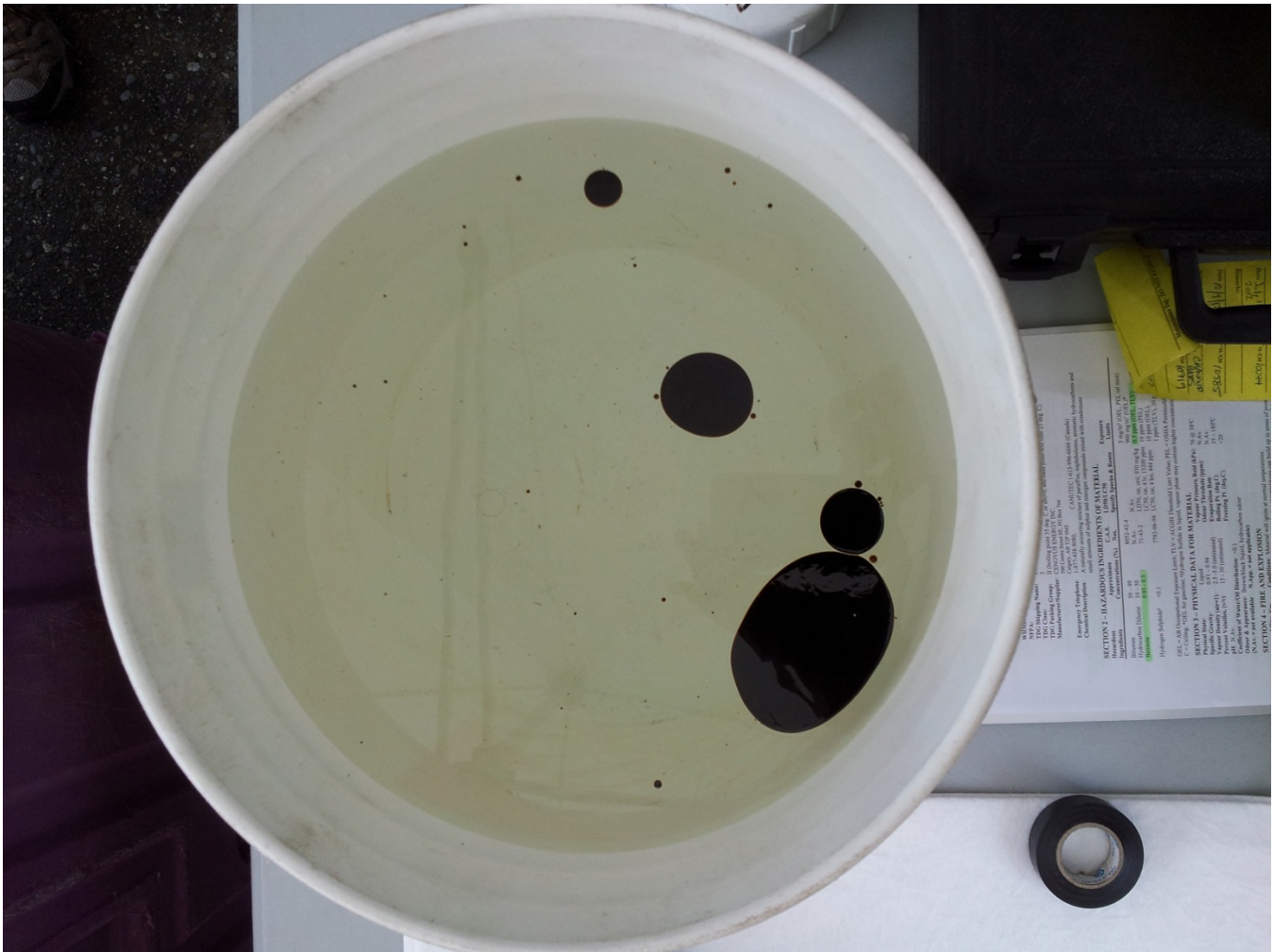


Figure 1: Slick Thickness versus Volume

Although Figure 1 indicates a linear increase of thickness with volume, a change of a few millimetres in the measured diameter would result in a constant thickness regardless of spilled volume. As well, the repeatability of the volume of each drop may not be exact, and the five drop slick actually resulted from the merging of a four-drop slick and a one-drop slick, which may have introduced some water-borne impurities into the combined slick.



Photograph 1 shows a typical picture of the oil slicks.



Photograph 1: Oil slicks in the pail: the 4-drop spill and the 1-drop spill are about to join at about the 4 o'clock position.

We also measured spreading of a 5-drop spill versus time:

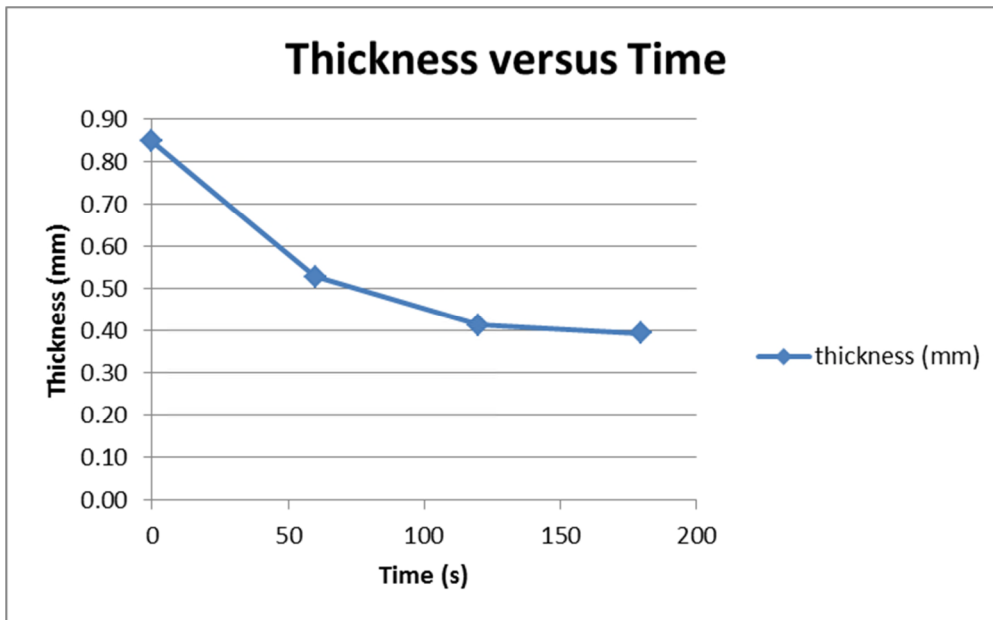
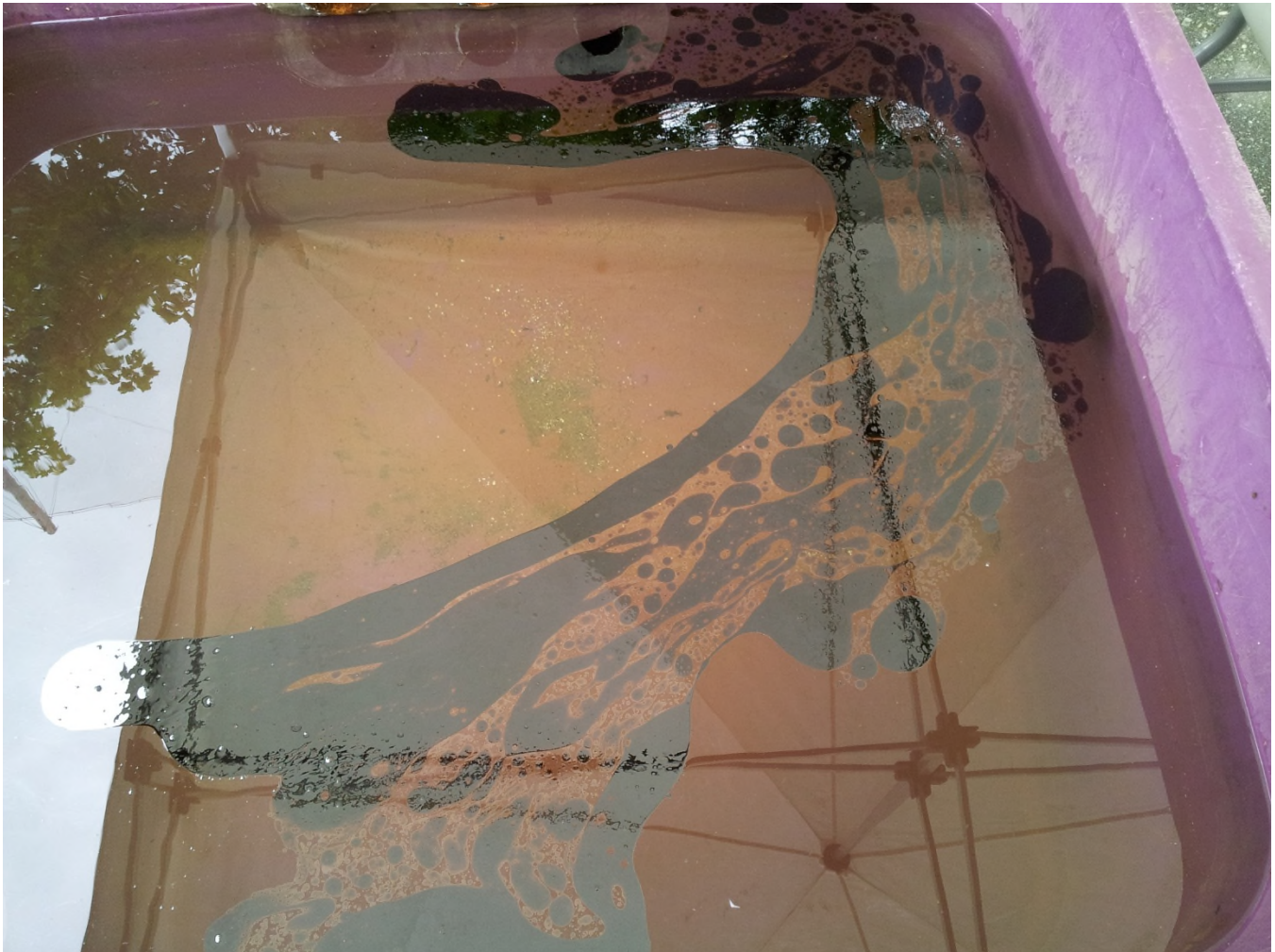


Figure 2: Thickness versus time for a 5-drop spill.

## 2.2 Second Test: Drops in a fish tank

Finally, we put 30 mL into the fish tank. Unfortunately, there was a fair bit of air injection during installation, so the slick was initially broken up into many patches. These were then swirled around by the circulation in the tank, driven by a small wind as shown in Photograph 2.



**Photograph 2: Oil slick in the fish tank swirled around by the circulation in the tank**



About an hour later, the swirls broke up into small circular patches, shown in Photograph 3.



**Photograph 3: Oil slick in the fish tank one hour after the release**



### 3.0 CONCLUSIONS

The conclusions are that even fresh dil-bit doesn't undergo the usual spreading that diesel or gasoline might do: it remains in a single small slicklet, with minimum circumference to area configuration: a circle. In the case of the fish tank spill, even a mild breeze set up surface currents that swirled the slick around the tank. The particular configuration, no beach, meant that very little oil contacted the sides of the tank, at least within the first few hours. As the slick in the tank broke up, it did form the classic thin/thick configuration, although the distinction between thin and thick sheens was extremely distinct in the observations described here, and it is difficult to know if the thin parts actually carried any significant amount of oil.

It is important to understand the physical processes we see in these experiments, in order to determine how to scale them up to a full-size spill. Early theories by Fay (1969) and Hoult (1972) are still used to understand the relative balance of forces in a spreading oil slick: gravitational, inertial, viscous and surface tension. However, these models don't seem to fit the observations. An alternative is to examine the effect of surface tension versus gravity spreading: the buoyant spreading tendency of the oil being opposed by surface tension, which wants to achieve a minimum surface area.

The thickness of a puddle of fluid in air, spreading over a solid surface is given by Eq. 1 below (P-G de Gennes et al., 2002):

$$h = \sqrt{\frac{2\gamma_{la}(1 - \cos \theta)}{g\rho}}$$

For the dil-bit slicks, the density should likely be replaced by the density difference with respect to water, since the gravitational spreading tendency depends on  $\Delta\rho \cdot gh$ , not  $\rho \cdot gh$ . However, it was noted that the oil slicks floated with what appeared to be a large fraction above the water, in which case, it may be appropriate to use just the oil density. The resulting thickness, for a range of contact angles and these two interpretations of the spreading process is given in Table 1 below. Two sets of density and surface tension values are considered, for the start of the Gainford trials in tank 9SB, and for the end of the trials.

**Table 1: Surface Tension Control of Oil Thickness**

Surface Tension (dyne/cm)	Rho_oil (g/cm <sup>3</sup> )	Theta (deg)	h (delta rho) (mm)	h(rho) (mm)
37	0.925	180	14.2	4.0
37	0.925	90	10.0	2.9
37	0.925	20	2.5	0.7
37	0.925	0	0.0	0.0
51	0.975	180	28.9	4.6
51	0.975	90	20.4	3.3

---

51	0.975	20	5.0	0.8
51	0.975	0	0.0	0.0

The above theory, either for the case where one considers the oil density alone or the density difference, seems to support the observations. Further work is need to examine the degree to which dil-bits “wets” the water surface, and also to determine to what extent the surface tension of dil-bit differs from natural crude oils, for which there is greater literature on the behaviour at sea. However, the observations and the above theory certainly seem to support the concept of maintaining a minimum slick thickness of 1 mm when doing the evaporation calculations.

## 4.0 RECOMMENDATIONS

The following are the key recommendations:

1. The experiment should be repeated, but with better measuring tools, a larger tank, and with product at various stages of weathering
2. The amount of oil in the “thin” slick should be determined.
3. A physical chemist should be engaged to review and upgrade the surface tension analysis presented above.
4. Test should be developed to extend the procedure to allow scaling up to real-world conditions: what are the effects of waves, both large and small, and what are the effects of typical surface current shear, on the slick behaviour: do the slicklets behave differently in more energetic environments.

---

## 5.0 REFERENCES

Pierre-Gilles de Gennes; Françoise Brochard-Wyart; David Quéré (2002). Capillary and Wetting Phenomena—Drops, Bubbles, Pearls, Waves. Alex Reisinger. Springer. ISBN 0-387-00592-7.

## 6.0 LIMITATIONS OF REPORT

This report and its contents are intended for the sole use of Trans Mountain and their agents. EBA Engineering Consultants Ltd. does not accept any responsibility for the accuracy of any of the data, the analysis, or the recommendations contained or referenced in the report when the report is used or relied upon by any Party other than Trans Mountain, or for any Project other than the proposed development at the subject site. Any such unauthorized use of this report is at the sole risk of the user. Use of this report is subject to the terms and conditions stated in EBA's Services Agreement. EBA's General Conditions are attached to this report.

# TECHNICAL MEMO

ISSUED FOR USE

<b>TO:</b>	Bikramjit Kanjilal, Trans Mountain	<b>DATE:</b>	July 18, 2013
<b>C:</b>		<b>MEMO NO.:</b>	2
<b>FROM:</b>	Aurelien Hospital and Jim Stronach, EBA	<b>EBA FILE:</b>	V13203022
<b>SUBJECT:</b>	Validation for the Oil Spill Model SPILLCALC: Evaporation and Oil-Sediment Interaction		

## 1.0 INTRODUCTION

Evaporation and oil-sediment interaction are two key weathering processes to assess the potential impact of an oil spill on the environment. Both have been calibrated and validated against lab experiments.

The evaporation process has been validated against the Gainford experiments conducted in May 2013 at Gainford, AB. The oil-sediment interaction process has been calibrated against the paper: "Effects of Dispersants on Oil-SPM Aggregation and Fate in US Coastal Waters" July 2008 by Ali Khelifa, Merv Fingas and Carl Brown.

## 2.0 GAINFORD EXPERIMENT HINDCAST

The time-history of oil density in the Gainford Tank S9B was hindcast using EBA's SPILLCALC model, and a pseudo-component decomposition provided by Stantec. The major parameters of the hindcast, provided by Jose Rios, Polaris, were:

- Dimensions of the tank: Approximately 12.64 m<sup>2</sup> x 1.4 m water depth;
- Thickness of oil installed: Approximately 11.7 mm on 5/16/2013;
- Water Salinity: 20 – 21 ppt;
- S9B had no induced wind. Using a hand held wind meter we measured < 2 MPH across the 11 days, SPILLCALC used a wind speed of 0.8 m/s;
- Water temperature S9B: Ave.: 14.9 °C Max.: 22.0 °C Min.: 9.0 °C

The relatively thick layer of oil, greater than 10 mm, and the generally accepted observation that evaporation can be either atmospheric boundary layer limited, or limited by the diffusion rate within the oil slick, led us to examine the formulation of the evaporation rate in SPILLCALC. Previous to the investigations reported here, we used the mass transfer equation as presented by, e.g., McKay, Fingas, etc.:

$$Q_i = K_i * F_i * P_i * MF_i$$



Where  $Q_i$  is the evaporation rate (moles, or mass or volume per second per  $m^2$  of area) for each pseudo-component,  $K_i$  is the mass transfer coefficient, typically with a  $7/8$  dependence on wind speed,  $F_i$  is a conversion factor for the units of  $Q_i$ , and includes the ideal gas constant  $R$  and temperature  $T$ ,  $P_i$  is the pressure of the pure substance, and  $MF_i$  is its mole fraction.

Using the above equation alone, it was found that the density of the oil in the numerical model hindcast increased much faster than was observed at Gainford. It was assumed that the reason for this disagreement was that the computed evaporation rate was too high. We then set out to explore whether the rate of diffusion of the volatiles from within the slick to the surface limited the rate at which the mass transfer flux at the oil-air interface could carry away the volatiles. A one-dimensional diffusion equation was solved at every model time step, for each pseudo-component, representing the diffusion within the oil slick:

$$dC/ct = d/dz(A dC/dz)$$

Due to the thickness of the oil, the oil layer was divided between ten sub-layers in the vertical, representing a vertical discretization of 1.17 mm. The mass transfer equation provides the top boundary condition for the diffusion equation. The mole fraction considered in the mass transfer equation is the mole fraction in the top layer of the oil. The flux into the bottom layer was set to zero, although it could ultimately be set to the rate of dissolution. There are thus specific boundary condition at the top and the bottom of the oil slick. The diffusion equation was then solved using a Crank-Nicholson method. Thereby, as volatiles were removed from the top millimetre of the slick, the evaporated rate decreased because of the lower concentration in the top layer. It was also found that the evaporative flux declined quickly, as the volatile components could not be supplied quickly enough by diffusion from the interior. Thus, the concentration in the top layers dropped fairly rapidly.

The diffusion within the oil layer is characterized by a diffusion coefficient. Literature indicates that the order of magnitude for volatile hydrocarbons such as pentane diffusing inside diluted bitumen ranges between  $1.e-9$  to  $1e-11 m^2/s$ . As an example, diffusivities reported by Afsahi and Kantzas (2006) estimated pentane diffusion in Cold Lake bitumen to have a coefficient of  $1.25.10^{-7} cm^2/s$ , or  $1.25.10^{-11} m^2/s$ . Since evaporation and diffusion processes concern a vast range of hydrocarbons, each with specific properties, a representative diffusion coefficient was selected for the mixture. The choice of the coefficient was mainly driven by reproducing the Gainford Tank 9B experiment and varies with time to reproduce changes occurring inside the oil layer due to the loss of volatile: its composition becomes more viscous and contains heavier hydrocarbons, leading to a decrease in the diffusion coefficient. Figure 1 below provides a comparison between the observed and computed densities in the Gainford experiment.

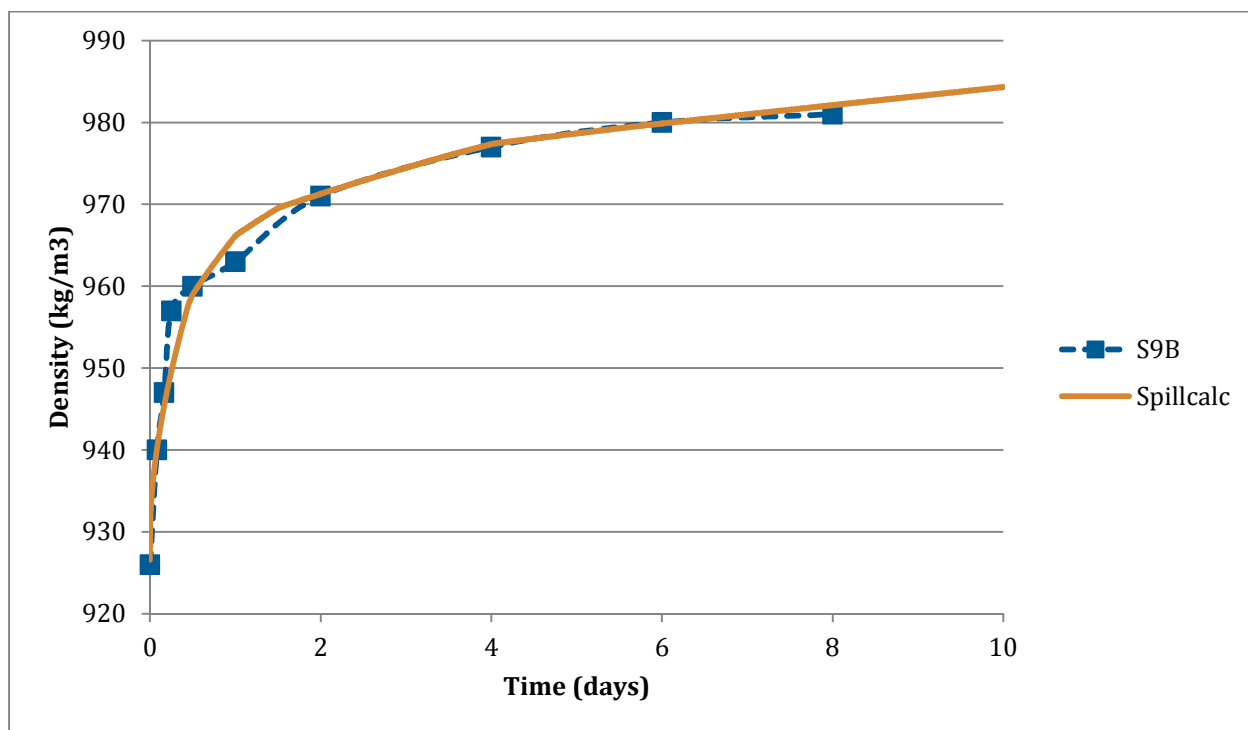


Figure 1: Observed and hindcast density time-series.

The agreement is very good. To achieve this level of agreement, we adjusted the diffusion coefficient as follows:

Table 1: Diffusion Coefficient

From Hour X to Hour Y	Diffusion Coefficient (m <sup>2</sup> /s)
Hr 0 – Hr 11	5.0e-10
Hr 11 – Hr 12	3.0e-10
Hr 12 – Hr 24	2.0e-10
Hr 24 – Hr 36	1.0e-10
Hr 36 – Hr 96	5.0e-11
Hr 96 – Hr 240	2.0e-11

### Application to the Marine Spill:

The same diffusion coefficients were used for stochastic and deterministic modelling, and the time variation of diffusion coefficient shown in Table 1 was implemented in both types of simulation, using the start of the spill as the time origin for the temporal variation in diffusion coefficient.

In addition to the diffusion, the area covered by the slick plays a major role in the evaporation subroutine. The spreading experiment which was conducted at the WCMRC facility showed that the lateral spreading of

the oil is limited and that a minimum thickness is observed. This minimum thickness is 0.4 mm, as described in the Spreading Observation Memo. As a result, an effective area was used in the evaporation process, based on the volume of oil in one cell and the minimum thickness it can reach. The ratio of the effective area over the area ranges between 0 to 1. At the beginning of the simulation, the effective area is very close to the cell area, since the oil stays very concentrated close to its release point. As time goes by, the effective area becomes smaller, representing the patchiness behavior of the oil.

### 3.0 OIL-SEDIMENT INTERACTION

The aggregation of suspended particulate matter (SPM) such as fine sediment with oil, forming oil-mineral aggregations (OMA) can be a key process in freshwater environment, where sediment concentration is usually higher than in the marine environment.

J.R. Payne developed in 1987 an equation which can describe oil-droplet and SPM interaction:

$$R = 1.3 * \sqrt{\frac{\epsilon}{\nu}} * k_a * C_0 * C_p$$

With R the rate of loss of free oil droplets in mass per unit volume per unit time.  $C_0$  and  $C_p$  are the concentration of oil droplets in the water and the concentration of SPM in the water respectively, in mg per litre.  $K_a$  is a lumped parameter that includes unknown information such as the sticking efficiency and size dependency.  $\epsilon$  is the energy dissipation rate per mass of fluid and is based on Delvigne and Sweeney' paper "Natural Dispersion of Oil",  $\epsilon$  is a function of the squared wave height.  $\nu$  is the kinematic viscosity of water. This equation has been implemented in SPILLCALC.

The calibration and the validation of the SPILLCALC oil-sediment interaction module was conducted using data reported in a paper by Dr. Ali Khelifa, Dr. Merv Fingas and Dr. Carl Brown: "Effects of Dispersants on Oil-SPM Aggregation and Fate in US Coastal Waters" July 2008.

Khelifa's experiment involved oil and sediment dropped into a reaction vessel subject to a certain level of agitation. The level of agitation was quantified through the energy dissipation rate, which ranged between 0.1 to 0.4  $\text{m}^2/\text{s}^3$ . Different types of sediments were used in the study: the most relevant sediment for the calibration of our model is the natural sediment from the shores of the Colombia River Delta, Washington, USA. The percentage of oil interacting with sediment was measured for different concentrations of sediments.

The oil spill model, SPILLCALC, uses time-varying wave data computed by SWAN and time-varying sediment concentration computed by H3D to calculate the interaction of oil with sediments, making it difficult to reproduce laboratory conditions. Hence, for the validation against Kheilafa et al., the energy level,  $\epsilon$ , was forced to a range of values: 0.1 and 0.4  $\text{m}^2/\text{s}^3$  to reproduce lab conditions. Also the sediment concentration was set to 25, 50, 100 and 200 mg/L in order to compare the model results with the lab study.

The choice of  $K_a$ , which represents a lumped parameter that includes unknown information such as the sticking efficiency and size dependency, was driven by reproducing the lab experiment.

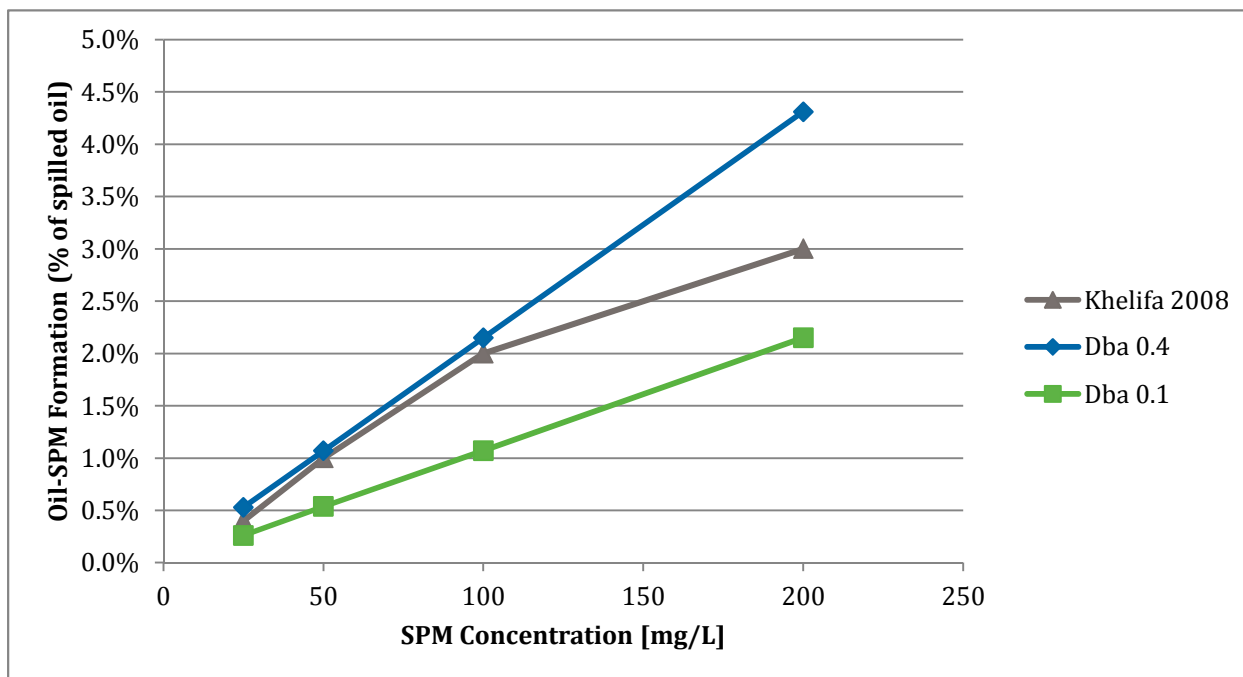


Figure 2: Percentage of Oil-SPM Interaction

The agreement is very good, recognizing that the energy in the reaction vessel was not constant but ranges between 0.1 and 0.4 m<sup>2</sup>/s<sup>3</sup>. The best agreement is achieved for values of sediment concentration lower than 100 mg/L, which will be typical conditions in the Fraser River and in the marine environment.

A value of 1.e-5 m<sup>3</sup>/kg was used for the sticking parameter Ka. J.R. Payne indicated in “Oil/Suspended Particulate Material Interactions and Sedimentations”, 2003, that values for Ka would range between 1.e-5 m<sup>3</sup>/kg to 3.e-4 m<sup>3</sup>/kg, according to lab testing. The value that SPILLCALC uses is in agreement with Payne’s coefficient values. ADIOS2 uses a constant for all sediment types: 1.e-4 m<sup>3</sup>/kg, which also falls within Payne’s coefficient values.



---

## 4.0 REFERENCES

Khelifa, A., M. Fingas and C. Brown, 2008. "Effects of Dispersants on Oil-SPM Aggregation and Fate in US Coastal Waters". Final Report to the Coastal Research Response Center, University of New Hampshire, July 2008, 38 pp.

## 5.0 LIMITATIONS OF REPORT

This report and its contents are intended for the sole use of Trans Mountain and their agents. EBA Engineering Consultants Ltd. does not accept any responsibility for the accuracy of any of the data, the analysis, or the recommendations contained or referenced in the report when the report is used or relied upon by any Party other than Trans Mountain, or for any Project other than the proposed development at the subject site. Any such unauthorized use of this report is at the sole risk of the user. Use of this report is subject to the terms and conditions stated in EBA's Services Agreement. EBA's General Conditions are attached to this report.

# APPENDIX C

## SHORELINE RETENTION INFORMATION

---

# Methods for Estimating Shoreline Oil Retention

prepared for

**EBA Engineering  
Vancouver, BC**

prepared by

**John R. Harper, P.Geo, Ph.D.  
Coastal & Ocean Resources  
Victoria, BC**



**Coastal and Ocean Resources**  
*a MER company*

---

## Procedures for Fine Estimating Potential Oil Retention from Spill Modeling

---

As part of the support for spill modeling associated with assessment of accidental DilBit spills, Coastal & Ocean Resources (Coastal & Oceans), assembled a shoreline GIS dataset and then provided algorithms for estimating initial oil retention, should a Dilbit spill reach the shoreline. This document describes the procedures used to develop the dataset and the assumptions used in estimating potential oil residence.

### 1.0 Compiling the Coastal GIS Dataset

There are existing coastal habitat mapping datasets for the Strait of Georgia, Puget Sound, Juan de Fuca Strait and the West Coast of Vancouver Island. These are collectively referred to as the ShoreZone datasets and are managed by the Integrated Land Management Branch in BC and the Department of Natural Resources in Washington State. Coastal & Oceans collected imagery data and compiled the mapping data for these dataset so is familiar with the data content and limitations.

The BC and Washington datasets were combined in GIS and selected attributes attached to each shore unit. The combined dataset stretches from northern Vancouver Island to Grays Harbor in Washington and also includes entire Puget Sound and the Strait of Georgia (Fig. 1). The selected attributes were deemed most relevant to the spill modeling exercise (Table 1).

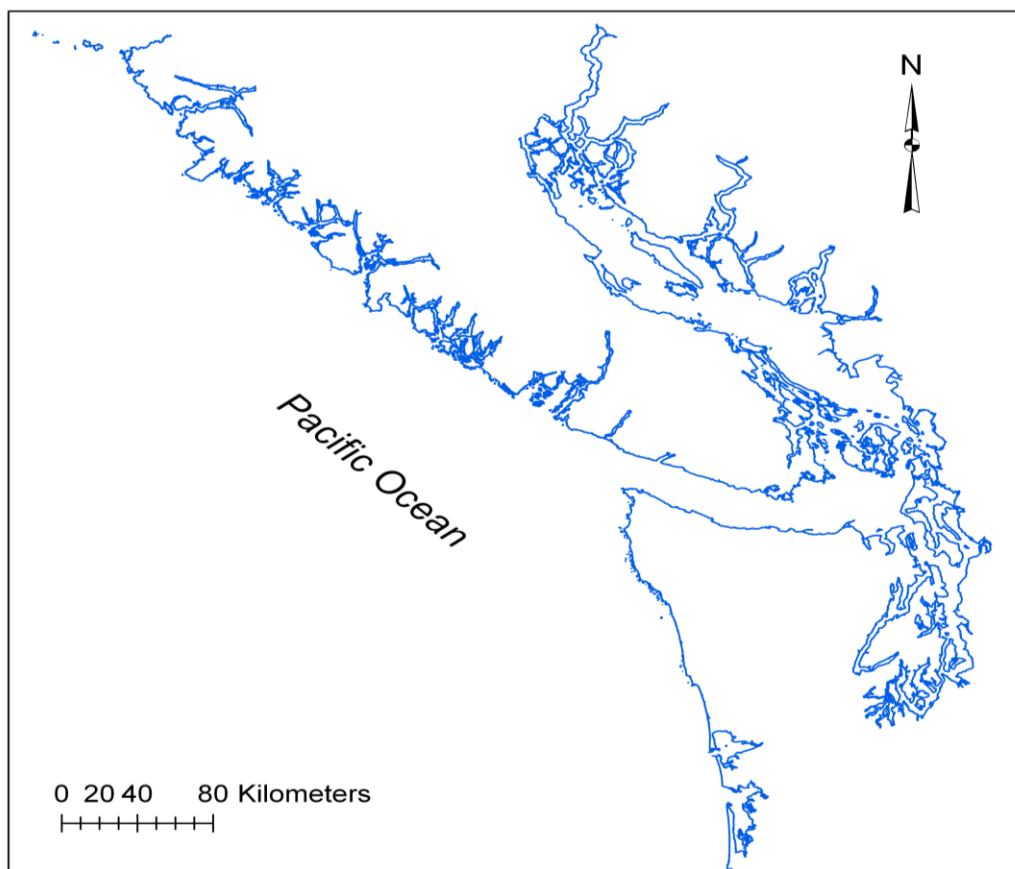


Figure 1. Extent of digital shoreline dataset compiled for the spill modeling



**Table 1 Attributes Attached to the Digital Shoreline Units**

<b>Attribute</b>	<b>Description or Source</b>
<i>Coastal Class</i>	One of 35 classes summarizing the overall character of the shore unit. From the BC and Washington ShoreZone datasets
<i>Exposure</i>	One of six Exposure classes from BC and Washington ShoreZone datasets. Classes include: <i>Very Exposed</i> , <i>Exposed</i> , <i>Semi-exposed</i> , <i>Semi-protected</i> , <i>Protected</i> and <i>Very Protected</i> .
<i>ORI</i>	One of five estimated classes of Oil Residence Index taken from the BC and Washington ShoreZone datasets. Classes are: (1) day to WEEKS; (2) WEEKS to months,(3) weeks to MONTHS; (4) MONTHS to years and (5) months to YEARS.
<i>Marsh</i>	All units where the Saltmarsh biobands was noted. Taken from the BC and Washington ShoreZone datasets.
<i>Upper Intertidal Substrate</i>	The substrate coding for the upper intertidal substrate, the most likely location for oil to strand. Taken from the across-shore component table of the BC and Washington datasets.
<i>Spill Shore Type</i>	A derived shore type based on the upper intertidal substrate classification and used for estimating retention of oil stranding on the shore.
<i>Unit Length (m)</i>	The along shore length taken from the GIS data. This is the approximate alongshore length of the digital high water line
<i>ITZ_Width</i>	The intertidal zone width in meters.
<i>Revised Width (m)</i>	This is the ITZ_Width for most units. But for some units (Strait of Georgia) this attribute is missing: for those units with blanks, widths were estimated from the Coastal Class where <i>narrow</i> units had an estimate of 15 m and <i>wide</i> units and estimate of 166m.
<i>Intertidal Area (m<sup>2</sup>)</i>	The Unit Length times the Revised Width

Some units were missing the Wave Exposure attribute (89 units) and these were updated using fetch data. The ShoreZone mapping includes considerable detail in intertidal substrate – each unit is systematically characterized in terms of morphology and substrate from the supratidal zone to the lower intertidal zone (Fig. 2). For this exercise, the upper intertidal zone was the greatest interest and the upper intertidal substrate description of each shore unit was included in the selected attribute table (Table 1). The Shore Type may differ from the upper intertidal substrate characterization as it is a generalized summary of the complete unit. In that spills mostly affect upper intertidal areas, and lower intertidal areas typically have much lower retention, we used the upper intertidal across-shore substrate description as the most accurate representation for use in spill retention.

There are 26,000 original shore segments in the ShoreZone spill modeling dataset. These were further subdivided to assist with the modeling so the unit lengths are subdivided to <100m, resulting in 172,000 shore segments for modeling. There are 15,911 km of shoreline in the modeling area.

Figure 2 shows the general substrate types for the project area. For spill sensitivity assessment, it is important to note that about 10% of the shoreline is estuary with marshes. While the outer coasts of Washington and British Columbia are considered high wave exposure, they actually comprise a relatively small proportion of the coast and most of the region is low wave exposure (Fig. 3); an estimated 83% of the shoreline is classified as low energy and 17% as high energy.

## Defining Spill Shore Types for DilBit Spill Modeling

Thirteen “Spill Shore Types” were defined to assessing shore oil retention. These Spill Shore types represent a combination of substrate and wave exposure (Table 2). They are similar to ESI and the Environment Canada shore types but reflect some of the unique aspects of Pacific Northwest shorelines. One important assumption incorporated into these Spill Shore Types is that low energy shorelines almost always have an extremely fine subsurface substrate (sand or mud), even though the surface veneer is coarse pebble, cobble or boulder (Fig. 4). This observation is significant in that low-energy shorelines (83% of the coast) will have limited oil penetration due to the fine nature of the substrate. Coarse (pebble, cobble, boulder), high energy shorelines may be coarse to considerable depths, increasing permeability and potential stranded oil retention

The ShoreZone dataset maps both alongshore units but also across-shore substrate (Fig. 5). We examined the dataset for upper intertidal substrate types, the most likely location that oil will strand.

There are a great number of combinations of substrate attribute and the ten most-commonly occurring are included in Table 3. There are 720 unique combinations of substrate in the upper intertidal zone for BC-Washington ShoreZone dataset. Queries were run to reduce this to 13 Spill Shore Types. Table 3 illustrates how the most commonly occurring upper intertidal substrates are assigned to one of the 13 *Spill Shore Types*.

The frequency of occurrence of the 12 Spill Shore Types is based on the summations of alongshore lengths (Fig. 6; Table 4). An estimated 31% of the shoreline is classified as *rock* and only about 7% is classified as *highly permeable substrate*. Various combinations of sand &

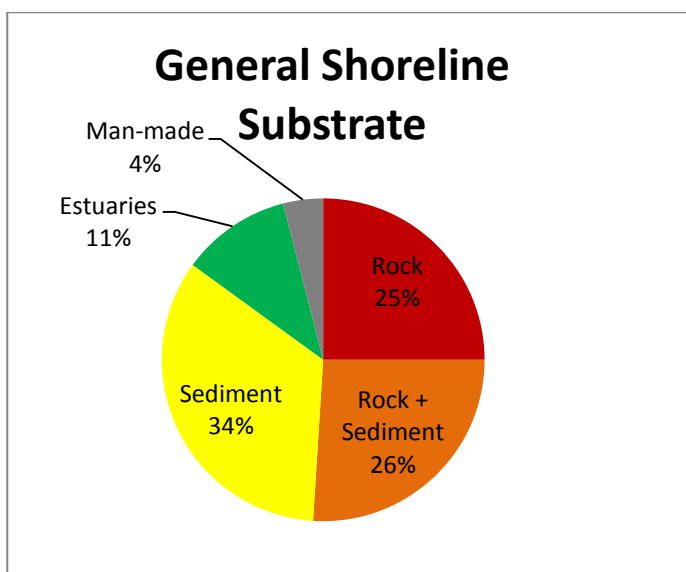


Figure 2. General occurrence of shoreline substrate, based on the BC shoreline classification system. Note that estuaries comprise about 11% of the shoreline length and combination of rock & sediment 26% - these are veneers of sediment over rock or discontinuous rock outcrops within a beach.

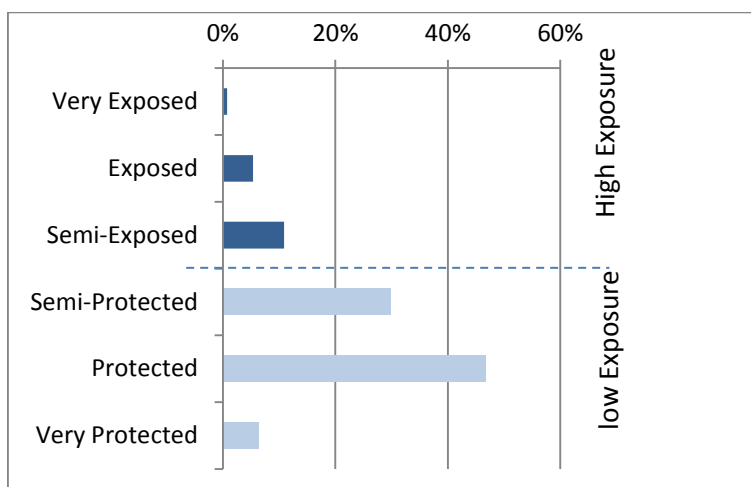


Figure 3. Summary of wave exposure in the project area.

gravel (sand, pebble, cobble, boulder) comprise the remaining 60%. Marshes occur along about 12% of the shoreline.

**Table 2. Spill Shore Types defined for Project.**

Exposure	Upper Intertidal Substrates	No	Code	Spill Shore Type
Low (VP, P, SP)	Rock	1	LE_R	Rock, low energy: assumed to be impermeable
	Rock w pebble, cobble veneer	2	LE_VR	Rock w veneer, low energy; a discontinuous veneer of pebble, cobble or boulder over rock
	Pebble veneer	3	LE_V	Pebble veneer over sand; a single layer of pebbles overlying sand, typical of low energy shorelines; stranded oil may attach to pebble but sand in subsurface limits penetration.
	Cobble or boulder veneer	4	LE_CV	Coarse veneer over sand; a single layer of cobbles or boulders overlying sand; sand limit subsurface penetration
	Sand or mud	5	LE_S	Sand or mud which typically has high water content and limits viscous oil penetration.
	Rip Rap	6	LE_RR	Course boulders or sometime concrete rubble that is commonly used as shore protection.
	Marsh	7	LE_M	Marsh
	Wood	8	LE_W	Wood bulkheads, generally assumed to be pilings and therefore somewhat porous.
High (VE, E, SE)	Rock	9	HE_R	Impermeable rock surfaces; joint and fracture patterns may allow some oil retention
	Rock with coarse veneer	10	HE_VR	Boulder and cobble overlying bedrock creates potential for stranded oil retention
	Boulder, cobble beaches (also includes few rip-rap sections)	11	HE_C	Coarse boulder or cobble beaches assumed to have high penetration potential; may include coarse beaches associated with rock platforms; although high energy, penetration may result in lengthy persistence.
	Sand w pebble, cobble or boulder	12	HE_SG	Combinations of sand and various forms of gravel (pebble, cobble, boulder); and matrix is assumed to minimize penetration.
	Sand	13	HE_S	High energy sand beaches; sand will limit viscous oil penetration; sand is likely to be highly mobile so has the potential to bury stranded oil.



Figure 4a. Typical surface veneer of pebble-cobble sized sediment commonly found on BC shorelines. Such substrate would be considered highly permeable with potentially significant oil penetration.



Figure 4b. Surface veneer scrapped away, revealing a fine-sand substrate. The permeability of the subsurface is much lower, limiting oil penetration.

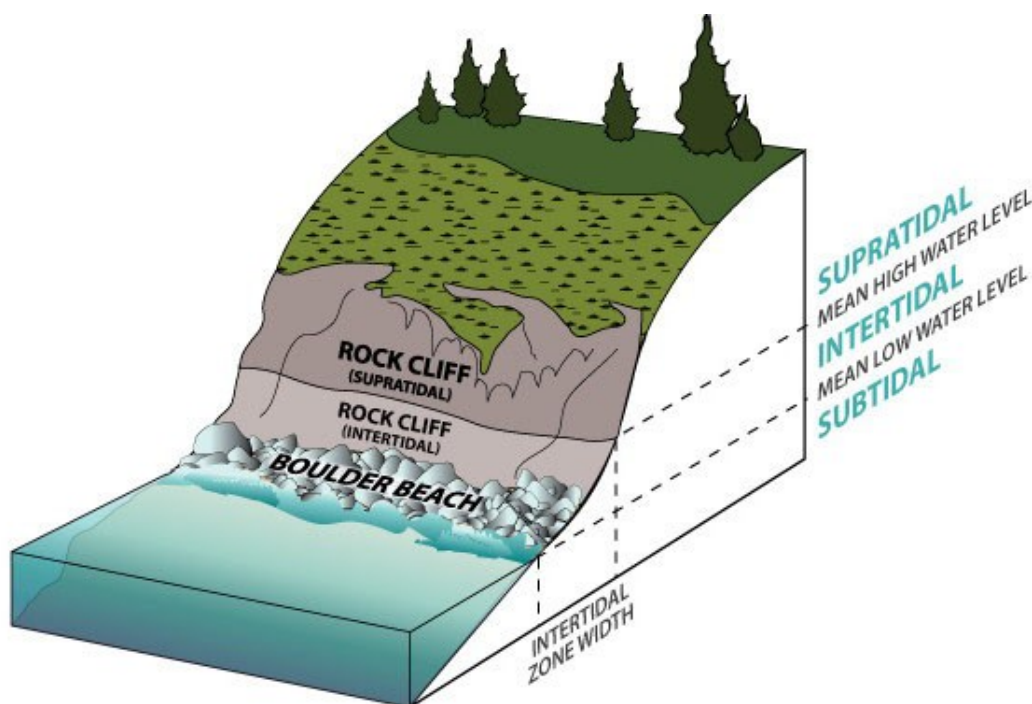


Figure 5. Schematic representation of the across-shore description of morphology and substrate that is recorded in ShoreZone for each alongshore unit. In this example, the upper intertidal is bedrock and the lower intertidal is boulder beach.

**Table 3 Example of Ten Most Common Upper Intertidal Substrates and their Conversion to a Spill Shore Type**

Code for Upper Intertidal Substrate	Translation of Code	Number Shore Units	Spill Shore Type	Spill Shore Type Description
R	Rock, low energy	29,507	LE_R	Rock, low energy
R	Rock, high energy	9,912	HE_R	Rock, high energy
Csp	Sand & pebble, low energy	7,344	LE_V	Pebble veneer over sand, low energy
Cs	Sand, low energy	6,704	LE_S	Sand, low energy
Cps	Pebble & sand, low energy	3,100	LE_V	Pebble veneer over sand, low energy
Cs	Sand, high energy	2,809	HE_S	Sand, high energy
Ar	Rip-rap, low energy	2,654	LE_RR	Rip-rap, low energy
Cp/Cs	Veneer of pebble over sand, low energy	2,373	LE_V	Pebble veneer over sand, low energy
Csp	Sand & pebble, high energy	2,104	HE_S	Sand, high energy
Csg	Sand & gravel, low energy	2,076	LE_V	Pebble veneer over sand, low energy

Note: there are 1,121 unique combinations of Upper intertidal substrate and energy.



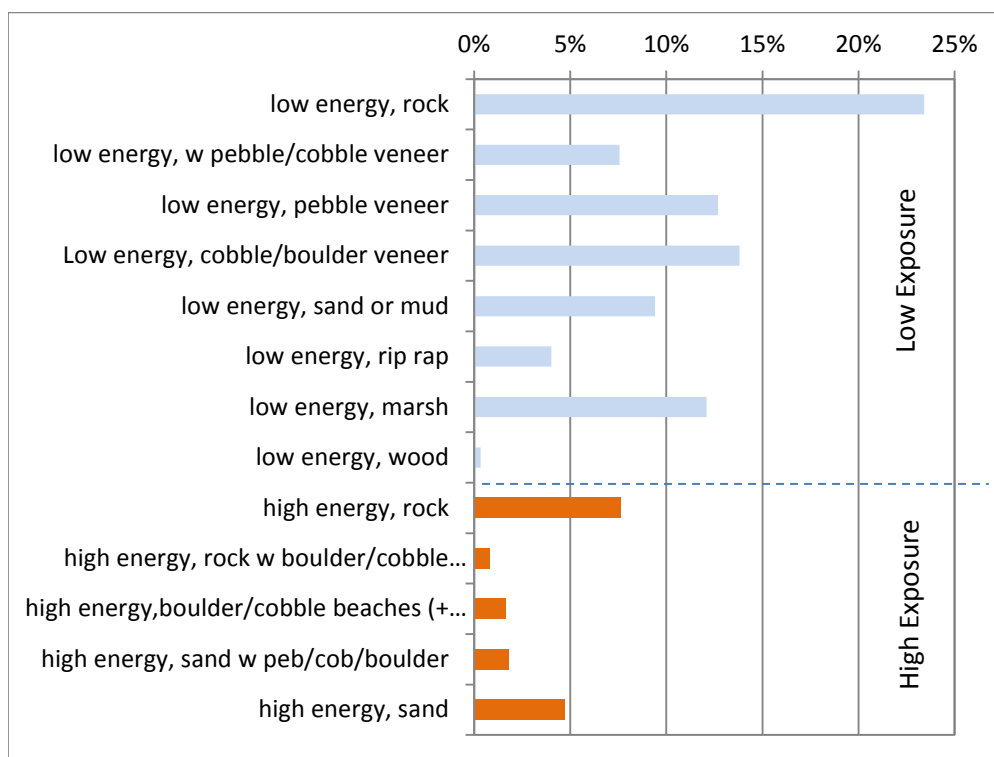


Figure 6. Upper intertidal shore types and exposure used as the basis for spill retention modeling.

**Table 4 Summary of Spill Shore Type Occurrence in Modelling Area**

Exposure	No	Description	% Length	Sub-total
Low Exposure	1	rock	23%	83%
	2	veneer over rock	8%	
	3	pebble veneer over sand	13%	
	4	cobble/boulder veneer over sand	14%	
	5	sand	9%	
	6	rip-rap	4%	
	7	marsh	12%	
	8	wood bulkheads	0%	
Hig Exposure	9	rock	8%	17%
	10	cobble/boulder veneer over rock	1%	
	11	cobble/boulder	2%	
	12	sand & gravel	2%	
	13	sand	5%	

## Oil Retention Assumptions and Estimated Initial Retention

One of the challenges for the spill modeling component is to estimate potential retention volumes on shorelines, should a spill contact the shoreline. Because there have been few spills of DilBit, there is no published information on oil retention in coastal sediments. Published values of DilBit viscosity (Table 5) indicate that weathered DilBit is likely to have very high viscosities.

A number of different bitumen oil types are summarized in Table 5; it is not entirely certain how these bitumen oil types compare to the proposed product being shipped from the Vancouver terminal. At this point, it is assumed that the weathered CLB and MKH/MRB oil types are most representative of the proposed product. Both temperature and degree of weathering (evaporation) will substantially alter viscosities. Modeling by Belore (2010a) indicates potential viscosities ranging from 2,000 to 100,000 cP. Belore (2010a) also states that “*if this MKH oil emulsifies, it will attain very high viscosities and densities.*” For a first-order approximation, it appears that weathered bitumen is likely to have viscosities in the range of 10,000 to 100,000 cP.

A number of oils were used in the Stranded Oil in Coarse Sediment Experiments (SOCSEX; Harper and Kory 1995) and the most viscous of these tests oils were IFO-180 and Bunker C oils (Table 5). The weathered bitumen oil types (MRB/MKH) tested by Belore (2010a) show similar viscosity ranges to Bunker C (20,000 to 100,000 cP). Oil penetration and retention into sediments is substantially related to oil viscosity (Harper and Kory 2010a) so these comparison provide some insight into the potential penetration and retention of weathered bitumen into coastal sediments if stranded.

**Table 5 Comparison of Dilbit Dynamic Viscosity with Previously Tested Oils**

Sources	Notes	Viscosities (summer)	Viscosities (winter)
Belore (2010a) Table 3.3	CLB bitumen type	“@ 15° C” 0% evaporation, 368.0 cP 14.3% evaporation, 9,227 cP 17 % weathered, 14,486 cP	“@ 1° C” 0% evaporation, 1,363 cP 14.3% evaporation, 57,548 cP 17 % weathered, 98,625 cP
Belore (2010a) Table 3.4	MKH bitumen type	“@ 15° C” 0% evaporation, 241.9 cP 14.3% evaporation, 1,377 cP 17 % weathered, 2,573 cP	“@ 15° C” 0% evaporation, 977.0 cP 14.3% evaporation, 6,487 cP 17 % weathered, 15,205 cP
Belore (2010a) Fig. 4-4 and 4-16	MRB bitumen type (“equivalent to MKH”, p. 4-5); “if MKH oil emulsifies, it will attain <i>very high viscosities</i> ” (p. 4-5)	3hr, 10,000cP 6 hr, 35,000 cP 9 hr, 55,000 cP 12 hr, 70,000 cP 24 hr, 100,000 cP	3hr, 2,000 cP 6 hr, 10,000 cP 9 hr, 11,000 cP 12 hr, 20,000 cP 24 hr, 80,000 cp
S. L. Ross (2012, Fig. 11)	CLB Temperature 15°C	2,000 to 1,000,000 cP plateaus around 200,000 cP	
SOSEX (Harper and Kory 1995; Fig. 6a, 6g)	IFO-180 Fuel Oil at 15°C	2,000 cP	
	IFO-180 Fuel Oil at 0°C		11,000 cP
	Bunker C at 15°C, not emulsified	12,000 cP	
	Bunker C at 0°C, not emulsified		100,000 cP

Adhesion properties or “stickiness” may also influence retention of stranded oil in sediments. Belore includes a tabular comparison of bitumen oil types as compared to more common oil types, including some oils tested in the SOCSEX experiments. These adhesion values are summarized in Table 6. The adhesion values suggest that some bitumen oil types have similar adhesive properties to Bunker C and some (MKH) are closer to the IFO-180 oil types.

**Table 6 Adhesion Properties of Oils**

Oil Type	% Evaporation	Adhesion (g/m <sup>2</sup> )
Cold Lake Bitumen	0%	98
Condensate (CLB)	14%	146
(Belore 2010a; Table 3-5)	17%	131
Mackay River Heavy bitumen-synthetic (MKH);	0%	52
(Belore 2010a; Table 3-5)	9%	57
	13%	60
Bunker C (SOCSEX; Harper and Kory 1995; Fig. 7)	0%	90
	6%	125
IFO-180 (SOCSEX; Harper and Kory 1995; Fig 7)	0%	48
	2.5%	62

#### Oil Retention in Sediments Assumptions

There is no published information on the retention of stranded bitumen oil types in sediment. As such, we make a number of assumptions on potential penetration and retention of weathered bitumen. As a first

approximation, weathered bitumen oil is most closely approximated by weathered Bunker C oils where viscosities are likely to be in the range of 10,000 to 100,000 cP. Table 7 shows measured viscosities and associated sediment retention values for a variety of coarse sediments (finer sediment “plugged” or were essentially impermeable to these viscous oil types.). Figure 7 shows the data plotted for oil retention in larger sediments (medium to very large

**Table 7 Measured Oil Retention**

Oil Type	Viscosity (cP)	Oil Retention (L/m <sup>3</sup> )		
		Medium Pebbles	Large Pebbles	V. Large Pebbles
Bunker-6%, 2°	160,000	288	157	85
Bunker-0%, 2°	80,000	197	94	77
Bunker-0%, 5°	50,000	213	130	51
Bunker-0%, 10°	30,000	155	47	24
Bunker-0%, 15°	15,000	52	68	5
IFO-2.5%, 2°	13,000	60	30	5
IFO-2.5%, 15°	3,000	18	5	0.1

Data from SOCSEX II (Harper and Kory 1995)

pebbles) for the documented ranges of viscosities of Bunker C and IFO-180 oils. For the range of anticipated viscosities of a weathered DilBit (Table 5), the associated retention values (in L/m<sup>3</sup>) range from 75 to 300 L/m<sup>3</sup>. At viscosities above 100,000 cP, medium pebbles are beginning to “plug” and become impermeable, suggesting that a weather DilBit spill will only penetrate the coarsest sediments (boulder, cobbles) which are relatively rare in the project area.

For the purposes of the modeling, we made assumptions of the penetration potential, the retention potential and the surface layer potential (thickness of oil that remains attached to the beach surface but not actually permeating the sediments).

1. Assume that weathered DilBit will have <1 cm of penetration in sands, < 5 cm in pebbles and < 10 cm in cobbles (Harper and Kory 1995; Table 13).

2. Assume retention of 300 L/m<sup>3</sup> for sand, 200 L/m<sup>3</sup> for pebble and 100 L L/m<sup>3</sup> for cobbles (Harper and Kory Table 21)
3. Assume a layer of weathered oil above the sediments of 1 cm for rock, sand, pebbles and cobbles.

The implication of these assumptions for the various Spill Shore Types are summarized in Table 8. The volumetric retention in litres per square metre is summarized in Column 9. This value includes a subsurface volume (Col 7) and surface thickness or coating (Col 8).

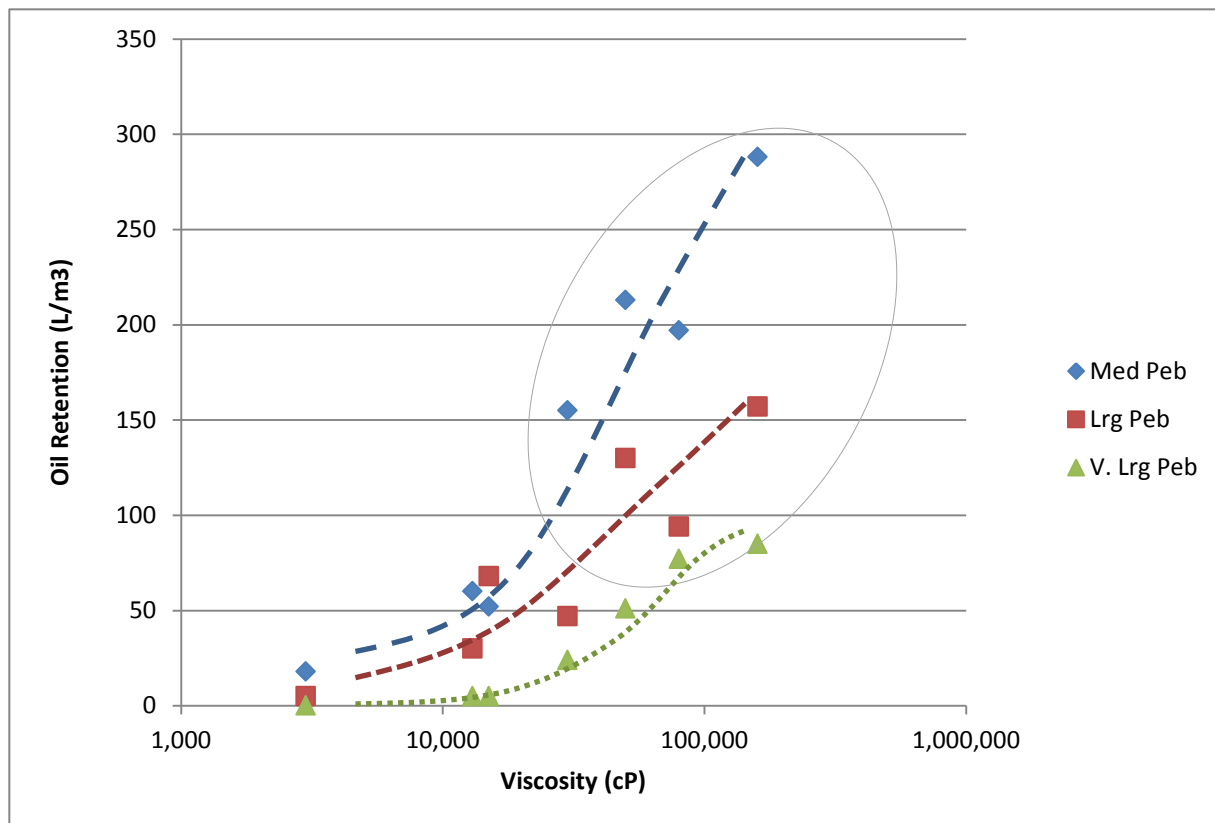


Figure 7. Oil retention values in coarse sediments as a function of changes in oil viscosity. The oval indicates the most likely range of weathered DilBit viscosities and associated sediment retention.

**Table 8 Initial Oil Retention Estimates.**

1	2	3	4	5	6		7	8	9
	Shore Type	Description	Penetration (cm)	Conc (L/m3)	Thick- ness (cm)		Vol in Sediment L/m2	Vol in Surface Layer L/m2	Total Volume (L/m2)
1	LE_R	Rock	0	0	0.5		0	5	5
2	LE_VR	Rock w pebble, cobble veneer	1	100	0.5		1	5	6
3	LE_V	Pebble veneer	2	200	0.5		4	5	9
4	LE_CV	Cobble or boulder veneer	10	100	0.5		10	5	15
5	LE_S	Sand or mud	1	300	0.5		3	5	15
6	LE_RR	Rip Rap	30	100	0.5		30	5	35
7	LE_M	Marsh	1	300	1		3	10	13
8	LE_W	Wood	2	300	0.5		6	5	11
9	HE_R	Rock	0	0	0.5		0	5	5
10	HE_VR	Rock with coarse veneer	20	200	0.5		40	5	45
11	HE_C	Boulder, cobble beaches (also includes few rip-rap sections)	30	200	0.5		60	5	65
12	HE_SG	Sand w pebble, cobble or boulder	1	300	0.5		3	5	8
13	HE_S	Sand	1	300	0.5		3	5	8
14	LE_L	Log boom modifier	0	0	1		0	2	2

Note: Shore type 14, Log Booms, assume coating thickness of 1 cm with 20% coverage within the boom. This retention might be best thought of as either

Log Booms in the Fraser River present a special challenge/



## References

Belore, R. 2010a. Properties and fate of hydrocarbons associated with hypothetical spills in the at the Marine Terminal and in the confined channel assessment area. Contract Report by SL Ross Environmental Research Limited, Ottawa, ON, for the Enbridge Northern Gateway Project, 132 p.

Belore, R. 2010b. Properties and fate of hydrocarbons associated with hypothetical spills in the open water area. Contract Report by SL Ross Environmental Research Limited, Ottawa, ON, for the Enbridge Northern Gateway Project, 44 p.

Harper, J.R. and M. Kory 1995. Stranded oil in coarse sediment experiments. Contract Report by Coastal & Ocean Resources Inc., Sidney, BC for Environment Canada, Edmonton, AB, 60p.

SL Ross 2012. Meso-scale weathering of Cold Lake Bitumen/Condensate Blend. Contract Report by SL Ross Environmental Research Limited, Ottawa, ON, 27p.

## APPENDIX A

### Field Observations of Shoreline Types and Substrate

---

#### Introduction

As part of the spill modeling assessment and shoreline oil retention estimates, a short field program was conducted on lower Vancouver Island beaches to assist with the validation of mapping and oil retention assumptions. The field program collected observational data to help answer two questions:

- Does the ShoreZone mapping data (see Howes 2001; Berry et al 2001) capture the essential elements of the shoreline morphology and substrate, especially as they relate to spill potential retention and residence?
- Are assumptions about the substrate valid, especially permeability as these can significantly affect initial oil retention values?

#### Field Surveys

Surveys were conducted around a low-tide window from 20-30 May 2013. A total of 57 ShoreZone units were surveyed (Figure A-1). The following procedures were used within each unit:

##### Shore Unit Classification Observations

The observers provided a “field estimate” of the ShoreZone shore type. This is one of the 36 Shore Types (also referred to as BC Class) in the BC ShoreZone system. Shore Types are a summary indicator of morphology, substrate and width of each alongshore unit. Units were selected for the survey with a bias towards sand & gravel substrates and easy accessibility to improve survey efficiency. A variety of shoreline exposures are included in the data, although the vast majority of the stations fall into the low wave exposure regime (Table A-1).

Observers walked most of the unit, collected at least one representative unit photo and took more detailed observations of surface and subsurface sediments. Observations were systematically recorded on field data sheets.

The observers used the same procedure that mappers used when classifying aerial videography. This procedure allows a “ground interpretation/classification” to be compared to the “aerial interpretation/classification” used in the ShoreZone mapping. It is

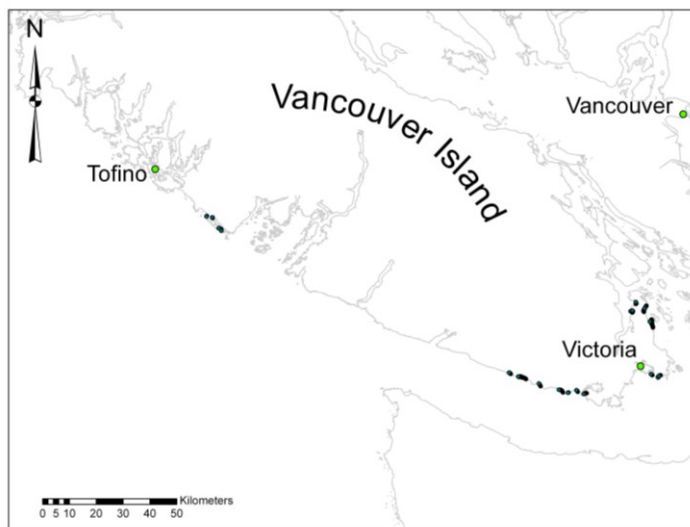


Figure A-1. Survey locations.

assumed that an interpretation made on the ground is “correct” and allows validation of the aerial mapping data. This ground interpretation/classification of the *Shore Type* is the primary attribute required to validate the mapping data.

#### Substrate Observations

The glaciated shorelines of BC and Washington often include a patch-work of rocky shorelines and sediment shorelines. Substrate is known to be a significant factor in potential oil retention during accidental spills. Some substrates are relatively impermeable (e.g., rock, mud, sand) and usually do not retain much oil whereas others are quite permeable (pebble-cobble-boulder), where oil can permeate into the subsurface with relatively high retention rates. As such, *permeability* of shoreline substrate is a critical variable for estimating the retention volume of oil stranded on the shoreline.

Observations of surface and subsurface substrate were made at a series of plots within the upper intertidal zone of each shore unit. Depending on the substrate character, five or less plots were photographed to show the surface sediment and the immediate subsurface sediment; a total of 272 plots were photographed. Figure A-2 shows an example of paired photos for the same plot. Observers carefully removed the surface sediment layer to reveal the subsurface layer.

A senior geologist classified the surface and subsurface substrate in each photo.

We also considered a permeability test similar to a “perk test” where a fixed volume of water was emptied into a standpipe and allowed to drain; the drain time then provides an objective, relative measure of permeability. However, drain times were comparatively long so fewer plots could have been surveyed. The perk test was abandoned after the initial tests.

## **Results**

#### Shore Type Classifications

Table A-2 summarizes the matches between ground and aerial classifications. The data indicate that only 60% of the Shore types showed a match (or close to match) and there appeared to be a bias of aerial mappers to map substrate finer than it appears on the ground (i.e., under-estimating the coarse fraction). We noted that some of the mapping data (Ucluelet, Juan de Fuca Strait) is over 30 years old and the mapping was based on considerably lower resolution imagery than the 2001 Washington and 2005 Saanich Peninsula ShoreZone mapping. We have noted these discrepancies before in trying to compare ground and aerial classification data (Harper and Morris 2007; Harney et al 2008). Because spatial occurrence of sediment is highly

**Table A-1 Summary of Surveyed Exposures**

Energy Class	Exposure Category	No Segments
<i>High Energy</i>	Exposed	3
	Semi-Exposed	15
<i>Low Energy</i>	Semi-Protected	27
	Protected	12
<i>Totals:</i>		57

**Table A-2 Ground & Aerial Classifications**

Ground to Aerial Classification	No.	%
Exact or close matches	38	60%
Ground Observations coarser	13	21%
Ground Observations finer	6	10%
Mismatch	6	10%
	63	100%

patchy and variable, it may actually be more difficult for ground mappers to evaluate the percent occurrence of the various substrate categories that are used to estimate the summary indicator of the unit (i.e., shore-type class).

Given the uncertainty in the mapping of shore types (Table A-2), one might ask how this would affect potential shoreline oil retention estimates. If the substrate matrix (the sediment size controlling permeability so that for a mixture of pebble and sand, the permeability will be controlled by the sand) for the various shore-type classes is examined, the difference is not as great (Table A-3). The sediment matrix matches in ~79% of the comparisons. We also went through the segment data to look at the comparison of estimated permeability based on the ground and aerial interpretation/observations assuming that the stranded spill would be a heavy or viscous oil (*low permeability* in rock, sand or mud substrate, *moderate permeability* in pebble substrate and *high permeability* in cobble/boulder substrate). Results of the classification of permeability are summarized in Table A-4 and indicate that in terms of permeability, the ground and aerial interpretation/classification agreed in 90% of the comparisons.

**Table A-3 Sediment Matrix in Ground & Aerial Classifications**

Ground to Aerial Classification	No.	%
Same matrix	50	79%
Different matrix	13	21%
<i>Totals:</i>	63	100%

**Table A-4 Permeability Estimates from Ground & Aerial Shore-Type Classifications**

Ground to Aerial Classification	No.	%
low ground, low aerial	50	85%
high ground, high aerial	3	5%
high ground, low aerial	3	5%
low ground, high aerial	3	5%
<i>Totals:</i>	59	100%

#### Substrate Observations

The surface and subsurface photos were classified in terms of Wentworth size categories (Table A-5). The data are used to test the hypothesis: *most low-energy gravel surface sediments are thin and underlain by a sand layer that would be relatively impermeable to viscous oil during a spill stranding.*

Example photos are included in Figure A-2 showing that surface veneers of gravel are often a single clast thick and the subsurface is usually sand. Table A-6 summarizes the permeability classification from 270 plots. These data show that the hypothesis is generally supported by the field observations.

**Table A-5 Sediment Classification**

Sediment Category	Code	Size (mm)
Boulder	B	>256
cobble	C	64-256
pebble	P	4-64
granule	G	2-4
Sand	S	0.0625-2
Mud	M	<0.0625

Example: PS = pebble (>50%) and Sand (<50%)  
SPG = sand (>33%), pebble (<sand), granule (<pebble))

The hypothesis really addresses *low-energy* locations (*Semi-Protected* or *Protected* exposure); there were 60 low-energy plots where surface conditions were classified as *high* or *moderate* permeability (Table A-6). Permeability classifications from the *low-energy* sites show that the vast majority of observations support the hypothesis (82%). A few of these sites with *moderate* permeability in the subsurface (five plots) were associated with rip-rap or seawalls where elevated energy levels are likely.










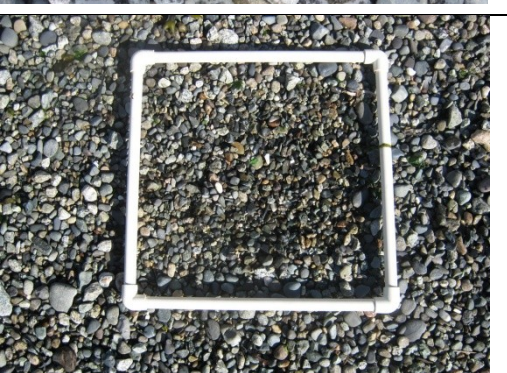
Surface	Subsurface	Description
		A. Plot 306D, a low energy site, upper intertidal zone
		B. Plot 320B, low energy site, upper intertidal zone.
		C. Plot 610B, a moderate energy site, upper intertidal zone (near Jordan River).
		D. Plot 312C showing a location where both surface and subsurface are <i>moderately</i> permeable.

Figure A-2. Examples of plot photos of surface and subsurface sediments.



## Discussion

This modest field program examined approximately 54 km of shoreline that is included within the BC ShoreZone dataset (57 shore units). The intention of the program was to provide a level of confidence in the approximations used in estimating oil retention from spill models. In particular we wanted to make the case that ShoreZone mapping was an appropriate tool to support modeling of oil retention. The survey examined actual ground conditions in comparison to the ShoreZone mapping data (collected between 1980 and 2007).

The ground verification showed about a 60% match between aerial interpretation/classification and ground interpretation/classification (Harney et al 2008; Harper and Morris 2007). This is similar to previous verification studies of ShoreZone and resulted in more detailed mapping rules after 2007. But the ShoreZone datasets used in this project pre-dated the refined mapping rules. When the data comparisons are examined in terms of initial oil retention, the comparison of aerial and ground data indicate a 80 to 85% agreement (Tables A-3, A-4). That is, for most of the shoreline examined, the ShoreZone mapping data appears to correctly predict the permeability of shore sediment observed during this ground survey.

A secondary objective of the field survey was to test the hypothesis that *low-energy gravel beaches (pebble, cobble, boulder) are usually only a thin veneer of gravel over sand*. This is an assumption that was used in the modeling and has important implications to the permeability of these beaches and ultimately to oil retention from a spill. *Impermeable* substrates will have lower retention than *permeable* shorelines, which may act like a “sponge” to retain oil. Shoreline substrate and permeability were observed at 270 plots where both surface and immediate subsurface sediments were photographed (Fig. A-2). Of the 60 plots with *low-wave exposures* and *moderate to high* permeability (pebbles, cobbles, boulders), over 80% had impermeable sediment (mud, sand granules) in the immediate subsurface (Table A-7). These data support the assumption that most low energy shorelines will have limited penetration into subsurface sediments and that most oil retention will occur as surface slick on the beach surface.

**Table A-6 Permeability Comparisons of Surface and Subsurface**

Permeability		Observations	
Surface	Subsurface	No	%
low	low	184	68%
moderate	low	66	24%
moderate	moderate	17	6%
high	low	1	0%
high	high	2	1%
<b>TOTALS:</b>		<b>270</b>	<b>100%</b>

**Table A-7 Summary of Low-Energy Plots**

Permeability		No	%
Surface	Subsurface		
moderate	low	49	82%
moderate	moderate	9	15%
high	high	2	3%
<b>Totals:</b>		<b>60</b>	<b>100%</b>

## References

- Berry, H.D., Harper, J.R., Mumford Jr., T.F., Bookheim, B.E., Sewell, A.T., & Tamayo, L.J. (2001). The Washington State ShoreZone Inventory User's Manual. Olympia, WA: DNR Nearshore Habitat Program.
- Harney, J.N., J.R. Harper and M.C. Morris 2008. Report on the ShoreZone Ground Verification Study Conducted in Sitka, Alaska (May 2008) (ver. 5). Prepared by Coastal & Ocean Resources Inc., Victoria, BC for Prepared for: NOAA National Marine Fisheries Service and Nature Conservancy (Juneau, Alaska) 62p.
- Harper, J.R., and Morris, M.C. 2008. BC ShoreZone Field Verification Project. Report prepared for BC Ministry of Environment 39 p.
- Howes, D.E. 2001. BC Biophysical Shore-Zone Mapping System— A Systematic Approach to Characterize Coastal Habitats in the Pacific Northwest. Proceedings of the 2001 Puget Sound – Georgia Basin Conference, Seattle.

APPENDIX B  
Fraser River Addendum

---

**Table B-1 Fraser River Shore Types**

2009 Shore Type	Code	% Occurrence	SSS ShoreType	Code	% Occurrence
Rip Rap	RR	35%	Rip rap	LE_RR	35%
Artificial Marsh	AM	2%	Marsh	LE_M	51%
Fringing Marsh	FM	49%	Marsh	LE_M	
Beach	B	5%	Sand beach or mudflat	LE_S	7%
Mudflat	MF	2%	Sand beach or mudflat	LE_S	
Impermeable	IM	7%	Rock	LE_R	7%

**Note:** 204 km of South Arm mapped downstream of the Port Mann Bridge.

A previous shore-typing scheme was utilized for most of the shoreline below Annacis Island. This shore-typing scheme mapped six shore types (Table B-1). The equivalent four shore types for the Salish Sea Shoreline Shore Types are also identified in Table B-1.

Intertidal widths were estimated from satellite imagery and the FREMP on-line atlas ortho-photographs.

The South Arm of the Fraser River was assumed to be an entirely *Protected* wave exposure environment and all shore types in the river assumed to be *low energy* shore types.

Once the SSS Shore types were assigned, the same procedures were used to estimate the potential oil retention should a slick reach the shoreline.

Log booms within the river presented a special challenge as there is little documentation of oil retention on log booms. The total area of log-booms was estimated from a satellite image. Log booms are uniformly 20 m in width and we digitized a line segment along the centre axis of each log boom. The area of the log boom is calculated as the length of the line segment times the average width (20m). Some oil would coat the outer boom sticks of the boom and some would likely be carried under the boom and re-emerge within the boom. We assumed an average coverage of 20% of the total boom area and would receive a uniform coating of 1 cm. A single square metre of boom would have a retention of 2 L/m<sup>2</sup>.

# APPENDIX D

## BURRARD INLET SPILLCALC VALIDATION

---

# TECHNICAL MEMO

ISSUED FOR USE

<b>TO:</b>	Bikramjit Kanjilal	<b>DATE:</b>	July 31, 2013
<b>C:</b>	Jim Stronach, Aurelien Hospital	<b>MEMO NO.:</b>	N/A
<b>FROM:</b>	Daniel Potts	<b>EBA FILE:</b>	V13203022
<hr/>			
<b>SUBJECT:</b>	SPILLCALC Validation against Westridge Hydrocarbon Accidental Release, Burrard Inlet, 2007		

## 1.0 DOCUMENT OBJECTIVE

This technical memo describes the validation of SPILLCALC against the 2007 spill in Burrard Inlet at Kinder Morgan's Westridge Terminal.

## 2.0 INTRODUCTION

At 12:32 p.m. on 24 July 2007, a backhoe accidentally ruptured a pipeline carrying crude oil in Burnaby, BC. Approximately 224 m<sup>3</sup> of oil escaped the pipeline, some of which entered city storm sewers and was released into Burrard Inlet near Kinder Morgan's Westridge Terminal.

EBA used SPILLCALC to hindcast the trajectory of the released oil as a validation of the model. Predictions made by SPILLCALC were compared against observations reported in the Environmental Impact Statement (EIS; Stantec, 2010) as well as archived news articles available online.

## 3.0 MODEL INPUTS

SPILLCALC relies on surface currents computed by H3D. EBA implemented H3D in a nested configuration, with a 125-m resolution model of Burrard Inlet nested within a 975-m resolution model of the Strait of Georgia. Inputs to these models are summarized below.

### 3.1 Strait of Georgia H3D Implementation

The model bathymetry was the same as that used for the stochastic and deterministic simulations for Trans Mountain, described in the main report: Modelling the Fate and Behaviour of Marine Oil Spills for the Trans Mountain Expansion Project" (EBA, 2013). Fraser River daily flows were included, with median monthly temperatures and clay concentrations; no other rivers were included in the Strait of Georgia model. Water elevation boundary conditions were derived from tidal harmonic constants. Temperature and salinity boundary conditions were derived from ROMS 2012 data. Temperature and salinity initial conditions were taken from existing H3D model output for 1 July 2012. Wind and other meteorological inputs were taken



from Vancouver Airport data and Halibut Banks buoy data. The model was run from 1 July 2007 to 30 August 2007.

### 3.2 Burrard Inlet H3D Implementation

The model bathymetry was the same as that used for the stochastic and deterministic simulations for Trans Mountain, described in the main report: *Modelling the Fate and Behaviour of Marine Oil Spills for the Trans Mountain Expansion Project* (EBA, 2013). No river inflows were included. Water elevation, temperature and salinity boundary conditions were provided by the Strait of Georgia model. Temperature and salinity initial conditions were duplicated from the 2011 H3D inputs, which correspond to late August or early September. Wind data were derived from Calmet outputs. Other meteorological inputs were taken from Vancouver Airport data and Halibut Banks buoy data. The model was run from 1 July 2007 to 30 August 2007. Surface currents were archived every 15 minutes.

### 3.3 SPILLCALC Implementation

In addition to surface currents, SPILLCALC requires wind data; the properties, volume, timing and location of the oil release; and shore oil retention properties.

- The wind input was the same as that used for the Burrard Inlet H3D model.
- Oil properties were derived from information in Table 1.1 of the EIS. The oil was represented by eleven pseudo-components, whose properties were based on the corresponding Cold Lake Blend pseudo-components. The densities of each pseudo-component were decreased by 1.7% to force the overall density to match that given in Table 1.1 (925 kg/m<sup>3</sup>). According to Table 1.1, volatiles made up 15.9% of the mass of the oil released. Based on the adjusted densities of the pseudo-components, this corresponds to 21.3% by volume.
- Table 2.3 of the EIS reports that 5.636 m<sup>3</sup> of oil was estimated to have been released to Burrard Inlet, excluding recovered oil and volatilization. Since volatile pseudo-components made up 21.3% of the oil volume, the release volume input to SPILLCALC was  $(5.636 \text{ m}^3) / (100\% - 21.3\%) = 7.16 \text{ m}^3$ .
- Emergency responders contained and ultimately recovered most of the oil that entered the sewers, using booms, vacuum trucks and skimmers. According to Table 2.1 of the EIS, the first report of oil coming out of the sewer was at 1:35 p.m. on 24 July (one hour after the rupture), and the first booms were deployed at 2:15 p.m. By 4:40 p.m. on 26 July most of the oil was removed from inside the boomed area. In the intervening time, small amounts of oil escaped from the boomed area as a result of wave action. Therefore, the oil release in SPILLCALC was assumed to occur at a steady rate over a period of 51 hours, from 1:35 p.m. on 24 July to 16:35 p.m. on 26 July.
- The location of the sewer outflow was estimated based on a photo in a news article (CBC, 2007). The estimated coordinates of the outflow were 49° 17.306' N, 122° 57.507' W. This point is at the foot of Cliff Avenue, about 600 m downhill from the site of the pipeline rupture.
- The oil retention properties of the shoreline were as described in the main report: *Modelling the Fate and Behaviour of Marine Oil Spills for the Trans Mountain Expansion Project* (EBA, 2013). In the region of interest, oil retention capacities ranged from 70 to 2900 L/m.

The SPILLCALC model was run from the start of the oil release until no oil remained on the water surface.

## 4.0 RESULTS

The model ran for about 85 hours, terminating at 3:00 a.m. on Saturday 28 July 2007, at which time there was no oil remaining on the water surface. At the end of the simulation, 76.1% of the oil volume was on shore, 22.2% had evaporated and 1.7% had dissolved – see the simulation mass balance in Figure 4.1. The evaporated fraction included the 21.3% volume of volatiles plus 0.9% from the heavier pseudo-components. Aside from a small dissolved fraction, all the remaining oil reached and was retained on the shore.

The SPILLCALC predictions were validated against observations in the EIS and new reports, as follows.

### 4.1 Validation of Shore Impacts

Figure 4.2 shows the SPILLCALC prediction of oil retained on shore. The maximum predicted oil retention on shore was 69 L/m, adjacent to the release location. At the same location, the shore retention capacity is 1245 L/m. Nowhere was the shore capacity exceeded; therefore, all oil that reached shore was 100% retained. SPILLCALC does not simulate re-suspension of beached oil.

Figure 4.3, reproduced from the EIS, summarizes the observations of shore impacts. The observations are qualitative, categorizing the oil impacts as heavy, moderate, light, very light, or none in each surveyed shore segment. These categories are illustrated with sample photos in the EIS, but are not quantitatively defined. Therefore, only a qualitative comparison of Figures 4.2 and 4.3 can be made. Overall, the two figures show good general agreement:

- The heaviest observed shore oiling was adjacent to the spill site, from the Chevron refinery to Barnet Marine Park. The heaviest predicted shore oiling was in the same area, although perhaps more localized to the release point.
- Moderate oiling was observed on the shore near the Dollarton Highway beginning near the Second Narrows and extending to Cates Park. SPILLCALC also predicted oiling along this shoreline.
- Light oiling was observed along the south shore at the Second Narrows. SPILLCALC also predicted oiling along this shoreline.
- Very light oiling was observed in Belcarra Bay. SPILLCALC also predicted oiling in the bay.
- No oil was observed in Port Moody; neither did SPILLCALC predict any oil impact there.

There were also some differences between the observed and predicted shore impacts:

- No shore oiling was observed south of Belcarra Bay; however, SPILLCALC predicted oiling there.
- No shore oiling was observed north of Cates Park and around Deep Cove; however, SPILLCALC predicted oiling there.

The oiling predicted south of Belcarra Bay is likely due to the uncertainty in the timing of the oil escape(s) from under the containment booms. The predicted oiling occurred midday on Thursday 26 July, from oil

released that morning. If much oil did not escape from the booms that morning, the shoreline oiling would not be predicted.

The oiling predicted around Deep Cove is patchy, with many unoiled sections. It is possible that the predicted slight degree of oiling actually occurred and escaped detection. Alternately, the model may have incorrectly predicted the oil trajectory due to uncertainty in the release timing or errors in prediction of local wind or currents around Deep Cove. Note that tar balls and sheen were observed on the water in this area (see next section) despite the lack of shore impacts.

## 4.2 Validation of Slick Motion

The time history of the slick motion was validated against descriptive reports of oil observations in the EIS and in archived news items. Section 2.1.1.1 of the EIS, titled “Oil Dispersion Throughout Burrard Inlet,” provided several notes useful for this validation. The “pie plates” referred to in the EIS texts are tar balls, which are also predicted by SPILLCALC.

- “The greatest concentration of oil was reported east of Second Narrows and west of Port Moody. Oil in this area initially consisted of pie plates and sheen, with sheen noticeably increasing on July 29.... Mousse first appeared on July 30. By August 2 only a few patches of sheen and mousse remained outside of the spill site.” (EIS, page 2-5)
  - The greatest predicted concentrations of oil were in the same locations; predictions agreed with observations. The predicted lifespan of oil on water is underestimated by the model due to complete stranding of the oil on shore. In reality, oil on shore can be re-suspended and continue to move, but this mechanism is not supported in the model.
- “The westward movement of oil consisted of intermittent pie plates between First Narrows Bridge and Second Narrows Bridge, with the most westerly observation being a patch of sheen about 1 km east of First Narrows. By August 2, there were no further signs of oil west of the Second Narrows Bridge...” (EIS, page 2-5)
  - SPILLCALC predicted some oil passing west of the Second Narrows Bridge predawn on 27 July. All of this oil either struck the north shore or moved back east by midafternoon with the change of tides. Predictions agreed with observations.
- “The eastward movement of oil into Port Moody began July 29 and was followed by sheen reports.... The last reports of mousse and sheen in Port Moody were on August 1....” (EIS, page 2-5)
  - The model stopped before 29 July and predicted no oil going to Port Moody. The absence of oil observations at Port Moody before 29 July agrees with model predictions.
- “Throughout the surveys there were reports of scattered pie plates and sheen in the Deep Cove area of Indian Arm and about 1 km further north. This oil was most evident on July 27 and decreased steadily thereafter.” (EIS, page 2-6)
  - SPILLCALC predicted oil entering Indian Arm on the afternoon of 26 July. By 6:00 a.m. on 27 July most of this oil had hit shore, with the remainder also hitting shore within another 12 hours. The prediction is slightly early but the location matches observations.

- “Late Thursday night, ‘turkey-platter-sized globs’ of oil coated boats and docks on the shore in Belcarra Bay.” (Vancouver Sun, 2007)
  - The model predicted oil entering Belcarra Bay midafternoon Thursday 26 July. All the oil either struck shore or exited by 9:00 p.m. The predicted oil movement agrees with observations, except a slight difference in timing, which can be attributed to the uncertainty in the oil release timing.

Overall, the oil movement predicted by SPILLCALC agrees with recorded observations, apart from some slight differences in timing, and the early termination of the model due to oil stranding on shore.

## 5.0 CONCLUSIONS

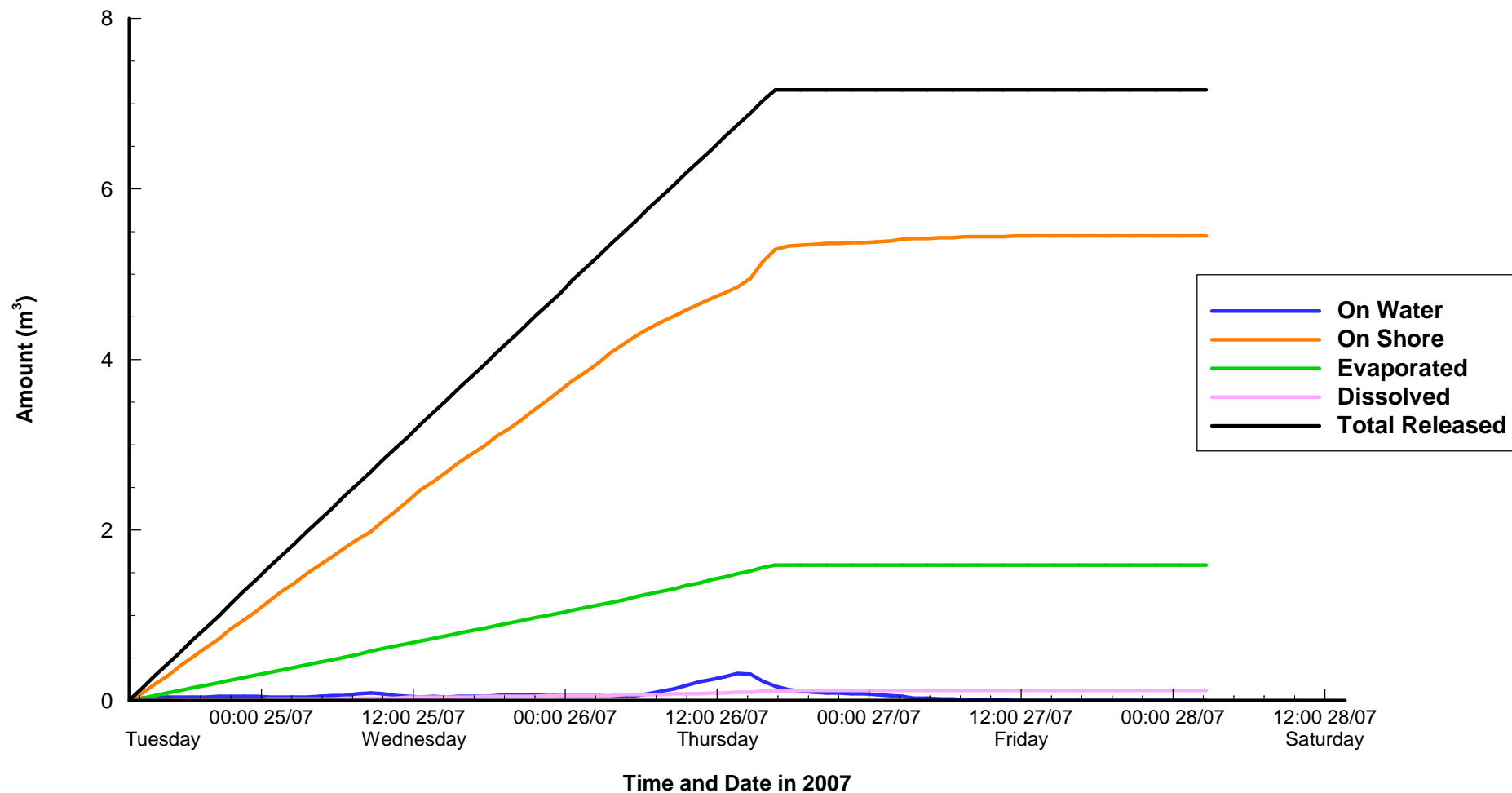
The predictions made by SPILLCALC of oil motion and shore impacts during the 2007 spill in Burrard Inlet were compared with recorded observations. The general movement of the oil, the locations of heavily affected shorelines and the extent of the affected area are in agreement. Some differences appear in the timing of the oil motion and the lifespan of oil on water. These differences are mainly attributed to uncertainty in the timing of the release and to the permanence of oil on shore in SPILLCALC.

## 6.0 LIMITATIONS OF REPORT

This report and its contents are intended for the sole use of Trans Mountain and their agents. EBA Engineering Consultants Ltd. does not accept any responsibility for the accuracy of any of the data, the analysis, or the recommendations contained or referenced in the report when the report is used or relied upon by any Party other than Trans Mountain, or for any Project other than the proposed development at the subject site. Any such unauthorized use of this report is at the sole risk of the user. Use of this report is subject to the terms and conditions stated in EBA’s Services Agreement. EBA’s General Conditions are attached to this memo.

## REFERENCES

- CBC, 2007. Cleanup continues on B.C. oil spill. <http://www.cbc.ca/news/canada/british-columbia/story/2007/07/24/bc-oilspill.html> Dated 24 July 2007; accessed 30 July 2013.
- Stantec, 2010. Environmental Impact Statement: Divisions B and D: Sewers, Foreshore, and Marine Environment – Westridge Hydrocarbon Accidental Release. May 2010.
- Vancouver Sun, 2007. Beaches closed as 'big black globs' of oil spread north. <http://www.canada.com/vancouver/news/story.html?id=e819bd23-bfb6-4427-9a9a-ddb2010f5049&k=79641> Dated 28 July 2007; accessed 31 July 2013.



## NOTES

Simulation Parameters:  
 Tracking time: up to 10 days  
 Release time: 13:35 24-Jul-2007  
 Release volume: 7.16 m<sup>3</sup>

Mass Balance After Simulation (m3):  
 On Water: 0.00 ( 0.0%)  
 On Shore: 5.45 (76.1%)  
 Evaporated: 1.59 (22.2%)  
 Dissolved: 0.12 ( 1.7%)  
 Total: 7.16 ( 100%)

STATUS  
ISSUED FOR REVIEW

CLIENT



## TRANS MOUNTAIN OIL SPILL STUDY

### Oil Mass Balance Summer, Site D

PROJECT NO.  
V13203022

OFFICE  
EBA-VANC

DWN  
DP

DATE  
July 31, 2013

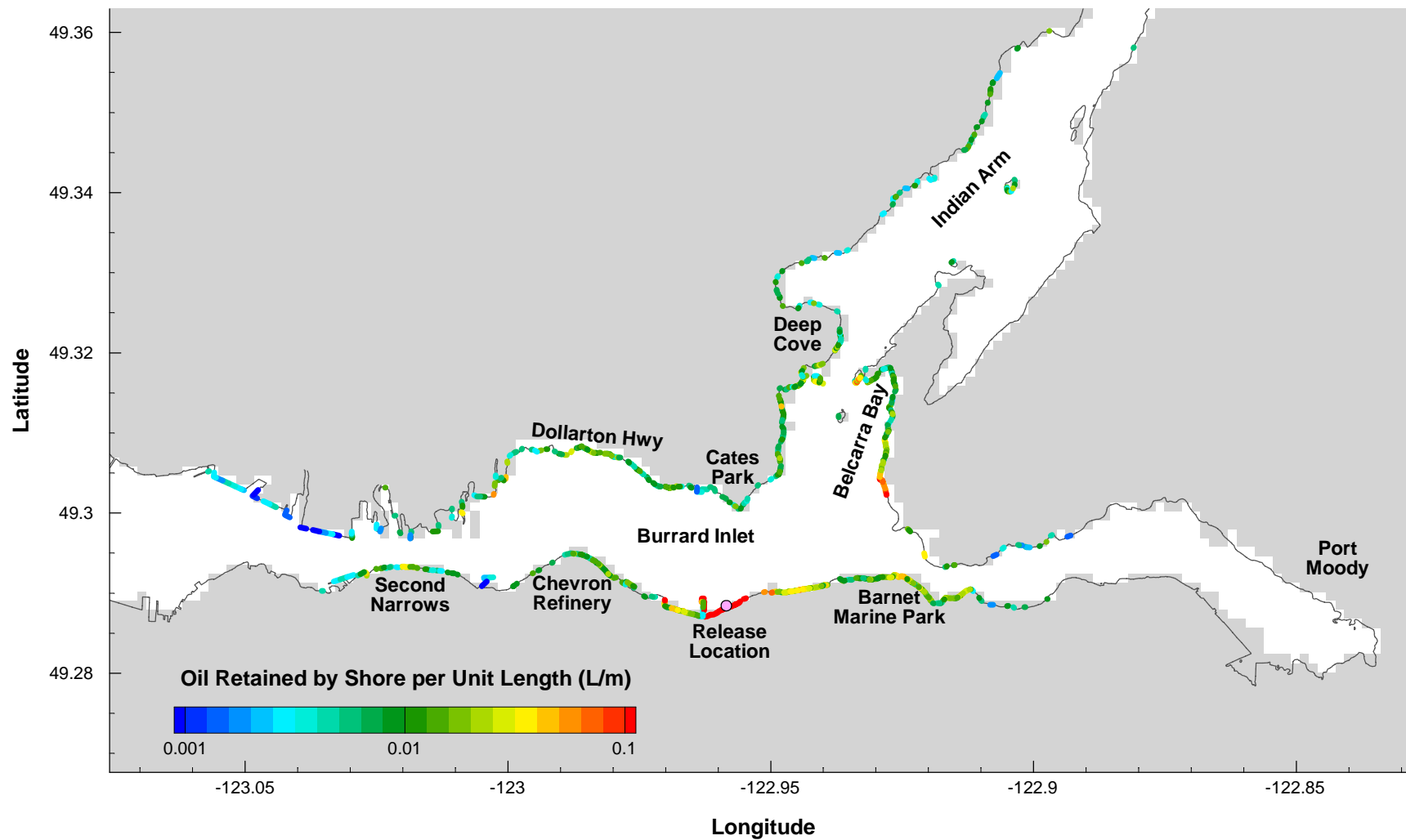
CKD  
JAS

APVD  
JAS

REV  
0

Figure 4.1





## NOTES

Maximum predicted oil retention on shore was 69 L/m adjacent to the release location. The total volume of oil retained on shore was 5.45 m<sup>3</sup>.

STATUS  
ISSUED FOR REVIEW

CLIENT



## TRANS MOUNTAIN OIL SPILL STUDY

### Simulated Shoreline Oiling: Westridge Hydrocarbon Accidental Release

PROJECT NO.  
V13203022

OFFICE  
EBA-VANC

DWN  
DP

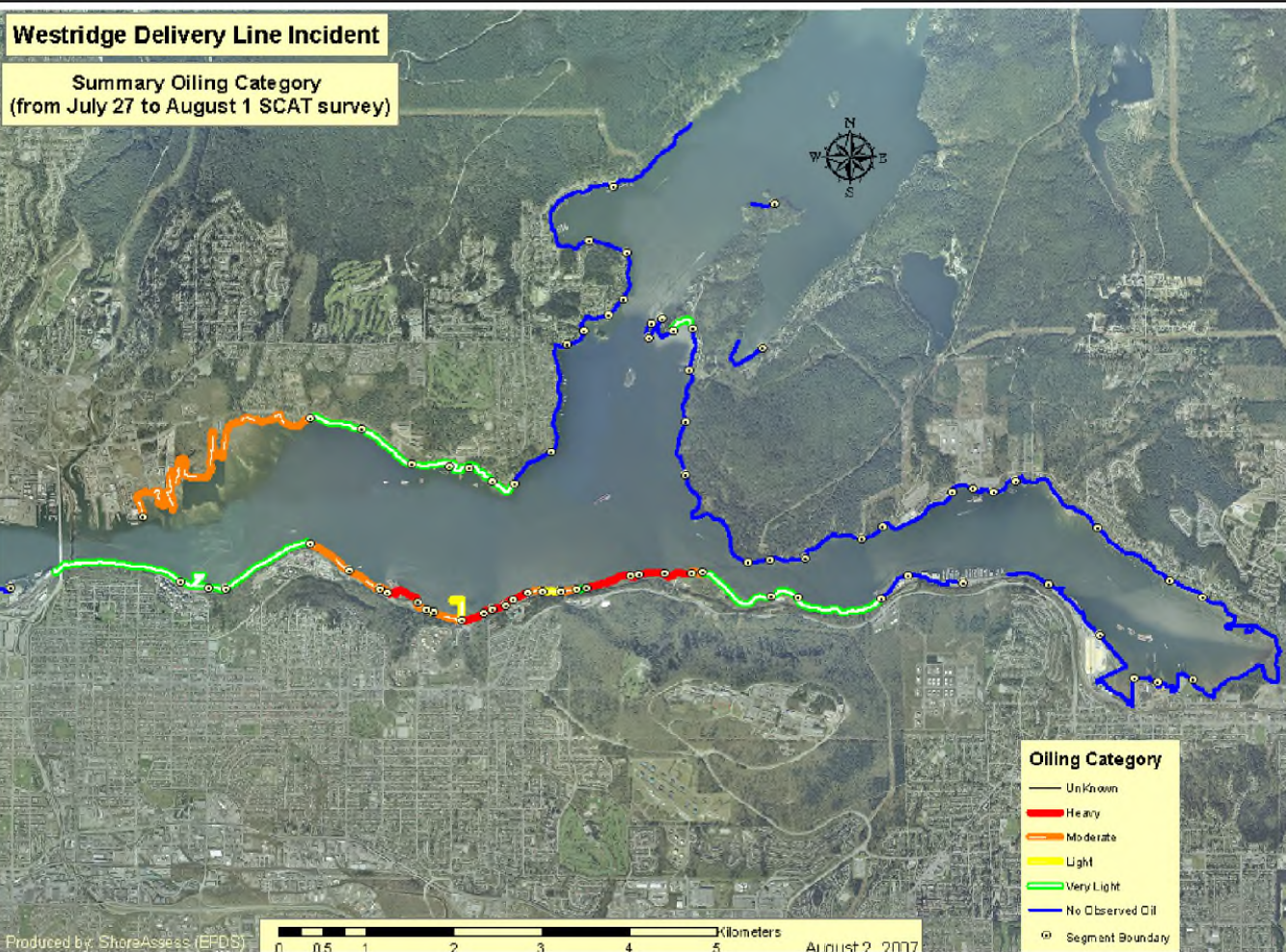
DATE  
July 30, 2013

CKD  
JAS

APVD  
JAS

REV  
0

Figure 4.2



P:\2010\Westridge\05-Final Report\BI\_validation\_2007\figures\shoresline\_oiling\_EIS\shore\_oiling\_EIS\_figure.lay

**Jacques Whitford**  
AXYS  
Jacques Whitford AXYS Ltd.  
4370 Dominion Street  
Burnaby, British Columbia  
V6G 4L7  
Tel. (604) 436 3014  
Fax. (604) 436 3752

**KINDER MORGAN**  
CANADA INC.

#### SUMMARY OILING CATEGORY

PROJECTION	UTM - ZONE 10	DRAWN BY	SB
DATUM	NAD 83	CHECKED BY	
DATE	20-Oct-07	FIGURE NO.	3.3

## NOTES

Reproduced from "Environmental Impact Statement: Divisoins B and D: Sewers, Foreshore and Marine Environment - Westridge Hydrocarbon Accidental Release" by Stantec (formerly Jacques Whitford AXYS), May 2010.

STATUS  
ISSUED FOR REVIEW

#### CLIENT



## TRANS MOUNTAIN OIL SPILL STUDY

### Shore Oiling Summary Map from Stantec EIS

<b>PROJECT NO.</b> V13203022	<b>DWN</b> DP	<b>CKD</b> JAS	<b>APVD</b> JAS	<b>REV</b> 0
<b>OFFICE</b> EBA-VANC	<b>DATE</b> July 30, 2013			

**Figure 4.3**

# APPENDIX E

## STOCHASTIC MODELLING RESULTS

---

# APPENDIX F

## EBA'S GENERAL CONDITIONS

---

---

# GENERAL CONDITIONS

## DESIGN REPORT

This report incorporates and is subject to these “General Conditions”.

---

### 1.0 USE OF REPORT AND OWNERSHIP

This Design Report pertains to a specific site, a specific development, and a specific scope of work. The Design Report may include plans, drawings, profiles and other support documents that collectively constitute the Design Report. The Report and all supporting documents are intended for the sole use of EBA's Client. EBA does not accept any responsibility for the accuracy of any of the data, analyses or other contents of the Design Report when it is used or relied upon by any party other than EBA's Client, unless authorized in writing by EBA. Any unauthorized use of the Design Report is at the sole risk of the user.

All reports, plans, and data generated by EBA during the performance of the work and other documents prepared by EBA are considered its professional work product and shall remain the copyright property of EBA.

### 2.0 ALTERNATIVE REPORT FORMAT

Where EBA submits both electronic file and hard copy versions of reports, drawings and other project-related documents and deliverables (collectively termed EBA's instruments of professional service), only the signed and/or sealed versions shall be considered final and legally binding. The original signed and/or sealed version archived by EBA shall be deemed to be the original for the Project.

Both electronic file and hard copy versions of EBA's instruments of professional service shall not, under any circumstances, no matter who owns or uses them, be altered by any party except EBA. EBA's instruments of professional service will be used only and exactly as submitted by EBA.

Electronic files submitted by EBA have been prepared and submitted using specific software and hardware systems. EBA makes no representation about the compatibility of these files with the Client's current or future software and hardware systems.

### 3.0 ENVIRONMENTAL AND REGULATORY ISSUES

Unless so stipulated in the Design Report, EBA was not retained to investigate, address or consider, and has not investigated, addressed or considered any environmental or regulatory issues associated with the project specific design.

### 4.0 CALCULATIONS AND DESIGNS

EBA has undertaken design calculations and has prepared project specific designs in accordance with terms of reference that were previously set out in consultation with, and agreement of, EBA's client. These designs have been prepared to a standard that is consistent with industry practice. Notwithstanding, if any error or omission is detected by EBA's Client or any party that is authorized to use the Design Report, the error or omission should be immediately drawn to the attention of EBA.

### 5.0 GEOTECHNICAL CONDITIONS

A Geotechnical Report is commonly the basis upon which the specific project design has been completed. It is incumbent upon EBA's Client, and any other authorized party, to be knowledgeable of the level of risk that has been incorporated into the project design, in consideration of the level of the geotechnical information that was reasonably acquired to facilitate completion of the design.

If a Geotechnical Report was prepared for the project by EBA, it will be included in the Design Report. The Geotechnical Report contains General Conditions that should be read in conjunction with these General Conditions for the Design Report.

### 6.0 INFORMATION PROVIDED TO EBA BY OTHERS

During the performance of the work and the preparation of the report, EBA may rely on information provided by persons other than the Client. While EBA endeavours to verify the accuracy of such information when instructed to do so by the Client, EBA accepts no responsibility for the accuracy or the reliability of such information which may affect the report.